Regulation of actin dynamics by phosphoinositides during epithelial closure

A thesis submitted to the University of Manchester for the degree of
Doctor of Philosophy
in the Faculty of Life Sciences

2013

Karen Anne Pickering

Table of Contents

Word count: 65,835

List of figures

List of tables

Abstract

The University of Manchester

Karen Anne Pickering

Doctor of Philosophy

Regulation of actin dynamics by phosphoinositides during epithelial closure

September 2013

Epithelia act as protective barriers and it is therefore essential that wounded epithelia are rapidly repaired to maintain barrier function. Cells surrounding epithelial wounds become motile following wounding, which involves generating dynamic actin structures that drive closure of the wound. These actin structures include filopodia which are important in the final stage of epithelial closure in which the opposing epithelial edges are joined together. The molecular mechanisms that trigger wound edge cells to become motile are not well understood. Using *Drosophila* wound healing and the morphogenetic process dorsal closure as models, we find that phosphatidylinositol 3,4,5-triphosphate (PIP_3) regulates epithelial closure by promoting the formation of filopodia at epithelial edges. PIP_3 accumulates at epithelial edges and genetically depleting PIP_3 results in reduced filopodia and defects in epithelial closure. We demonstrate that the GTPase Rac and guanine nucleotide exchange factor Myoblast City function downstream of PIP_3 to promote filopodia formation. We also demonstrated that the scaffolding protein Par3/Bazooka and the lipid phosphatase PTEN are responsible for restricting the localisation of PIP_3 and consequently the downstream signals to the epithelial leading edge, so acting to determine the location of filopodia formation. This project reveals a novel mechanism by which actin protrusions, required for epithelial closure, are formed in response to epithelial damage. Additionally, we have identified an additional role for PIP_3 in regulating the extrusion of cells from epithelial sheets in the Drosophila embryo. This finding implicates PIP_3 in the regulation of tissue homoeostasis, and could contribute to our understanding of tumour initiation as unregulated tissue growth can result in the formation of tumours.

Declaration

No portion of the work referred to in the thesis has been submitted in support of an application for another degree or qualification of this or any other university or other institute of learning

Acknowledgements

Firstly I would like to thank my supervisor Dr. Tom Millard, for his support and guidance over the past 4 years. I am eternally grateful for the opportunity that he has given me, and without his support and guidance I would not have been able to complete this project.

I also wish to thank all of the members of the Millard lab, past and present, Juliana, Gina and Yutaka, who have made the lab a friendly and welcoming place to work. I am especially grateful for all of the technical help that they have given me over the course of the project. I am truly grateful for Gina, who has been a great support for me throughout, has had to put up with all my rants and has always been there with chocolate when needed.

Additionally, within the faculty of life science, I would like to thank my advisor Dr. Andreas Prokop for his input and suggestions throughout this project which have been insightful and invaluable. I would also like to thank members of his lab whose input in our shared lab meetings has been greatfully received, most notably Natalia and Robin. Additionally I would like to thank Professor Enrique Amaya and all the members of The Healing Foundation who have provided help and guidance whenever required.

Special thanks goes to the core facilities within the faculty of life sciences, including the fly facility, and in particular to Sanjai, for helpful discussions and his knowledge on where to obtain reagents. In addition, I would like to thank the Bioimaging department, in particular to Peter and Roger, as without their help getting trained on all the microscopes and at times, getting them to work, this project would not have been possible. I also wish to thank the DNA sequencing facility, as without their expertise we would not have had confidence in one of our lines or have been able to generate transgenic fly lines required for this project.

My project would not have been possible without the continuous funding and support from The Dowager Countess Elanor Peel Trust and The Healing Foundation, for which I am eternally grateful.

Finally, I would like to thank my friends and family who have gotten me through the past 4 years, My friends, for being there for me with chocolate and wine (when needed), and for my wonderful Mum, who has supported me unconditionally both emotionally and financially. Without my Mums love and support I would not have had the courage to return to University, or the persistence to make it through. For that I am forever grateful.

Abbreviations

A or AC	Actin-binding protein 1
Abp1	Acidic region
ADP	Adenosine diphosphate
ADF	Actin Depolymerising Factors
aPKC	atypical Protein Kinase C
Arp2/3	Actin Related Proteins
ATP	Adenosine triphosphate
Baz	Bazooka
BMP	Bone Morphogenetic Protein
C	Central region
CA	Constitutively active
C1	Protein kinase C conserved region 1
Cdc42	Cell division control protein 42 homlogue
cDNA	Complementary Deoxyribose nucleic acid
cGMA	Constitutive GFP Moesin
CHO	Central Nervous System
CNS	Chinese Hamster Ovary
DC	Dorsal Closure
ddH_2O	Distilled Water
DHR	Dbl homology
DHR	Dock Homology Region
DME	Dorsal Most Epidermal cells
DNA	Deoxyribonucleic acid
Dock	Dedicator of Cytokinesis
DMSO	Dimethyl Sulfoxide
DN	Dominant Negative
Dpp	Decapentapleigic
DSHB	*Drosophila* Studies Hybridoma Bank
EDTA	Ethylenediaminetetraacetic actin
EGF	Epidermal Growth Factor
EGFR	Epidermal Growth Factor Receptor
ELMO	Engulfment and Cell Motility
En	Engrailed
Ena	Enabled
Erk	Extracellular-signal Related Kinase
F-actin	Filamentous actin
FITC	Fluorescein isocyanate
G-actin	Globular actin
GAP	GTPase Activating Proteins
GBD	GTPase Binding Domain
GDF	GDI displacement factors
GDI	GDP dissociation inhibitors

GDP	Guanosine diphosphate
GEF	Guanine Nucleotide Exchange Factors
GFP	Green Fluorescent Protein
GPH	GFP tagged domain of Grp-1
GSK3	Glycogen Synthase Kinase-3
GTP	Guanosine triphosphate
JNK	c-Jun N-terminal Kinase
KCl	Potassium Chloride
LB	Lysogeny Broth
LBA/IPTG	Lysogeny Broth Agar/Isopropyl-Beta-D-Thiogalactoside
MAPK	Mitogen Activated Protein Kinase
MBC	Myoblast City
MDCK	Madin-Darby Canine Kidney
$MgCl_2$	Magnesium Chloride
MRLC	Myosin Regulatory Light Chain
mTORC2	Mammalian Target of Rapamycin Complex 2
Na_2HPO_4	Disodium phosphate
NaOH	Sodium Hydroxide
NPF	nucleation promoting factors
NaCl	Sodium Chloride
NEB	New England Biolabs
PCR	Polymerase Chain Reaction
PDGF	Platelet Derived Growth Factor
PDGFR	Platelet Derived Growth Factor Receptor
PDZ	domain present in PSD-95, Dlg and ZO1/2
PH	Pleckstrin homology
PI	Phosphatidylinositol
PI(3)P	Phosphatidylinositol 3-phosphate
$PI(3,4)P_3$	Phosphatidylinositol 3,4-biphosphate
PI(4)P	Phosphatidylinositol 4-phosphate
PI3K	Phosphoinositide 3-kinase
$PI(4,5)P_2$	Phosphatidylinositol 4,5-biphosphate
PIP_3	Phosphatidylinositol 3,4,5-triphosphate
PLC	Phospholipase C
PKB/akt	Protein Kinase B
PTEN	Phosphatase and Tensin homologue
PxxP	Poly Proline region
RBD	Ras Binding Domain
Rok	Rho associated Kinases
Scar	Suppressor of cyclic AMP receptor
SDS	Sodium Dodecyl Sulphate
SH2	Src Homology 2
SH3	Src Homology 3
Sif	Still life
SOC	Super Optimal Broth
Sra1	Specifically Rac Associated protein-1

TE	Tris and EDTA buffer
TRITC	Tetramethylrhodamine-5-(and-6)-Isothiocyanate
UAS	Upstream activating sequence
VASP	Vasodilator-stimulated phosphoprotein
WASP	Wiskott-Aldrich syndrome protein
WAVE	WASP-family verprolin-homologous
WH2	Wasp-homology 2
Wt	Wild Type

Chapter 1: Introduction

Actin plays a central role in controlling cell morphology and precise regulation of actin dynamics is required for a variety of processes such as morphogenesis, wound healing and immune cell migration (Martin and Lewis 1992; Jacinto *et al.* 2000; Wood *et al. 2002;* Wood *et al.* 2006; Yoo *et al.* 2010). There are two main types of protrusions that actin can form; filopodia, that are long, thin needle like bundles of actin (Mogilner and Rubinstein 2005) and lamellipodia that are a flat cross-linked network of actin (Small 1995), both of which play an important role in cell movement, however, filopodia have been shown to have an additional role in joining epithelial edges together. Given the importance of actin in key biological processes it is essential that we understand how its dynamics are regulated at the molecular and cellular levels and how it functions *in vivo*. This introduction will describe how actin dynamics are regulated, in particular during tissue morphogenesis and repair.

1.1 Actin dynamics at the leading edge:

A variety of proteins regulate the assembly and organisation of actin filaments at the leading edge of migrating cells and these are required for the formation of actin protrusions. Actin filaments can push on the plasma membrane to form actin protrusions, and the type of actin protrusion formed depends on the architecture of the actin filaments present at the plasma membrane; filopodia are formed by bundled actin filaments that push against the membrane to form a long, needle-like protrusion, whilst lamellipodia are formed from a thin, cross-linked network of actin filaments pushing against the membrane. (Small 1995; Mogilner and Rubinstein 2005). This section describes the regulation of actin dynamics at the leading edge and how lamellipodia and filopodia are formed.

1.1.1 Actin

Actin is a 43kDa nucleotide binding protein that can polymerise to form linear filaments. Polymerised actin is known as filamentous actin (F-actin), while monomeric actin is known as globular actin (G-actin) (reviewed by Goley and Welch 2006). Each actin monomer has a barbed (fast growing) end and a pointed (slow growing) end and they associate in a pointed to barbed end conformation in actin filaments (with respect to the leading edge), with polymerisation occurring primarily at the barbed end (reviewed by Pollard and Borisy 2003).

Various actin-sequestering proteins, such as thymosin-β4 and profilin, both of which form 1:1 complexes with actin monomers, can modulate actin polymerisation. However, they do so in

different manners; thymosin-β4 inhibits the exchange of bound nucleotides and so inhibits polymerisation (as ADP-actin polymerises 5-10 times slower than ATP-actin), whereas profilin promotes nucleotide exchange and as such acts as an enhancer of actin polymerisation (Mockrin and Korn 1980; Goldschmidt-Clermont *et al* 1992). Goldschmidt-Clermont *et al*. (1992) showed that even where the levels of thymosin-β4 is high, and thus rates of polymerisation should be low, the rate of nucleotide exchange on actin monomers can be greatly varied by small changes in the concentration of profilin, implicating profilin as the rate limiting factor of polymerisation. Shortly after monomers are incorporated into filaments, the bound ATP is hydrolysed to ADP, meaning that recently formed filaments mostly consist of ATP-actin, while older filaments are largely composed of ADP-actin (reviewed by Pollard and Borisy 2003).

1.1.2 Nucleation of actin filaments

The nucleation of new actin filaments is energetically unfavourable under cellular conditions, so nucleators and their activators are required to generate new actin filaments. One key nucleator, the Arp2/3 complex, can be activated by specific nucleation promoting factors (NPFs) (Skoble *et al.* 2001). There are two classes of NPFs; class I and class II (reviewed by Goley and Welch 2003). Wiskott-Aldrich syndrome protein (WASP) is a class I NPF, and is characterised by a WCA domain; consisting of a WASP-homology-2 (WH2) domain, a central (c or cofilin homology) domain and an acidic (A) domain (Marchand *et al.* 2001; Chereau *et al*. 2005; Goley and Welch 2006). The WCA domain of WASP interacts with Arp2/3 invoking a conformational change resulting in the activation of the Arp2/3 complex. Specifically, the C region of the WCA domain interacts with the Arp2 subunit, whilst the A region interacts with the Arp3 subunit, bringing Arp2 and Arp3 into close contact. The WH2 domain of the NPF then interacts with and delivers an actin monomer to this site, forming a complex consisting of Arp2, Arp3 and an actin monomer. This trimer acts as a nucleation site for a new actin filament (Friden 1983; Goley *et al.* 2004; Boczkowska *et al.* 2008; Weston *et al.* 2012). Class II NPFs, such as cortactin and actin-binding protein-1 (Abp1) are characterised by the ability to bind Arp2/3 but not G-actin, however, they are able to bind F-actin which is required for the activation of Arp2/3 (Uruno *et al* 2001). As Arp2/3 alone has a low basal nucleating activity, and WASp and N-WASP are expressed in an auto-inhibitory conformation, external signals are required to relieve the auto-inhibition and promote the nucleation of actin filaments. (Mullins *et al.* 1998; Rohatgi *et al.* 2000).

1.1.3 Elongation of actin filaments

Once a filament has been nucleated, it undergoes elongation where actin monomers are added to the barbed end. Elongation occurs when profilin associates with the barbed end of an actin monomer, thus allowing the actin-profilin complex to bind to the barbed end of an

existing filament but blocking binding to the pointed end (Pollard and Cooper 1984; Pring *et al.* 1992). Rapid filament elongation soon depletes the cytosolic actin monomer pool, resulting in slower elongation. There are two mechanisms that can compensate for this; the inhibition of elongation by capping proteins and the depolymerisation of actin filaments by cofilin. Both mechanisms help maintain the level of actin monomers in cells.

1.1.4 Maintenance and depolymerisation of actin filaments

Actin polymerisation can be halted by the addition of capping proteins such as CapZ (found in muscle (Caldwell *et al.* 1989)) and Gelsolin (shown to be present in mice among other higher eukaryotes (Witke *et al*. 1995)) to the barbed end of filaments. Once bound, the capping protein prevents the addition of further actin monomers. There are two important outcomes from capping actin filaments; firstly, capping limits the length of actin filaments. This is important as it has been shown that shorter filaments are stiffer than longer filaments, and as such are more effective at pushing the membrane (DiNubile *et al.* 1995; Svitkina *et al.* 1997; Svitkina and Borisy 1999). Secondly, capping filaments restrict where the membrane can be pushed. Only filaments that are in contact with the membrane are capable of pushing it forward, therefore capping restricts the use of actin monomers to areas where the membrane extension needs to occur (reviewed by Cooper and Schafer 2000). Whilst capping proteins prevent the extension of actin filaments, anti-cappers, such as Ena/VASP, work by binding to the barbed end of an actin filament, preventing the addition of capping proteins, but still allowing the elongation of the filament (Bear *et al.* 2002).

'New' actin monomers, required for polymerisation, are added to the cytoplasmic pool by the depolymerisation of existing actin filaments. ADF/cofilins are a family of small proteins that can bind to ADP-actin filaments and promote their depolymerisation (Carlier *et al.* 1997). The interaction between ADF/cofilins and ADP-actin can change the twist of the actin helix making it more accessible to severing into shorter filaments (McGough *at al.* 1997). Once the ADP-actin is dissociated from the actin filament, profilin competes with ADF/cofilin for the monomer. The profilin in the newly formed profilin-actin complex promotes the dissociation of ADP, and as there is more ATP then ADP in cells, nucleotide-free actin preferentially binds to ATP allowing it to be readily available for polymerisation (Rosenblatt et al 1995; Vinson *et al.* 1998; Blanchoin and Pollard 1998).

Severing of a capped actin filament by ADF/cofilin has been shown to promote actin polymerisation by increasing the number of free barbed ends in a network (Ghosh *et al.* 2004). These free barbed ends may be capable of pushing the membrane forward or could provide new sites for branching by the Arp2/3 complex. Depolymerisation is thus important for further polymerisation. This depolymerisation of ADP-filaments by ADF/cofilin, nucleotide exchange

by profilin and then reincorporation at the barbed end is known as treadmilling and is the mechanism used to push the membrane forward by a dynamic actin network (Figure 1).

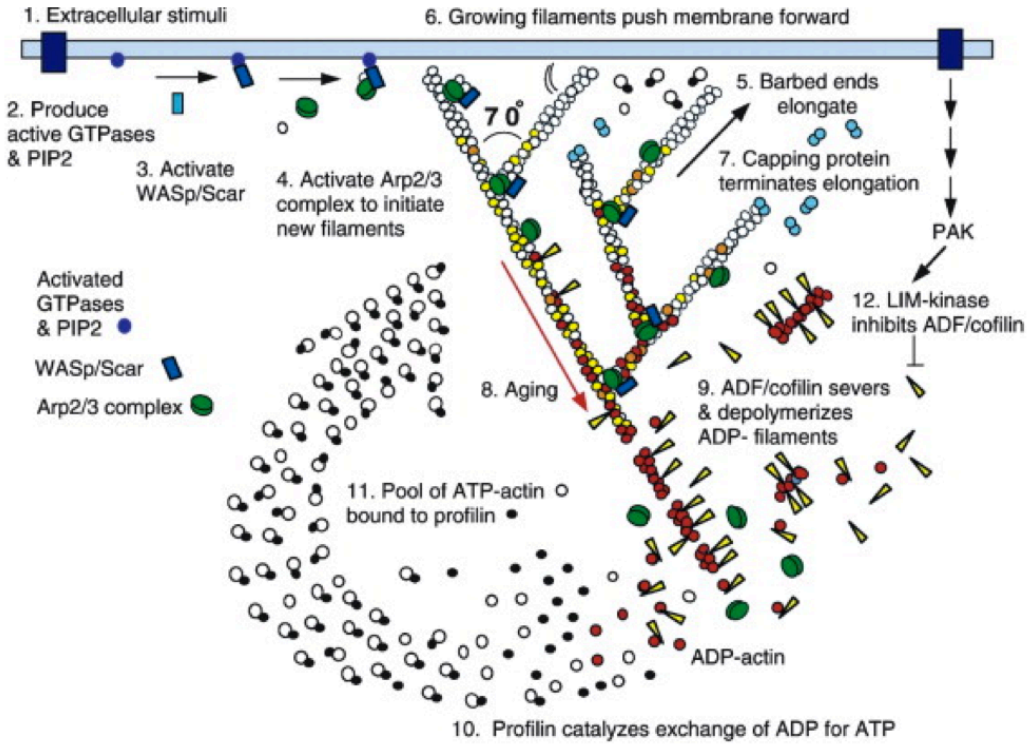

Figure 1. Schematic displaying the treadmilling model for leading edge protrusions. 1) Extracellular signals stimulate receptors 2) activating Rac-family GTPases and PIP2 that activate 3) WASp/SCAR proteins. 4) WASp/SCAR stimulate association of Arp2/3 complex with an actin monomer. 5) Rapid elongation at the barbed end of the filament 6) pushes the membrane forward. 7) Capping proteins terminate elongation. 8) Filaments age by hydrolysis of ATP bound to each actin subunit, followed by the dissociation of the γ-phosphatase. 9) ADF/cofilin promotes phosphate dissociation, severs ADP-actin filaments and promotes ADP-actin dissociation from the ends of filaments. 10) Profilin catalyses the exchange of ADP for ATP returning subunits to 11) the pool of ATP-actin units bound to profilin ready for polymerisation. 12) Rho-family GTPases also activate PAK and LIM kinase which phosphorylates ADF-cofilin. This tends to slow down the turnover of filaments. Pollard and Borisy 2003. Copyright obtained from Elsevier

1.1.5 Filopodia formation at the leading edge.

As mentioned previously, filopodia are needle-shaped cellular protrusions containing parallel bundles of actin filaments. They were first observed live by Gustafson and Wolpert when studying Sea Urchin embryo development (Gustafson and Wolpert 1961), and were found to be highly dynamic. Our understanding of the regulation of filopodia has increased greatly over

the past two decades, however, the mechanism by which filopodia are initiated is currently under debate. There are two proposed models of filopodial initiation; the convergent elongation model and tip nucleation model both of which are discussed in more detail below;

1.1.6 Convergent elongation model

The convergent elongation model was first proposed by Svitkina *et al.* (2003), who hypothesised that filopodia originate from a branched actin network from which a group of actin filaments converge, bundle and elongate to form filopodia. Ena/VASP and profilin elongate barbed-end filaments, by the continuous addition of actin monomers. These elongation factors are capable of oligomerisation, linking several actin filaments together. The parallel filaments are bound together by fascin (an actin cross-linker), resulting in an actin bundle (Figure 2). It is thought that fascin contains two actin binding sites, one C-terminal and the other at the N-terminus of the protein allowing it to bind two actin filaments simultaneously, resulting in bundling (Jansen *et al*. 2011). Interestingly, Work by Zanet *et al.* (2012) showed that fascin also has a role in filopodia formation, independent of its role in actin bundling and it is thought to act at the filopodial tip in promoting the formation and growth of protrusions. Over time, the original Arp2/3 molecule responsible for nucleation of the filament will dissociate leaving free 'pointed' ends (accessible for treadmilling), indicating that the Arp2/3 complex is not required for filopodial maintenance (reviewed by Svitkina and Borisy 1999).

Evidence supporting the convergent elongation model includes work by Machesky and Insall (1998), which showed that disruption of Arp2/3 localisation inhibited the formation of filopodia in macrophages. Subsequent work has shown that filopodia emerge from a pre-existing lamellipodial network (Svitkina *et al.* 2003). Additionally, cell-free systems have shown that Arp2/3, alongside the bundling protein fascin, can reconstitute the formation of filopodial bundles (Vignjevic *et al.* 2003; Haviv *et al.* 2006). These studies all support the convergent elongation model of filopodia initiation.

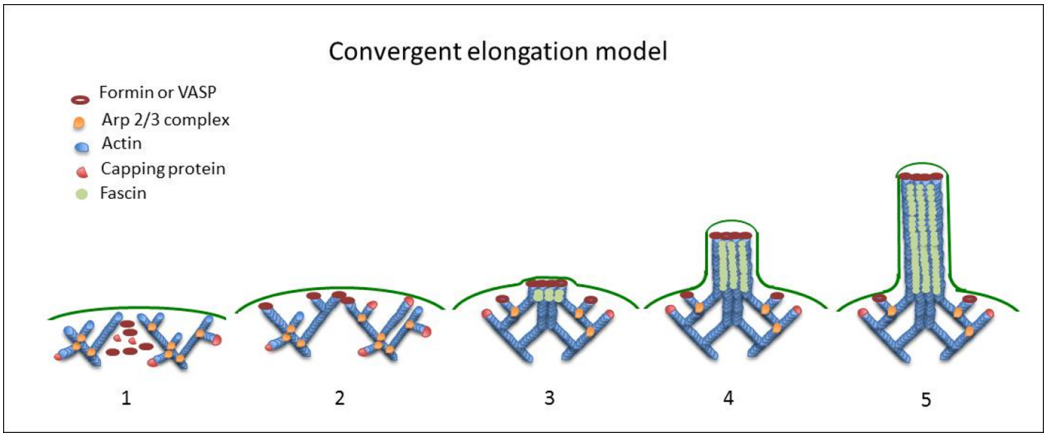

Figure 2. Mechanistic model of filopodia initiation by the convergent elongation model. 1) Branched actin network is formed by Arp2/3 mediated nucleation. 2) Elongation factors (such as Formins or VASP) promote continuous elongation of some barbed ends. 3) Interaction between several barbed ends results in converged filaments. 4) Parallel cross-linked filaments result in a protruding bundle. 5) Over time, the Arp2/3 complex leaves the network resulting in free pointed ends. Model adapted from Yang and Svitkina 2011.

1.1.7 Tip nucleation model

The tip nucleation model proposes that filopodia are formed by a membrane-bound cluster of formins. This formin cluster nucleates new actin filaments close to one another and is capable of maintaining their elongation. These elongated filaments are then cross-linked by fascin, resulting in the formation of a filopodia (as shown in Figure 3). The tip nucleation model does not require a pre-existing filament network (reviewed by Yang and Svitkina 2011).

The formin mDia is the main candidate to play a role in filopodia formation, however despite experiments to prove its role in filopodia initiation, mDia is initially distributed along the leading edge and later accumulates at the tips of newly formed filopodia (Yang *et al.* 2007). Despite this, formins are still thought to play a vital role in the tip nucleation model, arguments for which are based on two sets of data; firstly, increasing or decreasing levels of formins affects filopodia number, inducing and inhibiting filopodia respectively (Schirenbeck *et al.* 2005; Matusek *et al*. 2008) and secondly, filopodia still persist even when the Arp2/3 complex or its activators are downregulated (Steffen *et al.* 2006). The first experimental evidence for this theory showed that filopodia number and length were significantly reduced in primary neuron cultures where dDAAM (a *Drosophila* formin) was lost (Matusek *et al*. 2008). However it could be argued that as formins have the ability to work as elongators as well as nucleators, these data could be consistent with both models of filopodia formation (Yang and Svitkina 2011).

The second study in support of the tip nucleation model showed that in VA-13 fibroblasts, which have reduced levels of the WAVE complex (an activator of Arp2/3), the formation of both filopodia and lamellipodia are inhibited (Steffen *et al*. 2006). However, when Cdc42 was overexpressed in WAVE deficient cells, the number of protruding filopodia was increased although no lamellipodia were formed. This increase in filopodia, in cells with reduced WAVE but active Cdc42, indicated that filopodia could be formed in a WAVE-independent manner. The authors proposed that as WAVE is an activator of the Arp2/3 complex, the WAVE null cells should not have any active Arp2/3 and as such any filopodia observed in these were formed in an Arp2/3 independent manner. However, the results of this study has been recently been disputed due to the way the images were processed (Yang and Svitkina 2011). When the images were re-analysed (by Yang and Svitkina 2011), it was suggested that the depletion of the Arp2/3 complex may result in a decrease in the overall number of filopodia in cells, contradicting the work as evidence supporting the tip nucleation model.

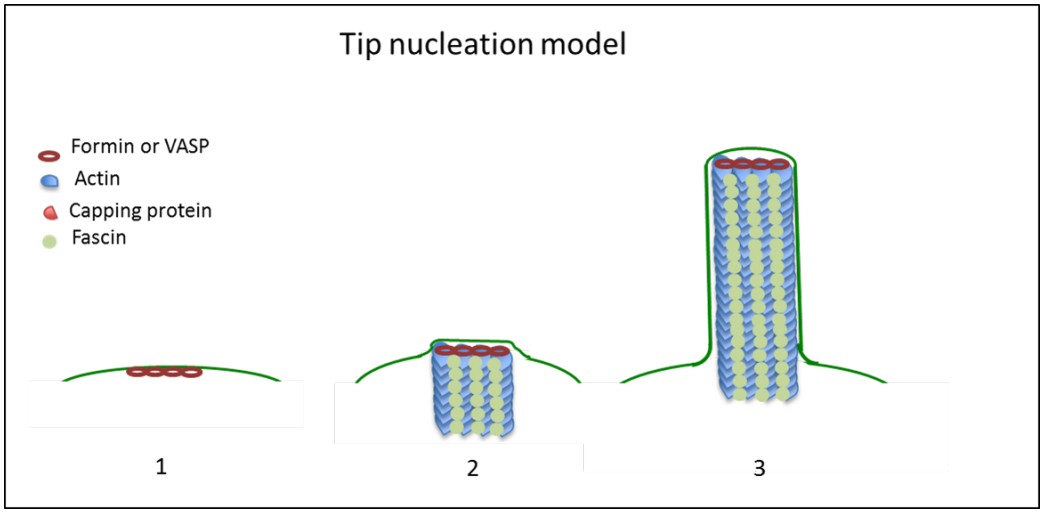

Figure 3. Mechanistic model of filopodia initiation by the tip nucleation model. 1) Activated formin accumulated at the plasma membrane. 2) Formin clusters nucleate actin filament formation and maintain their elongation. 3) Elongating filaments are cross-linked by fascin, forming an actin bundle. Image adapted from Yang and Svitkina 2011

Despite there being less evidence present for the tip nucleation model it is likely that the two models of filopodia formation can co-exist together, especially considering the various conditions in which filopodia are formed. Work by Gonçalves-Pimentel *et al*. (2011) showed that in primary neurons, the absence of either Arp2/3 or formins resulted in a reduction of the number of filopodia, however, the elimination of both completely abolished the formation of filopodia. This supports the hypothesis that both models of filopodia formation are correct.

1.2 Regulation of actin dynamics by the Rho family GTPases

The Rho GTPases are highly conserved members of the Ras superfamily. They are small (20-30 kDa in size), monomeric GTP-binding proteins that play a key role in the regulation of the actin cytoskeleton (reviewed by Bishop and Hall 2000). Rho GTPases act as molecular switches that exist in two conformational states, an active GTP-bound state and an inactive GDP-bound state. In the active, GTP-bound state, Rho GTPases can interact with a variety of effector proteins to co-ordinately regulate their behaviour. Switching between states is controlled by Guanine Nucleotide Exchange factors (GEFs), which promote the exchange of GDP for GTP, resulting in the activation of GTPases, and GTPase activating proteins (GAPs) which promote the dephosphorylation of GTP to GDP so inactivating GTPases (reviewed by Schmidt and Hall 2002). Adjacent to the bound nucleotide within Rho GTPases are two switch regions that undergo a conformational change upon binding to GTP, indicating the activation state of the GTPase to effector proteins (Ihara *et al.* 1998; Dvorsky and Ahmadian 2004). In addition, the activation state of GTPases is further controlled by GDP Dissociation Inhibitors (GDIs), which bind the GDP-bound GTPase and prevent nucleotide exchange, thus reducing the amount of GDP-GTPase available for activation (Moissoglu *et al*. 2006). This inhibition can be relieved by GDI Displacement Factors (GDFs), which displace the GDI from the GTPase/GDI complex, releasing the GDP-GTPase for activation by GEFs (Chaung *et al.* 1993) (Figure 4).

To date, 22 members of the Rho GTPase family have been identified in mammals (reviewed by Vega and Ridley 2007) with the best-studied members being Rho, Rac and Cdc42. *In vitro,* each of these proteins has been shown to regulate the actin cytoskeleton in a specific manner, with Rho regulating actin stress fibres/actin cable formation, Rac primarily regulating membrane ruffling and lamellipodia formation and Cdc42 regulating filopodia formation (Nobes and Hall 1995). However, the roles and regulation of each of the GTPases are less well defined *in vivo*, and it appears that there is also substantial cross talk between them (Nishimura *et al*. 2005). This section will outline our current knowledge of roles of Cdc42, Rho and Rac in the regulation of the actin cytoskeleton and how they contribute to cellular and organismal processes.

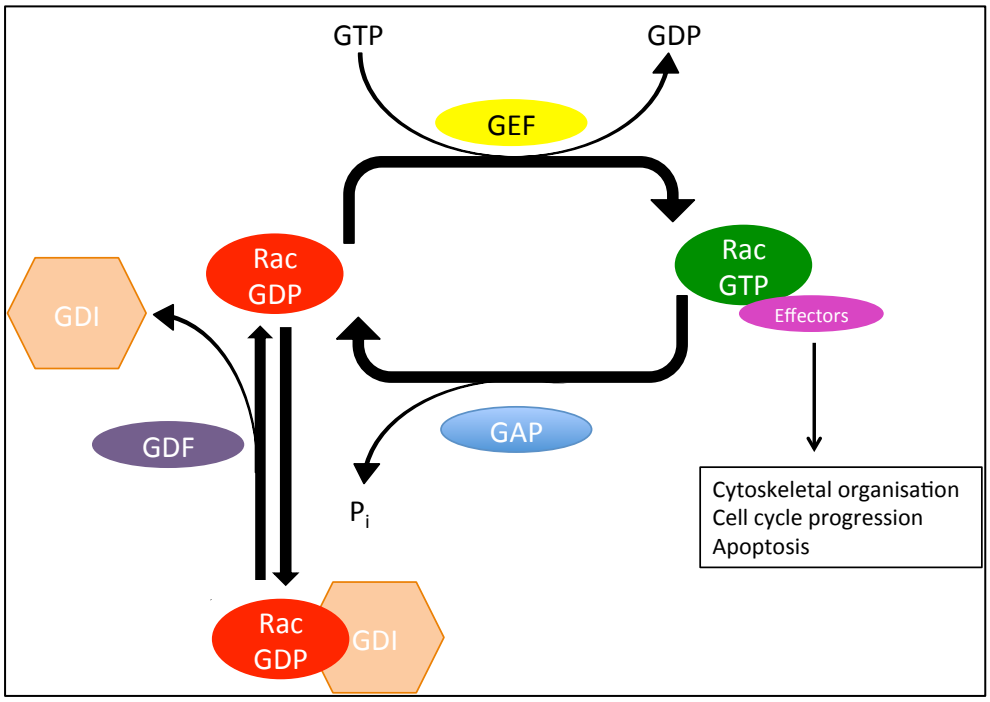

Figure 4. The Rac GTPase cycle. Rac GTPases are recruited to the membrane where GEFs promote the exchange of GDP for GTP, and GAPs dissociate GTP and promote the exchange for GDP. GDI's associate with GDP-bound Rac, preventing its activation by GEFs. GDFs are able to dissociate GDI's from the Rac-GDP/GDI complex, exposing it to activation by GEFs. Figure adapted from Schmidt and Hall 2002.

1.2.1 Cdc42

1.2.1.1 Cdc42: Cellular functions

Cdc42 has two main cellular functions; the regulation of actin assembly and the regulation of cell polarity (Adams *et al.* 1990; Nobes and Hall 1999; Genova *et al*. 2000; Yang *et al*. 2006). Whilst these two functions are distinct, they are often associated with one another and are both important during cell migration. Cdc42 is required for the formation and maintenance of both apicobasal polarity required for the correct development of epithelia, and planar polarity in which cells orientate themselves in a two-dimensional plane perpendicular to the apicobasal axis (reviewed by Drubin and Nelson 1996; reviewed by Gibson and Perrimon 2003).

In many cell types, including mouse embryonic fibroblasts, mouse neurons and *Drosophila* epidermal cells, reducing the levels of Cdc42 results in the reduction in the number and length of filopodia, which can have a dramatic effect on the ability of a cell, to migrate (Nobes and Hall 1995; Kozma *et al*. 1997; Wood *et al.* 2002; Yang *et* al. 2006; Garvalov *et al.* 2007). Cdc42 regulates the actin cytoskeleton by relieving the auto-inhibition of the NPF WASP/N-wasp. The inhibition of WASP/N-wasp occurs between the N-terminal G-protein binding region (including a Cdc42/Rac interaction motif and a basic region) and the WCA C-terminal

domain (Kim *et al*. 2000), Cdc42 can bind to the G-protein binding region, resulting in the release and exposure of the WCA domain allowing it to recruit and activate the Arp2/3 complex (Miki *et al*. 1998; Rohatgi *et al.* 2000), so acting as an upstream regulator in the nucleation of actin filaments required for actin protrusion formation. Alternatively, Cdc42 can regulate the actin cytoskeleton through cofilin. Garvalov and colleagues (2007) identified Cdc42 as an upstream regulator of cofilin and in neurons lacking expression of Cdc42, an increase in the amount of phosphorylated (inactive) cofilin was observed. Cofilin is required for the disassembly of existing actin filaments (Carlier *et al*. 1997), generating free actin monomers and as such is required for the formation of new actin filaments essential for the formation of filopodia. These data show that Cdc42 is able to generate free barbed ends, required for actin protrusion formation.

Cdc42 was first proposed to have a role in establishing and controlling cell polarity in the division of yeast where it localises to the bud site, early in the yeast cell cycle (Adams *et* al. 1990; Ziman *et al*. 1993). Although strains of yeast lacking Cdc42 continue to grow, they fail to bud and polarise correctly (Adams *et al*. 1990). Supporting the observations in yeast, work in epithelia such as MDCK cell culture and *C.elegans* implicate a role for Cdc42 in regulating apicobasal polarity which is required for the formation of a functional epithelium (reviewed by Gibson and Perrimon 2003). In MDCK cells, Cdc42 interacts with the Par polarity complex (consisting of Par6, Par3 and aPKC) creating a quaternary complex, which is required for the formation of tight junctions. This interaction has also been shown to be vital in the development of epithelial cell-cell contacts in *C.elegans* (Joberty *et al.* 2000). In 1999, Nobes and Hall, also demonstrated the role of Cdc42 in establishing planar cell polarity and migration in response to a scratch wound in a monolayer of Swiss 3T3 cells. Loss of Cdc42 resulted in a loss of the ability of cells to polarise in response to wounding, with the Golgi complex of wound edge cells failing to realign and a reduction in cell movement towards the wound (Nobes and Hall 1999). The role of Cdc42 in cell polarisation has also been shown in *Drosophila* hemocyte (macrophage-like cell) migration towards a wound. Although *cdc42*-/- hemocytes were able to migrate towards wounds, the route taken was frequently indirect, suggesting a defect in polarity (Stramer *et al.* 2005). The effect of loss of Cdc42 on hemocyte migration was less severe than observed *in vitro* by Nobes and Hall, suggesting that the importance of Cdc42 in cell polarisation and migration may be dependent on the system.

1.2.1.2 Cdc42 in organismal processes

Cdc42 is important for development in a variety of organisms, including *Drosophila* and mice. *Drosophila* embryos lacking Cdc42 undergo developmental arrest part way through embryogenesis (germband retraction) (Jacinto *et al.* 2000). Additionally, Cdc42 was shown to be vital for the development of the embryonic epithelium, in particular in the elongation of epithelial cells into a columnar shape, required for the maintenance of the epithelial monolayer

(Genova *et al*. 2000). It has also been shown to be vital during *Drosophila* dorsal closure (henceforth DC) and will be discussed in more detail in section 1.4.5.4 (Jacinto *et al*. 2000). In vertebrate development, Cdc42 has a crucial role in the patterning of the lung (Wan *et al*. 2013). Mice with specific knockdown of Cdc42 in respiratory cells die at birth from respiratory failure. The lungs fail to develop properly due to a loss of cell polarity, which results in the disruption of actin-based cell migration processes essential for lung development. Additionally, defects are observed in branching morphogenesis resulting from improper alignment of mitotic spindles leading to cell division occurring perpendicular to the epithelium monolayer (Wan *et al*. 2013).

Additionally, Cdc42 has also been shown to be involved in the progression of cancer, with a reduction in levels of Cdc42 sufficient to inhibit lung cancer metastasis in the mouse (Reymond *et al.* 2012). However, the role of Cdc42 in cancer metastasis is not fully understood, as reducing its levels has varying results depending on the cancer type. Knockdown of Cdc42 in moderately metastatic breast cancer cells results in an inhibition of migration and invasion, whereas in highly metastatic breast cancer cells the migration and invasion was enhanced with Cdc42 reduction (Zuo *et al*. 2012). This demonstrates the complex roles Cdc42 plays in cancer cell migration and that more work is required to further elucidate exactly how Cdc42 regulates metastasis. These data highlight the vast range of processes in which Cdc42 is involved during development and its importance in the regulation of actin dynamics and cell polarity.

1.2.2 Rho

Madaule and Axel first identified Rho GTPase in the mollusc in 1985 where it was shown to contain domains required for membrane attachment. Soon after its identification, Rho was shown to be important in cell morphology with increased active Rho resulting in elongated cells while Rho inhibition caused cells to round up (Paterson *et al.* 1990). These phenotypes were due to Rho acting on the actin cytoskeleton and in particular, regulating the formation of contractile actin structures and focal adhesions in Swiss 3T3 cells (Ridley and Hall 1992). The formation of actin stress fibres can be induced by each of the three main mammalian isoforms (RhoA, RhoB and RhoC) (Chardin 1989; Ridley and Hall 1992; Hall *et al*. 1993). The function of each of the isoforms was reviewed by Wheeler and Ridley (2004) who outlined RhoA as important for tail retraction and disassembly of adhesions at the rear of the cell, Rho B retards growth factor receptor trafficking and localises to endosomes, and Rho C is diffuse throughout the cytoplasm (Wheeler and Ridley 2004). A fourth Rho, RhoH evolved independently and is mainly expressed in haematopoietic cells, and a role for functional differentiation of T-cells has been suggested (Li *et al.* 2002).

1.2.2.1 Rho in cell migration

The role of Rho in cell migration has primarily been associated with the formation of actin stress fibres and turnover of focal adhesions. The formation of stress fibres at the rear of a migrating cell promotes tail retraction, whilst the turnover of focal adhesions is required for cells to crawl over and adhere to a given substrate (Ridley and Hall 1992; Yamana *et al.* 2006). Rho is required for effective cell migration during scratch wound assays. Pre-treatment with exoenzyme C3 (a specific inhibitor of Rho) resulted in a significant delay in the healing of a scratch wound in a culture of corneal epithelial cells when compared to control cultures. Inhibiting Rho resulted in a loss of actin bundles usually observed running parallel to the wound edge, that are required for directional migration of the epithelial sheet (Yin *et al.* 2008). The importance of Rho in cell migration has also been shown in *Drosophila* hemocytes migrating to a wound. In *rho* mutant embryos, hemocytes appear to elongate in the direction of the wound, however they cannot free from existing adhesions and appear tethered in place (Stramer *et al*. 2005).

Rho regulates the formation of actin stress fibres and contractile actin cables through activating Rho-associated kinases, which promote the phosphorylation of the regulatory light chain of myosin (MRLC). Rho-associated kinases work in two ways; they phosphorylate myosin phosphatase, thus inactivating it as well as directly phosphorylating MRLC itself (Kawano *et al*. 1999; reviewed by Bishop and Hall 2000). Phosphorylated MRLC stimulates the ATPase activity of Myosin heavy chain, promoting assembly of contractile actomyosin structures (Amano *et al*. 1996; reviewed by Bresnick 1999).

1.2.2.1 Rho in organismal processes

The formation of a contractile actin cable is vital in many processes throughout development including *Xenopus* development, in particular in the process of convergent extension, with altering levels of Rho disrupting gastrulation. Rho (alongside Rac) is required for the polarisation of intercalating cells with disruption of these GTPases resulting in the failure of cells to elongate and complete convergent extension (Tahinci and Symes 2003). The authors also found Rho to be important for the lifespan of protrusions in *Xenopus* explants, with inhibition of Rho resulting in shorter lived protrusions, however, how Rho regulated this has not yet been determined. Additionally Rho has been implicated in the stabilisation of cell-cell junctions, for example, during *Drosophila* trachea formation Rho plays a role in the turnover of E-cadherin. This turnover of E-cadherin is required for tracheal branching and increasing Rho levels increased the amount of stable E-cadherin at junctions (Warrington *et al*. 2013). Rho is also vital for the process of *Drosophila* DC, and will be discussed in more detail in section 1.4.5.4.

Despite the vital roles Rho has in development of *Drosophila* and *Xenopus*, no role has yet been identified in the development of mice. Knockouts of *rhoB* and *rhoC* are viable with no developmental defects (Liu *et al*. 2001; Hakem *et al.* 2005), and as yet, no *rhoa* null mice have been made. However, a mouse strain with keratinocyte-restricted deletion of RhoA also displayed no adverse effects, with the skin developing normally (Jackson *et al*. 2011). These results suggest that there could be redundancy between the Rho isoforms in mice and as such single knockout mice do not display defects. Rho has also been shown to be vital for re-epithelialisation in a variety of systems, and will be discussed in more detail in section 1.4.2.1.

Given what is known about the role of Rho in development and wound healing, it is not surprising that Rho is also involved in tumour formation and metastasis. In the two *rho* knockout mouse models available, although no developmental defects were detected, differences in tumourigenesis were observed. The loss of RhoB in these mice resulted in an increase in tumours, leading to the conclusion that RhoB protects against tumourigenesis (Liu *et al.* 2001). RhoC, whilst not important in tumour initiation, appears to play a role in metastasis with a loss of RhoC resulting in a reduction in tumour metastasis (Hakem *et al*. 2005).

1.2.3 Rac

The third well-characterised Rho GTPase subgroup is the Rac family, of which there are 4 members in mammals; Rac1, Rac2, Rac3 and RhoG. Rac proteins are important for the regulation of lamellipodia and membrane ruffle formation (Ridley *et al*. 1992b; Nobes and Hall 1995), and in mice, the three Rac isoforms have different expression patterns; Rac1 is the best studied of the isoforms and is expressed ubiquitously, Rac2 is mainly restricted to haematopoietic cells (Shirsat *et al*. 1990; Moll *et al*. 1991; reviewed by Heasman and Ridley 2008), and Rac3 is most abundant in the brain (Haataja *et al.* 1997). RhoG is widely expressed and also has a role in the in the regulation of the actin cytoskeleton, in particular, it is able to activate Rac1 through Rac activating proteins, GEFs (Vincent *et al*. 1992; Katoh *et al.* 2005).

1.2.3.1 Rac in the actin cytoskeleton and cell migration

Rac proteins regulate the actin cytoskeleton, in particular, the formation of lamellipodia, by activating nucleators, such as the Arp2/3 complex (how these activate actin filament formation is discussed in section 1.1.2) (Steffen *et al*. 2004). Rac-GTP activates the Arp2/3 complex by binding to specifically-Rac associated protein-1 (Sra-1), which is a component of the Scar/WAVE complex. Binding of Rac to Sra-1 results in the activation of Scar/WAVE, which directly binds to and activates the Arp2/3 complex (Steffen *et al.* 2004).

During neutrophil cell migration, different Rac isoforms play different roles; Rac1 plays a role in uncapping actin filaments by promoting phosphoinositide association with capping proteins, thus resulting in their dissociation, whilst Rac2 activates cofilin and Arp2/3 (Hartwig *et al.* 1996; Yang *et al.*1998; Sun *et al*. 2007). Both of these processes are vital for the generation of free-barbed ends required for actin polymerisation. *In vitro,* Rac1 regulates the formation of lamellipodia in a wide range of cells including fibroblasts and epithelial cells (reviewed by Ridley 2001), however, its role in neutrophils is more complicated. *Rac1* null neutrophils form multiple lamellipodia and can still migrate, but they are unable to detect a chemoattractant gradient (Sun *et al*. 2004), whilst r*ac2* null cells can orientate towards a chemoattractant, but cannot migrate towards it. However, work by Gu *et al.* suggests that in macrophages, actin protrusions may be formed independent of Rac, as cells lacking expression of both Rac1 and Rac2 can migrate at a similar speed to wild type cells (Gu *et al*. 2003). *In vivo* analysis has also shown the importance of Rac in the formation of lamellipodia and cell migration. In zebrafish neutrophils, Rac is required for the formation of lamellipodia and for efficient migration towards wounds (Yoo *et al.* 2010). Consistent with this, *Drosophila* embryonic hemocyte migration towards a wound is impaired in embryos lacking expression of Rac (Stramer *et al.* 2005). These data suggests a role for Rac in the regulation of actin protrusions required for efficient cell migration.

1.2.3.2 Rac in organismal processes

Hakeda-Suzuki and colleagues (2002) showed that in *Drosophila,* Rac is required for a multitude of developmental processes, and that when the function of all three *rac* genes (*rac1, rac2 and mtl*) are absent, embryogenesis cannot be completed (Hakeda-Suzuki *et al*. 2002; Ng *et al*. 2002). One of the defects observed during the development of triple *rac* null embryos, is a failure to complete DC but the presence of any one of the *rac* genes is sufficient to rescue the defect. Rac has been shown to be vital for the process of DC during *Drosophila* embryogenesis and will be discussed in more detail in section 1.4.5.5. Rac is also important in other developmental processes in the *Drosophila* embryo, such as myoblast fusion and development of the nervous system (Hakeda-Suzuki *et al*. 2002; Ng *et al*. 2002). Myoblast fusion involves a variety of processes including migration, recognition and adhesion, all of which are crucial for correct fusion (reviewed by Abmayr and Pavlath 2012) and it is likely that actin rearrangements play a part in some of these processes. Hakeda-Suzuki *et al.* demonstrated that *rac1* and *rac2* were required for myoblast fusion (Hakeda-Suzuki *et al*. 2002), however, their exact role during this process is as yet unknown.

During the development of the nervous system, axon guidance, growth and branching must be tightly controlled for proper development. In *Drosophila* it was shown that Rac was involved in all three of these processes; axon branching is highly sensitive to the loss of Rac GTPases with heterozygous *rac1* knockouts eliciting defective branching. Axon guidance defects were

also seen with loss of Rac1 alone, although defect occurrence and severity increased with loss of the other *rac* genes, with the most defects seen in triple mutant animals. Axon growth was least affected by the loss of Rac, and defects were only seen in neurons lacking all three Rac genes (Ng *et al*. 2002). This study demonstrates the requirement for Rac in all aspects of development of the nervous system.

Rac is also vital for the development of the *Xenopus* embryo, in particular during the process of gastrulation. Overexpression of Rac during gastrulation was able to induce the formation of both lamellipodia and filopodia, in contrast to *in vitro* work where Rac has only been able to induce lamellipodia formation (Nobes and Hall 1999; Tahinci *et al*. 2003). In the absence of Rac, gastrulation defects were observed, which can be caused by a failure of cell polarisation required for forward movement of the tissue needed for efficient gastrulation. In these embryos, although the total number of protrusions was unaffected, the number of protrusions associated with the long axis of axial-mesoderm cells was reduced (these protrusions are required to stiffen the tissue and enable it to move forward to complete gastrulation (Keller *et al.* 2000)). This work indicates a role for Rac in the polarisation and distribution of the actin cytoskeleton required for proper gastrulation in *Xenopus* embryonic development. Rac is also required in mammalian development, with a vital role in the formation of the nervous system. Tahirovic *et al.* showed that in mouse *rac1* knockout growth cones, WAVE is lost from the plasma membrane, suggesting that Rac recruits the WAVE complex to the periphery, initiating actin remodelling at the sites of growth (Tahirovic *et al* 2010).

Unsurprisingly, Rac is also involved in cancer progression. It is overexpressed in a variety of tumours and is important in malignancy; however, no mutations resulting in the activation of Rac itself have been discovered (Rihet *et al.* 2001). Overexpression of Rac has been observed in lung and testicular cancer. In both cases increased levels of Rac is associated with cancer cell proliferation and tumourigenicity. In testicular cancer it was observed that higher levels of Rac1 correlated with increased progression of the cancer (Kamai e*t al.* 2004; Kissil *et al.* 2007). Additionally, Rac3 is also overexpressed in some cancers and is hyper-activated in breast cancer (Mira *et al*. 2000).

1.2.4 Interactions between the GTPases in cell migration/protrusion formation

The idea that each Rho family GTPase has a district function is complicated by the fact that there appears to be substantial cross-talk between members of the family. For example, activation of Cdc42 leads to activation of Rac in cultured fibroblasts (Ridley *et al.* 1992b; Nobes and Hall 1995). Injection of Cdc42 alone into confluent fibroblasts resulted in the formation of lamellipodia, however when co-injected with a Rac inhibitor, lamellipodia were no longer formed (Nobes and Hall 1995), suggesting that Cdc42 was regulating the formation of lamellipodia in a Rac-dependent manner. The ability of Cdc42 to activate Rac has also been

shown in neuroblastoma cells where Cdc42 induces lamellipodia in a Rac-dependent manner through the Par polarity complex. Cdc42 binds to Par6 (part of the Par polarity complex), and inhibition of this interaction resulted in a loss of Cdc42-induced lamellipodia, however filopodia were unaffected. Interestingly Par3 (another member of the Par polarity complex), was shown to bind to Tiam1 (A specific Rac GEF), implicating the Par complex as a mediator of Cdc42 activation of Rac (Nishimura *et al.* 2005) (Figure 5).

Interestingly, Rac antagonises the activity of Rho in NIH.3T3 fibroblasts, with expression of active Rac downregulating Rho activity. Over activation of Rho, however, did not affect Rac activity, suggesting that this inhibition is uni-directional (Sander *et al.* 1999). The ability of Rac to inhibit Rho activity is independent of JNK signalling or changes on the actin cytoskeleton (as actin has been shown to contribute to signalling feedback loops (discussed in section 1.3.6) suggesting that Rac is able to antagonise Rho at a GTPase level, and this balance between Rho and Rac determines cell morphology and migration in these cells (Sander *et al*. 1999).

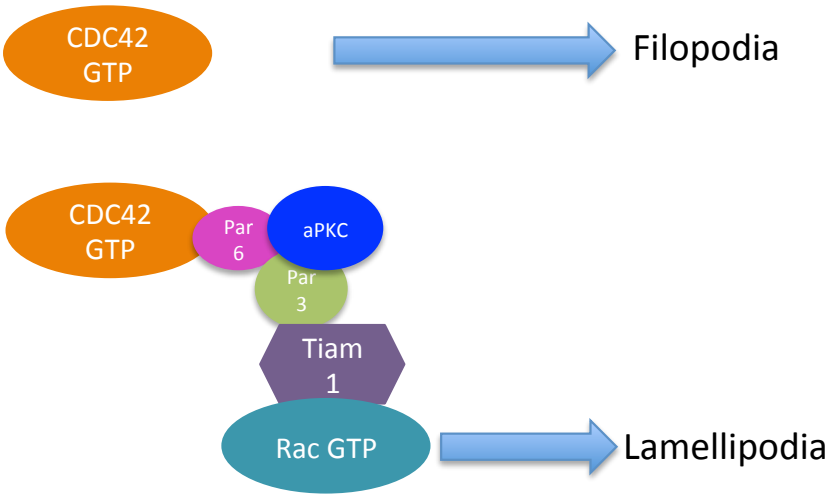

Figure 5. Interaction between the GTPases. Cdc42 can regulate the formation of filopodia, but can also bind Par6 (part of the aPKC polarity complex), then Par 3 can bind Tiam1, recruiting and activating Rac, so forming lamellipodia.

1.2.5 GEFs

As discussed previously, Rho GTPases exist in two conformational states, an active GTP-bound form and an inactive GDP-bound form, which are interconverted by the action of GEFs and GAPs (Garrett *et* al, 1989; Hart *et al*. 1991). GEFs activate GTPases by promoting the dissociation of GDP making way for the association of GTP (which due to its high intracellular levels is energetically favourable) and GAPs bind to GTP-bound GTPases and accelerate

hydrolysis of the GTP-subunit to GDP, thus inactivating it (Scheffzek *et al.* 1997; reviewed by Govek *et al.* 2005). GEFs and GAPs play a critical role in transmitting signals from receptors to Rho GTPases. This section will primarily discuss the action and regulation of Rac specific GEFs.

Rho GTPase GEFs can be divided into two sub-families; typical Dbl homology–pleckstrin homology domain (DH-PH)-containing GEFS, of which there are around 69 in mammals (reviewed by Rossman *et al*. 2005), and atypical Dock180-related proteins containing the Dock homology region (DHR)-2 domain, of which there are 11 in mammals (reviewed by Côte and Vuori 2002). The specificity of GEFs varies, with some GEFs having multiple substrates (such as Vav1 that can activate Rac, Cdc42 and Rho), while others are specific to one GTPase (such as FDG1 for Cdc42) (Zheng *et al.* 1996; Olsen *et al*. 1996).

1.2.5.1 DH-PH GEFs

The DH domains of different GEFs share little homology with one other; however, their structure is highly conserved, with 2 alpha helices (CR1 and CR3) exposed on the surface of the GEF. These alpha helices are part of the GTPase interaction region (Aghazadeh *et al* 1998; Soisson *et al*. 1998). The interaction between the DH domain of GEFs and the GDP-bound GTPase results in the release of GDP from the GTPase and due to the high intracellular ratio of GTP: GDP, GTP binds to the nucleotide-free GTPase, resulting in its activation (reviewed by Cherfils and Chardin 1999; Govek *et al.* 2005). The PH domain of GEFs is situated C-terminal to the DH domain and has two proposed functional roles; firstly, it autoinhibits the activity of the DH domain (by binding to the coiled-coil region inactivating the GEF) and secondly it targets the GEF to the required location of action (by binding to membrane bound phosphoinositides) (Harlan *et al.*1994; Rossman *et al.* 2002). Although the DH-PH domain is the most common motif in GEFs, other functional domains are present which are likely to be involved in linking upstream receptors to GEFs. These domains include SH2, SH3 and PDZ domains, among others (Figure 6).

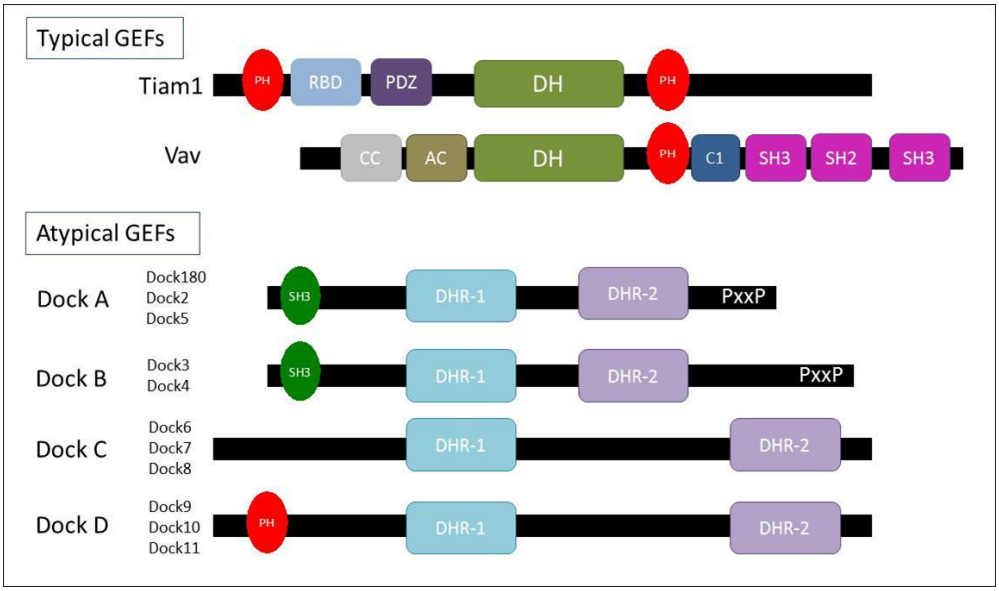

Figure 6. Structure of mammalian GEFs. Domains shown are DH (Dbl homology domain), PH (Pleckstrin homology domain), SH3 (Src homology 3 domain), C1 (Protein kinase C conserved region 1), PDZ (domain present in PSD-95, Dlg and ZO1/2), AC (acidic region), SH2 (Src homology 2 domain), RBD (Ras-binding domain), DHR-1 (Dock homology region 1), DHR-2 (Dock homology region 2) and PxxP (poly proline region) (Schmidt and Hall 2002; Côté and Vuori 2007).

Tiam1 is a typical Rac-specific DH-PH GEF that most likely exists in an auto-inhibited conformation, as deletion of its N-terminal region, results in its constitutive activation (Michiels *et al.* 1997; Worthylake *et al.* 2000; reviewed by Mertens *et al.* 2003). Although the method of autoinhibition has not been determined for Tiam1, in the case of Vav, two methods of autoinhibition exist; firstly, the N-terminal alpha helix can interact with the DH domain blocking access to the GTPase binding site. This can be relieved by phosphorylation of a tyrosine residue within the alpha helix (Aghazadeh *et al*. 2000). Secondly, interaction between the coiled-coil region and the PH domain also results in inhibition of GEF activity, and can be relieved by interaction between the PH domain and phosphoinositides (discussed in section 1.3.4) (Das *et al.* 2000; reviewed by Bustelo 2000). Aside from regulating the auto-inhibition of DH-PH GEFs, the PH domain has also been implicated in the translocation of the GEF to the required site of action. Tiam-1 has two PH domains and the N-terminal PH domain alone is responsible for its localisation by binding to phosphoinositides (Michiels *et al*. 1997). However, this binding it not always required for translocation of DH-PH GEFs to the plasma membrane, for example, Vav can be recruited to cell surface receptors through interaction between its SH2 domain and adapter proteins (Margolis *et al.* 1992; Fleming *et al*. 2000).

In *Drosophila,* Still life (Sif, the homologue of Tiam1) is vital for the development of synaptic terminals. Still life is expressed in the brain and the ventral nerve cord during embryogenesis.

When a truncated form for Sif was expressed, the development of the nervous system was disrupted, primarily by either axons failing to reach the muscles or failing to develop terminal arbors. The authors proposed that Sif was a Rac-specific GEF, required for proper axonal extension and motor terminal arborisation in addition to inducing membrane ruffling (Sone *et al.* 1997). Additionally, Sif regulates the formation of actin protrusions on the basal surface of *Drosophila* epithelial cells (Georgiou and Baum 2010). The authors proposed that phosphoinositides recruited Sif to the basal domain of the epithelial cell where it activated Rac, Scar and Arp2/3 complexes to promote the formation of filopodia.

1.2.5.2 Atypical GEFs

Dock180 proteins are atypical GEFs as they lack the typical DH-PH domains, however they contain two Dock homology regions (DRH1 and 2) and so far 11 Dock proteins have been identified. These GEFs can then further be subdivided into 4 subfamilies as shown in Figure 6 (reviewed by Côté and Vuori 2007). Dock180 is a well-studied atypical Rac-specific GEF, and both DHR domains are important for its function (Kiyokawa *et al* 1998). The DHR-1 domain is important for recruitment of Dock180 by phosphoinositides and will be discussed in more detail in section 1.3.4. The DHR-2 domain interacts with the nucleotide-free form of Rac and is required for Rac activation. Loss of the DHR-2 domain renders Dock180 unable to activate Rac and inhibits cell migration (Lu *et al.* 2005; reviewed by Côté and Vuori 2007). In addition to the DHR domains, Dock A and B subgroup proteins also contain an N-terminal SH3 domain that can bind to the DHR-2 region, concealing the DHR-1 domain and inhibiting the activity of Dock180. Additionally, expression of constructs lacking the SH3 domain resulted in the increase of active Rac by 1.5 fold (Lu *et al*. 2005), suggesting that this domain plays a role in inhibiting the activity of Dock180.

Elmo (mammalian Ced-12) is an evolutionarily conserved protein that can form a complex with Dock180 by binding to the SH3 domain. This interaction releases the SH3-DHR-2 binding, relieving auto-inhibition of Dock180 (Lu *et al*. 2005) (Figure 7A). It has also been suggested that ELMO can play a role in the increasing the GEF activity of Dock180. The Dock180/nucleotide-free Rac complex forms an additional binding site, to which the PH domain of Elmo can bind. This binding of Elmo results in a stabilisation of the complex, facilitating the GEF activity of Dock180 (Lu *et al*. 2004) (Figure 7b).

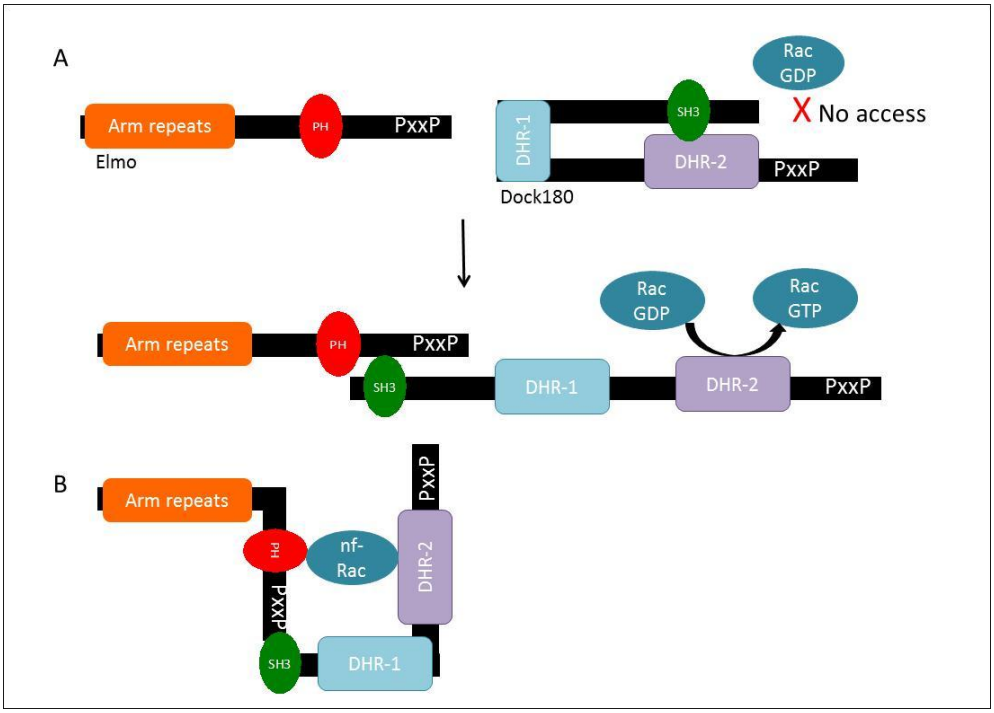

Figure 7. Interaction between Elmo and Dock180. A) A large portion of the C-terminus (the PxxP and part of the PH domain) of Elmo is required for interaction with the N-terminal SH3 domain of Dock180. In the inhibited form, the DHR-2 is inaccessible to Rac-GDP, and binding of Elmo to Dock180 relieves the inhibition, exposing the DHR-2 for Rac-GDP binding and GEF activity. B) The PH domain of Elmo can also bind to and stabilise the Dock180/nucleotide free Rac complex, increasing the affinity of Dock180 towards nucleotide Rac and its GEF activity. Adapted from Côté and Vuori 2007.

The *Drosophila* homologue of Dock180, myoblast city (MBC), has been shown to be vital for a variety of developmental processes, including muscle development, DC and development of the nervous system. Embryos lacking expression of MBC, display a lack of differentiated muscle, with myoblasts failing to elongate and fuse with one another thus failing to form multinucleate syncytia required for muscle formation (Rushton *et al.* 1995). Additionally, embryos with reduced levels of MBC display DC and neuronal defects (Erickson *et al.* 1997; Nolan *et al.* 1998). In embryos lacking expression of MBC, a range of phenotypes are observed during DC, which will be described in section 1.4.5.5. When the axonal outgrowth was studied in embryos lacking expression of MBC, the commissures of some embryos were spaced incorrectly and in some cases the longitudinal connectives did not undergo proper fasciculation (Nolan *et al.* 1998). The authors speculated that the defects observed in embryos lacking expression of MBC could be due to abnormal migration of cells required for each of these developmental processes.

Given the roles of the GTPases in development, wound healing and cancer, it is not surprising that GEFs are also important for these processes. For example, *tiam1* knockout mice are more resistant to Ras-induced tumour formation. Of those that did form, a slower growth rate than controls was observed, however, a greater percentage of these tumours became malignant. This suggests that Tiam1 is important for regulating different aspects of tumour development, through increasing the levels of Rac activity (Hordijk *et al.* 1997; Malliri *et al*. 2002). The vast amount of work that has been carried out on the GTPases and their activators implicates them as important regulators of the actin cytoskeleton in many different processes including development, wound healing, and cancer development and progression.

1.3 Phosphoinositide signalling

Phosphoinositides are membrane lipids consisting of a 6-carbon inositol ring linked to a phospholipid (reviewed by Falkenburger *et al*. 2010). There are 9 different phosphoinositides, differing in the number and position of phosphates on the inositol ring. Phosphoinositides act as signalling molecules that control a variety of processes including cell migration, cell survival and correct spindle orientation (reviewed by Vanhaesebroack 2012). A number of different enzymes catalyse the phosphorylation and dephosphorylation of different positions on the inositol ring and their action controls phosphoinositide levels (Figure 8).

One of the best-studied phosphoinositides is phosphatidylinositol 3,4,5-triphosphate (PIP_3), which was first discovered in 1989 by Auger *et al.* who showed that phosphorylation of phosphatidylinositol 4,5-biphosphate ($PI(4,5)P_2$) by phosphoinositide 3-kinase (PI3K) formed PIP_3. Antagonising this reaction is phosphatase and tensin homologue (PTEN), which dephosphorylates PIP_3 back to $PI(4,5)P_2$ (Maehama and Dixon 1998; reviewed by Vanhaesebroeck *et al*, 2012). Since its discovery, PIP_3 has been implicated in many processes including cell migration, survival and growth (Leevers *et al*. 1996; Zhou *et al.* 1998; Gao *et al.* 2000). In most cases, it is the localisation and levels of PIP_3 which are vital for ensuring these processes occur correctly and these are controlled by PI3K and PTEN. These enzymes will be discussed in more detail in the following section.

1.3.1 PI3K

Phosphoinositide 3-kinases (PI3Ks) were first identified in 1988 as enzymes that phosphorylate the 3-OH group of phosphoinositides (Whitman *et al.* 1988). PI3Ks phosphorylate three different phosphoinositides: phosphatidylinositol (PI), phosphatidylinositol 4-phosphate (PI(4)P) and $PI(4,5)P_2$; to yield phosphatidylinositol 3-phosphate (PI(3)P),

phosphatidylinositol 3,4-biphosphate ($PI(3,4)P_2$) and PIP_3 respectively (Auger *et al.* 1989) (Figure 8).

The PI3K family and its functions have been studied in great detail as altering the level of activity of PI3K can, with over-activation of PI3K cause cancers and inactivation of PI3K cause myopathies and neuropathies (Ma *et al.* 2000; Blondeau *et* al. 2000; Varma *et al.* 2005). This section will outline the different classes of PI3K enzymes and then focus on the regulation and functions of class I enzymes.

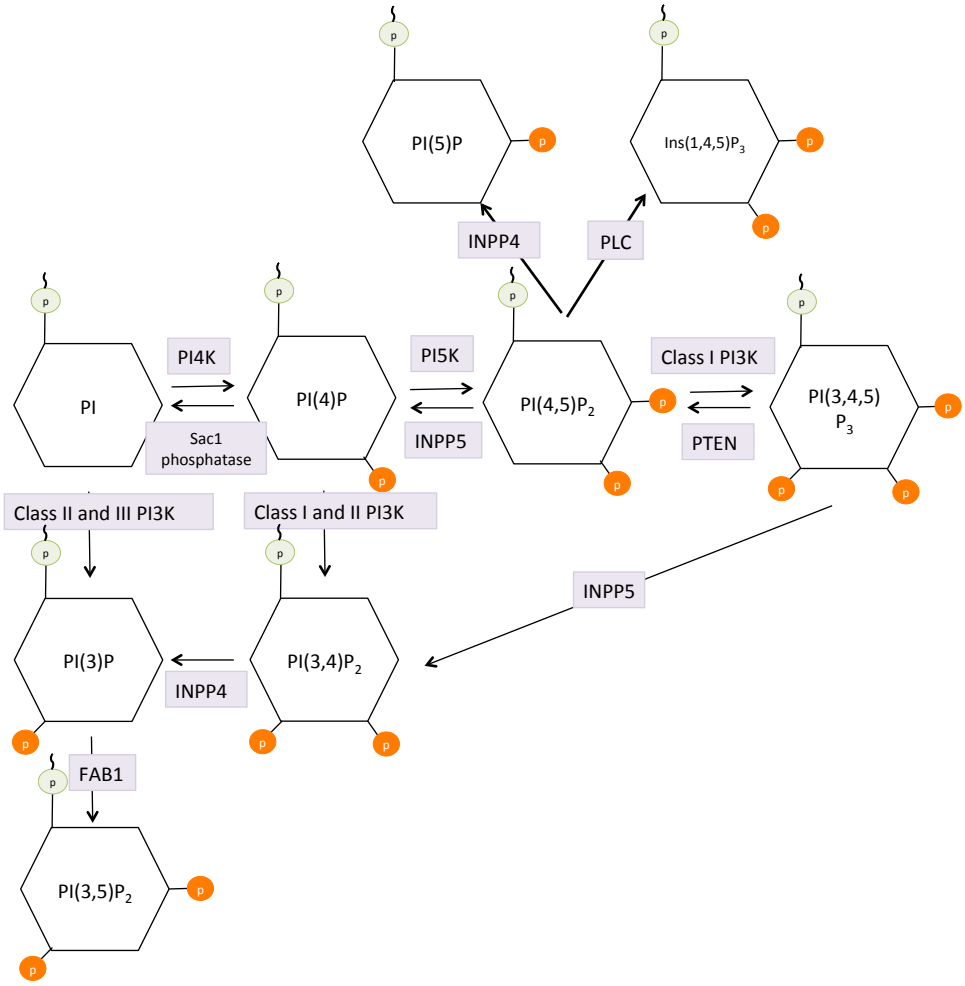

Figure 8. The kinases and phosphatases involved in the regulation of the phospholipids. The main metabolic pathways involved in the formation and dephosphorylation of phosphoinositides. Class I PI3K activated by cell surface receptors where Class II and probably Class III PI3Ks play a key role in the regulation of vesicular trafficking through the endosome-lysosome system. FAB1, PI(3)P 5-kinase, INPP5, inositol polyphosphate 5-phosphatase; PLC, Phospholipase C; PTEN, phosphatase and tensin homologue; INPP4, inositol polyphosphate 4-phosphatase type 1. Adapted from Vanhaesebroeck *et al.* 2012

1.3.2 Classes of PI3K

There are 8 mammalian isoforms of PI3K, divided into 3 functional classes. The classes, isoforms and functions are described below, with Figure 9 outlining the domains specific to each class.

1.3.2.1 Class I PI3K

In vertebrates, there are 4 isoforms of class I PI3K (PI3K p110 α, β, γ, δ), divided into two sub-classes, all of which can phosphorylate both PI(4)P and $PI(4,5)P_2$ to yield $PI(3,4)P_2$ and PIP_3 respectively (Vanhaesbroeck *et al*. 2012) (see Figure 9). Class I PI3Ks are recruited to the plasma membrane in response to specific stimuli through interactions with receptors or adapter proteins (Auger *et al.* 1989). The primary functions of class I PI3K are to regulate cell size, motility and survival. The class I family is divided into 2 subclasses (Class IA and Class IB) based on their mechanisms of action. There are three catalytic subunits of PI3K in the class IA group; p110 α, β and δ; p110 α and β have been shown to play different roles in mouse development with p110α being required for cell survival while p110β regulates cell proliferation (Benistant *et al.* 2000; Vanhaesbroeck *et al.* 2012). Class IA catalytic subunits are activated primarily through a p85 adaptor subunit, which binds to the N-terminal p85 binding region of p110. The p85 subunit binds to phosphorylated receptor tyrosine kinases through SH2 and SH3 domains thus linking extracellular cues to activation of PI3K (Dhand 1994).

The sole catalytic subunit of class IB is p110γ and it differs from the class IA subunits in its N-terminus, as it lacks a p85 binding site. Instead, p110γ contains a domain that binds to p101 (denoted as PH in Figure 9). p110 associates with G-protein coupled receptors and is activated by interaction with Gβγ subunits (Brock *et al.* 2003). The main role of p110γ appears to be as a regulator of inflammation and immune responses, for example it is involved in neutrophil migration towards a wound (Wymann et al 2003; Yoo *et al. 2010*). Drosophila have a single Class I PI3K (PI3K92E) implicated in regulation of cell growth and survival (MacDougall *et al.* 1995)

1.3.2.2 Class II

Class II PI3Ks are the least well-studied class of PI3K, however it is known that *Drosophila* has one class II PI3K (MacDougall *et al.* 1995) (PI3K68D) while mammals have 3 isoforms; PI3K-C2α, PI3K-C2β and PI3K-C2γ. The class II PI3Ks contain the C2-like, PIK and kinase domains common to all PI3Ks, however they vary in their additional membrane binding sites (Figure 9). The class II PI3Ks are found in most tissues (Kok *et al.* 2009) and are stimulated by extracellular signals, including growth factors and integrin engagement (Shaw *et al*. 1997;

Brown and Sheperd 2001). As yet, no defined role for this class of PI3Ks has been described, however *in vitro*, they can phosphorylate PI and PI(4)P, but not PI(4,5)P_2 (Misawa *et al*. 1998).

1.3.2.3 Class III

Vps34 is the only Class III and PI3K PI is the only substrate of this enzyme. So far, all eukaryotes investigated have a homologue of this enzyme (reviewed by Foster *et al*. 2003). Vps34 has no additional domains from the common regions shared with all PI3K isoforms (reviewed by Cain and Ridley 2009) (Figure 9). Vps34 has been implicated in endosome fusion and is localised mainly on intracellular membranes (Schu *et al.* 1993; Wurmser 1999). Additionally, it is also involved in a variety of intracellular trafficking events including autophagy, phagosome formation and transport at the nuclear membrane (Kihara *et al.* 2001; Vieira *et al.* 2001; Roggo 2002).

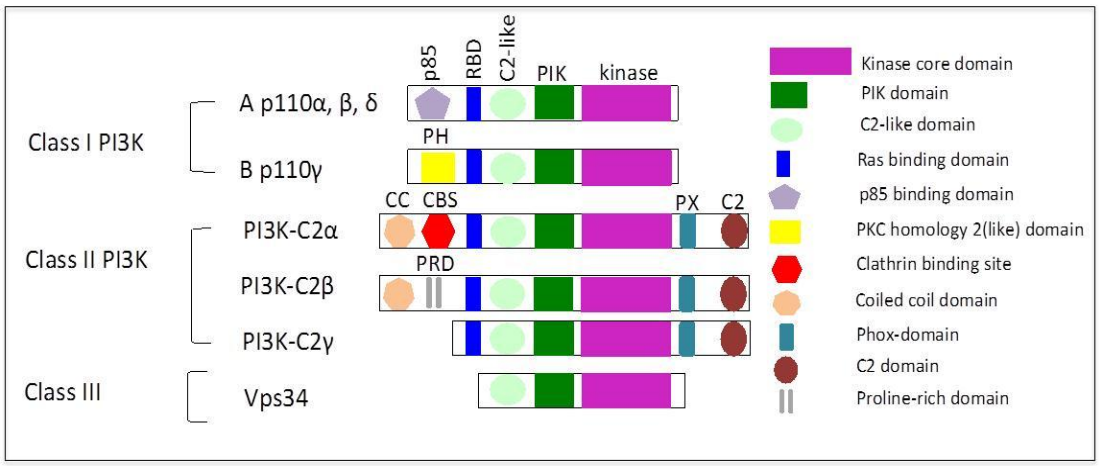

Figure 9. Domain organisation of the three PI3K classes. The three classes of PI3K, showing the domain order for each PI3K isoform. Schematic adapted from Cain and Ridley

1.3.3 Regulators of class I PI3Ks

The PI3K signalling pathway is activated in response to a variety of signals. In 1990, Ruderman *et al.* showed that when insulin production was stimulated in CHO cells, the products of PI3K (PI3P, PI(3,4)P_2, PIP_3) were increased. It was subsequently found that insulin binding causes the insulin receptor to phosphorylate the insulin receptor substrate protein, which recruits and binds specific SH2 domain-containing proteins including the p85 regulatory subunit associated with PI3Kp110α resulting in PI3K activation (Pons *et al*. 1995; reviewed by Saltiel and Pessin 2002). The GTPase Ras has also been identified as an upstream activator of PI3K. Ras-GTP directly interacts with and activates the p110 catalytic subunit of PI3K (Sjolander *et al*. 1991; Rodriguez-Viciana *et al*. 1994). It has also been shown

that stimulation of EGF results in activation of the Ras/PI3K pathway to form actin protrusions, implicating EGF as an external stimuli that can activate the PI3K signalling pathway (Sossey-Alaoui *et al*. 2005; Yip *et al.* 2007)

1.3.4 Effectors of class I PI3Ks

One domain common to many class I PI3K effectors is the pleckstrin homology (PH) domain. The PH domain is loosely conserved and consists of about 120 amino acids. Different PH domains bind to different PIs, for example the PH domain of Tiam1 can bind to PIP_3 while the PH domain of PLC-δ can bind to $PI(4,5)P_2$ (Haslam *et al*. 1993; Mayer *et al.* 1993; Lomasney *et al.* 1996; Sander *et al.*1998). One of the best studied PH domain containing effectors of PI3K is Akt (also known as PKB), which is activated rapidly in response to growth factor stimulation in a PI3K-dependent manner (Burgering and Coffer 1995). Akt activation requires two phosphorylations, one dependent on the PI3K pathway and the other mediated by the mammalian target of rapamycin complex 2 (mTORC2) (Stokoe *et al*. 1997; Sarbassov *et al*. 2005). Akt has many substrates in a variety of processes including GSK3 in the insulin signalling pathway (Cross *et al*. 1995), p21 and p27 in cell cycle regulation (Zhou *et al.* 2001; Viglietto *et al*. 2002) and tuberous sclerosis 2, which is a tumour suppressor. It is through these pathways that Akt regulates cell growth and survival (Leevers *et al.* 1996; Brunet *et al.* 1999; Potter *et al*. 2002).

PI3K also regulates Rho family GTPase activity, as some GEFS and GAPs for the GTPases, contain PH domains (or a DHR-1 domain in atypical GEFs) that bind PIP_3 (Chhatriwala *et al.* 2007; Campa *et al*. 2009). This regulation of GEFs and GAPs by phosphoinositides is likely to underlie many of the effects of PI3K on actin dynamics and cell migration (reviewed by Di Paolo and De Camilli 2006; Yoo *et al.* 2010). The relationship between phosphoinositides and GEFs is complex, as GEFs can bind both $PI(4,5)P_2$ and PIP_3, in some cases with very different results. In the case of the Rac GEF Vav, binding to $PI(4,5)P_2$ results in the interaction between the DH and PH domains, causing inhibition of the GEF, while PIP_3 binding relieves this autoinhibition, activating the GEF (Han *et al.* 1998). Alternatively, the Rac GEF Tiam1 can bind to phosphoinositides through its N-terminal PH domain, with binding to PIP_3 and $PI(3,4)P_2$ resulting in an increase in its GEF activity, whilst binding to $PI(4,5)P_2$ had no effect (Fleming *et al*. 2000). Additionally, both Rac and Cdc42 can bind directly to PI3K in a GTP-dependent manner, resulting in PI3K activation and production of PIP_3 (Tolias *et al*. 1995).

The atypical GEF Dock180, has also been shown to interact with PIP_3 despite not containing the DH/PH domains normally seen in GEFs, as it has two dock homology regions (DHRs), which contains DH and PH-like domains that are sufficient for PIP_3 binding (Côté and Vuori 2002; Côté *et al.* 2005). The DHR-1 domain of Dock180 can interact with phospholipids, in particular PIP_3 (Côté *et al*. 2005). Loss of the DHR-1 domain in CHO cells inhibited Rac-

dependent cell elongation and migration, despite levels of active Rac remaining unchanged, suggesting that the DHR-1 domain is required for the localisation of Dock180 to areas where there are high levels of PI3-kinase signalling, rather than having a direct function in Rac activation.

1.3.5 PTEN as an antagonist of PI3K

The phosphatase and tensin homologue (PTEN) is a negative regulator of PI3K and dephosphorylates PIP_3 at the 3-OH position to $PI(4,5)P_2$, additionally PTEN also has protein phosphatase activity (Meyers *et al.* 1998). PTEN was first identified in 1997, as a chromosome 10 gene in humans, which is completely or partially lost in some cancers (Li *et al*. 1997). Rapidly after the identification of PTEN loss in cancers, *pten* knockout mice were generated and showed the importance of PTEN in supressing the formation of tumours (Suzuki *et al*. 1998). Since the role of PTEN in cancer was identified, its role in various cellular functions has been investigated extensively. In *Drosophila*, there are three splice variants of PTEN, with PTEN2 and PTEN3 displaying 5 times more activity than PTEN1 (Maehama *et al*. 2004). The sole difference between these two splice variants is the presence of a 5 amino acid PDZ-binding motif at the C-terminus of PTEN2 (Maehama *et al* 2004). This additional PDZ binding domain allows PTEN to associate with membrane bound proteins (Von Stein *et al*. 2005), such as Bazooka (henceforth Baz, the *Drosophila* homologue of Par3). Von Stein *et al*. showed that this co-localisation of Baz and PTEN2 also correlated with the presence of $PI(4,5)P_2$ in *Drosophila* epithelia, suggesting that Baz recruits PTEN to the membrane to dephosphorylate PIP_3, so acting to restrict the localisation of PIP_3.

PTEN is mostly associated with the dephosphorylation of PIP_3 to $PI(4,5)P_2$, and as such can regulate many cellular functions. One way in which $PI(4,5)P_2$ regulates cellular processes is by the recruitment of annexin2 which in turn binds and sequesters Cdc42 to the plasma membrane. Whilst at the plasma membrane, Cdc42 can bind to the Par polarity complex promoting apical polarity (Martin-Belmonte *et al*. 2007). The establishment of polarity is vital in many processes including the formation of lumen and cell motility (Martin-Belmonte *et al*. 2007). In addition to cell polarity, PTEN also has been shown to have a role in cellular senescence and regulation of tumour microenvironment (Song *et al* 2012).

1.3.6 PI3K and PTEN in cell polarisation and migration

Since the generation of PI3K inhibitors (mainly pan-PI3K inhibitors such as wortmannin and LY294002) many cellular processes have been found to involve PI3K activity including membrane ruffling and actin rearrangements (Wymann and Arcaro 1994; Kotani *et al.* 1994). Work in *Dictyostelium* cells has shown the importance of PI3K in cell migration. In these cells, class I PI3K was shown to be required for the formation of actin filaments necessary for the

extension of pseudopodia, however these cells were still able to migrate when PI3K was lost (Zhou *et al.* 1998). More recently, work showed that during *Dictyostelium* chemotaxis, PI3K translocates to the leading edge, interestingly, at the same time, PTEN localises to the rear of the cell in a reciprocal manner (Funamoto *et al*. 2001; Funamoto *et al.* 2002). The authors showed that this specific localisation of PI3K to the front of chemotaxing cells was required for the formation of pseudopods and that PTEN was required for cell polarisation. In cells where PTEN levels were reduced, polarisation was not established and chemotaxis impaired due to a negative regulation of PI3K signalling pathways, as such multiple pseudopodia were formed (Funamoto *et al.* 2002).

PI3K has also been identified as an important regulator of hemocyte migration towards a wound in *Drosophila* although it is not required for developmental migration (Wood *et al.* 2006). When the levels of PI3K are reduced (by overexpressing dominant negative PI3K or injection of a PI3K inhibitor), the hemocytes, although being morphologically similar to wild-type counterparts (in the formation of dynamic lamellipodia and filopodia), fail to chemotax towards wounds. This failure in migration is due to an inability to polarise the existing actin cytoskeleton in the desired direction (Wood *et al*. 2006). PI3K, in particular PI3Kp110γ, has also been shown to be vital for directional migration of zebrafish neutrophils towards a wound. When zebrafish were treated with a p110γ specific inhibitor (AS-605240), neutrophils failed to migrate in the desired direction due to a reduction of PIP_3 at the leading edge (Yoo *et al* 2010). The importance of PI3K in cell migration has also been shown in mouse studies where PDGFRα was mutated in such a way that it was incapable of binding to and activating PI3K. This PDGFR mutation resulted in a specific cell migration defect that resulted in spina bifida (Pickett *et al*. 2008).

Research in *Dictyostelium* and other systems implicate PI3K as an important regulator of cell migration and chemotaxis, although recent work in *Dictyostelium* has shown that cells can still migrate in the presence of PI3K inhibitors, or when all *pi3k* and *pten* genes are mutated. However, these cells do have reduced migration speed suggesting that PI3K and PIP_3 are still required for efficient migration (Loovers *et al.* 2006). Cells lacking expression of PI3K exhibit a reduction in both basal and stimulated levels of F-actin, resulting in a delay in the reorganisation of the actin cytoskeleton to retract the old pseudopod and generate a new pseudopod (Funamoto *et al.* 2001). This work is consistent with the hypothesis that PI3K is not required for sensing a chemotactic gradient but is required for proper polarisation and migration of *Dictyostelium* cells (Nisho *et al.* 2007). PI3K has also been linked with leading edge actin re-organisation in zebrafish neutrophils as PIP_3 localises to the front of newly forming protrusions, whilst it is lost from retracting pseudopods. Additionally, when PI3K levels are reduced, F-actin is disturbed at the rear of the cell suggesting that it plays a role in anteroposterior polarity (Yoo *et al*. 2010). These data implicate PI3K as a regulator of the

actin cytoskeleton during directed cell migration; however how PI3K acts on the actin cytoskeleton is not fully understood.

In some systems it appears that PI3K participates in a positive feedback loop during cell migration, with downstream effectors of PI3K able to further increase its activity (Weiner *et al*. 2002). This suggests that PI3K is part of a signal amplification system that helps ensure that robust cellular responses are generated, even in response to weak signals (Ma *et al.* 2004). A model of local excitation and global inhibition has been proposed in the generation of a feedback loop, amplifying PI3K at the desired site, whilst downregulating or inhibiting it throughout the rest of the cell (Ma *et al*. 2004). This could be a mechanism by which a cell can detect shallow gradients of chemoattractant, increasing the activation of PI3K at the front of the cell, whilst recruiting PTEN to the rear of the cell dephosphorylating PIP_3. This would result in the accumulation of PIP_3 observed at the front of migrating cells required for directional migration (Devreotes and Janetopoulos 2003).

One example of local excitation and global inhibition is in zebrafish neutrophils migrating towards a wound, where PI3K can activate the small GTPase Rac (via PIP_3), and Rac can feedback to further activate PI3K (Yoo *et al.* 2010). Yoo and colleagues showed that activation of Rac through PI3K resulted in an upregulation of PIP_3 at the leading edge of migrating neutrophils. They observed that the accumulation of PIP_3 upon chemoattractant stimulus was specifically mediated by Rac activity. The presence of a feedback loop between Rac and PI3K could explain contradicting reports as to which functions upstream of the other (Zheng *et al.* 1994; Innocenti *et al.* 2003) (Figure 10).

A feedback loop between F-actin assembly and PI3K has also been observed in neutrophils, with treatment with latrunculin (an inhibitor of actin polymerisation) resulting in a decrease in PIP_3 levels. Actin polymerisation can also translocate PI3K to the plasma membrane of chemotaxing *Dictyostelium* cells (Sasaki *et al*. 2004), further validating the presence of a feedback loop between actin and PI3K activation (Figure 10). Additionally, it has recently been shown that microtubules can also regulate PI3K (Yoo *et al*. 2012). Depolymerisation of microtubules in zebrafish neutrophils completely abolished leading edge PIP_3 localisation, however the cells were still able to migrate in a PI3K-independent, but Rac-dependent manner (Figure 10). However, these cells were unable to migrate directionally towards a wound, suggesting that microtubule disassembly might render the cell unable to detect attraction signals by PI3K and as such is not able to activate downstream actin regulating pathways (Yoo *et al* 2012).

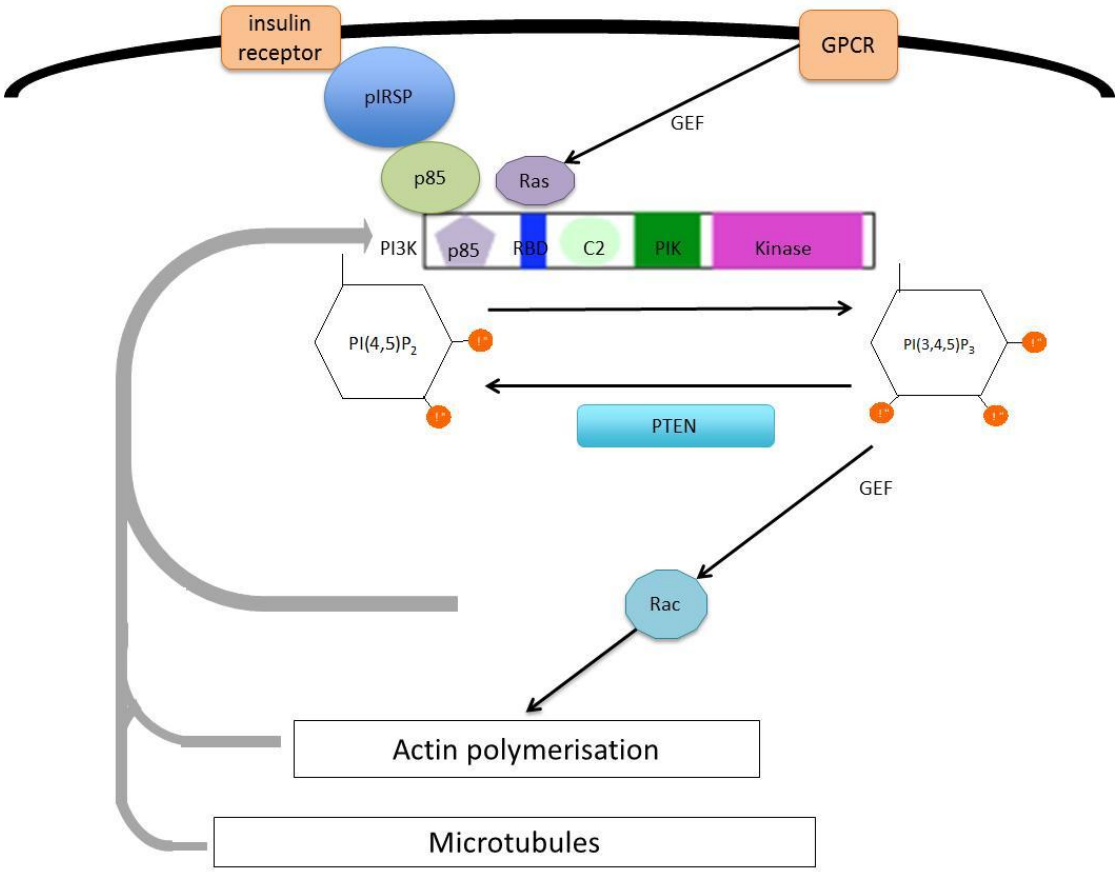

Figure 10. Positive feedback loops to amplify the PI3K signalling pathway. Extracellular stimuli induce the activation of the small GTPase Ras or the phosphorylation of IRSP, both resulting in binding to PI3K, either directly through the Ras-binding domain (RBD) or indirectly through the p85 subunit. This activates the downstream signalling pathways activating Rac, resulting in F-actin polymerisation. F-actin polymerisation translocates PI3K to the plasma membrane increasing the local PI3K activation. It is unclear how microtubules feedback onto PI3K, but it is known that they play a role in the recruitment of activation of PI3K (adapted from Charest and Firtel 2006).

1.3.7 PI3K and PTEN in development

Since the identification of PI3K and PTEN and the development of mutant alleles, it has been found that a variety of developmental processes involve these enzymes. PI3K plays an important role in regulating cell growth and size during development. During the development of the *Drosophila* wing imaginal disc, overexpression of PI3Kp110α (the sole class I PI3K in *Drosophila*) resulted in an overgrowth of tissue, and equally, when dominant negative PI3K was expressed, tissue growth was restricted (Leevers *et al*. 1996). Additionally, PTEN is also involved in cell growth and size. In *pten* mutants, *Drosophila* cells proliferate faster and are larger, resulting in an increased organ size (Gao *et al*. 2000). As these effects could be

supressed by mutations in *akt*, it is suspected that PTEN controls cell growth and size, through antagonizing the PI3K signalling pathway in *Drosophila* wing imaginal disc development (Gao *et al*. 2000). PI3K also plays a role in the lifespan in *C.elegans*, the gene *age-1*, which encodes a homologue of the PI3K catalytic subunit, is required for non-dauer development and normal senescence (non-dauer development is normal developmental progression where the dauer stage is a type of stasis) (Morris *et al* 1996). When *age-1* is lost, dauers form as opposed to progressing normally into non-dauer formation. It has thus been proposed that PI3K signalling, mediated by AGE-1 can control lifespan and the decision of the organism to progress out of dauer diapause.

The development of *Xenopus* embryos is also dependent on PI3K signalling, with increased expression of PI3K resulting in the development of double heads and dorsal axes, conversely when the activation of endogenous PI3K is inhibited, the embryos developed without apparent axial structures and a short tail (Peng *et al*. 2004). The work by this group suggested that PI3K is required for normal development of the dorsal axis. These data show the importance of PI3K in both cellular and organismal development.

1.3.8 PI3K and PTEN in epithelial organisation

Polarity is required for the proper development and function of an epithelium. In particular the formation of apical and basal domains is required to establish polarity and the localisation of proteins and lipids to the correct domains (Martin-Belmonte and Mostov 2008). Typically the apical domain of the epithelium is required to interact with the lumen whilst the basal membrane keeps contact with the extracellular matrix (reviewed by Gassama-Diagne and Payrastre 2009). PIP_3 is largely restricted to the basal domain, where it regulates the formation of actin protrusions that interact with the underlying basement membrane (Takahama *et al.* 2008). Re-localising PIP_3 to the apical surface of MDCK cells, results in a redistribution of basolateral proteins (such as syntaxin 4 and p58) and the formation of actin protrusions on the apical surface. This work indicates that PIP_3 is required to determine the basal domain of epithelial cells (Gassama-Diagne *et al.* 2006).

In MDCK cells, the apical domain is characterised by the accumulation of both $PI(4,5)P_2$ and PTEN. Apical accumulation of PTEN dephosphorylates PIP_3 to $PI(4,5)P_2$ in this domain, restricting PIP_3 to basal domain of the cells (Martin-Belmonte *et al.* 2007). At the apical surface, $PI(4,5)P_2$ interacts with annexin 2, which can then bind and recruit Cdc42 to the apical domain. Cdc42 in turn interacts with Par6 (part of the Par polarity complex). Histone-tagged $PI(4,5)P_2$ applied to the basolateral surface of MDCK cells resulted in ectopic implantation of $PI(4,5)P_2$ in this domain and the relocatisation of Cdc42 from the apical to the basal surface (Gassama-Diagne *et al.* 2006; Martin-Belmonte *et al.* 2007). Similarly, in the *Drosophila* embryonic epithelium and neuroblasts, PTEN is localised to the apical surface via

interaction with the scaffolding protein Baz (homologue of mammalian Par3), here PTEN dephosphorylates PIP_3 restricting it to the basal domain of cells and enriching the localisation of $PI(4,5)P_2$ at the apical domain (von Stein *et al.* 2005). However, in *Drosophila* photoreceptors, PIP_3 accumulates at the apical domain. One explanation for the difference between cell types is that there is a reduced level of PTEN at the apical domain of *Drosophila* photoreceptors, compared to MDCK cells, and as such apical PIP_3 dephosphorylation is reduced (Pinal *et al.* 2006).

1.3.9 PI3K and PTEN in wound healing

Given that PI3K and PTEN are important for cell polarisation and migration, it is unsurprising that they are also involved in wound healing. Work by Lai *et al*. in 2007 showed that PTEN is involved in epithelial wound healing of the lung. When an *in vitro* culture of lung epithelial cells was scratch wounded, inhibition of PTEN enhanced cell migration into the gap. A different study found that Akt is localised to wound edges in mice (Squarize et al 2010). Wounding of mice lacking epithelial *pten* displayed an increase in the rate of wound closure, due to an upregulation of the Akt/mTOR pathway at the wound edge, leading to an increase of proliferation. Additionally, in human and rat corneal monolayer scratch wound assays, PTEN was downregulated at the wound leading edge resulting in an increase in Akt activity. This upregulation of Akt led to an increased migration rate of wound edge cells, enhancing the speed of wound closure (Cao *et al*. 2011). Inhibition of PTEN also promoted wound healing in whole rat eyes, implicating PTEN in both *in vitro* and *in vivo* wound healing. These studies show that PTEN/PI3K signalling pathways are involved in wound healing, with a reduction in PTEN resulting in an increase of the PI3K/Akt signalling pathway.

1.3.10 PI3K and PTEN in cancer

All of the components of the PI3K signalling pathway are mutated or amplified in a range of cancers (reviewed by Yuan and Cantley 2008) with PTEN being one of the most frequently mutated tumour suppressors (Li *et al*. 1997). PTEN inactivation leads to the constitutive activation of the PI3K pathway and mutations of PTEN have been detected in 31% of glioblastoma cell lines, 100% of prostate cancers and 6% of breast cancer cell lines (Li *et al* 1997; Myers *et al.* 1998). Additionally PI3Kp110α is amplified in ovarian, cervical, head and neck cancers among others (Shayesteh *et* al. 1999; Ma *et al*. 2000; Samuels *et al*. 2004). Mutations of this gene in cancers results in either amplification or constitutive activation of PI3K and its downstream products (Campbell *et al*. 2004). Akt has also been shown to be amplified in multiple cancers, such as pancreatic, head and neck, with a mutation in its PH domain resulting in constitutive association with the plasma membrane (Bellacosa *et al*. 1995; reviewed by Engelman *et al*. 2006). This prolonged membrane association and activation of

Akt has been shown to transform cells in culture to cells with cancer-like characteristics (Carpten *et al*. 2007).

The vast amount of work that has been carried out on PI3K and PTEN over the past 3 decades implicates them as important regulators of the actin cytoskeleton in many different processes including development and wound healing. Additionally, given that they are implicated in a vast range of cancers, it is vital that further research is carried out to fully understand the roles these enzyme play during these events, to enable development of treatments and therapies.

1.4 Wound healing

The skin acts as a protective barrier, preventing exposure of the organism to infection, toxins and fluid loss. When this barrier is compromised, a clot is formed rapidly which acts as a temporary cover and also serves as a matrix over and through which cells can migrate during the repair process. Following this, inflammatory cells are recruited to the wound to kill invading pathogens and debris. Alongside the inflammatory phase, new tissue formation (including re-epithelialisation) occurs, during which wound edge epidermal cells migrate across the wound until they meet the opposing epidermal edge and fuse together, thus re-establishing the protective barrier (reviewed by Martin 1997). This process of re-epithelialisation is vital for restoring epithelial integrity and occurs in response to tissue damage in a wide range of epithelial tissues, including the gut, lung and cornea (Martin 1997; Bement *et al.*1993; Danjo and Gipson 1998; Lai *et al.* 2007; Cao *et al.* 2011). As this process appears to be conserved between tissues it is important that we understand the mechanisms and signalling pathways involved in re-epithelialisation.

1.4.1 Mechanisms of re-epithelialisation

The process by which cells move during re-epithelialisation varies between tissues and two different mechanisms by which wound edge cells migrate during re-epithelialisation have been observed; actin purse string closure and lamellipodial crawling (Martin and Lewis 1992; Wood *et al*. 2002). Actin purse string closure was first described by Martin and Lewis (1992), when they generated wounds in the chick embryo wing bud and observed the formation of an actin cable at the leading edge of the wound. They argued that the formation and contraction of this cable could provide the mechanical force required to drive wound closure (Martin and Lewis 1992). The actin cable is composed of actin and myosin filaments that are anchored to adjoining cells by E-cadherin at adherens junctions; this allows contractility to be obtained between neighbouring cells when filaments in individual cells contract (Brock *et al.* 1996; Danjo and Gipson 1998) (Figure 11). The actin cable is also present in other tissues during re-epithelialisation; for example, the actin cable has been observed in epithelial wounds in

Drosophila and mouse embryos, and also in eye corneal wounds in the adult mouse. In each case, disrupting the formation of the actin cable resulted in delayed or defective wound healing, indicating the importance of the cable (Danjo and Gipson 1998; McCluskey and Martin 1995; Wood *et al.* 2002). When the *Drosophila* epidermis is wounded, some cells are observed to be 'squeezed-out' from the leading edge contributing to the reduction of the wound area (Bement *et al.* 1993; Jacinto *et al.* 2001) (Figure 11.).

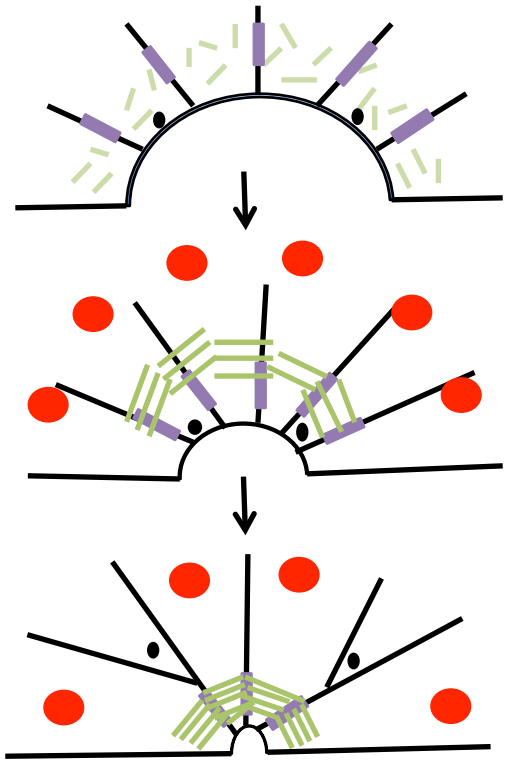

Figure 11. Schematic diagram illustrating how the contractile actin cable aids wound closure. The individual actin filaments (green bars) anchor to adherens junctions (purple bars). Contraction of the cable in each cell leads to a reduction of the wound area. As the wound area is reduced, some leading edge cells are squeezed out from the wound edge allowing the gap to constrict further. Black dots indicate cells that will leave the leading edge, red dots are nuclei. Adapted from Martin and Parkhurst. (2004)

Lamellipodial crawling rather than purse-string contraction appears to be the main mechanism of re-epithelialisation in adult mammalian skin and Drosophila larvae (Odland and Ross 1968; reviewed by Jacinto *et al.* 2001; Galko and Krasnow 2004). In this model of closure, large lamellipodia are formed at the leading edge of the migrating cell sheet that enables it to advance over the substratum. Actin cables and protrusions are often observed together (e.g. in the mouse cornea), suggesting that the two mechanisms can collaborate to close wounds (Danjo and Gipson 1998). In addition wound edge actin protrusions are important throughout wound closure and will be discussed in more detail below.

1.4.2 Signalling pathways in re-epithelialisation

In order to achieve re-epithelialisation, epithelial cells surrounding the wound have to undergo substantial changes in behaviour, including the re-organisation of the actin cytoskeleton to form an actin cable and/or actin protrusions. The signalling processes that regulate these changes are discussed below.

1.4.2.1 Rho family GTPases in re-epithelialisation

The GTPase Rho has been shown to be required for the formation of the actin cable during epithelial wound healing. In addition to the work in *Drosophila* (which will be discussed in section 1.4..3), the GTPases have also been shown to be required for re-epithelialisation in *Xenopus* embryos and in the mouse epidermis. Rho is vital for the formation of the actin cable during wound healing in the epithelium of *Xenopus* embryos. Within 12 seconds of wounding, Rho is recruited to the wound margin followed by the formation of an actin cable and accumulation of F-actin at cell junctions surrounding the wound. (Bement *et al.* 1999; Clark *et al*. 2009; Simon *et al.* 2012). The role of Rho in re-epithelialisation in mice is not well understood. Mouse embryonic fibroblasts lacking expression of RhoA or RhoB display a reduction in the rate of re-epithelialisation during *in vitro* scratch wound assays, however when wound healing was investigated *in vivo*, no delay in re-epithelialisation was observed. Wound healing in mice lacking expression of RhoC, has not been investigated. It is likely that the lack of a wound healing phenotype is as a result of redundancy between the Rho genes (Liu *et al*. 2001; Hakem *et al*. 2005; Jackson *et al*. 2011).

Cdc42 is required for the formation of actin protrusions during re-epithelialisation. In *Xenopus* embryos, Cdc42 was essential for the assembly of cortical actin during wound healing in early stage *Xenopus* embryos (Davidson *et al.* 2002). Overexpression of Cdc42 in *Xenopus* embryos resulted in a dramatic enhancement in the rate of wound healing, indicating a role for Cdc42-mediated protrusions in *Xenopus* re-epithelialisation (Davidson *et al.* 2002; Kofron *et al*. 2002; Yoshii *et al.* 2005). Additionally, during re-epithelialisation in later stages of *Xenopus* development, Cdc42 is activated at wound margins, followed by the accumulation of F-actin at cell junctions, demonstrating its role in wound healing throughout development (Clark *et al.* 2009; Simon *et al.* 2012). Cdc42 is also important during mammalian wound healing. Loss of Cdc42 from adult mouse epithelial cells resulted in impaired re-epithelialisation, due to a loss of F-actin cytoskeletal rearrangements required for efficient migration into the wound (Anttonen *et al*. 2012).

Rac is required for mouse epidermal wound healing, in particular for the migration of keratinocytes and fibroblasts into the wound. A delay in re-epithelialisation was observed when a dominant inhibitory mutant of Rac1 was expressed in either keratinocytes or

fibroblasts. *Rac* deficient cells in culture also displayed migration and adhesion defects, primarily as a result of reduced persistence of lamellipodia. This reduction of protrusion and adhesion also resulted in delayed healing in *in vitro* scratch wound assays (Tscharntke *et al.* 2007; Liu *et al.* 2009).

In addition to Rho GTPases, the small GTPase Ras is also required for *in vitro* wound repair. In cultured keratinocytes, activation of Ras results in the cells becoming more protrusive and forming larger lamellipodia. This effect of Ras on the cell morphology was independent of Erk activation and occurred as a consequence of PI3K-independent Rac activation. In scratch wound assays, keratinocytes with activated Ras closed the wounds quicker than wild-type controls, further demonstrating its role in wound healing (Tscharntke *et al.* 2005).

1.4.2.2 c-Jun NH_2-terminal Kinase in re-epithelialisation

c-Jun NH_2-terminal kinase (JNK) is a member of the evolutionary conserved sub family of mitogen activated protein kinases (MAPK), which is activated by cytokines and extracellular stress (reviewed by Weston and Davis 2002). JNK has been shown to play a key role in re-epithelialisation in a variety of systems (Rämet *et al.* 2002; Bosch *et al.* 2005; Okada *et al*. 2009). Wounding of the adult mouse cornea resulted in JNK activation at the wound edge in wild type mice, and reducing the levels of JNK activity (using a JNK specific inhibitor) resulted in impaired wound re-epithelialisation (Okada *et al.* 2009). The authors showed that during healing of the corneal wound, no proliferation occurred, indicating that JNK signalling is required for cell migration rather than proliferation.

1.4.3 *Drosophila* as a model of wound healing

Drosophila are genetically tractable and amenable to live imaging, and as such they are ideal to study the process of wound healing directly. Wounding can be carried out at all stages of *Drosophila* development, however only embryonic and larval wound healing will be discussed here.

1.4.3.1 Embryonic wound healing

One benefit of studying wound healing in *Drosophila* embryos is that the wounds heal quickly, with moderately sized wounds (≈ 200 μm in area) closing within 2 hours, allowing the whole process of wound healing to be observed in detail. Recent studies using laser pulses to wound the embryonic epidermis demonstrated that the wounds close using both actin purse string closure and lamellipodial crawling (Wood *et al*. 2002). In these wounds, both Rho and Cdc42 are vital for the formation of these crucial structures required for efficient re-epithelialisation.

Rho is vital for the formation of the actin cable during *Drosophila* embryonic wound healing, and when lost, wound edge cells fail to form a continuous actin cable and as such there was little, if any, contraction of leading edge cells, however, they are able to make and extend filopodia and lamellipodia (Wood *et al*. 2002). Although wounds in *rho* mutant embryos undergo a delay in initiating re-epithelialisation, once wound edge cells have begun moving, they do so at a rate similar to controls (Ridley and Hall, 1992; Wood *et al.* 2002). In these embryos, it appears that wound edge filopodia and lamellipodia are able to interact with and 'tug' on each other, providing sufficient driving force required to close the wound.

It has been demonstrated that actin protrusions assist wound closure throughout the whole process of re-epithelialisation (wounding of embryos lacking Cdc42, which are unable to generate actin protrusions, resulted in a delay in re-epithelialisation, although an actin cable was still present (Abreu-Blanco *et al*. 2012)). Additionally, actin protrusions are vital for the final phase of re-epithelialisation. Wood *et al*. (2002) wounded embryos with reduced levels of Cdc42 and observed a failure of wounds to completely heal, due to a lack of actin protrusions. Surprisingly, Rac does not appear to be required for *Drosophila* embryonic epidermal wound healing. When Wood *et al.* wounded *rac* mutant embryos; no observable difference was seen in the rate of wound closure (Wood *et al*. 2002).

Additionally, EGFR is a receptor tyrosine kinase, which is activated upon *Drosophila* embryonic wounding. EGFR activation leads to ERK signalling and has been shown to be required for effective wound healing (Geiger *et al*. 2011). However, in this study it was not shown how EGFR and ERK play a role in re-epithelialisation.

Due to the genetic tractability of *Drosophila*, genetic screens can be carried out to identify new regulators in the process of epithelial repair (Campos *et al.* 2010).

1.4.3.2 Larval wound healing

Larval epidermal wound healing differs slightly from that of embryonic wound healing in that no actin cable has been detected (Galko and Krasnow 2004). When the epidermis of the *Drosophila* larvae is wounded, cells at the wound edge maintained the regular shape observed directly before wounding. After 4 hours, some cells directly adjacent to the wound elongated towards the gap. By 8 hours, migrating cells covered most of the wound gap, and cells with multiple nuclei were observed. By 24 hours the wounds were completely closed, with cells still displaying an irregular cell shape and some containing 2-12 nuclei (Lesch *et al.* 2010).

Rac1 is required furing *Drosophila* larval epithelial wound healing, where it is required for the polarisation of wound edge cells (Baek *et al*. 2010). Interestingly, the authors also showed that during larval epithelial wound healing Rac was upstream of JNK in the assembly of actin

during larval wound healing (Baek *et al.* 2010). JNK is activated at wound edges and when its activity is reduced, wound healing is significantly delayed due to a failure of wound edge cells to migrate (Galko and Krasnow 2004). When the role of JNK was further examined by wounding the *Drosophila* wing disc with reduced levels of *basket* (*Drosophila* JNK) a delay in re-epithelialisation was observed due to a reduction in both actin cable and filopodia formation (Bosch *et al*. 2005).

Larvae are ideal for wound healing studies as large-scale genetic screens can be carried out (Lesch *et al*. 2010). A screen by Lesch *et al*. identified a set of genes required for larval wound healing that differed to those for embryonic wound healing. One major difference is that Rho is dispensable for larval wound healing, which is perhaps not surprising as re-epithelialisation in larva does not depend on the formation of an actin cable.

1.4.4 Differences between embryonic and adult re-epithelialisation

Although the role of Cdc42 appears to be conserved between embryonic and adult wound healing, the role of Rho and Rac in wound healing appears to be a bit more complicated. Rho does not appear to be required for re-epithelialisation in adult tissues. Despite mouse *rhoA* mutant keratinocytes displaying a reduction in migration *in vitro*, *in vivo* keratinocyte-specific knockout of *rhoA* did not result in a delay in re-epithelialisation (Jackson *et al*. 2011). This is consistent in *Drosophila* larval wound healing where a continuous actin cable is not formed and loss of Rho1 (by RNAi knockdown) did not result in a wound healing defect (Brock *et al.* 2012). However, the lack of observable phenotype during adult wound healing in *rhoA* deficient mice is likely due to redundancy with other Rho genes.

Whilst Rac is vital for successful re-epithelialisation in both *Drosophila* larval and mouse adult epidermal wounds (Tschartkne *et al*. 2007; Baek *et al* 2010), it appears that Rac is not required for wound healing in *Drosophila* embryos (Wood *et al* 2002). Epithelial wounds in *rac* mutant embryos, displayed no obvious defects in re-epithelialisation compared to controls (Wood *et al*. 2002). It appears, at least in *Drosophila*, that the importance of Rho and Rac in wound healing may be stage dependent, with Rho activity required for the formation of an actin cable during embryonic wound healing, but in larval stages, loss of Rho has no significant effect on wound healing (Wood *et al* 2002; Lesch *et al*. 2010), whilst Rac is dispensable for embryonic wound healing, but required for larval re-epithelialisation (Wood *et al.* 2002; Baek *et al.* 2010).

1.4.5 Developmental parallels with wound healing

During the course of embryonic development a variety of morphogenetic events occur that involve closure of gaps in epithelial sheets. Examples include *Drosophila* DC, mouse eyelid

fusion and neural tube closure (Macdonald *et al.* 1989; Jacinto *et al.* 2000; Harden 2002; Zenz *et al.* 2003). Research over recent years has revealed that these events frequently have strong mechanistic parallels with epithelial wound healing (Figure 12) (Martin and Parkhurst 2004; Wood *et al.* 2002). As these events are often easier to observe and manipulate than wounds, they make useful models for studying wound healing. The best studied developmental model of wound healing is *Drosophila* DC, which will be discussed in detail below.

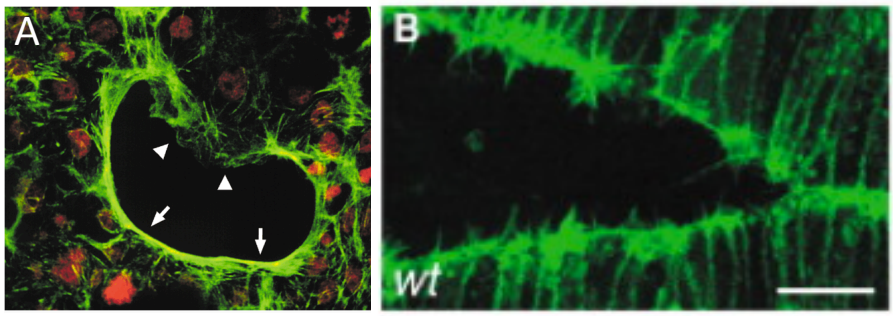

Figure 12. Mechanistic parallels between wound healing and DC. A) Shows the presence of both an actin cable (arrows) and actin protrusions (arrow heads) in a wound, and B) demonstrates the presence of both an actin cable and actin protrusions during the process of dorsal closure (Jacinto *et al.* 2001; Jacinto *et al.* 2002b). Scale bar in B represents 5 μm. Copyright obtained from Elsevier and NPG

1.4.5.1 *Drosophila* dorsal closure

DC is a morphogenetic event that occurs halfway through *Drosophila* embryogenesis. Prior to DC a hole on the dorsal side of the embryo is exposed as a result of germband retraction and must be closed in order for embryogenesis to proceed. DC is the process by which this hole is closed. The dorsal hole is closed by opposing epithelial edges sweeping over the amnioserosa (an extraembryonic epithelium that covers the hole), then fusing with one another at the dorsal midline to form a continuous epithelium (Young *et al.* 1993). Both the amnioserosa and the epithelium contribute to DC, and it involves a series of events that occur in order for it to proceed, which will be discussed in more detail below (Figure 13).

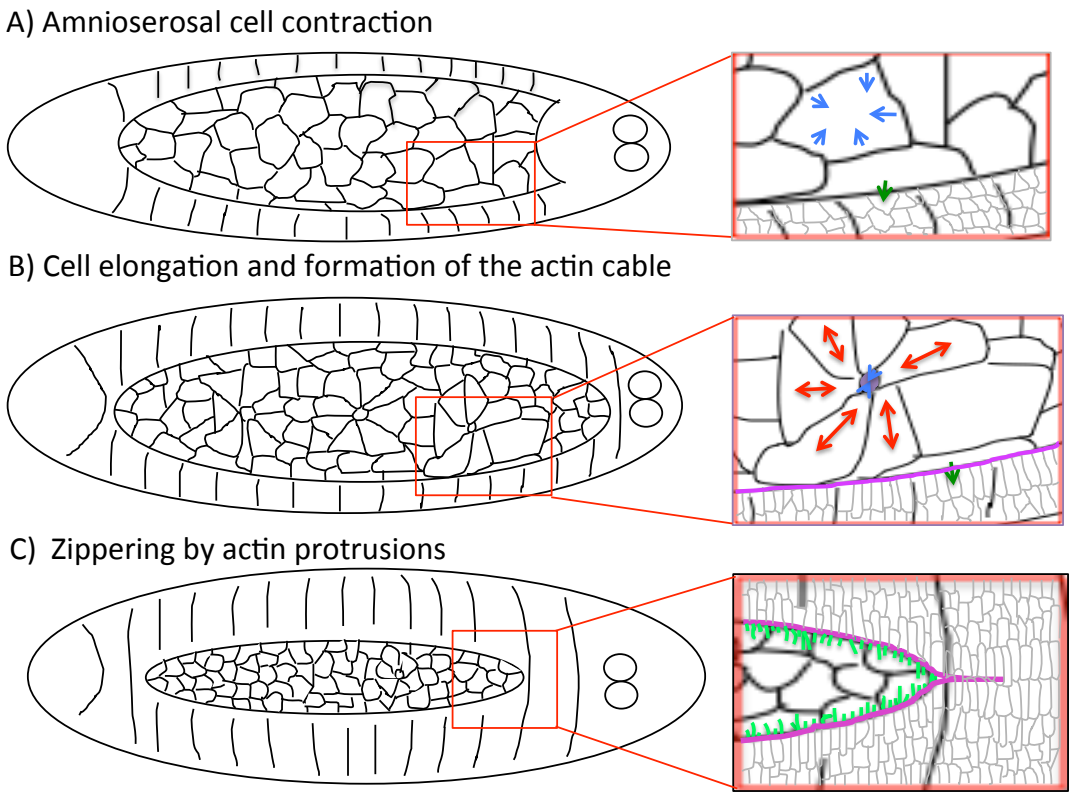

Figure 13. Schematic showing the mechanisms of DC. A) amnioserosa cell contraction - cells undergo pulsatile contractions (blue arrows), but the epithelial leading edge cells have yet to elongate (green arrow). B) Elongation of leading edge cell (green arrow) and formation of the actin cable (purple) – this takes place alongside amnioserosal contraction (blue and red arrows), with a subset being extruded from the extraembryonic tissue. The leading edge cells elongate in the direction of movement, with a contractile actin cable forming along the dorsal-most epithelial edge (purple cable). C) Zippering – filopodia (green lines extending away from the leading edge) at the canthi interdigitate to fuse together the two epithelial edges.

1.4.5.2 Elongation of leading edge cells

Prior to DC, JNK is active in both the amnioserosa and the epithelial leading edge (henceforth 'leading edge'). However, before leading edge migration commences, JNK is downregulated in the amnioserosa, but remains active in the leading edge, suggesting that this change in levels may act to signal the start of DC (Reed *et al*. 2001; Stronach and Perrimon 2002). At the onset of DC, JNK restricts the localisation of Decapentapleigic (Dpp) signalling (*Drosophila* homologue of BMP, and is a morphogen required for the pattern formation during embryonic and larval stages of development (Posakony *et al*. 1990)) to the leading edge region. This restriction of Dpp triggers cell elongation along the dorsoventral axis adding to the dorsalward movement of the leading edge, however how Dpp controls this elongation is not known

(Zeitlinger *et al*. 1997; reviewed by Martin and Wood 2002). This role of localised JNK signalling parallels wound healing in both *Drosophila* and mice, where JNK is shown to be upregulated in wound leading edge cells and it is required for cell migration into the wound (Galko and Krasnow 2004; Bosch *et al*. 2005; Okada *et al.* 2009).

1.4.5.3 Amnioserosal contraction

Amnioserosal cells undergo progressive changes as DC proceeds, apically constricting and shifting from a squamous to a columnar shape (Rugendorff *et al.* 1994). This reduces the surface area occupied by the amnioserosa and, as the epithelial leading edges are attached to the edge of the amnioserosa, this pulls the two epithelial edges towards one another. Harden *et al*. (2002) showed that Rac1 is required for the columnar elongation of amnioserosal cells, by regulating the formation of the apical actomyosin contractile apparatus, required for apical constriction. This contractile ring is restricted to the apical domain by the polarity protein Crumbs (Harden *et al*. 2002). Additionally, the PAR polarity complex also plays a role in regulating amnioserosa cell contraction, with myosin and the PAR complex forming an associated apical network (David *et al*. 2010). Repeated assembly and disassembly of apical actin networks cause amnioserosa cells to undergo pulsatile contractions, with each component of the PAR complex regulating distinct phases of contraction: Baz (Par3) controls the duration of the pulse, whilst Par6/aPKC control the relaxation times between pulses (David *et al*. 2010).

Although the apical constriction is the main cause of amnioserosa area reduction, cell delamination from the tissue also makes a contribution. As cells drop out of the amnioserosa, they appear to 'pull' the adjoining cells inwards to fill the hole left behind (Kiehart *et al.* 2000). However, an alternative explanation is that the surrounding cells elongate in the direction of the delaminating cell, and actively 'push' the delaminating cell out (Toyama *et al*. 2008; Solon *et al*. 2009). It has not been determined what causes cells to delaminate from the amnioserosa, however in other systems (*Drosophila* pupa, human and zebrafish epidermis), cell delamination from an epithelium occurs to maintain homeostasis of the cell layer in periods of growth (Marinari *et al.* 2012; Eisenhoffer *et al.* 2012). It is possible that during DC, amnioserosal cells delaminate due to overcrowding as a result of the advancing epithelial edges.

1.4.5.4 Actin cable contraction

At the boundary between the leading edge and the amnioserosa an actin cable is formed, which contracts throughout the process of DC. This contraction of the actin cable maintains tension along the leading edge and acts in a ratchet manner to sustain the reduction of the dorsal hole achieved by the amnioserosa (Jacinto *et al*. 2002b; Solon *et al*. 2009). One

regulator of actin cable formation is the homophilic adhesion molecule, Echinoid. At the onset of DC, Echinoid is lost from amnioserosal cells and this leads to the loss of Echinoid from the leading edge of dorsal most epidermal cells (DME), resulting in a planar polarised distribution of Echinoid in DME cells. This polarised distribution of Echinoid is required for the leading edge accumulation of actin regulators that drive the formation of the actin cable (such as F-actin, myosin and coracle) (Laplante and Nilson 2011). At the onset of DC Baz also redistributes away from the leading edge in DC, and although Baz can directly interact with Echinoid via the PDZ-binding motif (Wei *et al.* 2005), this interaction is not responsible for the redistribution observed during DC. In embryos lacking expression of Echinoid, re-expression of Echinoid lacking the Baz binding domain is sufficient to rescue the mutant defects observed, suggesting that the redistribution of Echinoid is not directly responsible for the distribution of Baz observed during DC (Laplante and Nilson. 2011). However, this restricted localisation of Echinoid and Baz allows accumulation of actin regulators to the front of the cell, to form the mechanical structures required for DC.

Rho1 is also required for the formation of the actin cable, and in embryos lacking zygotic expression of Rho1, the cable (formed under the control of maternally contributed Rho), is disassembled part way through DC. Although the movement of the leading edge does not fail, DC completes in a disorganised manner, due to loss of tension at the leading edge. Additionally, an increase in filopodial and lamellipodial protrusions are observed, which leads to improper alignment and puckering of the dorsal hole (Harden *et al.* 1999; Bloor and Kiehart 2002; Jacinto *et al*. 2002b). Jacinto *et al.* (2002b) proposed that during DC, the actin cable is also required to restrict excessive movement from the leading edge cells, ensuring that proper alignment and controlled epithelial fusion is achieved. Genetically, *rho*1 interacts with *zipper* (non-muscle myosin-II heavy chain) (Halsell et al 2000), and Rho kinases promote phosphorylation of the regulatory light chain of myosin (MRLC) (Kaneko-Kawano *et al.* 2012). The requirement for a Rho-mediated actin cable in DC is consistent with the known role of Rho in *Drosophila* embryonic wound healing, which is also dependent on Rho GTPase signalling (Wood *et al*. 2002). Additionally, Rho activity increases during *Xenopus* embryonic wound healing (Clark *et al.* 2009), and in both cases, loss of Rho results in a loss of actin cable. However, wound healing does not fail, instead, re-epithelialisation occurs through an increased amount of actin protrusions, which are able to 'pull' the wound closed.

Additionally, JNK is able to regulate the formation of the actin cable during DC, with embryos lacking JNK displaying a less prominent actin cable than controls. The authors proposed that this reduction in actin cable was due to the ability of JNK to increase expression of *chickadee* (*Drosophila* profilin) and as such, reduced JNK resulted in reduced actin polymerisation (Jasper *et al.* 2001). The role of JNK as a regulator of actin cable formation during DC is consistent with its role in wound healing in the *Drosophila* wing disc, where a reduction in JNK activity resulted in the loss of cable formation during re-epithelialisation (Bosch *et al.* 2005).

1.4.5.5 Actin protrusions

Filopodial actin protrusions are crucial for fusion of the two epithelial edges during DC. This occurs once the epithelial edges at either end of the dorsal hole are close enough so that filopodia from one leading edge can extend and touch the opposing edge (Jacinto *et al.* 2000). The points at either end of the dorsal hole where the two leading edges meet are known as the canthi. The two opposing edges are knitted together by filopodia at the canthi in a process resembling the closing of a zip, and hence has been given the name zippering. In addition to zippering together the epithelial edges, the leading edge filopodia also play an important role in ensuring correct alignment between the two leading edges by recognising 'matching' cells in the opposing leading edge. The molecular mechanism by which filopodia recognise matching cells is currently unknown (Millard and Martin 2008). As mechanisms of DC closely resemble epithelial fusion events seen in higher vertebrates, it is likely that the final 'knitting together' mechanism seen during fusion is highly conserved (reviewed by Jacinto *et al*. 2002a; Pai *et al*. 2012). In a similar manner to DC, filopodia are also important throughout wound healing, in particular during the final re-sealing phase, where filopodia are required to knit together the epithelial edges, completing the process of re-epithelialisation

The Rho family GTPases Cdc42 and Rac both play a role in regulating actin protrusion formation during DC. *rac1* mutant embryos display a reduction in both the actin cable and actin protrusions at the DC leading edge, resulting in inefficient zippering and an elongation of the dorsal hole (Harden *et al*. 1995; Woolner *et al.* 2005). An elongated dorsal hole is observed when the rate of zippering is reduced, often due to a reduction in the number of leading edge filopodia. Elongation of the dorsal hole occurs when contraction of the amnioserosa proceeds at the normal rate, but zippering is slower than normal. Thus the epithelial edges are drawn towards one another at a rate quicker than the remaining protrusions can zipper them together, causing the dorsal hole to appear longer and flatter than normal (Woolner *et al.* 2005). Consistent with the role of Rac in DC, *mbc* mutant embryos also display DC defects, including puckering along the dorsal midline, an elongated dorsal hole and large holes on the dorsal surface which is as a result of failure of the epithelial leading edges to fuse to one another (Erickson *et al.* 1997). During DC, DME cells elongate along the dorso-ventral axis, however, in embryos lacking expression of MBC, these leading edge cells fail to elongate and become rounded. Additionally, the levels of F-actin are reduced throughout embryos lacking expression of MBC, which would also contribute to the DC defects observed (Erickson *et al*. 1997).

The slow zippering rate observed in embryos with reduced numbers of protrusions is consistent with wound healing studies. When wounds were generated in mice with keratinocyte-specific knockdown of Rac1, re-epithelialisation was delayed due to a reduction in actin protrusions in wound edge cells (Tscharntke *et al.* 2007; Liu *et al.* 2009). However,

contrary to this, loss of Rac (and therefore lamellipodia) does not have a significant effect in *Drosophila* embryonic wound healing, presumably due to the ability of Rho-mediated actin cable and Cdc42-mediated protrusions to promote re-epithelialisation (Wood *et al*. 2002).

During DC, Rac can also act upstream of JNK. In *rac* mutant embryos, levels of DPP are significantly reduced, and Dfos fails to translocate to the nucleus, indicating a role for Rac in the regulation of JNK (Woolner *et al*. 2005). Additionally, embryos mutant for *hemipterous* (a JNK kinase) are unable to make filopodia and as a result undergo defective DC and segmental mis-alignment, in a similar manner to *rac* mutants (Jacinto *et al*. 2000). Interestingly, when wound healing itself was studied in *Drosophila* adults lacking expression of puckered (a downstream target of the JNK pathway), re-epithelialisation was delayed due to a lack of cytoplasmic protrusions, indicating a similar role for JNK in actin protrusion formation during re-epithelialisation (Rämet *et al.* 2002; reviewed by Martin and Parkhurst 2004). Cdc42 is also a regulator of filopodia formation during DC. In cells expressing a dominant negative form of Cdc42 a reduction in the number of filopodia is observed and the dorsal hole closes incompletely with gaps along the dorsal midline (Harden *et al.* 1999; Jacinto *et al*. 2000). A similar trend can be observed during re-epithelialisation, however, loss of Cdc42 from the epithelium of a *Drosophila* embryo, resulted in a complete failure of wound closure, due to a lack of protrusions required for the final re-sealing of the wound (Wood *et al*. 2002).

The anti-capping protein Ena has also been shown to promote filopodia formation during DC. Embryos lacking Ena zipper slowly, have fewer and shorter filopodia and display an elongated dorsal hole. When levels of Ena are increased, filopodia number and length are increased suggesting that Ena promotes both initiation and elongation of filopodia during DC (Gates *et al*. 2007). Although the role of Ena has not been shown directly in wound healing, it is likely that it plays a role as it is such a critical regulator of filopodial formation. In addition to actin being crucially important during DC, microtubules also required in the process of zippering (Lodish *et al.* 2000; Jankovics *et al.* 2006). When microtubules are depolymerised during DC, zippering is abolished (Jankovics *et al*. 2006). The role played by microtubules in zippering is currently not understood, although notably the number of leading edge filopodia is reduced when microtubules are depolymerised, suggesting they are able to regulate actin dynamics.

Although developmental events such as DC have been shown to be good models of wound healing, there are differences that must be taken into consideration; the process of wound healing is initiated by response to tissue damage, whereas DC is initiated by developmental cues. Additionally, inflammation and fibrosis cannot be addressed by these systems, which is why additional wound healing studies are important to verify any results.

1.5 Project aims

During both DC and epithelial wound healing, actin protrusions have been shown to be vital for effective epithelial closure (Jacinto *et al.* 2000; Wood *et al* 2002; Millard and Martin 2008; Abreu-Blanco *et al*. 2012). However, how these actin protrusions are regulated is not fully understood. We aim to determine upstream regulators of actin protrusion formation during DC and wound healing (Wood *et al*. 2002). During single cell migration, both in *Dictyostelium* and in zebrafish neutrophils, the phosphoinositide PIP_3 is important in identifying the front of the cell and regulating the formation of actin protrusions (Funamoto *et al.* 2001; Iijima and Devreotes 2002; Yoo *et al.* 2010). We therefore sought to determine if PIP_3 is also important for the regulation of cell polarity and actin protrusion formation during DC and wound healing. Additionally, we aimed to elucidate the downstream effectors of PIP_3 during these processes. We also investigated the cellular distribution of phosphoinositides during DC and wound healing and the mechanisms regulating their distribution. Finally, we also sought to determine whether phosphoinositide signalling plays a role in the extrusion of cells from epithelial sheets. These aims were addressed primarily using genetic and imaging approaches.

2. Materials and Methods

The following chapter outlines the materials and methods used throughout this project. All recipes are detailed in Appendix 1.

2.1 Genomic DNA extraction: Overnight egg lays from flies with the desired genotype were dechorionated by washing for 2 minutes with 50% v/v bleach solution (Fischer Scientific ♯S/5040/PB17). The embryos were collected into a sieve and washed thoroughly with de-ionised water. Once washed, the embryos were transferred to a clean apple juice plate and selected based on their genotype (e.g. by fluorescence selecting against GFP balancers) and stage. The stage of these embryos was not vital, but stage 16 or older embryos were preferred due increased amounts of genomic DNA present. 5 embryos were placed in a 1.5 ml microcentrifuge tube with 100 µl buffer A (100 M Tris 7.5, 100 mM EDTA, 100 mM NaCl, 0.5% SDS) and homogenised using a sterile plastic pestle. The homogenate was covered and incubated at 65^{O}C for 15 minutes, then placed in a microcentrifuge tube and centrifuged briefly, to pull down any condensation that may have collected on the lid of the tube during incubation. 100 µl 3M sodium acetate was added, mixed, incubated on ice for 10 minutes, and then centrifuged at 16000 x g for 10 minutes. From this, 150 µl of supernatant was transferred to new tubes where 90 µl of ice-cold isopropanol (Sigma-Aldrich ♯ I9030) was added, mixed and incubated at room temperature for 5 minutes to allow the DNA to precipitate. The tubes were then centrifuged for 15 minutes at 16000 x g, the supernatant removed and the tubes inverted onto a towel briefly. After a brief inversion, the pellet was washed with 200 µl of -20^{O}C 70% v/v ethanol followed by centrifuging for 10 minutes at 16000 x g, after which the resulting supernatant was removed. The tubes were inverted onto a towel and left to air-dry. Once dry, 50 µl TE (10mM Tris 7.5, 1mM EDTA 8.0) was added to the microcentrifuge tubes, mixed and then the tubes put at 65^{o}C on a heat block for 15-20 minutes to re-suspend the DNA. A final mix of the solution and then a quick spin was carried out to pull down the solution into the bottom of the tube. The DNA obtained from this extraction was stored at -20^{O}C until use.

2.2 PCR to amplify selected genes: A PCR reaction was carried out using 2 µl genomic DNA template, 1 µM forward primer, 1 µM reverse primer, 10 x appropriate reaction buffer (New England Biolabs (NEB) Thermopol buffer or Roche Applied Science high fidelity buffer), 0.2 µl taq (NEB Taq DNA Polymerase or Roche Applied Science), 25 µm dNTPs, (of a 25 mM stock) 50 mM $MgCl_2$ and water to make up to 20 µl. The PCR reaction cycle set up is shown in Figure 14. The high fidelity buffer and Taq polymerase were used when amplifying DNA for the generation of transgenics to increase the accuracy of amplification.

The final PCR product was run on a 1-2% agarose (w/v) gel (depending on product size) with 1:10000 safe-view (NBS Biologicals cat ♯ NBS SV1) for 25 minutes at 100mv and viewed using a UV gel dock (Labnet international)

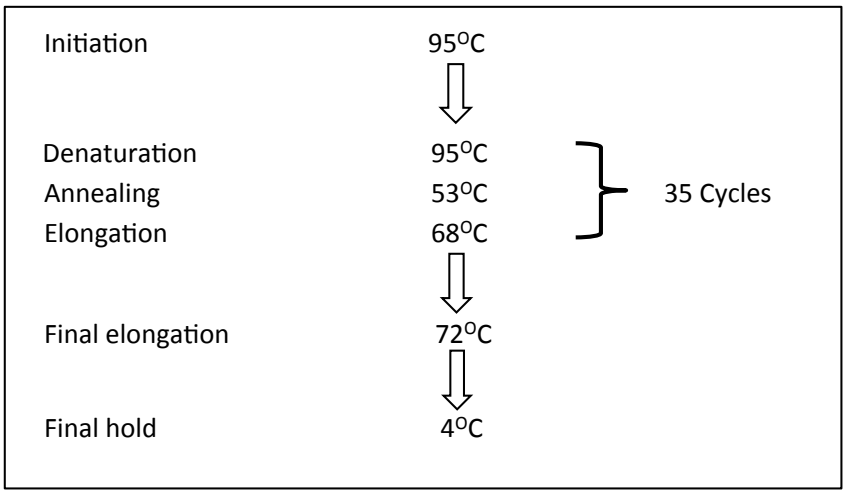

Figure 14. An outline of the PCR cycle used to amplify each of the *Drosophila rac* genes.

The primers used throughout this project are described in Table 1.

Primer	Forward/Reverse	Sequence (5'-3')
Rac1	F	GCT-ACA-CGA-CCA-ATG-CCT-TT
Rac1	R	CCA-GTT-TCT-TGT-CCC-TCA-GC
Rac2	F	AGG-CCA-TCA-AGT-GTG-TTG-TT
Rac2	R	CTC-AGG-CGA-TCG-TAG-TCC-TC
Mtl	F	GCT-ATC-CTA-CCC-GCA-GAC-AG
Mtl	R	GCG-GAG-CAC-TCC-ATG-TAT-TT
MBC	F	CGT-CTA-GAC-TAT-AAT-TTC-GAC-CGC-TGC-TC
MBC	R	CAG-CGG-CCG-CTA-TGA-GTG-TGT-GGA-GCG-AC
GPH	F	GG-GGT-ACC-ATG-GTG-AGC-AAG-GGC-GAG-G
GPH	R	TTT-TCT-AGA-TTA-ACT-CTT-GCT-GAG-TGC

Table 1. Primers used throughout the project. Primers used for both amplification of gene product and cloning of MBC and GPH, and for determining the presence or absence of the *rac* genes.

2.3 Cloning of PCR products: PCR products were purified using the Qiaquick PCR purification microcentrifuge kit (Qiagen cat ♯ 28104) following the manufacturer's protocol. Purified PCR product were then cloned into pGEM-T Easy following the manufacturer's protocol (Cat♯ A1360, Promega UK Ltd). Ligations were incubated at room temperature for 30 minutes. The pGEM-T easy vector is shown in Figure 15.

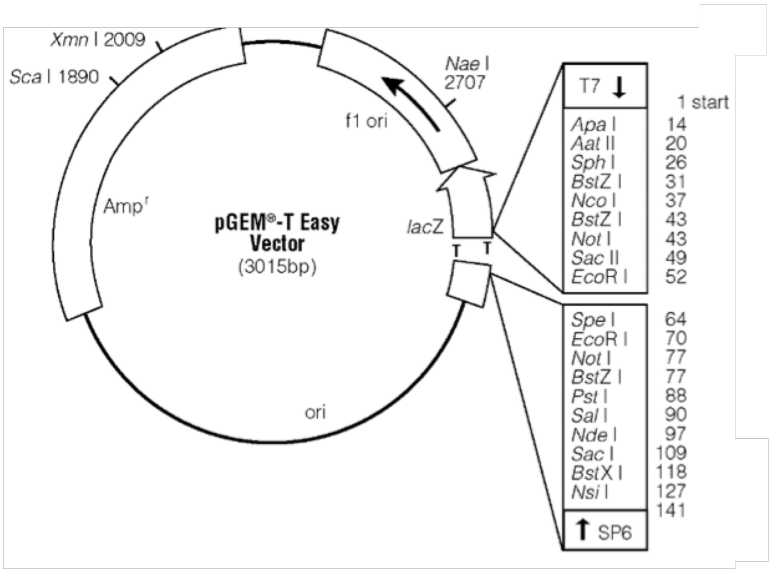

Figure 15. pGEM-T easy vector map showing the restriction sites. Purified PCR was ligated into vector. Map taken from Promega (2009)

Ligations were transformed into competent cells (NEB), by adding 3 µl ligation to 50 µl competent cells, gently mixing and standing on ice for 30 minutes. The reaction was then heat shocked for 30 seconds at 42^{O}C and then immediately returned to the ice for a further 2 minutes. 300 µl Super Optimal Broth (SOC, Invitrogen cat ♯ 46-0821) medium was added to the tubes, which were then incubated for 1 hour at 37^{O}C on a shaker. All 300 µl of the transformation was placed onto a Lysogeny Broth Agar/Isopropyl-Beta-D-Thiogalactoside (LBA/IPTG) plate and incubated at 37^{o}C overnight. LBA/IPTG plates were treated with 40 µl of 40 mg/ml X-gal (Bioline) prior to plating. Insertion of the PCR product was determined by blue/white selection (white colonies contained the insertion), after the overnight incubation.

Four white cultures from each transformation were picked and individually grown in 3 ml Lysogeny broth (LB) medium supplemented with 5 mg/ml ampicillin. The tubes were incubated overnight at 37^{o}C, shaking at 200rpm. Purification of the plasmid DNA from the bacterial cultures was carried out using QIAprep spin miniprep kit (Qiagen) according to manufacturer's protocol. Once purified, sample DNA concentration was then determined using a NanoDrop spectrophotometer (NanoDrop Technologies, ND-1000). The purified DNA was digested with *Eco* RI to confirm that the PCR product was present in the plasmid. The following reaction (Table 2) was incubated at 37^{o}C for 1 hour before running on a 2% (w/v) agarose gel (with a final concentration of 0.5 µg/ml ethidium bromide) at 100 volts for 20 minutes. The gel was visualised using a UV gel dock.

Restriction digest reactions (volumes in µl per reaction)	
Plasmid	3
EcoR1	0.5
10x Buffer H	2
H_2O	14.5

Table 2. Restriction digest reactions. Table shows the volumes required for a 20 µl restriction digest using EcoR1.

DNA samples for sequencing were prepared as follows: 200 ng template (as determined by the NanoDrop Spectrophotometer measurement), 4 pmol T7 primers in 10 µl of H_2O. The University of Manchester DNA Sequencing Facility performed the sequencing.

2.4 Fly stocks: All fly stocks used during this project were kept in vials containing food supplemented with yeast powder (produced by the Manchester University Preparation Stores). Stocks were maintained at 18^{O}C with flies transferred to new food vials every 2 weeks (a total of 2 tubes per fly line). Stocks that were either in regular use or were of reduced health were maintained at 25^{O}C with flies being transferred to new vials every 7 days.

2.4.1 Fly stocks used: w^{1118} flies were used as controls for all experiments. The following transgenes were used; ubiquitous GPH (tGPH – GFP-tagged grp1-PH domain under the control of the tubulin promoter, binds specifically to PIP_3) (Britton *et al*. 2002), ubiquitous GFP-moesin (cGMA) (Kiehart *et al.* 2000), ubiquitous GFP-E-Cadherin (Oda and Tsukita 1999) UAS-GFP-Moesin (UAS-GMA) (Dutta *et al.* 2002), UAS-m-Cherry-Moesin (Millard and Martin 2008), UAS-PTEN3 (Goberdhan *et al.* 1999), UAS-PTEN2 (Huang *et al.* 1999), UAS-GFP-PTEN2, UAS-GFP-PTEN3 (Pinal *et al.* 2006), UAS-m-Cherry-Baz (McGill *et al.* 2009), UAS-CA-Ras1 (Karim and Rubin 1998), UAS-CA-PI3K (Leevers *et al.* 1996), UAS-Rac1-wt (Luo *et al.* 1994), UAS-Alpha-Catenin (Oda and Tsukita 1999), UAS-Echinoid (Laplante and Nilson 2011). To express transgenes ubiquitously throughout the embryo *TubP*-Gal4 (Lee and Luo 1999) was used, *engrailed*-Gal4 was used to drive expression of transgenes in epidermal stripes (Brand and Perrimon 1993), *332.3*-Gal4 (Bloomington ♯ 5398; Wodarz *et al*. 1995) was used to drive transgene expression in the amnioserosa and *e22c*-gal4 (Jacinto *et al.* 2000) and *I67D*-Gal4 were used to express the transgenes in the embryonic epidermis. I67D-Gal4 was derived from DGRC Kyoto stock 106535. In addition, the following null alleles were used; $baz^{815\text{-}8}$ (Krahn *et al.* 2010), $pi3k92e^{A}$ (Weincove *et al.* 1999), $pten^{117}$ (Oldman *et al.* 2002), rac^{J10} and rac^{J11} triple mutants (Hakeda-Suzuki *et al*. 2002), mbc^{C1} (Rushton *et al.* 1995), $mbc^{D11.2}$ (Erickson *et al.* 1997), $still\ life^{ES11}$ (Sone *et al.* 2000) and akt^{04226} (Spradling *et al.* 1999).

2.4.2 Generation of transgenic lines: The following transgenic fly lines were generated during this project: UAS-m-Cherry-PH and UAS-GFP-PH, to allow visualisation of PIP_3 under the control of the UAS-Gal4 system, and UAS-m-Cherry-MBC and UAS-GFP-MBC to allow visualisation of *myoblast city* under the control of the UAS-Gal4 system.

Prior to cloning of MBC and Grp1-PH (PIP_3 specific binding domain) into pUASp expression vectors, which already contained the coding sequences for either GFP or m-Cherry (Millard and Martin 2008), restriction sites were added to the 3' and 5' ends of the cDNA along with additional bases to ensure that once cloned into the pUASp vector the cDNA was expressed in frame with the GFP or m-Cherry. Amplifying the MBC cDNA with primers listed in Table 1, inserted the *Not 1* restriction site at the 5' end and the *Xba 1* restriction site at the 3' end of the cDNA. Amplification of the Grp1-PH cDNA with primers listed in Table 1, inserted *Kpn 1* at the 5' end and the *Xba 1* restriction site at the 3' end of the cDNA. Once the restriction sites and additional bases were added, the cDNA was then subcloned into the pUASp vectors. Successfully subcloned variants were sent to BestGene Inc. for injection into *Drosophila* embryos. Injection of embryos was carried out according to BestGene's standard protocol, briefly, transgenic DNA is injected into early embryos that are yet to undergo blastoderm cellularisation. The DNA is injected alongside the P-element transposase, which both enter the pole cell nuclei and the transgenic DNA becomes incorporated into germline cell chromosomes. Injected offspring that that have inherited the transgene are identified via red eye colour and successful transgenic lines amplified. Once chromosome mapping has been carried out, the lines are maintained over balancer stocks (Ashburner *et al.* 2005).

In addition the line UAS-PTEN3-G137E was used. This line was generated by Deborah Goberdhan (University of Oxford) as follows: The G137E mutation was introduced into PTEN3 via an overlapping PCR strategy using the following primer pairs: 5'-cat aat tgc cat ggg ata tcc-3' and 5'-ccg gtg ctc **T**cc ttt cca gct tta ca -3' (NcoI site in *PTEN3* cDNA), and 5'-ctg gaa agg **A**ga gaa ccg gta cca tg-3' and 5'-cac ttg aac aaa cta gtt tgg-3' (SpeI site in *PTEN3* cDNA). These two PCR products were then used as templates in a subsequent PCR reaction with the NcoI and SpeI primers to generate a new PCR product that was cloned into PTEN3 cDNA and inserted in the transformation vector pUAST, which was then injected into embryos to generate of transgenics as described above.

2.4.3 Generation of maternal mutants (*pten*$^{117\ mat/zyg}$): To further investigate the role of PTEN during DC and wound healing, maternal mutants were generated by the following crosses, to provide embryos that were completely devoid of PTEN (Figure 16);

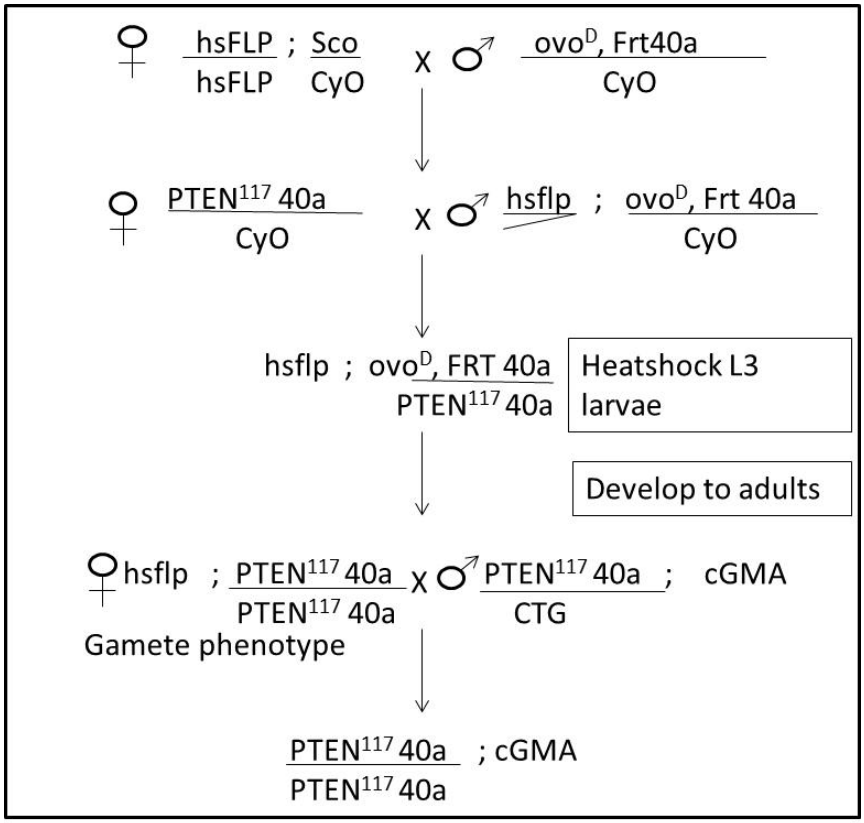

Figure 16. Generation of *pten* maternal mutants A crossing schematic of the generation of embryos lacking maternal and zygotic expression of PTEN

L3 larvae were heat shocked at 37^{o}C for 2 hours, to activate expression of the FLP recombinase in the gametes whilst undergoing meiosis. There are three possible outcomes from this protocol; 1) genetic recombination does not occur and the presence Ovo^{D} will prevent adult females from laying eggs, 2) Genetic recombination will occur and the gametes will have 2 copies of Ovo^{D}, in which case these adult females will not lay eggs or 3) genetic recombination does occur and the gametes will have 2 copies of the mutant *pten*^{117}. The adults from the third outcome will be crossed to *pten*$^{117/+}$ heterozygous null males with a GFP balancer. The embryos from this cross, when selected against the GFP balancer, will provide us with embryos that are maternally and zygotically null for *pten*. The above cross was also carried out with the final step crossing the females to males carrying tGPH to allow the study of PIP_3 in a maternally and zygotically null embryo.

2.5 Live imaging of *Drosophila* embryos

2.5.1 Preparation of embryos for live imaging: Flies of the desired genotype (or a cross that will provide offspring with the desired genotype) were placed in a cage containing an apple juice plate, supplemented with yeast paste, and kept at 25^{O}C. An overnight egg lay was used to obtain embryos of the required stage. To visualise the embryonic developmental stage, the embryos were dechorionated as described in section 2.1, transferred to a fresh

apple juice plate, and sorted for genotype (by fluorescence) and developmental stage using a Leica fluorescent microscope (Leica microsystems M165FC). Selected embryos were then aligned on a small square of apple juice agar, in the correct orientation (typically dorsal up). Embryos were oriented anterior-posterior (head to tail) left to right in a straight line. A 22x22 cm heptane glue coverslip was positioned carefully over the aligned embryos and slight pressure applied to ensure the embryos stuck to the coverslip. A small amount of halocarbon oil was placed on the embryos to prevent dehydration. The coverslip and embryos were transferred to a Lumox culture dish (Greiner #9607 7331) bridged by two 18x18 cm coverslips and held in place by two drops of nail polish (see Figure 17).

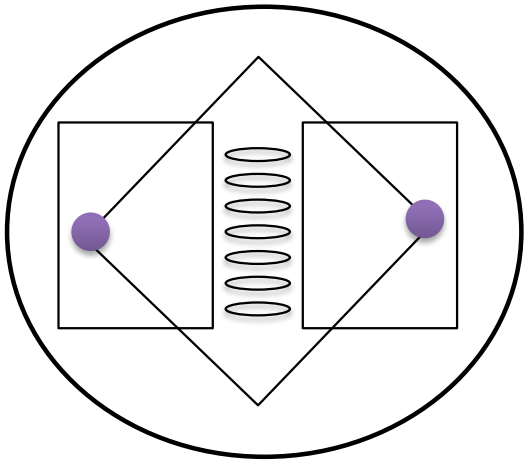

Figure 17. Schematic outlining embryo positioning on the live imaging dishes. Embryos (ovals in centre of the dish) are fixed to a heptane glue coverslip, which is then bridged between two coverslips with the embryos submerged in halocarbon oil for imaging. The cover slip is held in place by two drops of nail polish (purple dots).

2.5.2 Live imaging of embryos: Embryos were imaged using either a Leica TCS SP5 AOBS inverted or upright, or a Nikon A1 R confocal microscope. The use of confocal and the settings varied depending on the experiment, but in general imaging using the Leica SP5 confocal, the 63x 1.4NA oil immersion objective was used with a 1x confocal zoom (2x confocal zoom for filopodia studies). Standard confocal settings were as follows; pinhole 1 AU, 400Hz scan speed with bidirectional scanning, 512 x 512 was used initially with images taken at 1024 x 1024 for greater resolution. Images were taken using the following detection mirror settings; FITC or GFP constructs and Texas red or m-Cherry constructs; using the 488nm (10%), 594nm (50%) lasers respectively with HyD detectors for increased detection of emitted light. The laser powers were increased to 20% and 100% for 488nm and 594nm respectively if the standard PMT detectors were used. Images were acquired by sequential scanning and where Z stacks were taken, slices were captured 1 µm apart.

When using the Nikon A1 R the 60x oil immersion objective was used. As with the Leica microscope, the settings varied depending on the specific experiment, however, in general the resonant scan head was used, with the pinhole at 1.2 AU, 400Hz scan speed with bidirectional scanning and a zoom of 1 (2 for wounding experiments). Scan formats; 512 x 512, 1024 x 1024 or 1024 x 512. FITC or GFP constructs and Texas red or m-Cherry constructs were imaged using 488nm and 561 nm lasers respectively. For long time-lapse collection, multipoint imaging with the perfect focus facility was used, allowing the top slice of each embryo to be set uniquely resulting in multiple embryos being imaged without the imaging stack drifting out of focus.

2.5.3 Laser ablation of embryonic epidermis: Wounding of the *Drosophila* epidermis was carried out using a micropoint laser (Andor technology) attached to the Nikon A1 R confocal microscope. For wound analysis studies, the 60x oil immersion objective was used. The micropoint laser was set to a power level between 63 and 68 and fired when the epidermis was slightly out of focus, this resulted in a wound that took between 30-90 minutes to close. Embryos were wounded, alternating between control and mutant/transgenic embryos to ensure one complete set of embryos were not imaged before the others. The confocal settings for wounding were standardised as follows: Pinhole 1.2 AU, 16x resonant scanner, format 512 x 512 with a confocal zoom of 2. Embryos were imaged in 6 sections 0.8 µm apart. FITC or GFP constructs and Texas red or m-Cherry constructs were imaged using the 488nm and 561nm lasers respectively.

2.5.4 Image analysis: Images were analysed using either ImageJ software (wound healing studies) or Volocity 3D image analysis software (PerkinElmer) (zippering, dorsal hole and filopodia studies).

Dorsal hole ratios were determined using Volocity software by measuring the length and the width of the embryos during DC. Embryos were selected based on the width of the dorsal hole, selecting those that were mid-late DC, with a width of 0-50 µm in width).

Zippering analysis was carried out using Volocity software. Rate of zippering was calculated by observing how many frames it took each stripe to close a distance of 0.6 µM. The closure rate was determined for embryos that were classed as mid-late dorsal closure (in this case, this was determined by the number of stripes left to close with embryos ideally having 6-8 stripes remaining) (Figure 18).

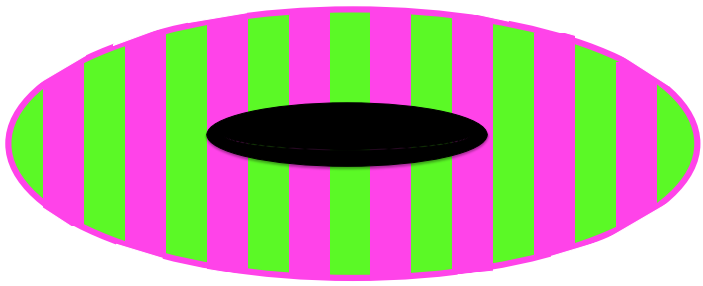

Figure 18. Schematic, demonstrating the stage required when undertaking zippering studies. Embryos were selected to be mid-late dorsal closure, and those imaged had 6-8 stripes left to close.

DC filopodial length and number were quantified using mid to late stage embryos where stripes are seen clearly (i.e. no adjoining amnioserosa cells expressing GFP) using the line function in Volocity software.

Wound closure analysis was carried out using maximum projected stacks in ImageJ. Using a Wacom Cintiq 12WX tablet (Wacom) and the free-hand draw tool with the measure function in ImageJ, the area of the wound was measured every frame (2 minutes intervals) by drawing around the edge of the wound. The total protrusion area was determined by then drawing around the visible protrusions and subtracting it from the total wound area. This could then be used to calculate the percentage of the wound area that consisted of protrusions.

The collected data from each experiment was transferred to Excel (2010) where average, standard deviation and error could be determined and displayed graphically. Statistical analysis was performed as stated in section 2.10.

2.6 Drug treatment of embryos: To pharmacologically inhibit the activity of PI3K, we treated embryos with LY294002 (Sigma Aldrich Cat ♯ L9908), a well-characterised PI3K inhibitor (Vlahos *et al.* 1994). Dechorinated, DC stage embryos were aligned on agar 'dorsal up' and mounted onto a heptane glue coverslip. The embryos were desiccated (in a tub with silica beads) for 2 minutes, then 1 x PBS was added. Using a needle holder on a Leica inverted microscope (Leica Microsystems DM IL LED) and a fine pulled needle (Appendix 1) the vitelline membrane on the posterior part of the embryo was pierced. The 1xPBS was removed and replaced with either 5mM DMSO or 5mM LY294002 and incubated for 50 minutes. The drug or DMSO solution was removed prior to wounding, and embryos were mounted as described in 2.6.1.

2.7 Immunofluorescence

2.7.1 Whole mount immunofluorescence staining of *Drosophila* embryos: Embryos of the desired genotype were bleached as described in 2.1 and fixed in a glass vial containing 1 ml 4% formaldehyde (diluted from 10% methanol free paraformaldehyde, Polysciences Inc) and 1 ml heptane (Sigma Aldrich ♯ 32287) on a roller for 45 minutes at room temperature. To devitinilise the embryos, the bottom layer of formaldehyde was removed and replaced by 1 ml 100% methanol (Fischer Scientific M/4000/17), the vial was shaken vigorously for 1 minute with fixed, devitinilised embryos sinking to the bottom of the vial. Once settled, the heptane (top layer) was removed and the embryos transferred, in the methanol, to a 1.5 ml microcentrifuge tube. The embryos were washed 3 times with 1 ml methanol (by removing old methanol and adding fresh methanol), this was then removed and 3 washes with PATX carried out in the same manner. When phalloidin staining was used methanol could not be used for de-vitinilisation, so this was instead carried out manually after the fixation. Manual de-vitinilisation was achieved by removing embryos from the formaldehyde using a glass pipette and placing them onto a strip of filter paper (with minimal transfer of heptane). The filter paper was then inverted onto double sided sticky tape stuck onto the inside of a lid from a 35 mm culture dish (Corning ♯ 430588) and gentle pressure was applied to transfer embryos to the tape. 1 ml PATX was placed onto the embryos promptly to prevent drying. A 27G needle was used to gently prick one end of the embryo and then apply slight pressure to the other end, removing the embryo from the membrane. De-vitellinised embryos were transferred to 1.5 ml microcentrifuge tube and rinsed with 1 ml PATX. Embryos were washed in 1 ml PATX, for 20 minutes on a roller, 3 times. Once washed, 400 µl of desired primary antibody at was added, and left overnight at 4^{O}C on a roller. The embryos were rinsed 3 times in 1 ml PATX, and then washed in 1 ml PATX, for 20 minutes on a roller, 3 times. Then 400 µl of the secondary antibodies were added and left rolling for 2 hours. The embryos were rinsed 3 times in 1 ml PATX, and then washed three times in 1 ml PATX, for 20 minutes on a roller. Once washed, the PATX was removed, leaving around 50 µl to transfer the embryos to a clean, labelled coverslip. Excess buffer was aspirated off, and 20 µl Vectorshield (Vector labs cat number H-1400) added to the slide with a coverslip placed on top, being careful to ensure no bubbles are made. The coverslip was left overnight in the dark to dry and then stored at -20^{O}C until viewed on a Leica SP5 confocal (Leica Microsystems GMBH). The antibodies used throughout this project are outlined in table 3.

Antibody	Concentration used	Supplier
Mouse anti-FasII	1:5	DSHB
Goat anti-GFP	1:500	Abcam
Rabbit anti-Bazooka	1:1000	Von Stein *et al.* 2005
Rat anti-E-Cadherin	1:500	DSHB
FITC-, Cy3 or Cy5 conjugated secondary antibodies (donkey)	1:100-200	Jackson Immuno Research
Tritc- or Alexa647-phalloidin	1:500-1000	Invitrogen

Table 3. Antibodies used throughout this thesis. A list of antibodies, dilutions and suppliers of the antibodies used throughout the thesis.

2.7.2 Embryonic flat preparation: To allow visualisation of CNS phenotypes, flat preparation of stage 16 embryos was performed following a previously published procedure (Budnik *et al*. 2006). Where visualisation of the dorsal hole was required, this procedure was adapted, to dissect embryos along the ventral surface to ensure the dorsal hole remained intact. Stage 14-15 embryos were used and dissected along the ventral surface keeping the dorsal side of the embryo intact for staining.

2.8 Cuticle preparations: Overnight egg lays from flies of the desired genotype (or those that would provide embryos of the desired genotype) were bleached as described in 2.1. Stage 16 embryos were selected based on their genotype (by fluorescence selecting against GFP balancers), transferred to a drop of water on a sylgard-coated cover slip (coverslips coated with a silicon-like gel) and de-vitinilised using a fine, sharp needle. The de-vitinilised embryos were then moved to a fresh slide with 50 µl water, placed on a heat block (at 70^{O}C) for 20-30 seconds and then transferred, using fine forceps, to 10-20 µl mounting medium (Hoyers medium) with a coverslip placed on top. The slide was returned to the heat block for 30 minutes after which a weight was gently placed on top of the slide and left overnight at 70^{O}C (or at least 2 hours). The cuticle preps were imaged under darkfield illumination using a Leica Axiovision upright microscope (Leica Microsystems GMBH) using the 20x objective and a darkfield condenser.

2.9 Statistical Analysis: All statistical analysis was performed using Prism 6 (GraphPad software). The normality distribution was first determined using Shapiro-Wilk normality test. Depending on the normality, data was analysed using appropriate parametric or non-parametric tests. For parametric tests, t-test, with Welch's correction or one-way ANOVA with Dunnets or Bonferroni ad hoc tests were performed. Where data was not normally distributed Mann-Whitney or Kruskal-Wallis with Dunn's multiple comparisons test were performed. All data analysis was performed to the $p \leq 0.05$ level of significance when compared to controls.

Chapter 3: Role of PIP_3 in *Drosophila* dorsal closure

PIP_3 has been implicated in a variety of processes including cell migration and actin reorganisation (Leevers *et al.* 1996; Zhou *et al.* 1998; Gao *et al.* 2000). Work in *Dictyostelium* cells demonstrated the importance of the PI3K signalling pathway in the formation of actin filaments necessary for the formation of pseudopodia (Zhou *et al.* 1998), in particular the specific localisation of PIP_3 to the front of migrating cells, where it reorganises the actin cytoskeleton (Funamoto *et al*. 2002). This polarised distribution of PIP_3 and rearrangements of the actin cytoskeleton is vital for efficient directional cell migration. The ability of PIP_3 to reorganise the actin cytoskeleton is not restricted to *Dictyostelium* cells. PIP_3 is also vital in the generation of pseudopods in migrating zebrafish neutrophils. During migration of neutrophils towards a wound, PIP_3 becomes localised to the front of the cell where it regulates the formation of actin protrusions (Yoo *et al*. 2010), again demonstrating the importance of PIP_3 in reorganising the actin cytoskeleton.

Directional migration is important in many developmental events in addition to single cell migration. Recent work investigated the role of PI3K signalling in neural tube closure and found that a reduction in the levels of PI3K resulted in a failure of cell migration along the neural midline, causing spina bifida in mouse embryos (Pickett *et al.*2008). Although this work did not directly implicate PIP_3 in the process of neural tube closure, it suggested that downstream components of the PI3K signalling pathway (of which PIP_3 is included), are important in cell migration during developmental events. The role of PIP_3 in actin cytoskeletal reorganisation has been well studied in single cell migration; however, its role in collective cell migration has not been investigated in detail.

As the PI3K signalling pathway has been shown to be required for collective migration during neural tube closure, we wanted to determine if PIP_3 is also required for the process of DC. Given that during DC, the formation of actin protrusions is vital to ensure effective epithelial fusion along the dorsal midline (Jacinto *et al.* 2000; Woolner *et al*. 2005; Millard and Martin 2008) and that PIP_3 has been shown to be important in the regulation of actin protrusions in single cell migration, we propose that PIP_3 may also be required for the process of *Drosophila* DC. By using *Drosophila*, we are able to investigate the role of PIP_3 during epithelial fusion in a genetically tractable model that is amenable to live imaging, allowing detailed study of the role of PIP_3 in cytoskeletal reorganisation during DC. A PDF of all figures shown in the results section can be found on the DVD inserted in the back of this thesis.

3.1 Localisation of PIP_3 in DC

To determine whether PIP_3 is important in DC, we first investigated its distribution during the process. To visualise the localisation of PIP_3, we used a fly line that expressed the PH domain of Grp1 tagged with GFP (GPH), a well characterised marker of PIP_3 (Britton *et al*. 2002). This construct was expressed ubiquitously throughout the embryo under the control of the tubulin promoter (tGPH). The ubiquitous expression of GPH enables us to clearly observe where PIP_3 accumulates throughout development. Live imaging of embryos expressing tGPH showed accumulation of PIP_3 at the leading edge, with a particularly pronounced localisation at the junctions between neighbouring epithelial cells along the leading edge (Figure 19 A and Bi). After the fusion of the leading edges, PIP_3 accumulation is lost approximately 6 cell widths behind the zippering canthi (Figure 18 Bii). When the localisation of PIP_3 was observed in more detail over time, by expressing UAS-GPH in *engrailed* stripes (using the *en*-Gal4 driver), it was observed that PIP_3 distribution is dynamic, changing significantly over time (Figure 19 Ci-iii). Time-lapse images show that within 10 minutes, PIP_3 is lost and then regained within leading edge epithelial cells.

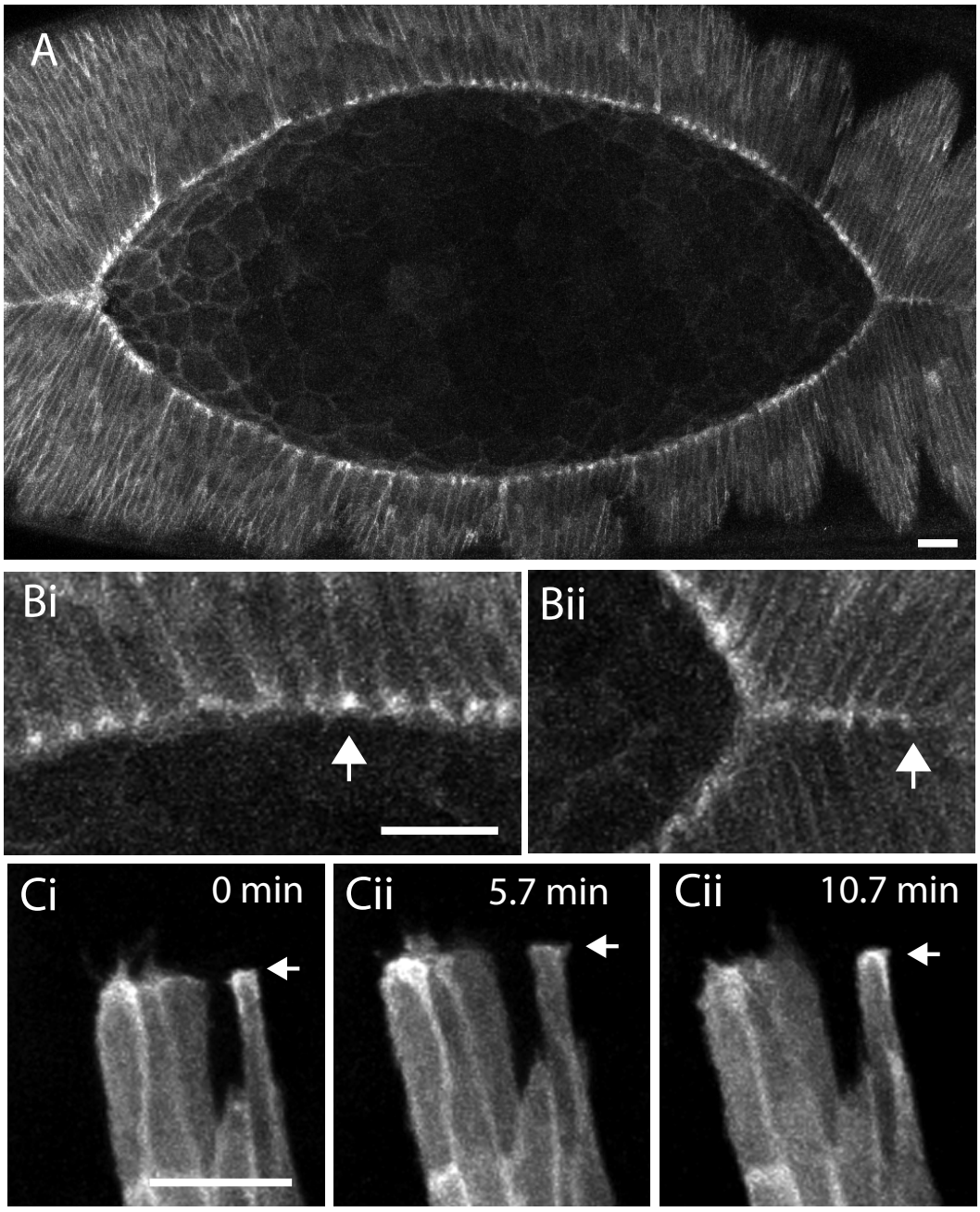

Figure 19. Localisation of PIP_3 at the leading edge during DC. A) Localisation of PIP_3 as visualised by expression of tGPH shows accumulation of PIP_3 at the DC leading edge. B) Accumulation is most pronounced at leading edge cell junctions (arrow) and Bii) the arrow indicates where PIP_3 is lost once epithelial fusion has completed. C) Expression of UAS-GPH in engrailed stripes shows transient localisation of PIP_3, the arrow indicates PIP_3 accumulation that is lost and then regained at the leading edge. All scale bars indicate 10 μm.

3.2 Manipulating PIP_3 levels during DC

3.2.1 Analysis of PIP_3 in mutant embryos

The specific localisation of PIP_3 during DC suggested that it might be playing a regulatory role. To establish what this role might be, we needed reliable methods of manipulating PIP_3 levels. The following section describes the methods used to manipulate PIP_3.

The use of mutants lacking expression of the key enzymes involved in the formation and elimination of PIP_3 provided one means of manipulating PIP_3 levels. Embryos lacking zygotic expression of PI3K (*pi3k92e*) (Weincove *et al.* 1999) are unable to phosphorylate $PI(4,5)P_2$ to PIP_3, except through residual maternal protein (Figure 20 A). Expressing tGPH in zygotic $pi3k92e^{A}$ mutants showed a decrease in GPHn associated with cell junctions, indicating a reduction in the levels of PIP_3 (as GPH binds specifically to PIP_3). However, the levels of PIP_3 in these embryos was variable with some retaining leading edge accumulation, most likely due to variable levels of residual maternally contributed protein (Figure 20 B and C).

The localisation of tGPH in embryos lacking zygotic PTEN ($pten^{117}$) (Oldman *et al.* 2002) was also observed. As PTEN dephosphorylates PIP_3 to $PI(4,5)P_2$, these embryos would be expected to display elevated levels of PIP_3. In embryos lacking zygotic expression of PTEN, most of the GPH had been recruited to the plasma membrane indicating an increase in PIP_3 levels. To further increase the levels of PIP_3, embryos lacking expression of maternal and zygotic PTEN were generated. In these embryos, no GPH was detected in the cytosol of DME cells, indicating the elevated levels of PIP_3 had sequestered all GPH to the membrane. The difference observed between the levels of PIP_3 in embryos lacking zygotic expression of PTEN to those lacking maternal and zygotic expression of PTEN indicates that maternally derived PTEN makes a substantial contribution to regulating PIP_3 levels during DC (Figure 20 Di, Dii).

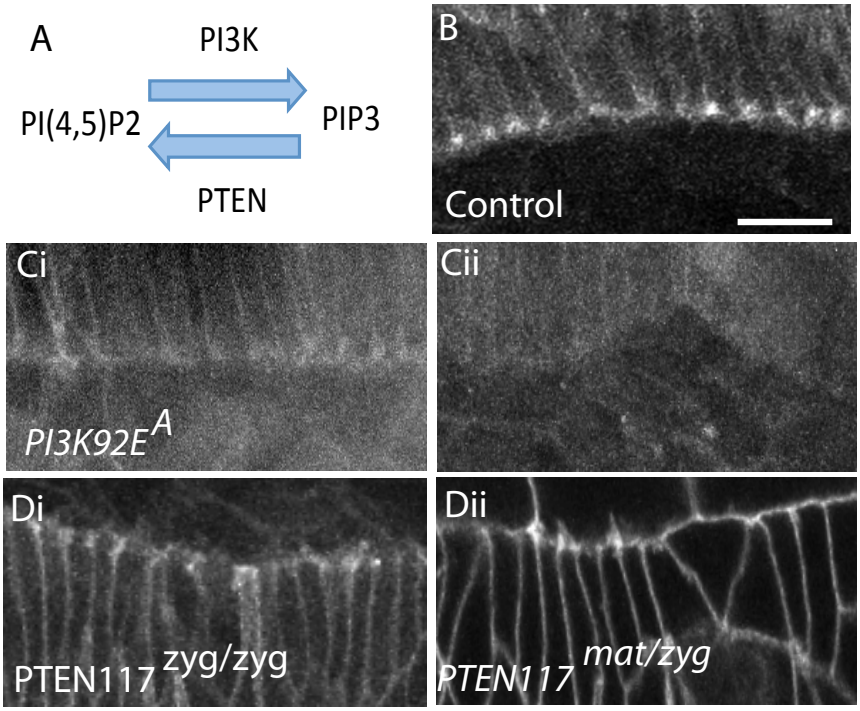

Figure 20. PIP_3 levels are altered in embryos mutant for components of the PI3K signaling pathway. A) Schematic showing that PI3K phosphorylates $PI(4,5)P_2$ to PIP_3, where PTEN antagonises this reaction. B) Shows levels of PIP_3 at the leading edge in control embryos. Ci and ii) show reduced levels of PIP_3 in embryos zygotically null for PI3K. Di) shows levels of PIP_3 in embryos lacking zygotic expression of PTEN, where Dii) shows levels of PIP_3 in embryos lacking maternal and zygotic expression of PTEN. Scale bar represents 16 μm.

3.2.2 Pharmacological inhibitors to reduce the levels of PIP_3

An alternative method of reducing PIP_3 levels was to use pharmacological inhibitors of PI3K. We used the well-characterised PI3K inhibitor LY294002 (Vlahos *et al.* 1994). By soaking embryos in which the vitelline membrane was punctured (using a fine pulled needle) in 5 mM LY294002 (in DMSO) we were able to reduce the amount of PIP_3 at the DC leading edge in some embryos (Figure 21). However, effect of the inhibitor was variable, with some embryos exhibiting normal levels of PIP_3 (Figure 21Bi, Bii). The variability is perhaps due to variation in the extent to which the vitelline membrane was punctured and as such variations in the amount of inhibitor reaching the DME cells.

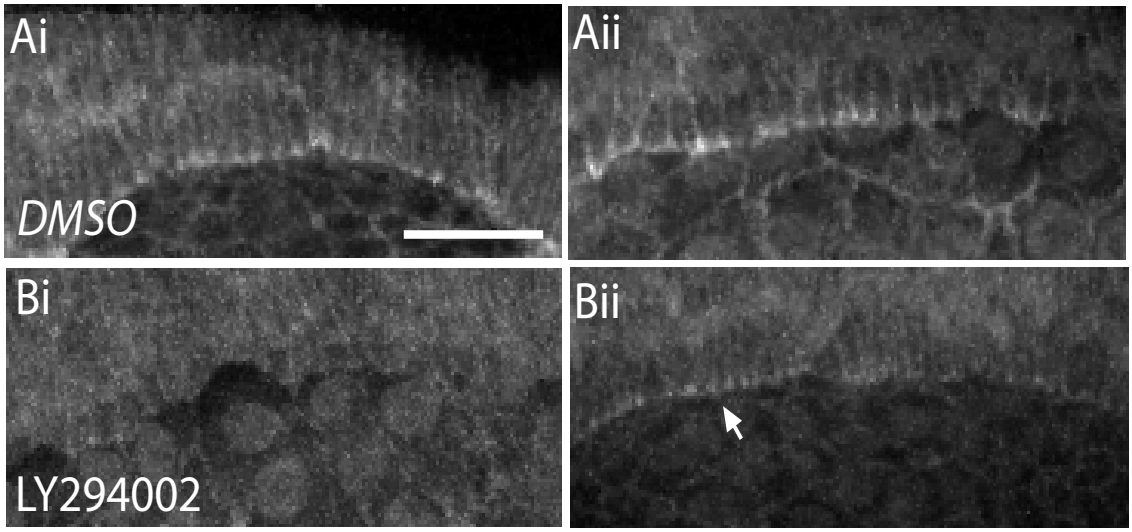

Figure 21. Reducing levels of PIP_3 during DC using pharmacological inhibitors. Ai, ii) Control embryos showing that soaking embryos in 5 mM DMSO did not affect the production or localisation of PIP_3. Bi, ii) Treatment with 5 mM LY294002 reduced the amount of PIP_3 present, however it was not consistent with some embryos still expressing PIP_3 (Bii arrow). Scale bar represents 16 μm.

3.2.3 Modulating levels of PIP_3 using transgene expression

As pharmacological and mutational approaches were not consistent in reducing the levels of PIP_3 during DC, we decided to take advantage of the genetic tools available in *Drosophila*, in particular the UAS-Gal4 system. As mentioned, PTEN is a phosphatase that can dephosphorylate PIP_3 to $PI(4,5)P_2$ (Maehama and Dixon 1998). Using the UAS-Gal4 system we were able to overexpress a splice variant of PTEN (UAS-PTEN3) (Goberdhan *et al.* 1999) in a subset of cells, so reducing PIP_3 levels specifically in these cells. There are two main splice variants of PTEN; PTEN2 (Huang *et al.* 1999) and PTEN3 (Goberdhan *et al*. 1999) with the sole difference being a 5 amino acid C-terminal PDZ binding domain, which allows PTEN2 to be recruited to specific cellular locations (Smith *et al.* 1999; Maehama *et al.* 2004). As PTEN3 lacks this domain, it is diffuse throughout the cell and as such was our splice variant of choice when trying to reduce the levels of PIP_3. Overexpressing UAS-PTEN3 under the control of *engrailed*-Gal4 (Brand and Perrimon 1993), allowed expression of UAS-PTEN3 in a subset of cells in the epithelium. Additionally, we co-expressed UAS-m-Cherry-moesin (Millard and Martin 2008) to allow the cells in which the transgene was expressed to be identified. These embryos also expressed tGPH to enable visualisation of PIP_3 levels during DC. The major benefit of using the UAS-Gal4 system is the presence of an internal control (non-*engrailed* stripes) alongside cells where transgenes are expressed (*engrailed* cells). Expressing UAS-PTEN3 in *engrailed* cells resulted in a consistent reduction of PIP_3 when compared to control embryos (Figure 22, A, B). As PTEN has also been shown to have protein phosphatase activity we also used a mutated form of PTEN (UAS-PTEN3-G137E) (Pickering *et al.* 2013), as a control. This mutated transgene has no lipid phosphatase activity, but is still able to dephosphorylate proteins. No change in levels of PIP_3 were observed upon expression of UAS-PTEN3-G137E (Figure 22 C), making this transgene a good control to ensure any effects observed whilst using UAS-PTEN3 are as a result of reduced PIP_3 and not of any changes in protein dephosphorylation.

UAS-PTEN3 thus provided a useful means of depleting PIP_3 in specific cells, but we also needed an equivalent approach to elevate PIP_3 levels. To do this, we used a constitutively active PI3-Kinase (UAS-CA-PI3K) (Leevers *et al.* 1996). Using this method, we were able to increase the levels of PIP_3 in a reproducible manner (Figure 22 D). Expressing UAS-CA-PI3K worked by overloading the cells with active PI3-Kinase. As an alternative approach we also expressed constitutively active Ras (UAS-CA-Ras) (Karim and Rubin 1998), as Ras has been shown to be an upstream activator of PI3-Kinase. Expressing UAS-CA-Ras in *engrailed* stripes also resulted in the increase of PIP_3, but not to the same extent as UAS-CA-PI3K, as CA-Ras increases the activity of endogenous PI3-Kinase, rather than increasing the total amount of PI3-Kinase present in the cell (Figure 22 E).

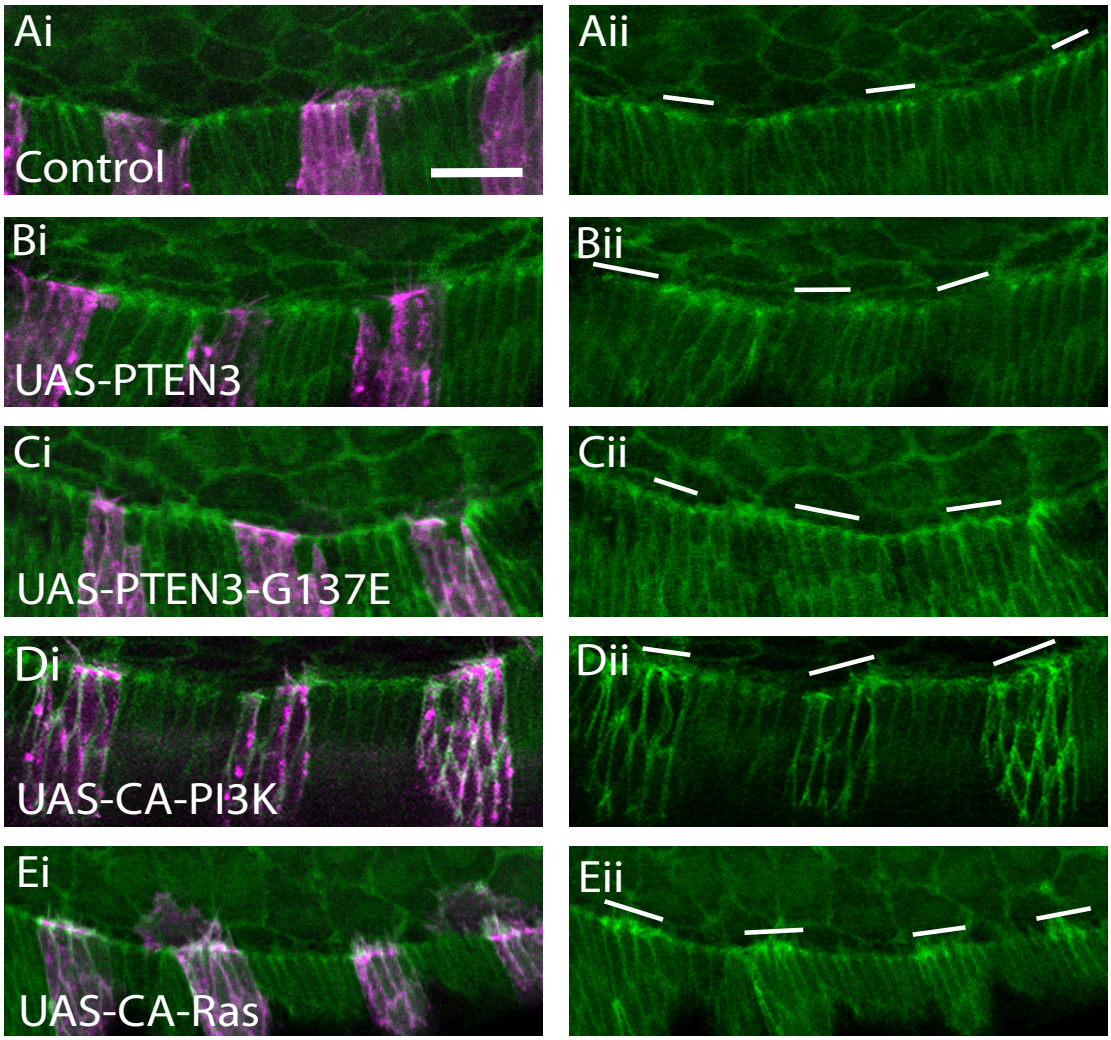

Figure 22. Genetic manipulation of PIP_3 levels. A) *en*-Gal4, UAS-m-Cherry-Moesin, tGPH showing that co-expression of UAS-m-Cherry-Moesin has no effect on PIP_3 levels. B) Expression of UAS-PTEN3 reduces levels of PIP_3 in *engrailed* stripes. C) UAS-PTEN3-G137E is not able to dephosphorylate PIP_3 when overexpressed. D and E) Expression of UAS-CA-PI3K or UAS-CA-Ras results in the increase of PIP_3 at the DC leading edge. Scale bar represents 15 μm

3.3 Effects of manipulating PIP3 levels on DC

To establish the role of PIP_3 at the leading edge during DC we first sought to determine the effects of altering the levels of PIP_3 throughout the embryonic epidermis. Overexpressing UAS-PTEN3 under the control of an embryonic ubiquitous driver, *tubP*-Gal4 (Lee and Luo 1999), we were able to reduce PIP_3 levels throughout the embryo. Additionally, we co-expressed UAS-GFP-Moesin to visualise F-actin where the transgene was expressed. Reducing the levels of PIP_3 in this manner resulted in an elongated dorsal hole with flattened leading edges when compared to controls (Figure 23 A, B, F). The length:width ratio of the dorsal hole was increased in embryos with reduced PIP_3 compared to controls (4.05 ± 0.27, to 3.51 ± 0.27 respectively p= 0.0019). We next investigated the effect of reducing PIP_3 levels by observing DC in embryos lacking zygotic expression of PI3K. These embryos exhibited a variety of phenotypes, probably reflecting varying levels of maternally-derived PI3K. 11% of zygotic *pi3k92e*^{A} mutants failed to survive to DC. Of the remaining embryos, 19% failed to complete DC and a further 11% closed, but exhibited marked puckering along the dorsal midline after closure, the remaining embryos closed without observable defect. The *pi3k92e*^{A} mutant embryos that reached DC exhibited the same elongated hole phenotype as those expressing PTEN3 (mean length:width ratio of 5.08 ± 0.52 compared to 3.51 ± 0.27 for controls p=0.0004) (Figure 23 A, C, F).

To study the effects of increasing the levels of PIP_3 on DC, we expressed UAS-CA-PI3K using *tubP*-Gal4. Increasing the levels of PIP_3 throughout the embryo resulted in a slight (but not significant) shortening of the dorsal hole, with the leading edges appearing more curved. The length:width dorsal hole ratio was slightly decreased by expression of CA-PI3K (3.16 ± 0.172 compared to 3.51 ± 0.22 for control embryos p=0.2422) although this was not statistically significant (Figure 23 A, D, F). We also observed DC in embryos lacking zygotic expression of PTEN (*pten*$^{117\ zyg}$). Consistent with expressing CA-PI3K, this also resulted in a slightly (but not significantly) shorter dorsal hole, with the leading edges displaying a more curved shape, with a length: width ratio of 2.95 ± 0.24. (p=0.3743) (Figure 23. A, E, F). To further analyse the effects of increasing the levels of PIP_3 in the embryo, we generated and analysed *pten*^{117} maternal and zygotic mutants (*pten*$^{117\ mat/zyg}$) expressing GFP-Moesin ubiquitously. 13% of *pten*$^{117\ mat/zyg}$ embryos arrested during development before reaching DC, and of those that reached DC, 8% failed the process completely, 54% displayed an abnormal dorsal hole (some elongated, some with a hole between the amnioserosa and leading edge and some with puckering along the dorsal midline) and 25% appeared normal (with eye-shaped dorsal hole). Of those that reached DC, we were able to carry out length:width ratio analysis and found that an increase in PIP_3 resulted in a significantly shortened dorsal hole (2.57 ± 0.14 for *pten*$^{117\ mat\ zyg}$ mutants compared to 3.51 ± 0.27 for control embryos p=0.0011) (Figure 23. G, H).

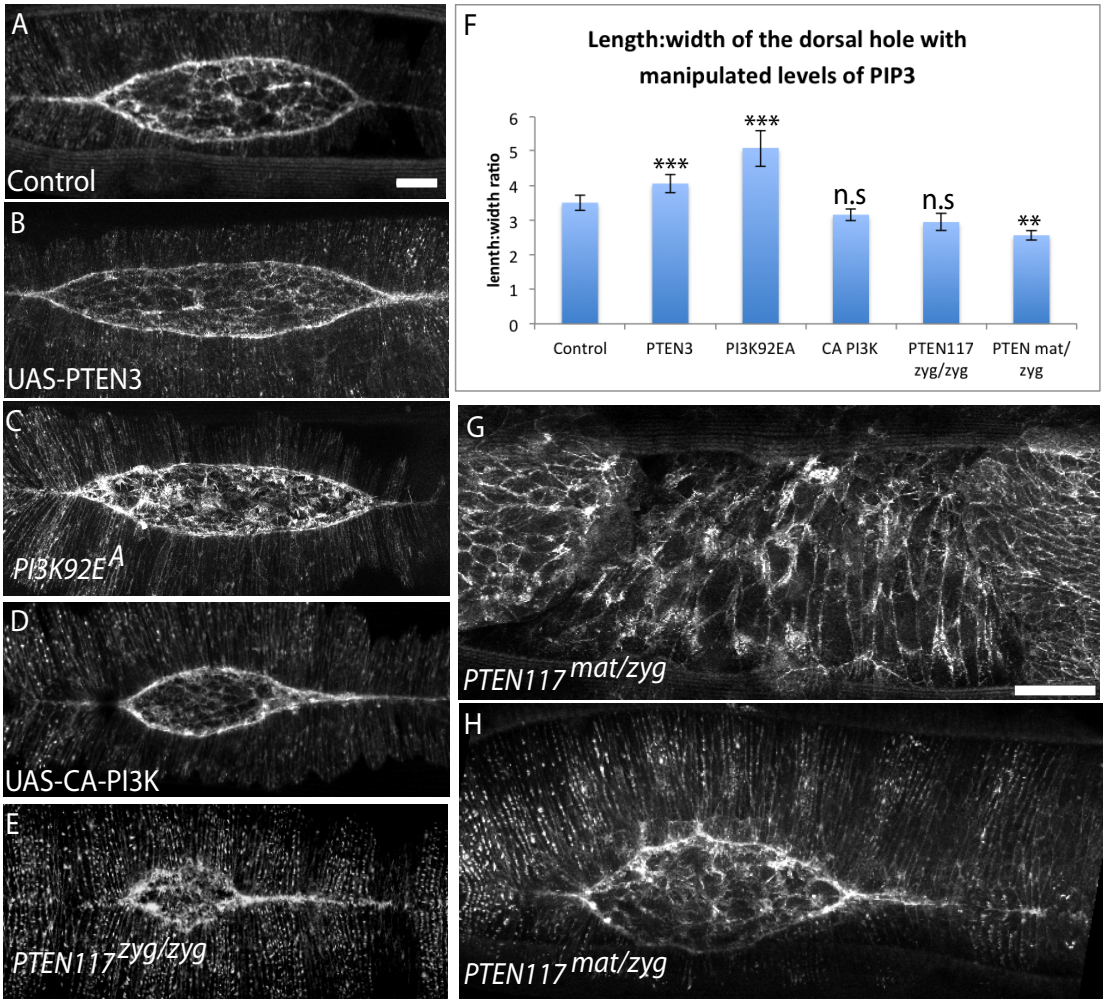

Figure 23. Manipulating levels of PIP_3 affects the geometry of the dorsal hole. A-E) Changes in the shape of the dorsal hole when levels of PIP_3 are either decreased (B,C) or increased (D, E). F) Quantification of length: width ratio indicating how much the dorsal hole has become rounded or elongated. G,H) Embryos lacking maternal and zygotic expression of PTEN display a variety of defects, with those reaching DC have a shortened dorsal hole. Scale bars represent 15 µm (A-E) and 31 µm (G,H)

3.4 Manipulating PIP_3 has an effect on the rate of zippering

It has previously been reported that an elongated dorsal hole can be due to failure or reduced efficiency of the fusion of the epithelial leading edges (Woolner *et al.* 2005). We therefore decided to investigate whether PIP_3 plays a role in the process of zippering. To do this, we expressed UAS-PTEN3 in the posterior compartment of each segment using the *engrailed*-Gal4 driver, alongside UAS-m-Cherry-Moesin (to allow visualisation of the cells expressing UAS-PTEN3) and cGMA (to visualise the F-actin throughout the embryo). The advantage of this strategy is that the transgene expression is limited to a subset of cells within the epidermis, allowing us to directly compare the behaviour of cells with depleted PIP_3 to that of cells with normal PIP_3 levels within the same leading edge. When UAS-PTEN3 was expressed in *engrailed* stripes we observed a significant reduction in the rate of zippering in engrailed stripes compared to neighbouring *non-engrailed* control stripes ($P<0.0001$) (the rate of zippering was quantified as described in section 2.5.4) (Figure 24, A,B, D). As a consequence of this delayed zippering, UAS-PTEN3-expressing cells often close after neighbouring non-PTEN3-expressing control cells, resulting in gaps along the dorsal midline (Figure 24 Bv).

To ensure the zippering defect observed on expression of UAS-PTEN3 is as a result of changes in PIP_3 levels, we analysed zippering in embryos expressing UAS-PTEN3-G137E. Expression of UAS-PTEN3-G137E in *engrailed* stripes, had no effect on the process of zippering when compared to non-*engrailed* cells ($p>0.9999$) (Figure 24 C). This suggests that the depletion of PIP_3 by PTEN3 is responsible for the observed zippering phenotype.

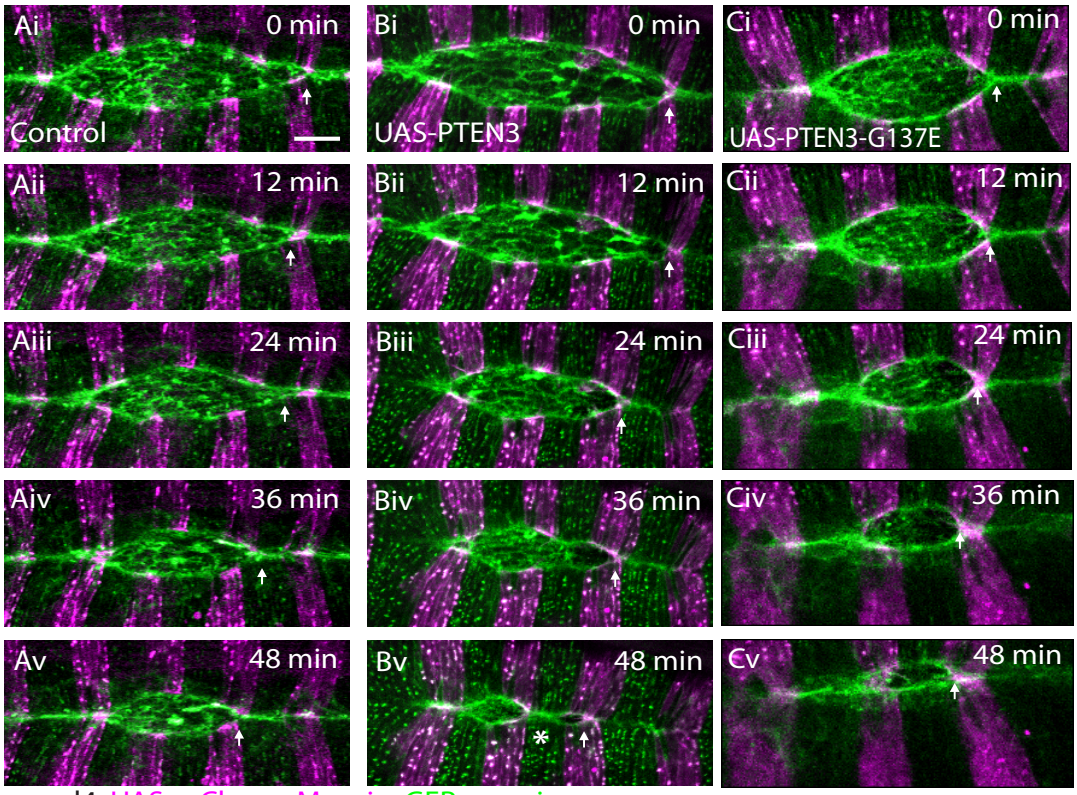

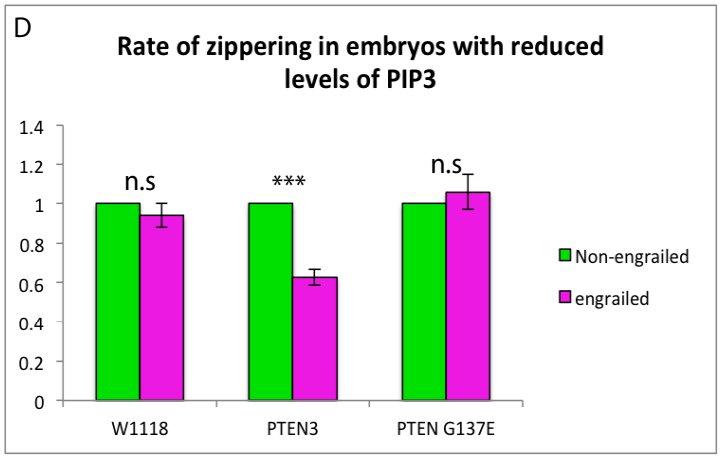

Figure 24. Reducing the level of PIP_3 reduces the rate of zippering. A-C) embryos expressing *en*-Gal4, UAS-m-Cherry-Moesin driving either A) control, B) UAS-PTEN3, C) UAS-PTEN3-G137E. Arrows indicate the position of the canthi at each timepoint, with the asterisk in Bv showing where defective zippering has occurred. D) Comparison of rates of zippering between *non-engrailed* (green) control stripes, and *engrailed* (magenta) stripes expressing the transgene indicated. *** Indicates zippering speed is significantly different from control stripes ($P<0.0001$), n.s. indicates $P>0.05$, error bars indicate S.E.M. Scale bar indicate 15 µm. Whole sequences are shown in movies 1-3 in appendix 2.

As reducing the levels of PIP_3 had a negative effect on zippering, we next sought to determine the effect of elevating PIP_3 levels. To achieve this, as previously, we expressed UAS-CA-PI3K under the control of *en*-Gal4. Additionally, UAS-m-Cherry-Moesin and cGMA were expressed to allow visualisation of *engrailed* cells and F-actin throughout the embryo. Increasing PIP_3 levels resulted in faster zippering in *engrailed* stripes compared to non-engrailed stripes ($p<0.0001$) (Figure 25 A, B, D). Interestingly, it appears that the stripes with elevated PIP_3 may begin zippering before the preceding control stripes have fused (Figure 25 Bv). Additionally, we also analysed the effect of expressing UAS-CA-Ras in *engrailed* stripes. This had the same effect as expressing CA-PI3K, with an increased rate of zippering in *engrailed* stripes when compared to non-*engrailed* stripes ($p<0.0001$). However, we did not observe *engrailed* stripes zippering prior to the completion of zippering of the preceding non-*engrailed* stripe (Figure 25 C, D). These data suggest that leading edge PIP_3 is a key regulator of zippering during DC.

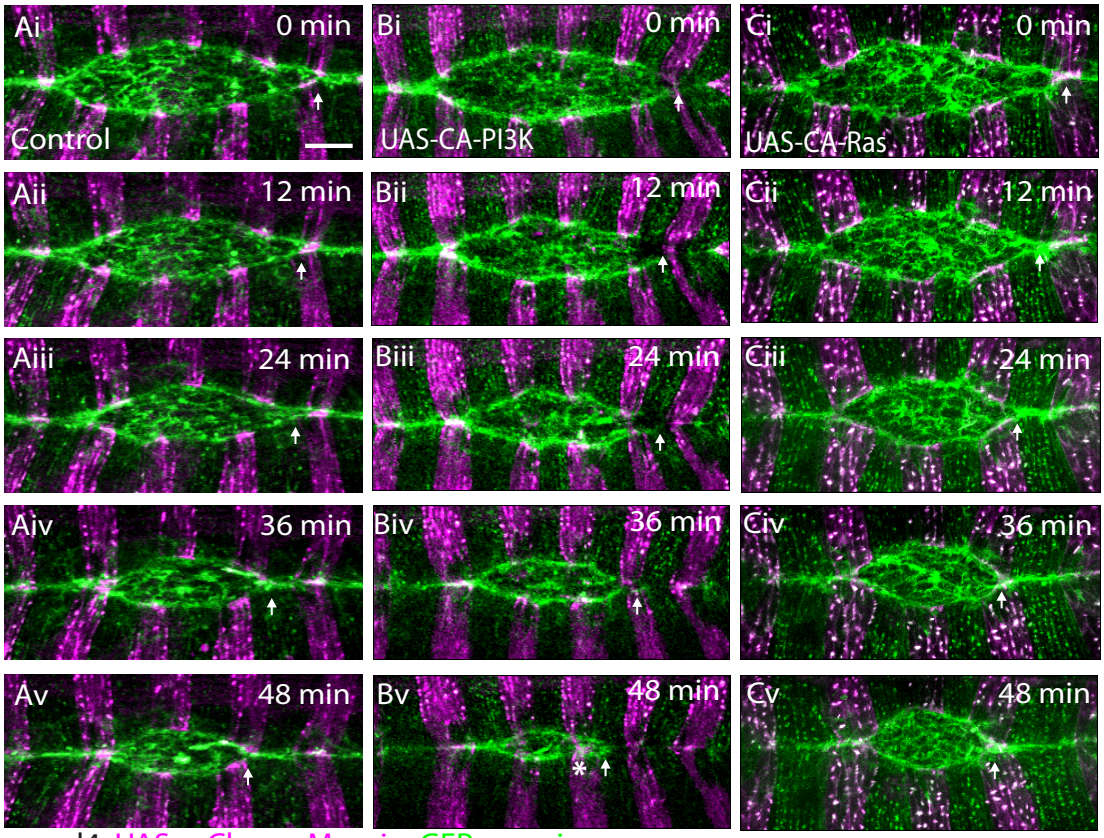

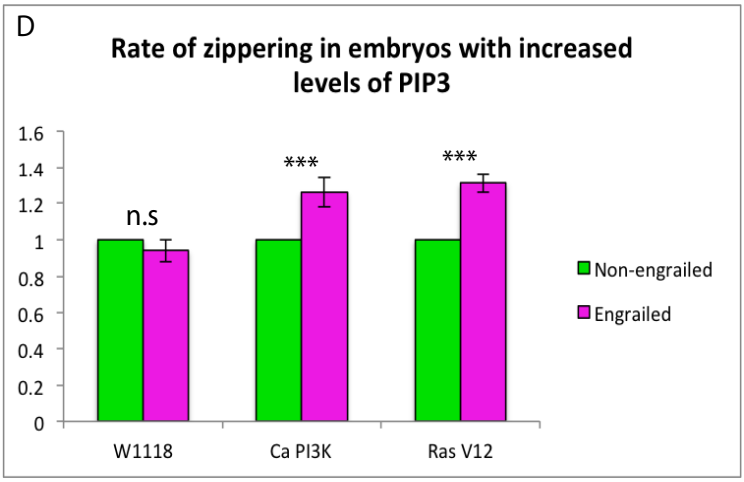

Figure 25. Increasing PIP_3 levels increases the rate of zippering. A-C) Embryos expressing either A) control, B) UAS CA-PI3K or c) UAS-CA-Ras transgenes in *engrailed* (magenta) stripes. Arrow indicate the canthi at each time point, and the asterisk in Bv) shows where dynamic filopodia are commencing zippering before the preceding control stripe has fully fused. D) Quantification of the rate of zippering in control *non-engrailed* (green) stripes vs *engrailed* stripes (magenta) expressing indicated transgene. n ≥ 10 for each transgene. *** Indicates significance of P>0.001 where n.s. indicates P>0.05. Error bars indicate S.E.M. Scale bars represent 15 µm. Whole sequences are shown in movies 1,4, 5 in appendix 2

3.5 PIP_3 is important for the regulation of filopodia during DC

As it has been reported that filopodia are key to the process of zippering during DC (Jacinto *et al.* 2002a), we hypothesised that manipulating PIP_3 levels might affect zippering by altering filopodial activity. To investigate this, we used *en*-Gal4 to drive expression of UAS transgenes to manipulate PIP_3 levels alongside UAS-GFP-Moesin (Dutta *et al.* 2002) to allow visualisation of leading edge filopodia. Reducing levels of PIP_3, by overexpressing UAS-PTEN3 resulted in a decrease in the number of filopodia per *engrailed* stripe from 5.93 ± 0.71 to 3.81 ± 0.47 ($p<0.0001$) (Figure 26 Ai, ii and B). To ensure any effects observed whilst using UAS-PTEN3 were as a result of PIP_3 dephosphorylation and not protein dephosphorylation, the effect of UAS-PTEN3-G137E expression on filopodia was also analysed. Expression of UAS-PTEN3-G137E did not affect filopodia number (5.96 ± 0.68 and 5.93 ± 0.71 filopodia per stripe were observed with expression of UAS-PTEN3-G137E or controls respectively $p> 0.9999$) (Figure 26 Av, B). Additionally, we analysed the number of filopodia in embryos lacking zygotic expression of PI3K and as such have reduced levels of PIP_3. Consistent with expressing UAS-PTEN3, in $pi3k92e^{A\ zyg/zyg}$ embryos, the number of filopodia observed at the leading edge was significantly reduced (4 ± 0.62 filopodia/stripe $p<0.0001$) when compared to control embryos (Figure 26 Avi, B).

To investigate the effect of increasing PIP_3 levels on the formation of filopodia, we overexpressed either UAS-CA-PI3K or UAS-CA-Ras (both of which result in an increase in PIP_3 levels). Overexpressing either of these transgenes resulted in a highly significant increase in filopodia number (11.57 ± 1.13 and 11.3 ± 0.96 for CA-PI3K and CA-Ras respectively $p<0.0001$ for both sets of data) (Figure 26 Aiii, iv, B). These data indicate that PIP_3 is important in the regulation of filopodia during DC.

We also analysed the effect of altering PIP_3 levels on the length of leading edge filopodia. Reducing the levels of PIP_3 resulted in shorter filopodia, (2.89 ± 0.27 μm in length in embryos overexpressing UAS-PTEN3 ($p<0.0001$), 2.99 ± 0.36 μm in embryos lacking expression of zygotic PI3K ($p<0.0001$) compared to 3.64 ± 0.27 μm in control embryos). However, overexpressing UAS-CA-PI3K did not have a significant effect on the length of filopodia (3.91 ± 0.28 in embryos overexpressing UAS-CA-PI3K $p=0.1331$) (Figure 26 D). Surprisingly, expression of UAS-CA-Ras was sufficient to increase the length of filopodia (4.27 ± 0.27 μm $p=0.0003$). These data implicate PIP_3 in the regulation of both filopodia number and length during DC.

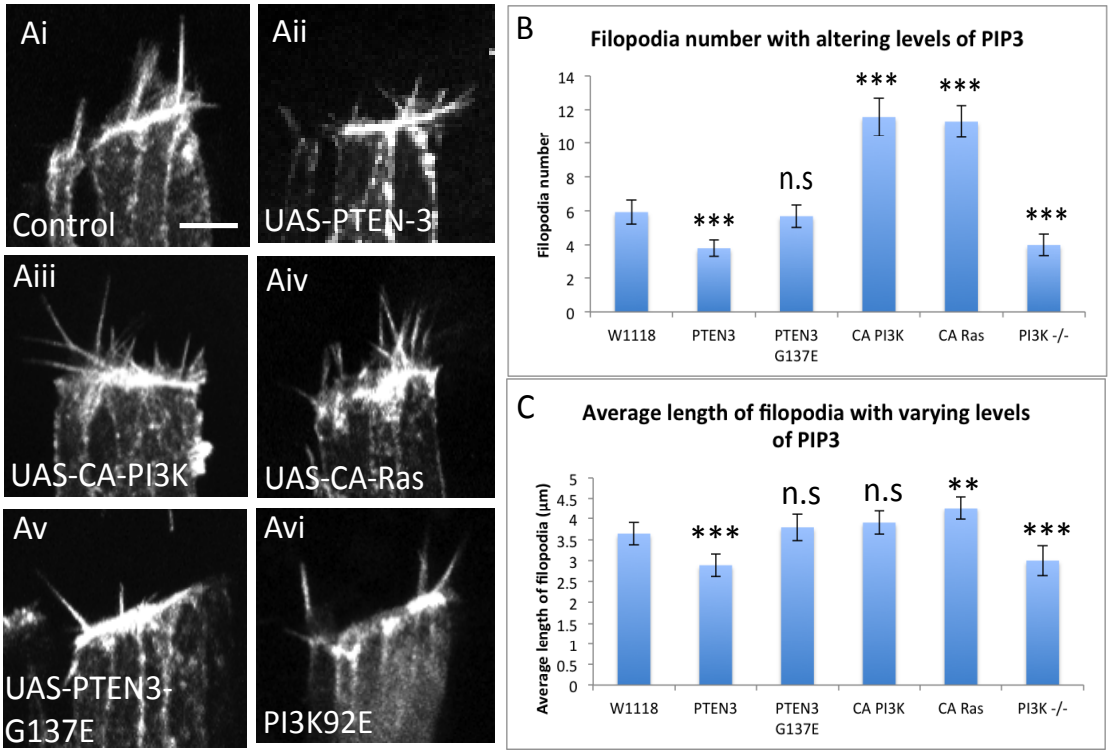

Figure 26. Effects of manipulating PIP_3 on filopodia number and length. Ai-v) snapshots taken from live imaging of embryos expressing transgenes in a subset of cells under the control of the *en*-Gal4 driver. Avi) Shows *en*-Gal4 driving expression of UAS-GFP-moesin alone in embryos lacking zygotic PI3K. B) Number of filopodia per *en*-Gal4 stripe expressing the indicated transgenes or in *pi3k92e*^{A} mutants. C) Length of filopodia in embryos expressing the indicated transgene. N ≥ 47 stripes from ≥ 11 embryos. *** indicates filopodia number is significantly different to control embryos (P<0.001), ** indicates (P<0.005 significance) and n.s. indicates no significant difference to the controls. Scale bars represent 5 µm

3.6 Wild-type Rac1 rescues the UAS-PTEN phenotype

To verify that the zippering defect observed upon depletion of PIP_3 is caused by the reduction in filopodial activity, we sought to increase the number of filopodia independently of PIP_3 levels to determine if this would rescue the DC defects observed when levels of PIP_3 were reduced. Rac1 is a well-known regulator of actin protrusions in a variety of contexts (Steffen *et al.* 2004; Stramer *et al.* 2005; Woolner *et al.* 2005; Yoo *et al.* 2010), and we observed expression of wild type Rac1 (UAS-Rac1-wt) increased the number of filopodia present during DC when it is expressed under the control of *en*-Gal4 alongside UAS-GFP-moesin (to visualise F-actin) (Figure 27 Biii). We sought to determine if co-expressing UAS-Rac1-wt and UAS-PTEN3 in *engrailed* stripes could rescue the DC defects observed when UAS-PTEN3 was expressed alone. We observed the levels of GPH in *engrailed* stripes co-expressing UAS-Rac1-wt and UAS-PTEN3 and did not observe an increase in levels of PIP_3, despite the increase in Rac present (Figure 27 A). This indicates that Rac regulates the formation of filopodia without affecting PIP_3 levels. When UAS-Rac1-wt was co-expressed alongside UAS-PTEN3 under the control of *en*-Gal4, in addition to UAS-GFP-moesin to visualise F-actin, we observed a rescue of the loss of filopodia phenotype observed when UAS-PTEN3 is expressed alone (W1118, 6.53 ± 0.53 filopodia; UAS-PTEN3, 4.86 ± 0.47 filopodia $p=0.0019$; UAS-Rac1-wt 10.27 ± 0.47 filopodia, $p= 0.0019$; UAS-PTEN3, UAS Rac1-wt 6.5 ± 0.58, $p>0.9999$) (Figure 27 B, C).

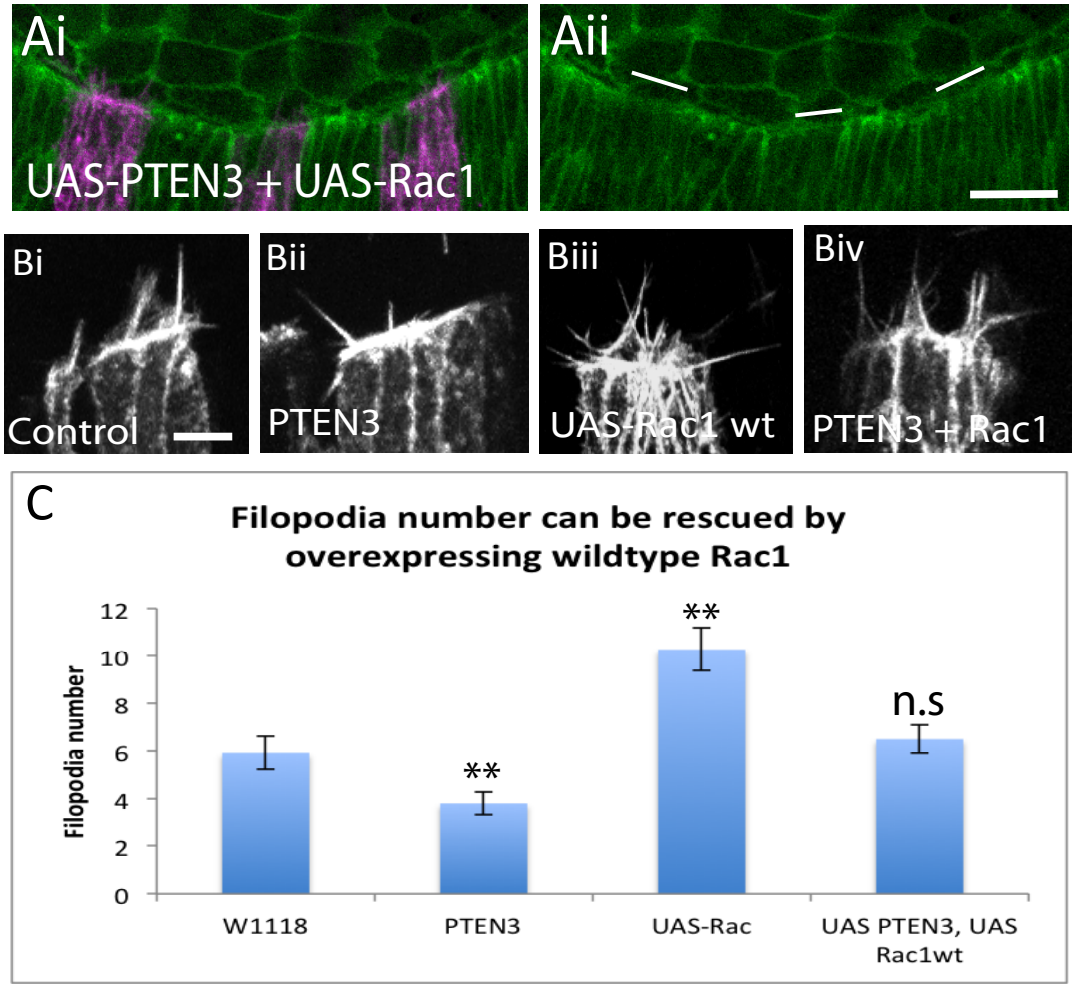

Figure 27. Rescue of the PTEN phenotype by expression of UAS-Rac1-wt. A) Co-expressing UAS-Rac1-wt alongside UAS-PTEN3 does not rescue the reduction in PIP_3 caused by expression of UAS-PTEN3 alone. B) Snapshots taken from live imaging embryos expressing the indicated transgene under the control of *en*-Gal4 driver. Quantification of the C) number of filopodia observed per stripe when *en*-Gal4 drives the indicated transcript. n ≥ 42 stripes from ≥ 10 embryos. ** indicates P<0.005 where n.s. indicates no significance between embryos expressing indicated transgene and control embryos. Error bars indicate S.E.M. Scale bar represents 5 μm

As co-expression of UAS-PTEN3 and UAS-Rac1-wt was able to rescue the filopodia number, we next investigated if it was also capable of rescuing the zippering defect observed with reduced levels of PIP_3. Expression of UAS-Rac1-wt in *engrailed* stripes was able to increase the rate of zippering along the dorsal midline (p=0.0171), when compared to control non-*engrailed* stripes. As in previous experiments, expression of UAS-PTEN3 reduced the rate of zippering (P=0.0254). When UAS-Rac1 and UAS-PTEN3 were co-expressed, the rate of zippering was comparable to control stripes (p>0.9999), indicating that expression of UAS-Rac1-wt is capable of rescuing the defects observed with expression of UAS-PTEN3 in a PIP_3 independent manner (Figure 28). These data suggest that PIP_3 contributes to zippering during DC by promoting filopodial activity at the leading edge.

3.7 PIP_3 is localised to sites of filopodia formation

As we have shown that PIP_3 is involved in the regulation of leading edge filopodia during DC, we next investigated the spatial and temporal relationship between the PIP_3 microdomains and filopodia formation. We live imaged embryos expressing UAS-m-Cherry-Moesin and UAS-GPH under the control of *en*-Gal4 to allow direct visualisation of PIP_3 and filopodia (Figure 29 A). This showed that significantly more filopodia arose from areas where PIP_3 was localised (61% compared to 39% filopodia not from PIP_3 microdomains, p<0.0001), and that the PIP_3 was localised to the base of the newly formed filopodia (n=22 embryos). The filopodia formed persisted longer than the microdomain of PIP_3, suggesting that PIP_3 is important in the initiation of filopodia rather than their persistence (Figure 29).

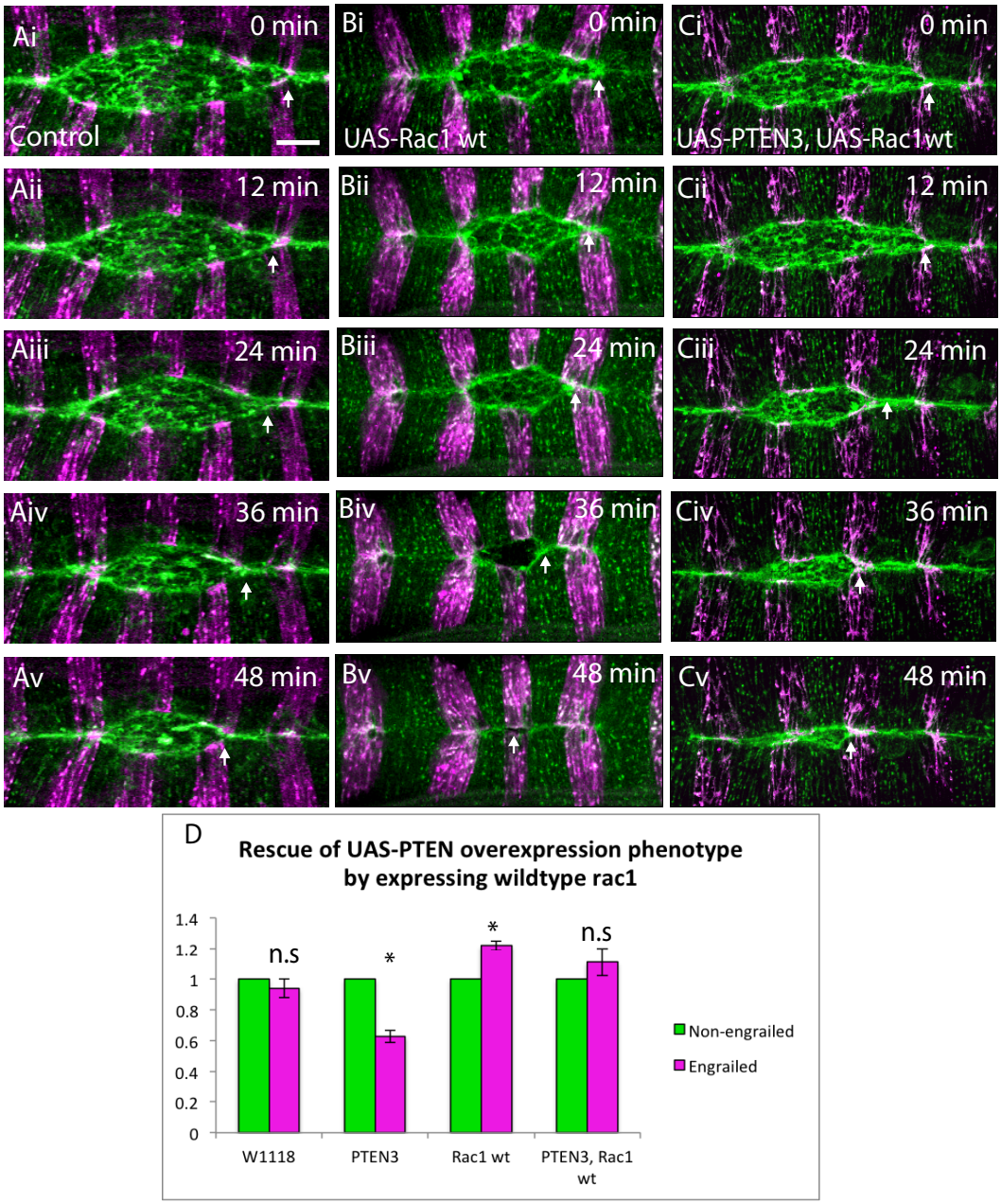

Figure 28. Expression of UAS-Rac1-wt rescues the zippering defect observed with reduced levels of PIP_3. A-C) exhibit stills take from time lapse movies in embryos expressing ubiquitous GFP-moesin (green) and UAS-Cherry-Moesin (magenta) under that control of *en*-Gal4. Embryos in B and C also express UAS-Rac1-wt and UAS-PTEN3, UAS-Rac1-wt respectively. Arrows indicate the location of the canthi in each image. D) Quantification of the effect of each of the transgenes on the rate of zippering when compared to the internal non-*engrailed* control. n ≥ 10 for each transgene. * indicates zippering is significantly different from control non-*en*-Gal4 stripes ($P<0.01$), n.s. indicates no significant difference. Error bars indicate S.E.M. Scale bars indicate 15 μm. Whole sequences are shown in movies 1, 6, 7 in appendix 2.

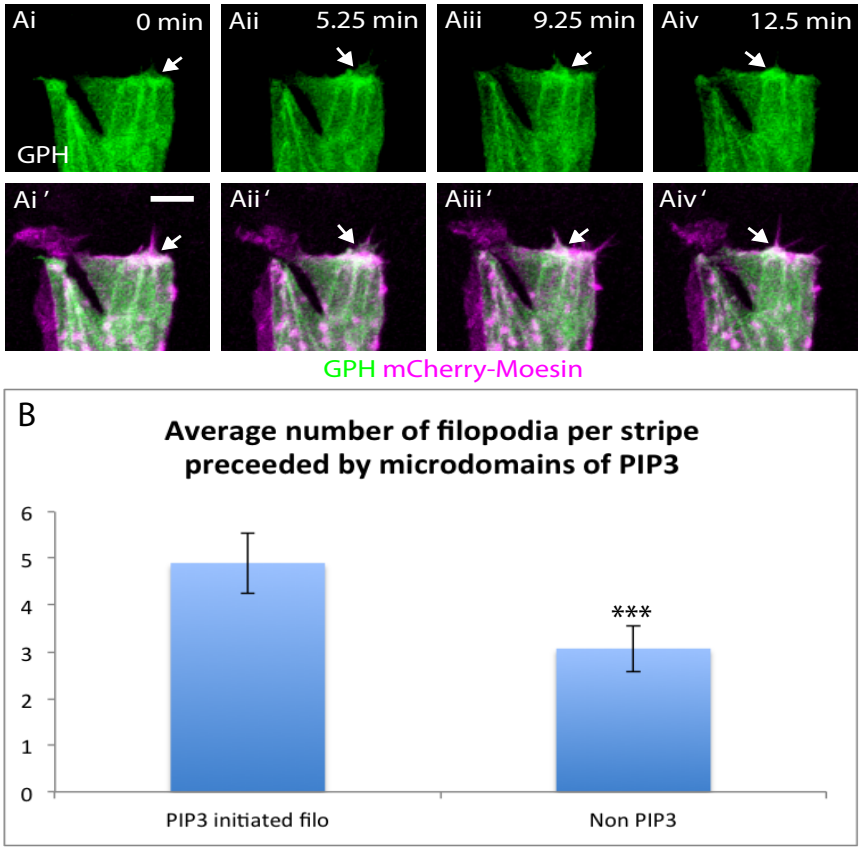

Figure 29. Correlation between PIP_3 localisation and filopodia formation. A) Time course of filopodia in an embryo expressing UAS-GPH and UAS-m-Cherry-Moesin under the control of *en*-Gal4, showing a correlation between leading edge PIP_3 accumulation and filopodia formation. B) Quantification of the number of filopodia formed preceded by a PIP_3 loci. *** indicates a significant difference between filopodia formed at an area with PIP_3 accumulation and those without ($P<0.001$). Error bars indicate S.E.M. Scale bar indicates 5μm. Whole sequence is shown in movie 8 appendix 2.

Chapter 3 discussion

3.8 PIP_3 is required for DC

PIP_3 has previously been shown to be involved in cell migration of *Dictyostelium* and neutrophils and also in the epithelial closure event neural tube closure (Funamoto *et al.* 2002; Pickett *et al.* 2008; Yoo *et al.* 2010). We therefore considered that it would be interesting to investigate whether PIP_3 might also play a role in DC.

Using tGPH (a PIP_3 marker), we observed PIP_3 to be localised at the front of DME cells, in particular, to cell junctions at the leading edge. This localisation is consistent with where dynamic actin rearrangements take place, in particular where actin protrusions are formed that are required for DC. These leading edge cell junctions have previously been identified as 'actin nucleation centres', as it is where the actin cable and actin rich protrusions first start to form (Kaltschmidt *et al*. 2002). Interestingly, actin regulating molecules such as Ena/VASP localise to the leading edge cell junctions in a similar manner to PIP_3 (Gates *et al*. 2007), suggesting that these regions could act as localisation points for actin regulators, ensuring that actin reorganisation occurs at the desired site. As PIP_3 accumulates in a similar pattern to previously identified actin regulators, it is possible that PIP_3 could be an upstream activator in the regulation of actin dynamics during DC. Interestingly, PIP_3 was not continuously associated with the leading edge during DC, but rather it was localised in a transient manner. This suggests that the presence of PIP_3 is not required continuously, and its leading edge accumulation could coincide with the dynamic assembly of actin protrusions observed during DC (Jacinto *et al.* 2000). We did not observe a difference in the leading edge actin cable in embryos with reduced levels of PIP_3 (figure 23), however, the thickness of the cable was not quantified, so it is possible that PIP_3 may also play some role in the polymerisation of actin required for actin cable formation. The localisation of PIP_3 at the leading edge could drive actin cytoskeletal rearrangements in a similar manner to those observed in neutrophil and *Dictyostelium* migration, establishing the front of the cell and promoting the formation of actin protrusions where required (Funamoto *et al.* 2001; Yoo *et al.* 2010). Once DC is complete, this specific junctional localisation of PIP_3 is lost, which could indicate that it is only necessary whilst actin assemblies are required for cell movement and fusion during DC.

To investigate the role of PIP_3 in DC, we determined that genetically altering its levels using the UAS-GAL4 system was the most consistent method to change the levels of PIP_3 either throughout the embryo or in a subset of cells. We also investigated the efficacy of pharmacological inhibitors and found they gave inconsistent results, possibly due to differences in the amount of inhibitor reaching the DME cells. Embryos zygotically null for components of the PI3K signalling pathway (*pi3k92e*^{A} and *pten*^{117}), although able to alter the

levels of PIP_3, were not as effective as genetically altering PIP_3 levels using transgenes, possibly due to the presence of maternally contributed protein in these mutants. Generating embryos lacking maternal and zygotic expression of PTEN was sufficient to dramatically and consistently increase the levels of PIP_3, however, using maternal mutants for PI3K was not possible. In addition, since PIP_3 signalling is known to regulate many processes in embryos, use of Gal4-driven transgenes was preferable as it allowed cell-specific disruption of PIP_3 signalling therefore minimising indirect effects due to defects in other tissues or cells. Altering levels of PIP_3 throughout the embryo resulted in changes in the shape of the dorsal hole, with reduced levels of PIP_3 (by expressing UAS-PTEN3 or using *pi3k92e*^{A} mutant embryos) resulting in an elongated dorsal hole, which has previously been associated with impaired fusion of the two leading edges during DC (Woolner *et al*. 2005). The defects observed in embryos with reduced levels of PIP_3 could be consistent with cells being unable to effectively determine a front and as such display impaired actin protrusion formation required for efficient epithelial fusion (Funamoto *et al*. 2001; Jacinto *et al*. 2000; Woolner *et al.* 2005). This result is comparable to studies in neural tube closure, where filopodia have been shown to be required for the fusion of the epithelial sheets, and a reduction in levels of PI3K resulted in spina bifida due to impaired epithelial fusion along the neural midline although in this case it is not known whether the impaired fusion is a direct result of reduced filopodia (Pickett *et al.* 2008; Pyrgaki *et al.* 2010; Pai *et al.* 2012).

Increasing the levels of PIP_3 (induced by expressing UAS-CA-PI3K or using *pten*^{117} zygotically null or maternally and zygotically null embryos) resulted in shortened dorsal holes, which could be consistent with epithelial fusion occurring at a faster rate than controls. This is consistent with our hypothesis of PIP_3 acting to control cytoskeletal rearrangements in DME cells required for efficient epithelial fusion. Embryos lacking maternal and zygotic expression of PTEN, in addition to the shortened dorsal hole, also displayed a range of phenotypes including embryos that arrested early in development. The failure early in embryogenesis could be explained by an increase in PIP_3 levels in all cells on all cell junctions. As both PTEN and PIP_3 have been linked to establishing cell polarity (Funamoto *et al.* 2002), a loss of PTEN could result in an inability of cells to undergo actin reorganisation at the correct location, required for early developmental events such germband retraction. The variation in defects observed in embryos lacking maternal and zygotic expression of PTEN could be explained by the ability of other pathways to regulate cell polarity, or that the expression level of PI3K and therefore PIP_3 levels could vary from embryo to embryo. These results implicate PIP_3 as a regulator of epithelial fusion during *Drosophila* DC.

3.9 PIP_3 regulates filopodia formation and zippering during DC

We demonstrate that PIP_3 is required for the regulation of filopodia at the front of DME cells and as such regulates the rate at which zippering occurs. Increasing levels of PIP_3 increases the number of filopodia present and increases the rate of zippering, whilst reducing PIP_3 levels, reduces the number of filopodia present and reduces the rate of zippering. It is likely that the changes observed in DC on altering PIP_3 levels is a direct result of changes in filopodia number. Filopodia have previously been shown to be vital for the process of zippering (Jacinto *et al*. 2000; Woolner *et al.* 2005), which is consistent with our observation during DC. In addition to having an effect on the formation of filopodia, it is possible that PIP_3 also acts to identify the front of the DME cells, so determining where actin rearrangements should occur (Zhou *et al.* 1998; Funamoto *et al.* 2002; Loovers *et al.* 2006; Nisho *et al*. 2007; Yoo *et al.* 2010).

In addition to affecting filopodia number, we show PIP_3 to be a regulator of filopodia initiation. We observed the preference for filopodia to be formed from microdomains of PIP_3 at the front of DME cells. This is consistent with previous work in neurons, where in response to a chemoattractant, filopodia are formed at sites of localised microdomains of PIP_3, which in turn drive the formation of localised patches of actin, a subset of which, give rise to filopodia (Ketschek *et al*. 2011). We also identified a possible role for PIP_3 in regulating the length of the filopodia. Reducing PIP_3 levels (by expressing UAS-PTEN3) resulted in shorter filopodia, however, increasing the levels of PIP_3 (by expressing UAS-CA-PI3K) did not have an effect on the length of filopodia. This could suggest that PIP_3 somehow plays a role in protecting the actin filaments from depolymerisation, however no link between PIP_3 and filament elongation/retraction has been shown. In contrast to the effect of expressing UAS-CA-PI3K, increasing levels of PIP_3 by expression of UAS-CA-Ras did result in an increase in filopodia length. This could be due to Ras acting upstream of other signalling pathways in addition to PI3K. One possibility could be via the Ras/Mek/Erk pathway, especially as in Glomerula epithelial cells, an increase in the level of Erk results in an increase in cortical F-actin, providing a possible additional link between Ras and filopodia (Bijian *et al.* 2005).

During these experiments, we demonstrate that manipulating levels of PIP_3 resulted in a change in both filopodia and zippering, but did not have an effect on segmental alignment. This is consistent with work carried out in neutrophils, where loss of PI3K resulted in defects in polarisation and migration, but not in sensing (Nisho *et al*. 2007). On the rare occasions where segmental misalignment was observed, it is likely that this defect was primarily due to the stripes with reduced levels of PIP_3 failing to zipper quick enough and so being pushed back from the leading edge.

It well documented that filopodia are required for zippering (Jacinto e*t al*. 2000; Wood *et al*. 2002; Woolner *et al*. 2005; Millard and Martin 2008), and we have demonstrated a role for PIP_3 in the regulation of filopodia, however, there was the possibility that the effects on zippering observed by decreasing levels of PIP_3 were a result of changes in other cell processes such as the adhesion of the two epithelial edges or the formation of septate junctions. However, we demonstrated that increasing the filopodia number independently of PIP_3 was sufficient to rescue all DC defects observed when PIP_3 levels were reduced. This indicated that the zippering defect observed with reduction of PIP_3 levels almost certainly is as a result of a reduction in filopodia number.

We have demonstrated a role for PIP_3 in the regulation of filopodia and zippering during *Drosophila* DC, however we do not see complete loss of filopodia or complete failure of DC. It is possible that we are not expressing sufficient UAS-PTEN3 to completely eliminate PIP_3. If we were to increase the number of copies of UAS-PTEN3 present, we might be able increase the PIP_3 removal further which might then completely eliminate filopodia. Alternatively, it is possible that there are multiple pathways working in a partially redundant manner to regulate the formation of filopodia. Cdc42 has been shown to be a regulator of filopodia both *in vitro* and *in vivo* (Nobes and Hall 1995; Kozma *et al.* 1997; Wood *et al.* 2002) through activation of the NPF WASP, which then activates the Arp2/3 complex. It is possible, that even when PIP_3 levels are reduced, Cdc42 is able to activate WASP and Arp2/3 to regulate the formation of filopodia, reducing any observable effects.

Although DC requires collective cell migration to achieve proper closure and previous work has demonstrated the importance of PIP_3 in single cell migration, it is likely that the role of PIP_3 is consistent between the two cell migration types, with its role being important in identifying the front of the cell, reorganising the actin cytoskeleton and determining the direction of movement (Sasaki *et al.* 2004).

3.10 Summary

We have shown that during DC, leading edge accumulation of PIP_3 is required for the formation of filopodia, which are vital to the process of zippering. In addition we demonstrate that there is a bias for the formation of filopodia from PIP_3 microdomains, perhaps suggesting that PIP_3 may be important for the initiation of filopodia. As PIP_3 is localised at leading edge junctions, which have previously been described as actin nucleation centres (Kaltschmidt *et al.* 2002), it is likely that PIP_3 has some function in regulating the activation of the protrusion-forming proteins stored at these cell junctions.

Chapter 4. Downstream effectors of PIP_3 in DC

We have demonstrated that PIP_3 is a regulator of actin protrusion formation during DC. This is consistent with previous work where PIP_3 has been shown to be vital for the reorganisation of the actin cytoskeleton in a variety of systems, including *Dictyostelium*, *Drosophila* and zebrafish cell migration (Funamoto *et al.* 2001; Funamoto *et al.* 2002; Wood *et al.* 2006; Yoo *et al.* 2010). However, how PIP_3 regulates the actin cytoskeleton is not well understood and appears to vary between systems. One way in which PIP_3 can regulate the actin cytoskeleton is through interaction with Rho GEFs, but the effect of this interaction appears to vary depending on the specific GEF. In HEK 293T cells, the Rho/Rac GEF Vav exists in an auto-inhibited conformation, however upon binding to PIP_3 this auto-inhibition is released, resulting in the activation of Vav (Das *et al*. 2000). Additionally, Tiam1 is a Rac specific GEF which likely exists in an auto-inhibited conformation and it has been proposed that binding to PIP_3 is capable of relieving this, thus promoting Rac activation (Fleming *et al*. 2000). PIP_3 has also been shown to be required for the recruitment of Dock180 to the cell membrane in HEK 293T cells by binding to the DHR-1 domain in Dock180, whilst the DHR-2 domain was required for binding to nucleotide free Rac (Côté and Vuori 2002). Unlike the interaction between PIP_3 and Tiam1, no role for the activation of Dock180 by PIP_3 has been identified, but PIP_3 may instead regulate Dock180 by controlling its localisation.

In each case, interaction between PIP_3 and Rac GEFs results in the activation of the specific GTPase and downstream signalling pathways required for the reorganisation of the actin cytoskeleton necessary for cell migration (reviewed by Ridley 2001; Sun *et al.* 2004; Yoo *et al.* 2010). This ability of PIP_3 to bind to and activate GEFs, so promoting the activation of GTPases has also been observed *in vivo*. In zebrafish neutrophils, PIP_3 activates Rac through Dock180 at the front of migrating neutrophils. This activation of Rac is required for the polarisation of the cell, polymerisation of actin and directional cell migration (Yoo *et al,* 2010). Given the interaction between PIP_3 and Rac specific GEFs in other systems, it is possible that in DC, PIP_3 regulates the actin cytoskeleton by regulating the activation state of Rac, which could then promote actin polymerisation in a Scar/Wave dependent manner (Steffen *et al*. 2004). Experiments were therefore performed to determine whether Rac and Rac-specific GEFs might act downstream of PIP_3 during DC.

4.1 Confirmation of *rac* mutant genotypes

To determine if Rac is a downstream effector of PIP_3, we chose to investigate the effect of loss of Rac during DC. Previous studies have demonstrated redundancy between the three Drosophila *rac* genes, therefore all three must be mutated to achieve complete loss of Rac function. Two triple *rac* mutant lines have previously been used extensively. These two lines

share the same deletions of *rac2* and *mtl*, but have different loss-of-function point mutations in *rac1*, which are known as $rac1^{J10}$ and $rac1^{J11}$. The *rac* triple mutant lines bearing these two mutations will henceforth be called rac^{J10} and rac^{J11} in this thesis (Figure 30). Due to a lack of observable phenotypes when initialy using these lines (the dorsal hole, CNS and musclulature appeared normal) (data not shown), we obtained the lines again and carefully checked that the reported mutations were present, as it is known that these triple mutant lines can be unstable (personal communication S. Woolner). To determine the absence of the *rac* genes we used two approaches; firstly, we observed the CNS and muscle phenotypes that had previously been described and secondly we molecularly determined the absence of *rac2* and *mtl*, and sequenced *rac1* to determine the presence of the reported point mutations (Hakeda-Suzuki *et al* 2002; Ng *et al*. 2002).

Carrying out neuronal flat preps and staining for FasII and F-actin, we were able to observe that embryos lacking expression of Rac exhibited defects in both axonal and muscular development (Figure 31 Ai-iii). Additionally, as the genotypes for both lines have been well characterised, using PCR we were able to determine the presence of *rac1* and the absence of *rac2* and *mtl* from both of the mutant lines as expected, indicating that they had either been partially or completely excised (Figure 31 B).

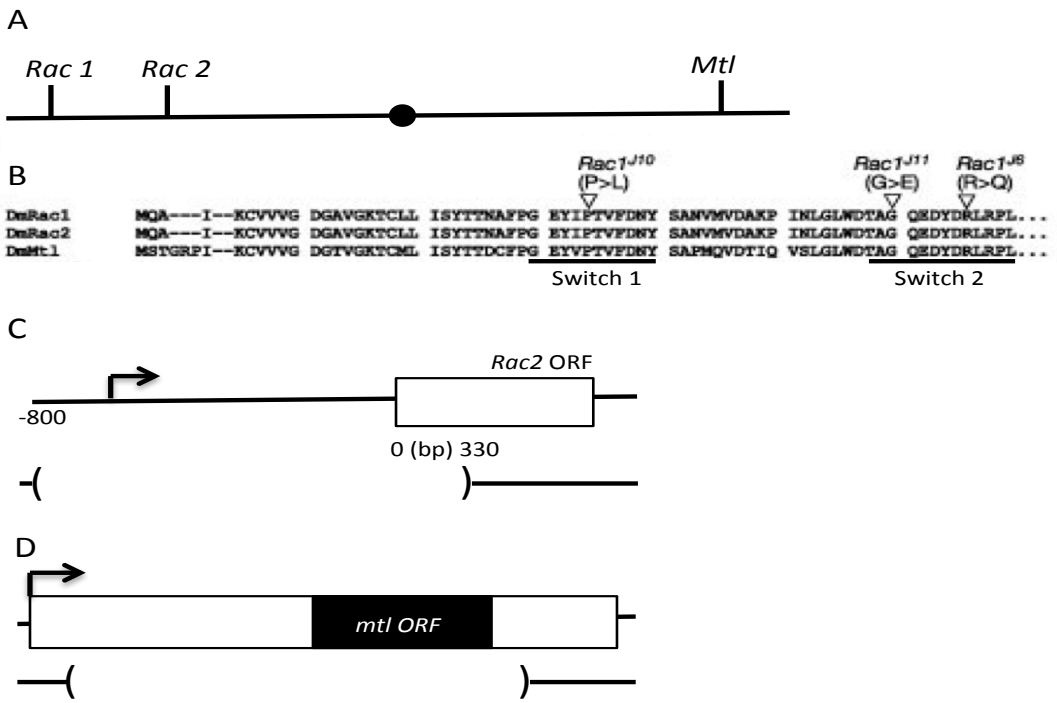

Figure 30. Schematic of Rac GTPase genes and mutant alleles A) Location of the three *rac* genes on the third chromosome. B) N-terminal residues of the 3 *rac* genes, also showing the 3 point missense mutations within the switch regions. C) Genomic organisation of *rac2* showing with the bracketed region deleted in the *rac* mutants. D) Genomic organisation of *mtl*, with the bracketed region indicating the 2068bp deleted region. The shaded region indicates the coding region of the gene (Hakeda-Suzuki *et al.* 2002; Ng *et al*. 2002)

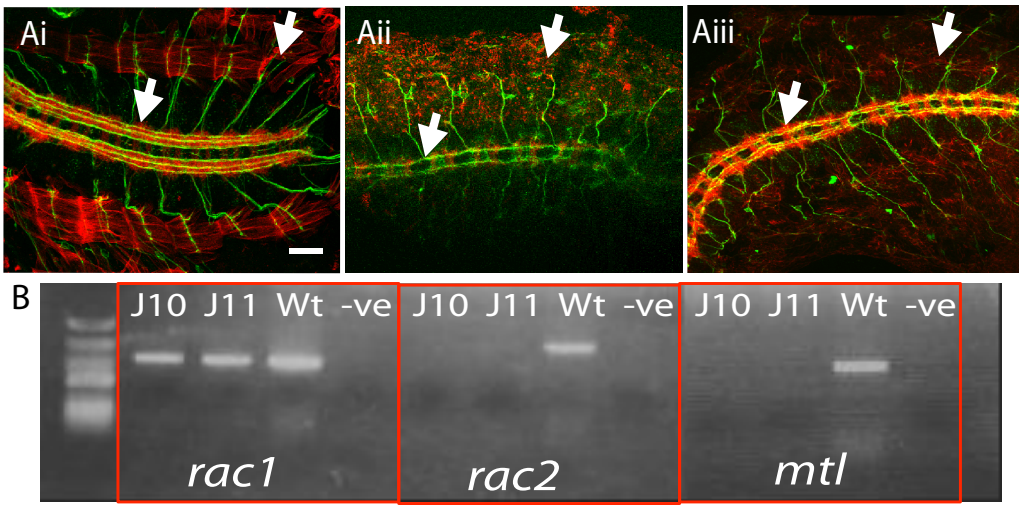

Figure 31. Profiling of *rac*^{J10} and *rac*^{J11} triple mutant fly lines. A) FasII staining of Ai) control Aii) *rac*^{J10} and Aiii) *rac*^{J11} mutant embryos with strong CNS and muscle phenotypes. Arrows in Ai) show normal muscle and CNS phenotype, where those in Aii and Aiii show dissociated muscle (red) and termination of axons and longitudional axons crossing the central midline. Scale bar represents 38 μm. B) PCR of the two *rac* mutant lines (with wild type controls) shows that the *rac1* gene is present and both *rac2* and *mtl* have been lost in both lines.

Both mutant alleles of *rac1* are caused by point mutations, and as such sequencing was required to confirm whether the mutation was present. In the case of *rac1*^{J10}, the point mutation is at codon 34, and is a change from a proline to a leucine, while *rac1*^{J11} has a mutation at codon 60, resulting in a change from lysine to glutamate. We found that these mutations were indeed present in the two lines (Figure 32). In addition to the two mutations that have been previously reported, we observed further mutations in our lines. For *rac1*^{J10}, two additional mutations were present, one at codon 78 which did not result in an amino acid change, and another at codon 119, which resulted in a change from arginine to histidine. This is a relatively conservative substitution in a short linker between two alpha helices and the residue is not conserved between GTPases or known to have an essential function (Hirshberg *et al.* 1997).

Rac1^{J11} had one additional mutation at codon 84 which did not result in an amino acid change. The presence of the expected point mutations in the *rac1* gene and the absence of *rac2* and *mtl*, identifies our lines as triple mutants which we could confidently use in further studies to investigate the effect of loss of Rac function. In addition, expressing a dominant negative form of Rac1 (Rac1-N17) has been reported to produce similar phenotypes to loss of all three Rac genes, providing an additional method to interfere with Rac signalling (Harden *et al.* 1995)

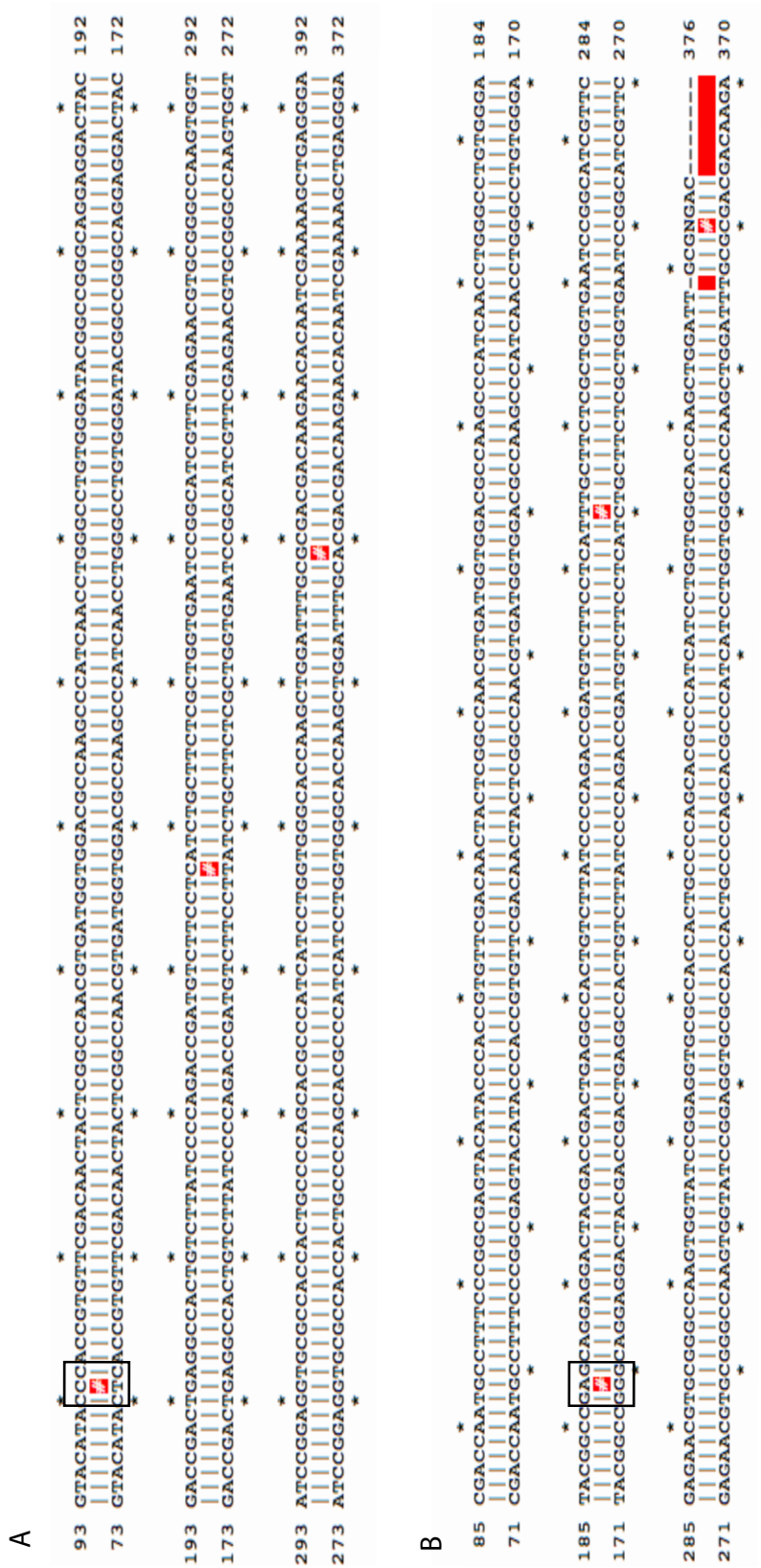

Figure 32. *Rac1* sequencing. Sequencing of A) *rac1*^{J10} and B) *rac1*^{J11} to identifying the presence of the point mutations at codons 34 and 60 respectively rendering the protein non-functional. Two additional mutations were identified in *rac1*^{J10} (codon 78 and 119), and one additional mutation in *rac1*^{J11} (codon 84), none of which resulted in a functional change.

4.2 Embryos with reduced levels of PIP_3 and Rac display similar phenotypes

To look for potential similarities between the effects of loss of Rac activity and reducing PIP_3 levels, we first investigated the effect of expression of dominant negative Rac during DC. Expression of either UAS-PTEN3 (to reduce PIP_3) or UAS-Rac1-N17 (dominant negative Rac1) under the control of *en*-Gal4, allowed analysis of the effect of expression of the transgenes on a subset of cells throughout DC. Additionally, UAS-m-Cherry-Moesin was expressed to visualise the cells in which the transgenes were expressed and cGMA was also expressed to allow visualisation of F-actin throughout the embryo. We observed that during DC, expression of either PTEN3 or Rac1-N17 occasionally resulted in the splaying of engrailed stripes at the DC leading edge. If the splaying is severe enough, segmental misalignment or puckering can occur along the dorsal midline as DC progresses (Figure 33 A-C). Expressing UAS-PTEN3 throughout the embryo under the control of *tubP*-Gal4 resulted in an elongated dorsal hole, which is also observed in in zygotic rac^{J11} mutant embryos (Figure 33 D-F). This phenocopying between embryos with reduced levels of PIP_3 or Rac suggests that the two may work in they same pathway.

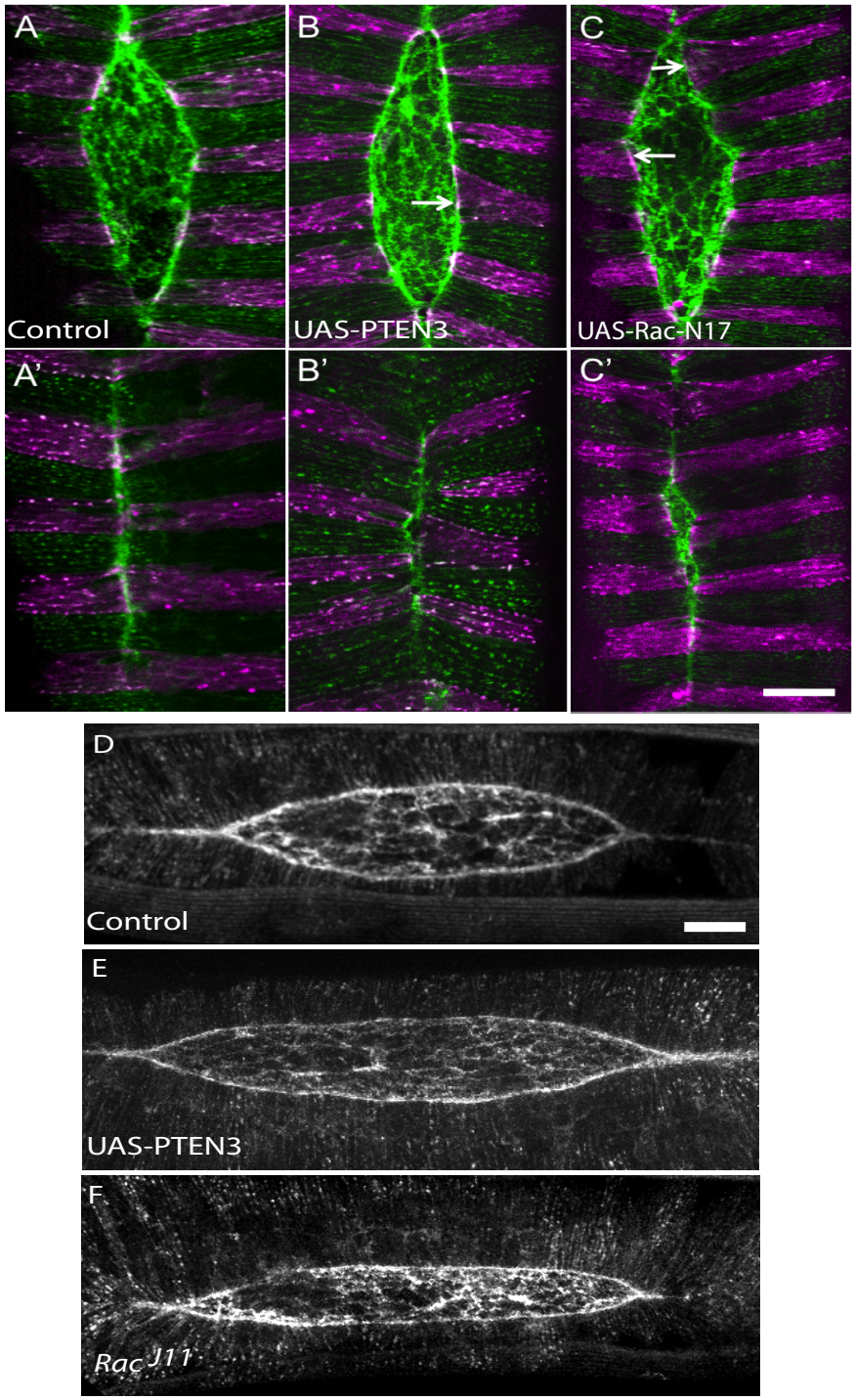

Figure 33. Similarities in DC defects in embryos with reduced levels of PIP_3 and those lacking expression of zygotic Rac. A, A') Control embryos displaying correct segmental spacing and alignment during DC and at the end of DC. B) embryos expressing UAS-PTEN3 in *engrailed* stripes (magenta), display splayed stripes (arrows), that can result in B') segmental mis-alignment. C) UAS-Rac1-N17 expression in *engrailed* stripes (magenta) also results in splayed stripes (arrows) and C') puckering along the dorsal midline. Similarities in DC phenotype in embryos with E) reduced levels of PIP_3 and in rac^{J11} mutants when compared to D) controls. Scale bar A-C represents 29 µm, and D-F 31 µm.

4.3 PIP_3 is upstream of Rac in the regulation of filopodia in DME cells

To determine if PIP_3 is upstream of Rac in DC, in particular in the regulation of filopodia formation, we investigated the effects of increasing the levels of PIP_3 in embryos lacking zygotic expression of Rac. If PIP_3 is upstream of Rac, increasing the levels of PIP_3 (by expressing UAS-CA-PI3K) should have no effect on filopodial number in embryos lacking Rac expression. Expressing UAS-CA-PI3K under the control of *en*-Gal4, along with UAS-GFP-Moesin (to visualise the F-actin), resulted in a significant increase in the number of filopodia observed, consistent with findings previously described in this thesis (9.85 ± 0.91 filopodia per stripe when compared to controls – 5.82 ± 0.63 filopodia per stripe, $p < 0.0001$). Loss of zygotic Rac expression resulted in a significant decrease in the number of filopodia at the DC leading edge (3.4 ± 0.51 filopodia per stripe, $p<0.0001$). Interestingly, expressing UAS-CA-PI3K in embryos lacking zygotic expression of Rac did not result in an increase in the number of filopodia (3.56 ± 0.47, rac^{J10} vs UAS-CA-PI3K;; rac^{J10} $p>0.9999$), suggesting that the capacity of CA-PI3K to increase filopodial activity is dependent on Rac. We also observed the effect on filopodia of expressing CA-PI3K in embryos with one copy of each Rac gene ($rac^{J10/+}$) and found that filopodia numbers slightly elevated from control levels (7.41 ± 0.55 filopodia per stripe $p=0.0054$). This suggests that the ability of CA-PI3K to enhance filopodia number is reduced when Rac activity is reduced but not eliminated. (Figure 34).

In addition to expressing UAS-CA-PI3K in rac^{J10} null embryos, we also expressed UAS-CA-PI3K alongside UAS-Rac-N17, as an alternative method of decreasing Rac levels within the embryo. As previously, expression of UAS-CA-PI3K resulted in the increase in the number of filopodia (9.34 ± 0.79 compared to 6.41 ± 0.53 for controls $p=0.0003$). Expression of UAS-Rac-N17 under the control of the *en*-Gal4 driver resulted in the decrease in the number of filopodia observed at the DC leading edge (5.16 ± 0.47 filopodia per stripe $p=0.0462$). Expressing UAS-CA-PI3K alongside UAS-Rac-N17 did not result in an increase in the number of filopodia present (5.59 ±0.67 filopodia per stripe), compared to expression of UAS-Rac-N17 alone ($p>0.9999$) (Figure 35).

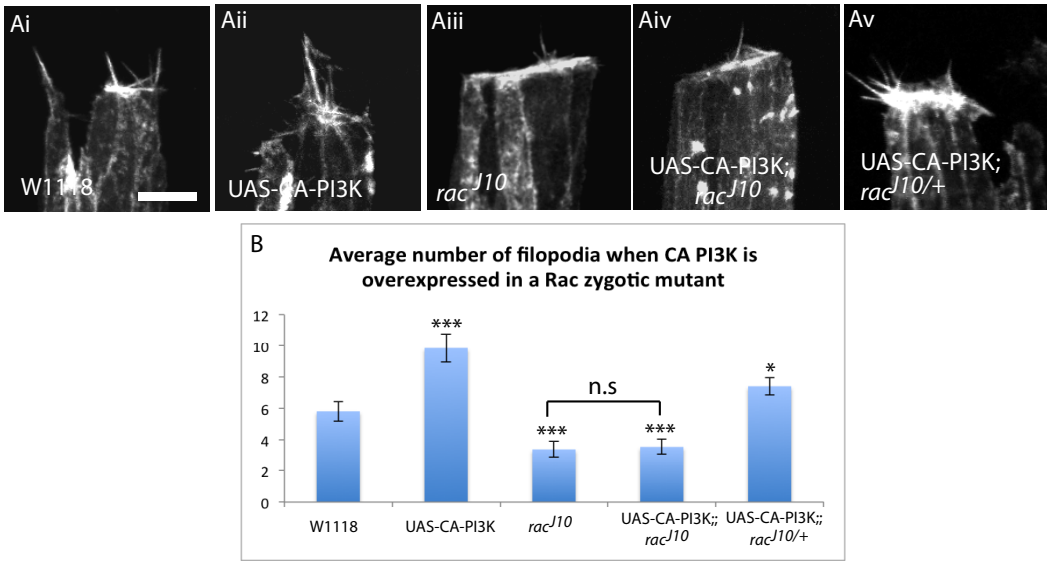

Figure 34. Increasing levels of PIP_3 in Rac zygotic mutants does not result in an increase in filopodia number. Ai-v) Live images taken of *engrailed* stripes expressing the indicated transgenes of mutant lines. B) Quantitation of the number of filopodia per stipe with varying levels of PIP_3 or Rac. n ≥ 46 stripes or ≥ 10 embryos. *** indicates a significant difference from control of P<0.001, * indicates a significant difference of P<0.01 where n.s. indicates no significant difference from the control. Error bars indicate S.E.M. Scale bar indicates 5 μm

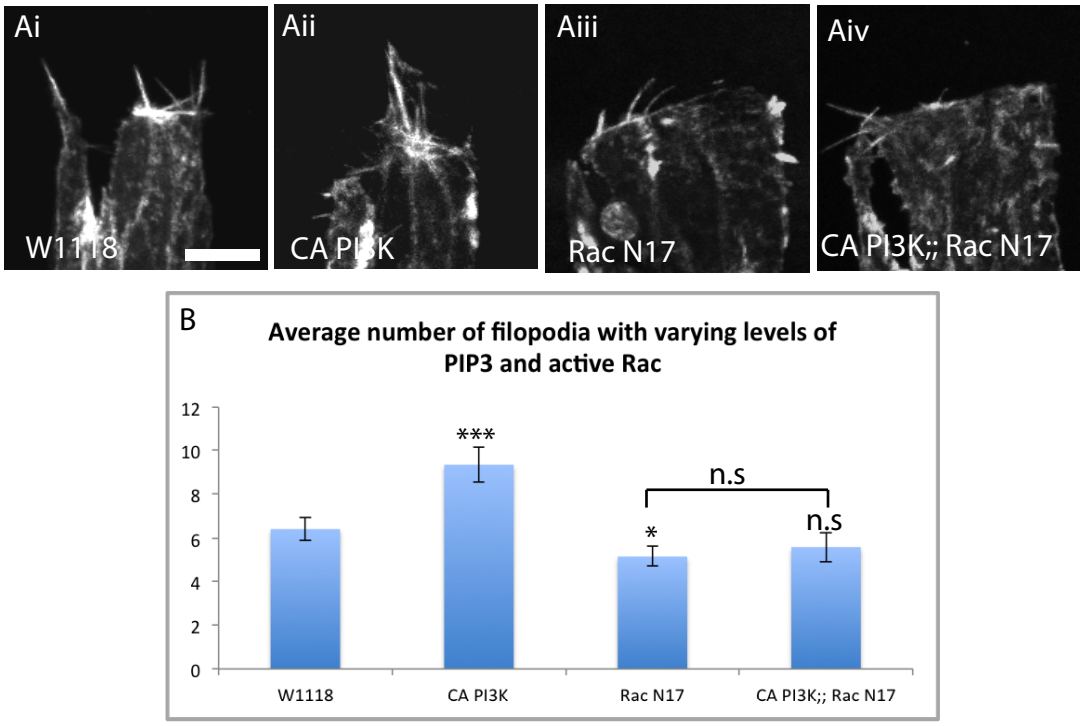

Figure 35. Increasing PIP_3 levels whilst expressing UAS-Rac-N17 does not result in an increase of filopodia. Ai-v) Live images taken of leading edge filopodia in embryos either expressing the indicated transgene or mutant for the indicated gene. B) Quantitation of filopodia number when the levels of PIP_3 and active Rac are altered. n ≥ 22 stripes, ≥ 6 embryos. *** indicates a significant difference with the control of P<0.001, * indicates a significant difference of P<0.01 and n.s indicates no significant difference. Error bars indicate S.E.M and the scale bar indicate 5 μm.

4.4 There is no positive feedback loop between Rac and PI3K in DC

As the presence of a positive feedback loop between Rac and PI3K has previously been described in zebrafish neutrophil migration (Yoo *et al.* 2010), we sought to determine whether a similar feedback loop might act during DC. If a feedback loop existed, we would expect that altering the levels of Rac would result in a change in PIP_3 levels. To investigate this, we observed the localisation of GPH in embryos lacking zygotic expression of Rac. Despite there being noticeable DC defects in rac^{J10} embryos, the distribution of GPH (and so PIP_3) remained unchanged, suggesting that reducing levels of Rac does not affect PIP_3 accumulation at the leading edge (Figure 36 A, B).

To further verify the absence of a positive feedback loop during DC, we altered the levels of Rac in *engrailed* stripes and observed the effect on leading edge PIP_3. To reduce the levels of active Rac, we overexpressed UAS-Rac-N17 under the control of *en*-Gal4 in embryos expressing tGPH in addition to UAS-m-Cherry-Moesin, to allow visualisation of where the transgenes are being expressed. In these embryos, no difference in the accumulation of PIP_3 was observed in stripes with reduced active Rac (Figure 36 C). Additionally, we also increased the levels of total Rac by expressing UAS-Rac1-wt under the control of *en*-Gal4. Interestingly, although we expected either an increase in PIP_3 or for PIP_3 levels to remain unchanged, we observed a decrease in PIP_3 at the leading edge (Figure 36 D).

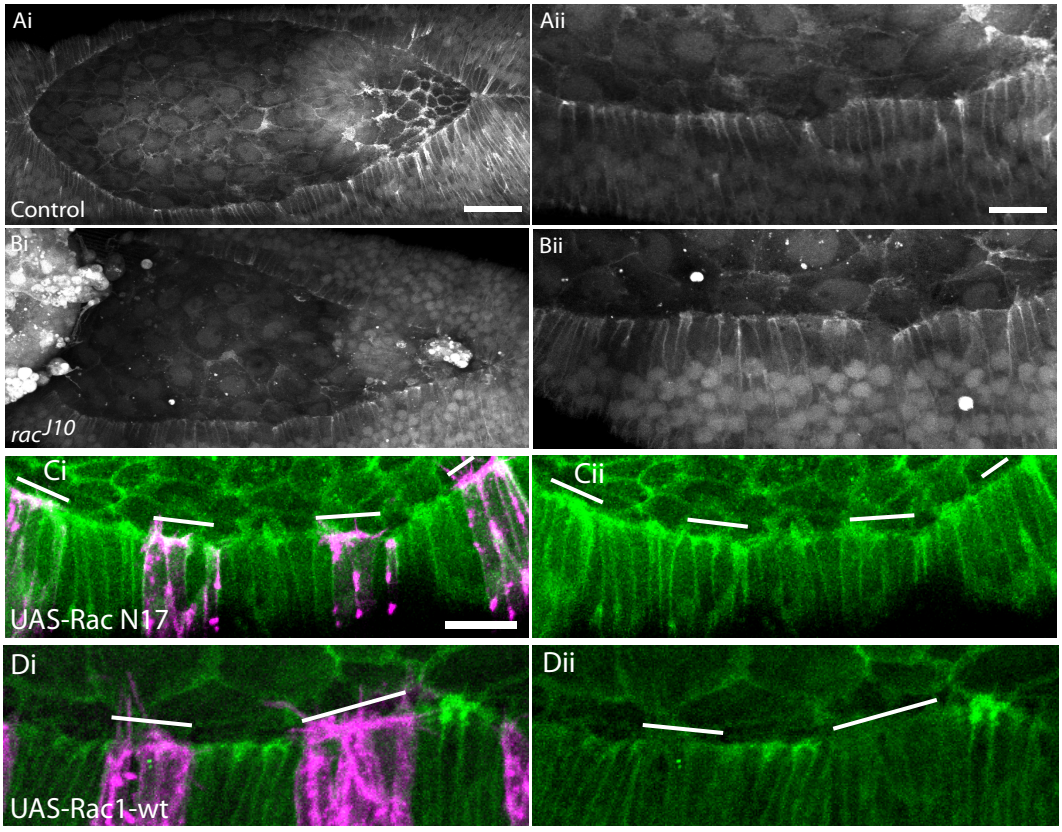

Figure 36. Increasing levels of Rac affects PIP_3 levels. GPH localisation in Ai, ii) wild type embryos and in B i and ii) embryos lacking zygotic expression of Rac^{J10}. Ci-ii) Expression of UAS-Rac-N17 alongside UAS-m-Cherry-moesin (magenta) under the control of *en*-Gal4 in embryos expressing tGPH. Di-ii) UAS-Rac1-wt expressed in *engrailed* cells (magenta) in embryos expressing tGPH. Scale bar indicates 12 μm for all images, except Ali and Bii where the scale bar represents 24 μm

4.5 Myoblast City (Dock180) as a PIP_3 effector/Rac regulator

As we have shown that PIP_3 is an upstream regulator of Rac during DC, we next sought to determine how PIP_3 regulates Rac. GTPases are activated by GEFs (which promote the exchange of GDP for GTP) and inactivated by GAPs (which inactivate the GTPase by promoting the hydrolysis of GTP to GDP). We therefore investigated GEFs as potential downstream targets of PIP_3.

In *Drosophila* there are 23 known Rho family GEFs, and of these we identified two good candidates to be Rac activators during DC; Myoblast City (MBC), the *Drosophila* homologue of Dock180, and still life (Sif) the homologue of Tiam1. MBC and Sif were good candidates as they both contain regions that bind to PIP_3 (either the PH domain in Sif or the DHR-1 domain in MBC), and are both Rac-specific GEFs (Micheils *et al*. 1995; Kiyokawa *et al.* 1998). ModENCODE expression data suggests that Sif expression is low in DC-stage embryos, whereas MBC is highly expressed throughout early embryogenesis (Graveley *et al*. 2011), we decided that MBC would be the better candidate to investigate first. In addition, MBC has previously been reported to exhibit defects in DC (Erickson *et al.* 1997) (Figure 37).

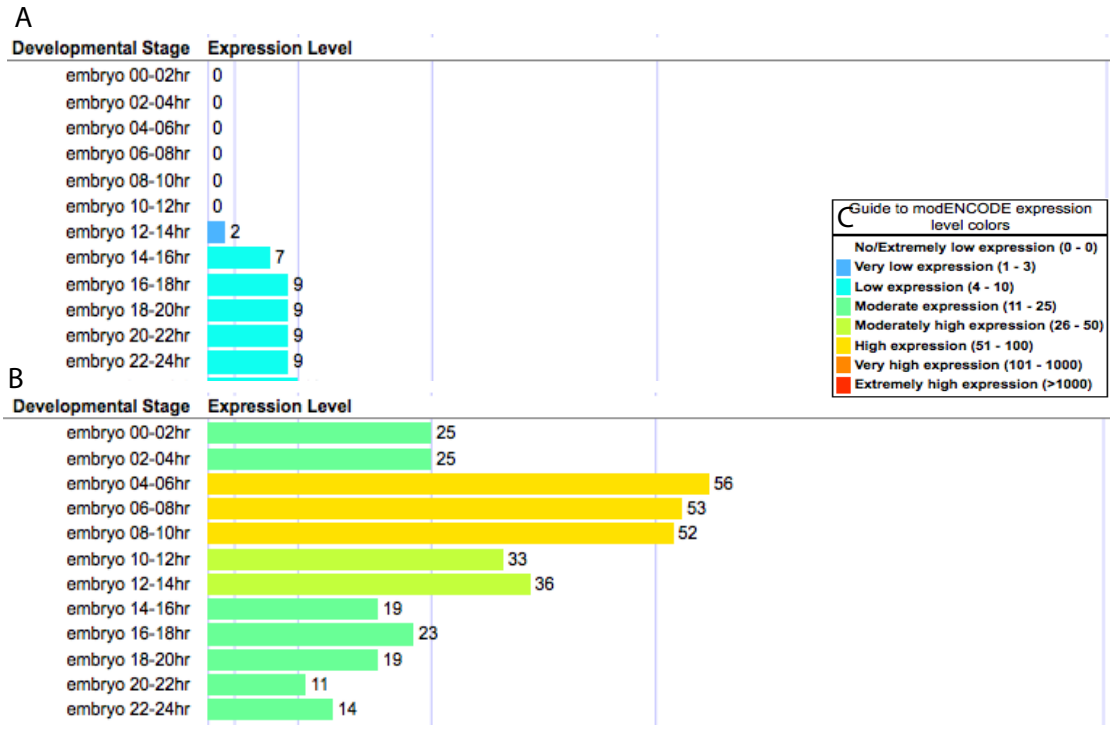

Figure 37. ModENCODE data for MBC and Sif. Expression profile of A) Still life and B) Myoblast city during development. C) Indicates levels of expression levels. Tables obtained from modENCODE Temporal Expression Data (Gravely *et al*. 2011).

4.5.1 MBC in DC

To determine whether MBC might link PIP_3 to Rac during DC, we first investigated the effect of loss of MBC on the shape of the dorsal hole. To do this we expressed GFP-moesin ubiquitously in embryos lacking zygotic expression of MBC. We used two distinct loss of function alleles of *mbc*: mbc^{c1} and $mbc^{d11.2}$. Both alleles exhibited a wide range of DC phenotypes (Figure 38. A, B); 38% of embryos displayed an elongated dorsal hole, 11% developed a hole between the amnioserosa and the dorsal leading edge, 27% of embryos had defects in head involution and/or tail retraction, 3% of embryos displayed an early embryonic defect, likely due to a failure of germband retraction to occur correctly and 21% appeared to have no DC defects (n = 37 embryos). To ensure that the defects observed were due to the lack of *mbc* expression, we observed DC in transheterozygous embryos ($mbc^{c1/d11.2}$). These embryos also exhibited DC phenotypes indicating that the defects observed were almost certainly due to a loss of MBC expression (Figure 38 C).

4.5.2 MBC is acting downstream of PIP_3 in DC

To assess if MBC is working downstream of PIP_3 in DC, we analysed the effects of increasing PIP_3 in mbc^{c1} mutant embryos. We assessed the number of filopodia in embryos expressing UAS-CA-PI3K, but lacking zygotic expression of MBC, with the rationale that, if MBC is downstream of PI3K, filopodia number should not increase with expression of UAS-CA-PI3K. As previously, expression of UAS-CA-PI3K in *engrailed* stripes (also expressing UAS-GFP-Moesin to visualise F-actin) resulted in an increase in the number of filopodia (10.32 ± 0.73 filopodia per stripe compared to 7.72 ± 0.68 filopodia per stripe in control embryos. $p = 0.002$). In embryos lacking expression of MBC a significant reduction in filopodia was observed (4.28 ± 0.61 filopodia per stripe, $p<0.0001$) (Figure 39. B, C, F). Expression of UAS-CA-PI3K in embryos lacking zygotic expression of MBC did not result in an increase in the number of filopodia (4.28 ± 0.49 filopodia per stripe) compared to embryos lacking expression of MBC alone ($p>0.9999$) (Figure 39 D, F). We also examined the effect of loss of one copy of MBC on the ability of CA-PI3K to induce filopodia. These embryos had filopodia number comparable to controls (7.85 ± 0.68 filopodia per stripe, $p > 0.999$) indicating that the ability of CA-PI3K to promote filopodia is limited when MBC levels are reduced (Figure 39 E, F). These results suggest that MBC is acting downstream of PI3K in the regulation of filopodia.

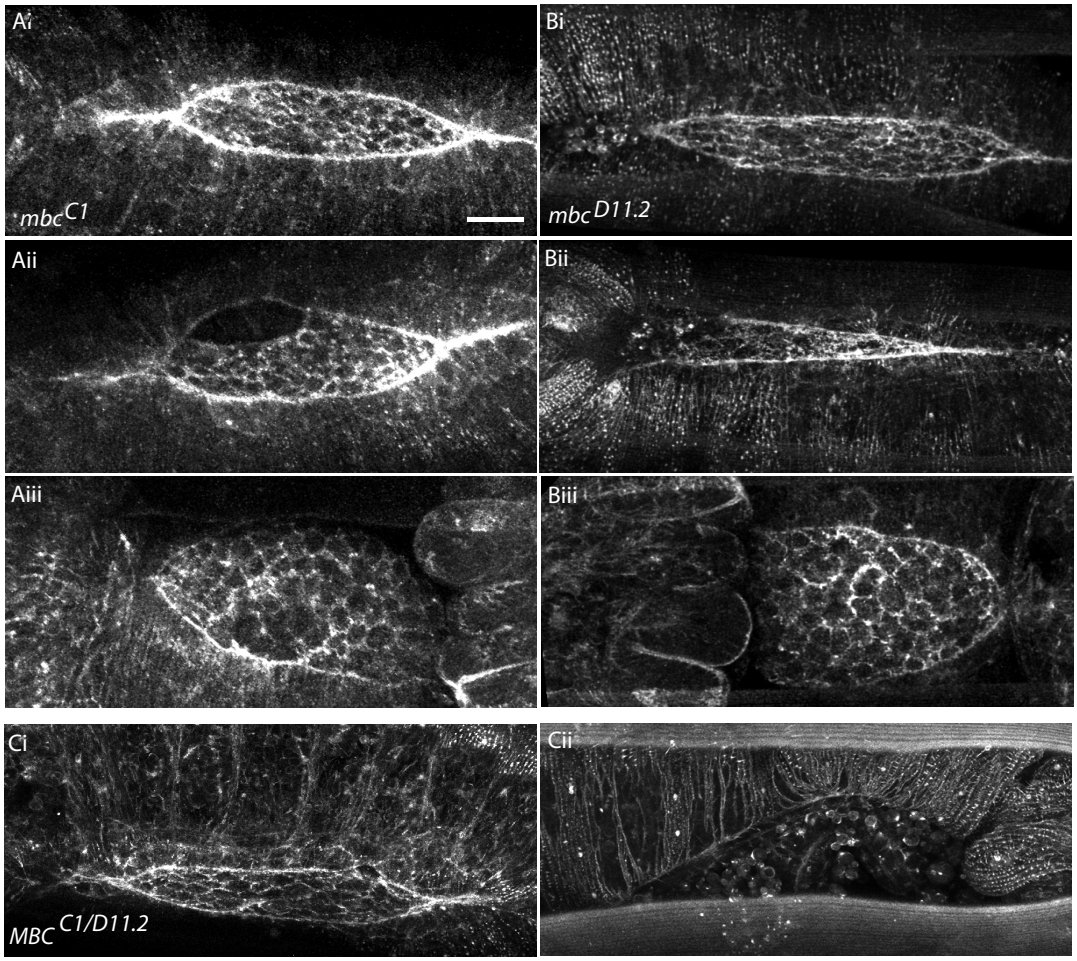

Figure 38. Embryos lacking zygotic expression of MBC exhibit DC defects. Embryos lacking zygotic expression of A) MBC C1 and B) MBC D11.2 exhibit a range of DC defects. C) Heteroallelic *mbc*$^{C1/D11.2}$ mutants also display a range of DC defects. Scale bar represents 24 µm.

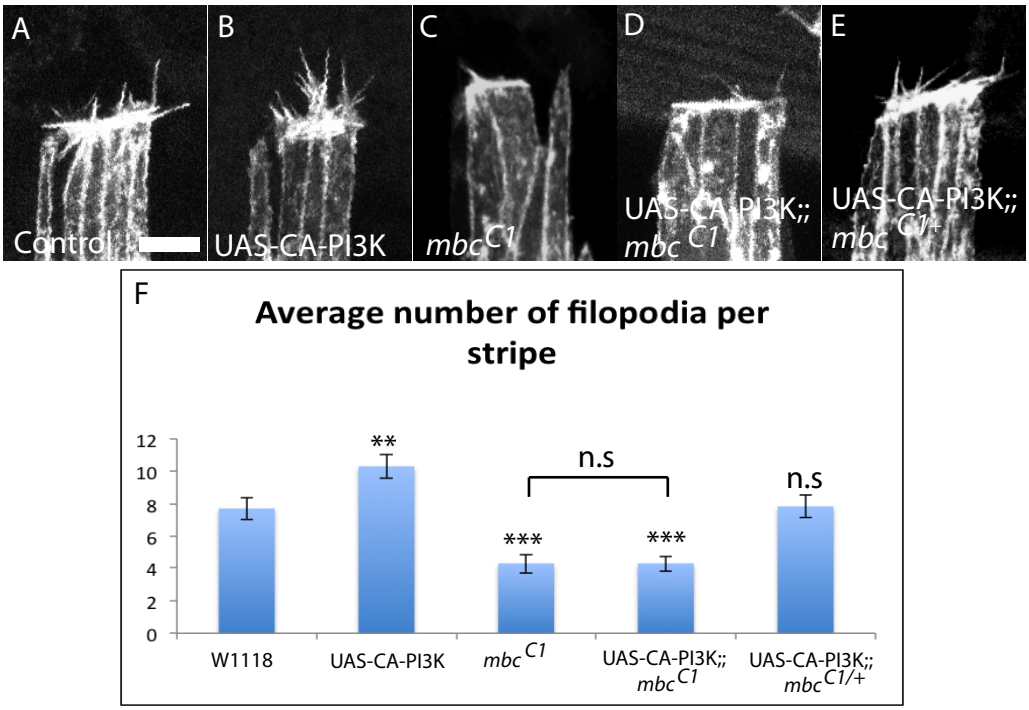

Figure 39. Expressing UAS-CA-PI3K in embryos lacking zygotic expression of MBC does not induce the formation of filopodia. A-E) Images of DC filopodia in embryos of the indicated genotype. F) Quantification of filopodia number in the genotype indicated. n ≥ 46 stripes or n ≥ 10 embryos. *** indicates a significant difference from the control of P<0.001, ** indicates a significant difference from the control of P<0.005 and n.s indicates no significant difference. Error bars indicate S.E.M and the scale bar represents 5um

4.5.3 MBC localisation is affected by a decrease in the level of PIP_3 during DC

To determine how MBC regulates filopodia downstream of PIP_3, we first investigated its localisation during DC. To visualise the localisation of MBC, we made a UAS-GFP-MBC transgene and expressed it throughout the embryo under the control of the *tubP*-Gal4 driver. MBC primarily localised to the DC leading edge, with some accumulation at junctions (Figure 40 A). Interestingly the localisation of UAS-GFP-MBC resembled the localisation of F-actin during DC.

Given that MBC appears to localise to the leading edge during DC, we next sought to determine if manipulating PIP_3 levels alters MBC localisation. We expressed UAS-GFP-MBC under the control of *en*-Gal4 and observed a localisation similar to that of F-actin, with GFP-MBC localising to cell junctions, most strongly at the leading edge (Figure 40 B). Reducing levels of PIP_3 by expressing UAS-PTEN3 under the control of *en*-Gal4, resulted in a reduction of GFP-MBC associated with cell junctions, with its distribution becoming more diffuse and cytosolic. However, the change in distribution of GFP-MBC was variable, with some cells retaining junctional localisation (Figure 40 Cv), whilst others lost it (Figure 40 Civ). Increasing PIP_3 levels by expressing UAS-CA-PI3K, appeared to result in a slight increase in the localisation of GFP-MBC to cell junctions (Figure 40 D).

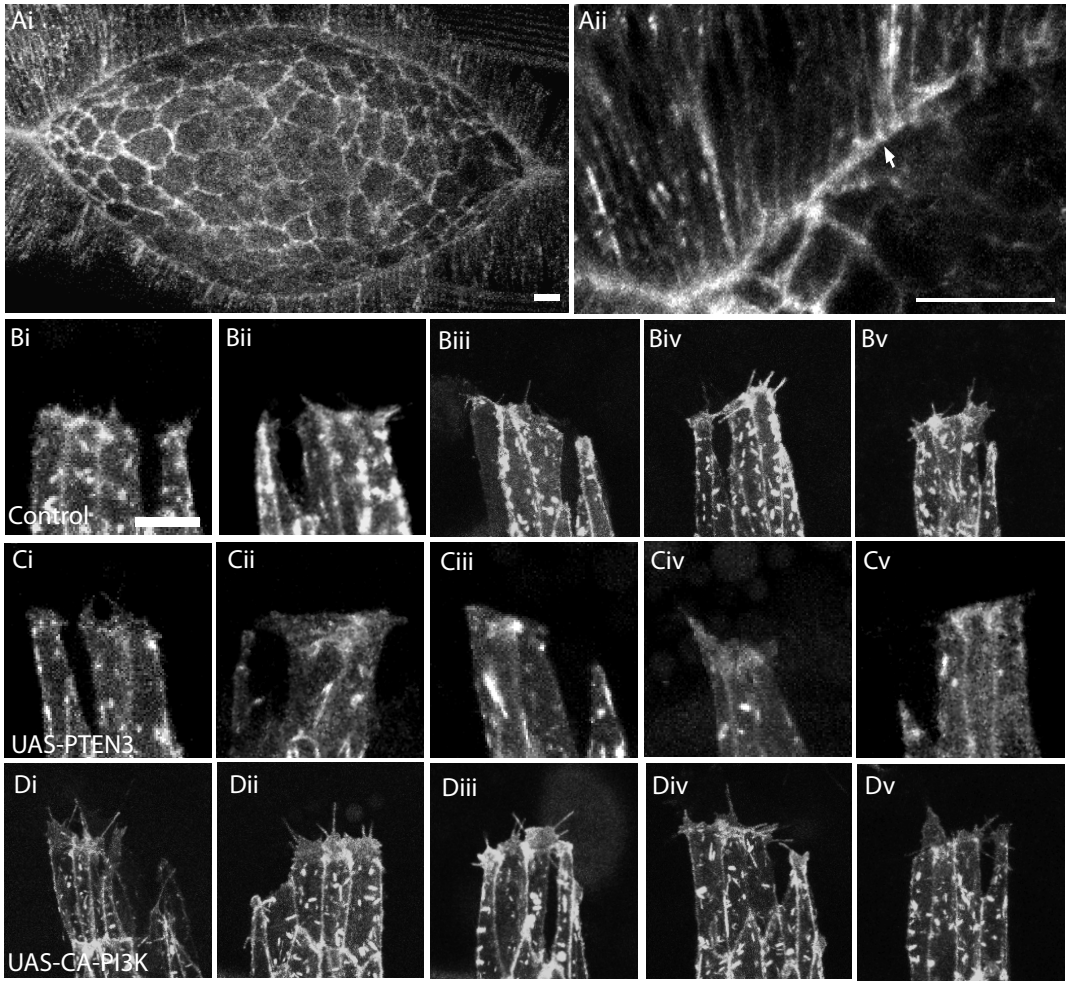

Figure 40. Localisation of MBC throughout DC A) MBC exhibits a junctional localisation at the DC leading edge in a similar manner to F-actin. Ai-Aii) GFP-MBC localises to the leading edge in particular to cell junctions (arrow). Localisation of MBC-GFP under the control of *en*-Gal4 in B) control embryos, C) in embryos expressing UAS-PTEN3 and D) in embryos expressing UAS-CA-PI3K. Each stripe represents a different embryo. Scale bar in A represents 20 μm, and the scale bar in B-D represents 5 μm.

4.5.4 Expression of UAS-Rac1-wt can rescue loss of filopodia observed in MBC mutants

To determine whether MBC is working upstream of Rac in the regulation of filopodia during DC, we analysed filopodia in embryos that lacked zygotic expression of MBC, but with elevated levels of Rac (UAS-Rac1-wt). If MBC is working by activating Rac, increasing the levels of Rac in a zygotic *mbc* mutant should rescue filopodia defects observed in mbc^{c1} embryos. As previously, expression of UAS-Rac1-wt under the control of *en*-Gal4 resulted in a significant increase in the number of filopodia present when compared to controls (11.63 ± 0.93 and 8.09 ± 0.72 respectively $p<0.0001$), whilst embryos lacking expression of zygotic MBC exhibited a significant reduction in filopodia number (4.27 ± 0.5, $p<0.0001$) (Figure 41 A-C, E). Overexpressing UAS-Rac1-wt in mbc^{c1} zygotically null embryos resulted in a significant increase in the number of filopodia observed compared to MBC null embryos (6.92 ± 0.84 and 4.27 ± 0.5 respectively $p=0.0097$) (Figure 41 D, E). Expression of UAS-Rac1-wt is therefore able to rescue the number of filopodia in embryos lacking zygotic expression of MBC suggesting that Rac is downstream of MBC during DC.

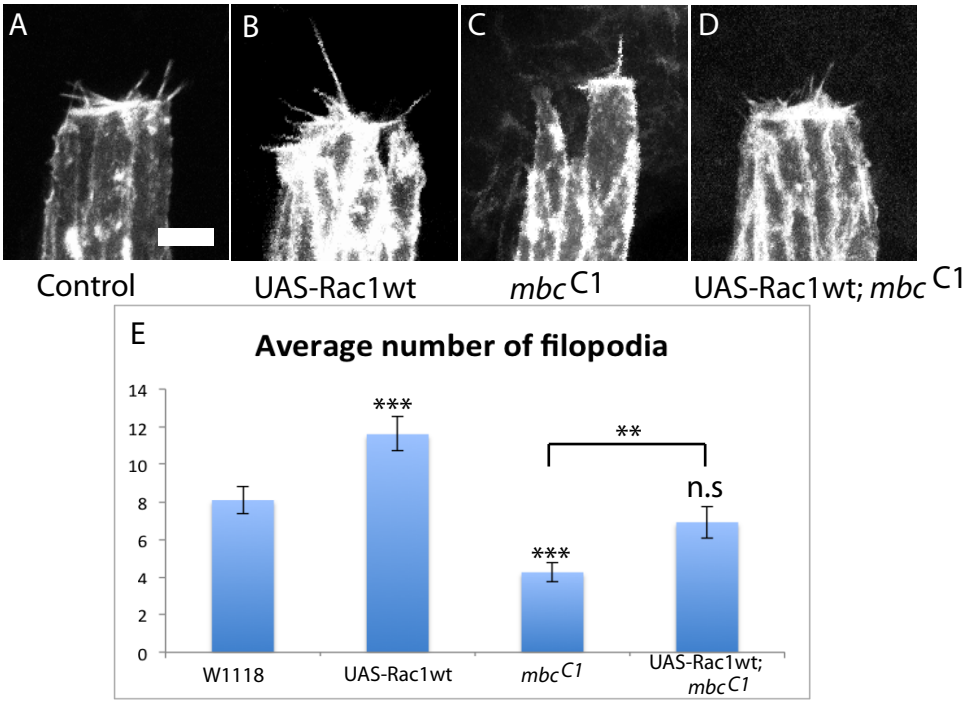

Figure 41. Overexpressing UAS-Rac-1wt in embryos lacking zygotic MBC expression rescues the loss of filopodia phenotype. A-D) show images of *engrailed* stripes expressing UAS-GFP-Moesin along with the indicated transgene or in the given mutant. E) Quantification of filopodia number in each genetic condition. n ≥ 24 stripes or n ≥ 10 embryos *** indicates a significant difference from the control of P<0.001, ** indicates a significant difference of P<0.005 and n.s. indicates no significant difference between test and controls. Error bars indicate S.E.M and the scale bar represents 5 µm.

4.6 Potential role of Still life during DC

Although our data suggested that MBC is acting downstream of PIP_3 during DC, we decided to investigate if the other potential GEF could also play a role in DC. To investigate whether Sif plays a role in DC, we expressed ubiquitous GFP-Moesin in embryos lacking zygotic expression of sif, using the sif^{ES11} mutant allele, and imaged DC. As expected, the control embryos exhibited the normal, eye shaped dorsal hole (Figure 42 A), whereas embryos lacking zygotic expression of Sif exhibited an elongated dorsal hole, with straight leading edges (Figure 42 B). Additionally, some embryos exhibited detachment of the amnioserosa from the leading edge, resulting in a disordered dorsal hole (Figure 42 Bii). These data suggest that, like MBC, Sif may play a role in DC.

4.7 Potential role of Akt during DC

Akt is a well-known downstream effector of PIP_3, and as such it is possible that it also plays a role during DC (Burgering and Coffer 1995). Using embryos lacking zygotic expression of Akt (akt^{04226}), we investigated whether it too might participate in DC. To establish if Akt has any role in DC, we first observed the effect of losing zygotic expression of Akt, with ubiquitous GFP-Moesin used to visualise F-actin. We observed a range of DC defects in these embryos with 42% of embryos displaying a normal dorsal hole (Figure 43 A, B), 25% of embryos showed an early embryonic defect, such as failure of the head to properly involute (Figure 43 D) and 33% displayed a DC phenotype, including an elongated dorsal hole (n = 16). Interestingly, one of the DC defects observed was detachment of the amnioserosa from the epithelial leading edge, when this occurred, the hole appeared to be treated like a wound with the formation of an actin cable and protrusions (Figure 43 C).

As a subset of embryos displayed DC phenotypes we next sought to determine if these embryos had filopodia defects. Expressing UAS-GFP-Moesin under the control of *en*-Gal4 in embryos lacking zygotic expression of Akt allowed visualisation of F-actin and so we were able to analyse the number of filopodia present at the front of DME cells. When levels of Akt were reduced, a small, but significant reduction in the number of filopodia were observed at the DC leading edge when compared to controls (6.59 ± 0.53 and 7.60 ± 6.59 filopodia per stripe respectively, $p = 0.0028$) (Figure 43 E, F).

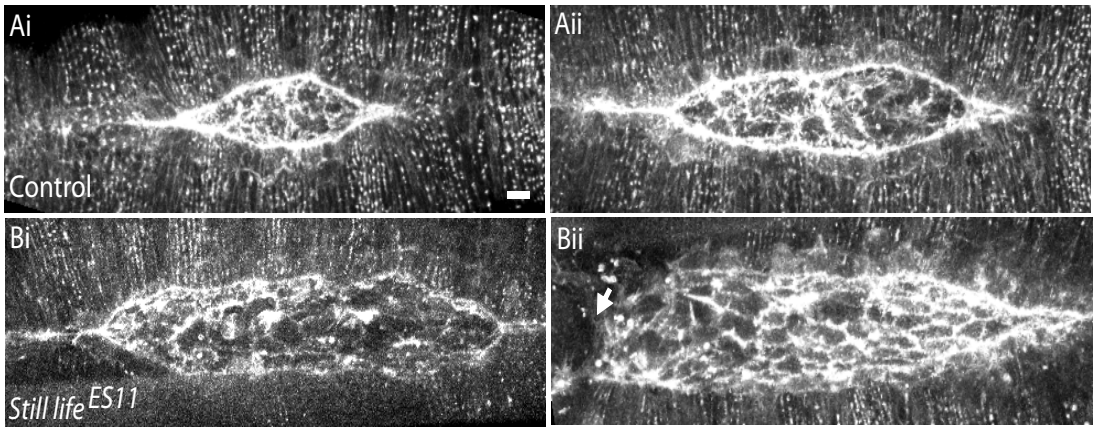

Figure 42. DC phenotypes observed in embryos lacking zygotic expression of Still life. Ai, ii) Dorsal hole observed in control embryos visualised with ubiquitous expression of GFP-moesin. Bi, ii) Shows examples of DC phenotype observed when zygotic expression of Sif is lost. Arrow in Bii indicates where the amnioserosa has separated from the leading edge. Scale bar represents 20 μm

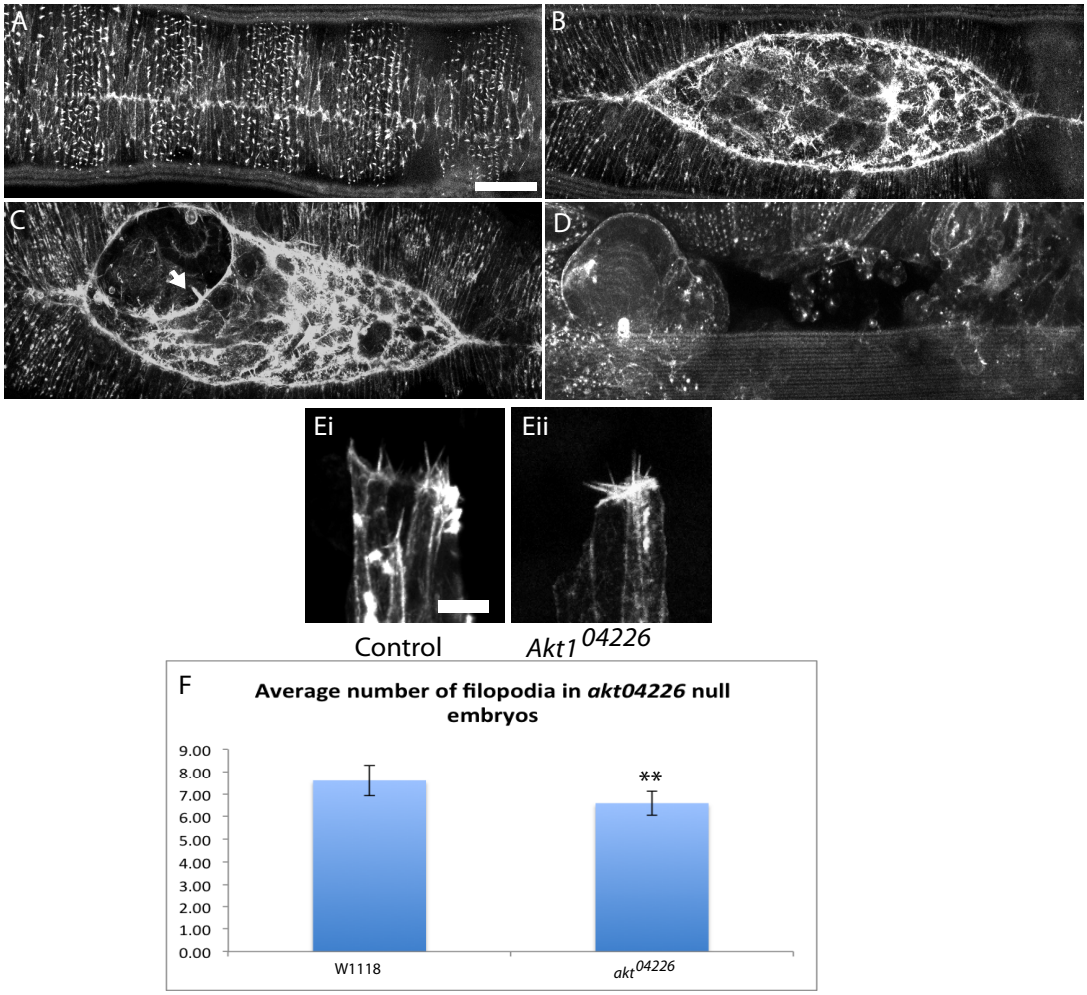

Figure 43. *akt*^{04226} mutant embryos display DC defects. A-D) *akt*^{04226} mutant embryos expressing cGMA display a range of DC defects including C) separation of the leading edge from the amnioserosa (arrow indicates the formation of filopodia and an actin cable) and D) early embryonic defects. Ei, ii) Embryos lacking zygotic expression of Akt display a significantly reduced number of filopodia as quantitated in F. ** indicates a significant difference from the control of P<0.005. Error bars indicate S.E.M and Scale bar represents 5 μm

Chapter 4. Discussion

We have shown that during DC PIP_3 regulates actin protrusion formation, and hence epithelial closure, however we do not know what functions downstream of PIP_3 in this process. To determine how actin protrusions are regulated by PIP_3 during DC, we sought to determine the downstream effectors in this signalling pathway. We took a candidate approach to identify other actin regulators, with one such candidate being the small GTPase Rac, as it is a well-studied regulator of actin protrusions during cell migration and developmental events and is regulated by PIP_3 in other contexts (Ridley 2001; Hakeda-Suzuki *et al*. 2002; Stramer *et al.* 2005; Woolner *et al.* 2005). Interestingly *Drosophila* embryos lacking expression of Rac exhibit an elongated dorsal hole in a similar manner to embryos with reduced levels of PIP_3 (Woolner *et al*. 2005).

4.8 PIP_3 is upstream of Rac in the regulation of filopodia during DC

That similar phenotypes were observed in embryos lacking zygotic expression of Rac or with reduced levels of PIP_3 indicated that these two molecules could be working in the same signalling pathway. We have shown previously that PIP_3 is required for DC, in particular in the formation of filopodia and as such it is vital for the process of zippering. Previous work has shown that Rac is also vital for the regulation of filopodia during DC, and when levels of Rac are reduced, zippering is impaired resulting in an elongated dorsal hole (Woolner *et al.* 2005), similar to the effect of reducing levels of PIP_3. As such, we hypothesised that PIP_3 and Rac are working in the same pathway to regulate the formation of actin protrusions at the front of migrating epithelial cells. This hypothesis is consistent with work in other systems where PIP_3 was shown to activate Rac in neutrophils through Rac specific GEFs (Weiner *et al.* 2002; Nishikimi *et al*, 2009; Yoo *et al*. 2010).

To obtain stronger evidence that Rac is downstream of PIP_3 during DC we carried out epistasis experiments to identify genetic interactions between the two signals. We elevated the levels of PIP_3 (using CA-PI3K) in embryos with minimal Rac activity, either using the rac^{J10} mutant or by expressing UAS-Rac-N17 under the control of *en*-Gal4. In both cases, increasing the levels of PIP_3 did not increase the number of filopodia when Rac activity was minimal, suggesting that Rac is necessary for PIP_3 to elevate filopodial activity. The finding that Rac regulates filopodia during DC is perhaps surprising, given that it is more normally associated with the regulation of lamellipodia (Ridley *et al.* 1992b; Nobes and Hall 1995). It is possible that the environment of the cell determines the type of actin protrusion formed and it is notable that filopodia are the predominant actin structure observed protruding from DME cells rather than lamellipodia. Additionally, it has been shown in epithelial cells in the *Drosophila* pupal developing thorax that the levels of Rac can influence which type of actin

protrusion is formed. High levels of Rac results in the formation of filopodia, whereas intermediate levels of Rac results in lamellipodial formation (Georgiou and Baum 2010). Consistent with this observation is our finding that expression of UAS-Rac1-WT during DC leads to an increase in filopodia rather than lamellipodia. During the course of the project, we attempted to observe the activation state of Rac directly using FRET-based activity sensors, however, in our hands, we were not able to detect changes in Rac activity using these sensors. As such we were unable to visualise the activation state of Rac during DC, and could only determine its presence downstream of PIP_3 genetically.

Activation of Rac at the leading edge of DME cells would be likely result in enhanced actin polymerisation, as Rac has been shown to activate the Scar/WAVE complex through interaction with Sra1 (a component of the Scar/WAVE complex), which can then directly bind and activate the Arp2/3 complex (Steffen *et al*. 2004). Although the Scar/WAVE complex is primarily associatied with the formation of lamellipodia, as is Rac, it is possible that in the case of DC, Scar/WAVE could be activated by Rac to form filopodia. It would be interesting to know if this interaction with the Scar/WAVE complex occurs during DC.

4.9 No evidence for a positive feedback loop between PIP_3 and Rac during DC.

It has previously been reported that during cell migration, whilst PIP_3 activates Rac, Rac is also able to activate PI3K in a positive feedback loop acting at the front of the cell (Weiner *et al.* 2002; Yoo *et al.* 2010). It is likely that this feedback loop amplifies local signalling at the leading edge of the cell so promoting robust actin polymerisation in response to weak signalling inputs. However, when we investigated the presence of a feedback loop in DC, we found that decreasing the levels of Rac did not result in a change in PIP_3 levels, suggesting that this feedback system probably does not operate during DC. Interestingly when we increased the total levels of Rac, we observed a decrease in PIP_3 levels, suggesting that whilst a positive feedback loop is not present, there may in fact be a negative feedback loop, which acts to restrict PI3K signalling when levels of Rac become too high. It is possible that this inhibition acts to prevent excess actin assembly. It could be hypothesised that this type of negative feedback loop might be present in more complex tissues where excess levels of PI3K have been linked to a variety of cancers (Shayesteh *et al.* 1999; Ma *et al.* 2000; Samuels *et al.* 2004). It is also possible that this feedback loop is vital to act as a 'stop' signal that is required when cells have reached their destination, such as once DC has been completed.

4.10 MBC is a PIP_3 effector in the regulation of Rac

As our data suggested that Rac is downstream of PIP_3 in the regulation of filopodia during DC, we next sought to determine how PIP_3 regulates Rac. Given that the activation state of GTPases is regulated by GEFs and GAPs, and that PIP_3 has been shown to bind to PH domain containing proteins, it was possible that PIP_3 could activate Rac via a PH-containing GEF, as occurs in other systems (Weiner *et al.* 2002; Nishikimi *et al.* 2009). Although MBC does not contain the typical PH domain, it does contain two Dock-Homology regions (DHRs), which contain DH-PH-like domains (Côté *et al*. 2005). Additionally, MBC is expressed during embryogenesis and embryos lacking MBC exhibit a DC phenotype, making it a good candidate for signalling downstream of PIP_3 in the regulation of Rac during DC (Erickson *et al.* 1997). We found that two different mutant alleles of *mbc*, mbc^{c1} and $mbc^{d11.2}$, both exhibited DC defects, including defects similar to those observed in embryos with reduced levels of PIP_3 or lacking expression of Rac, providing evidence that MBC might act as a link between PIP_3 and Rac. However, in addition to an elongated dorsal hole, these embryos also exhibited a range of other defects. It is likely that the variation in defects observed in embryos lacking zygotic expression of MBC is due to MBC being required for other morphogenetic processes (such as head involution and germband retraction) as well as a variation in maternal contribution of the protein.

Using genetic interactions we demonstrated that PIP_3 is upstream of MBC in the regulation of filopodia during DC, however we did not determine how PIP_3 regulates MBC. The link between Dock180 and PIP_3 has previously been demonstrated in LR73 cells (a CHO variant), where the authors demonstrated that an interaction occurred between PIP_3 and the DHR-1 domain of Dock180 (Côté *et al*. 2005). Although a direct link was not shown between Dock180 and actin protrusions, they did show that the interaction between Dock180 and PIP_3 was required for cell elongation and motility, which is consistent with our observation of MBC being required for actin protrusion formation at the front of DME cells required for efficient DC.

To evaluate how MBC links PIP_3 signalling to Rac activation, we generated transgenic flies containing GFP-tagged MBC that could be expressed under the control of the UAS-Gal4 system. Our finding that this construct localises to the leading edge of DME cells is consistent with it playing a role at the leading edge during DC. As we propose that MBC is a downstream target of PIP_3 we investigated the effect of altering PIP_3 levels on MBC localisation, and found that decreasing the levels of PIP_3 resulted in an overall loss of association of GFP-MBC with cell junctions and increasing the levels of PIP_3 slightly increased the association of GFP-MBC with cell junctions. Our observations are consistent with previous work, where PIP_3 has been shown to localise Dock180 via its DHR-1 domain to the front of migrating cells (Côté *et al.* 2005). We propose that during DC, as observed in previous work, PIP_3 is required for the localisation of MBC to the front of the cell, likely through interactions with the DHR-1 domain of

MBC. Additionally, as MBC/Dock180 exists in an auto-inhibited conformation, it is possible that PIP_3 could play a role in relieving this inhibition, in a similar manner to the GEF Vav (Tolias *et al*. 1995), although no work has yet demonstrated that PIP_3 can function in this manner.

We have determined genetically, that during DC both Rac and MBC are downstream effectors of PIP_3, as such we next sought to verify that that MBC is upstream of Rac in DC. Increasing levels of Rac in embryos lacking zygotic expression of MBC was sufficient to rescue the filopodia defect observed in *mbc*^{c1} embryos. This indicates that during DC, MBC is acting upstream of Rac, consistent with the fact that its homologue Dock180 is a Rac specific GEF (Brugnera *et al.* 2002).

From this work, we propose that during DC, PIP_3 accumulates at the leading edge, where it recruits and/or activates MBC. This leading edge MBC recruitment activates Rac and stimulates downstream signalling pathways required for the reorganisation of the actin cytoskeleton.

4.11 Alternative downstream effectors of PIP_3.

4.11.1 Potential roles of Still life and Akt during DC.

While the main focus of our studies linking PIP_3 to actin assembly in DC was MBC, we also briefly investigated two other known targets of PIP_3. The first of these was the Rac GEF Still life. Given that Sif contains two PH domains, of which the N-terminal PH domain is required for its localisation and PIP_3 binding (Michiels *et al*. 1997; Fleming *et al.* 2000), we sought to determine if it is a downstream target of PIP_3 during DC. We did not initially investigate Sif as recent high-throughput sequencing by the ModEncode consortium had failed to detect any expression of Sif before 12 hours post fertilisation, which is the approximate time of the onset of DC (Graveley *et al*. 2011). Surprisingly however, embryos lacking expression of Sif exhibited an elongated dorsal hole, similar to those observed in embryos with reduced levels of PIP_3. In addition to the elongated dorsal hole, we also observed instances where the amnioserosa detached from the epithelial leading edge. Notably, we only looked at one mutant allele, so we cannot rule out the possibility that the phenotype was caused by a second mutation on the mutant chromosome and would need to use a second allele to confirm the result. These observations, if confirmed, would suggest that Sif could have some role during DC, however due to time constraints, we were unable to test this further. If Sif was able to regulate the formation of filopodia, we would hypothesise that during DC, it would be acting to regulate the activation state of Rac, given that it has been shown to be upstream of Rac signalling in fibroblasts (Michiels *et al*. 1995). This would suggest the ability of GEFs to work

in a redundant manner, and may help explain why some embryos lacking zygotic expression of each GEF do not exhibit DC phenotypes (although this could also be explained by variable maternal contribution). It would be interesting to observe DC in embryos lacking expression of both Sif and MBC, if the observed phenotypes were enhanced, this could suggest that the GEFs work in a reducndant manner during DC.

Akt is a well-known PH-domain containing effector of PIP_3, and as such could also act during DC. Interestingly, we observed a wide range of phenotypes in akt^{04226} null embryos, ranging from completion of DC without fault to failure to reach DC. When analysed, we found there to be a small but significant decrease in the number of leading edge filopodia in embryos lacking zygotic expression of Akt, when compared to controls. Whilst Akt appears to be playing important roles during development, given the nature of the defects, it is difficult to conclude whether this reduction in filopodia is a contributory factor. Typically, defects associated with reduced numbers of filopodia include an elongated dorsal hole, and whilst this phenotype is observed, the presence of early embryonic defects and separation of the amnioserosa from the epithelial leading edge suggests that the phenotypes likely have other causes. Further supporting this is that whilst significant, the decrease in filopodia number is modest, suggesting that Akt is not an important regulator of filopodia and this change in filopodia number may be a somewhat indirect effect of loss of Akt.

4.12 Summary

From our work, we have deduced that during DC, PIP_3 recruits (and possibly activates) MBC, which then regulates the activation state of Rac at the leading edge of DME cells. This PIP_3-MBC-Rac pathway is responsible for regulating the formation of filopodia required for DC and is consistent with other studies (Côté *et al*. 2005; Yoo *et al.* 2010). The link between PIP_3 and Rac has been reported previously in single cell migration (Weiner *et al.* 2002; Nishikimi *et al.* 2009; Yoo *et al.* 2010), and as mentioned previously (Chapter 3) the pathways required for single cell migration could also be required for collective migration during DC. In contrats to results in single cell migration (Nishikimi *et al*. 2009; Yoo *et al* 2010), there does not appear to be a positive feedback loop between Rac and PIP_3 during DC, as decreasing Rac did not result in a loss of PIP_3 accumulation at the leading edge, and increasing Rac surprisingly resulted in a decrease of PIP_3. This could suggest the presence of a negative feedback loop, preventing levels of PIP_3 from reaching excessive levels. This inhibition of PI3K could be beneficial in the control of cell growth, in particular from a point of preventing cancerous growth as high levels of PI3K have been reported in many cancer types (Shayesteh *et al.* 1999; Ma *et al.* 2000; Samuels *et al.* 2004; Carpten *et al.* 2007).

Although we did not determine how PIP_3 recruits MBC during DC, given previous work, it is likely that the PH-binding region of PIP_3 is able to bind to the DHR-1 domain of MBC (Côté *et al*. 2005). Previous works showed that loss of the DHR-1 region inhibits cell migration in CHO-cells but does not have an effect of the ability of the GEF to activate Rac. From this, we hypothesise that in our system, MBC could be recruited to sites of PIP_3 accumulation, increasing Rac activity in these locations.

Whilst the main focus of this project was the PIP_3-MBC-Rac pathway, we briefly investigated the presence of other PIP_3 effectors that could be responsible for filopodia formation in DC. From the presence of an elongated dorsal hole in sif^{ES11} embryos, it is possible that Sif is also a regulator of filopodia. It could be that Sif is working to activate Rac independently of PIP_3, or it could be acting in a redundant manner to MBC. It would be interesting to see if loss of both MBC and Sif enhanced the phenotypes observed in embryos lacking expression of one of these GEFs. If so this could suggest the GEFs work in parallel in the regulation of the actin cytoskeleton.

Finally, given that a well-known effector of PIP_3 is Akt, we investigated its role in DC. Although there appeared to be a DC phenotype, there were also early embryonic defects and the reduction in number of filopodia was modest, suggesting that defects observed with loss of Akt, are likely due to other roles Akt plays during development (such as cell growth and survival (Leevers *et al.* 1996; Brunet *et al.* 1999; Potter *et al*. 2002)), as opposed to regulation of the actin cytoskeleton.

Chapter 5. Exploring the mechanisms regulating PIP_3 levels at the DC leading edge

We have shown that PIP_3 localises specifically to the front of DME cells in a polarised manner, where it regulates actin protrusion formation. However, we do not know what causes this leading edge accumulation of PIP_3. The levels and distribution of PIP_3 can be regulated either by controlling the production or metabolism of PIP_3, or by a combination of both (Whitmann *et al.* 1988; Li *et al*. 1997; reviewed by Vanhaesebroeck *et al.* 2012). Regulated metabolism of PIP_3 by PTEN has been shown to play a major role in regulating PIP_3 levels and cellular distribution in a variety of contexts (Gao *et al.* 2000; Funamoto *et al.* 2002; von Stein *et al*. 2005). For example, in *Dictyostelium* PTEN exhibits a reciprocal localisation with PIP_3, and is required to maintain the leading edge gradient of PIP_3 observed in these cells (Funamoto *et al*. 2002). If this gradient is lost, cells fail to reorganise their actin cytoskeleton, do not generate pseudopodia and fail to undergo directional cell migration (Funamoto *et al*. 2002; Nisho *et al*. 2007). PTEN also seems to be particularly important in regulating PIP_3 levels in epithelia. In both MDCK cells and in the *Drosophila* epithelium, the reciprocal localisation of PTEN and PIP_3 is important for the establishment of apicobasal polarity, with PIP_3 restricted to the basal domain of the cells, as PTEN is recruited to the apical domain where it dephosphorylates PIP_3 (von Stein *et al*. 2005; Martin-Belmonte *et al*. 2008). Although this work demonstrates the importance of the relationship between PTEN and PIP_3 in establishing apicobasal polarity, it is possible that the same mechanisms regulate the planar polarity of DME cells during DC.

Using genetic techniques available, we therefore investigated if PTEN is responsible for the specific PIP_3 accumulation observed during DC. Additionally, we wanted to determine other upstream regulators required for PIP_3 accumulation at the leading edge. Tom Millard and Juliana Alves-Silva made substantial contribution to the research described in this chapter.

5.1 PTEN as a regulator of PIP_3 localisation

PTEN exhibits a polarised distribution during cell migration in a reciprocal manner to PIP_3 accumulation (Funamoto *et al.* 2002). PTEN is vital in regulating the polarised distribution of PIP_3 by dephosphorylating PIP_3 where PTEN levels are high. It is possible that PTEN distribution during DC is responsible for generating the PIP_3 accumulation observed in DME cells. To investigate if PTEN might regulate the accumulation of PIP_3, we sought to determine the localisation of PTEN during DC.

As mentioned previously, there are two main splice variants of PTEN in *Drosophila* (PTEN2 and PTEN3). As no antibodies sufficiently sensitive to detect endogenous PTEN were available, we expressed GFP-tagged forms of PTEN2 and PTEN3 (Pinal *et al.* 2006) under

the control of the *engrailed* driver and live imaged the embryos to determine the localisation of each of the PTEN isoforms during DC. We observed different localisations for the two variants during DC; PTEN3 was distributed homogenously throughout the cytoplasm and nucleus (Figure 44 Ai), whilst PTEN2 localised strongly to cell junctions (Figure 44 Aii). Interestingly, UAS-PTEN2 was absent from the cell junctions at the leading edge, in a reciprocal manner to the observed localisation of PIP_3 (Figure 44 Aii, Aiii).

5.1.1 Polarisation of PIP_3 in leading edge cells is controlled by PTEN

As PTEN2-GFP and GPH (PIP_3) display a reciprocal localisation in DME cells, we investigated if PTEN2 could be responsible for the planar polarised distribution of PIP_3 observed at the DC leading edge. To investigate if PTEN was responsible for the generation of the PIP_3 gradient, we investigated the distribution of GPH in $pten^{117\ zyg}$ or $pten^{117\ mat/zyg}$ embryos. During this experiment, measuring the fluorescence intensity of GPH along DME cell junctions provided a way of objectively quantifying the gradient of PIP_3 in these cells. In control embryos, the levels of PIP_3 were increased at the leading edge and then rapidly decreased with distance away from the front of the cell, reaching a basal level 3-4 μm back from the leading edge (Figure 44Bi, C). Interestingly embryos lacking zygotic expression of PTEN, whilst still displaying an accumulation of leading edge PIP_3 similar to that observed in control embryos, had a higher basal level further back on lateral cell junctions (Figure 44 Bii, C). This demonstrates that PIP_3 is less polarised in $pten^{117}$ embryos than in controls, although a gradient of PIP_3 is still observed.

In DC stage embryos there is frequently still substantial amounts of maternal protein, therefore our $pten^{117}$ mutant embryos may still have significant quantities of maternally-derived PTEN. To remove this possibility we generated maternally and zygotically null embryos to ensure that PTEN was completely absent. In these embryos, whilst PIP_3 levels were still highest at the leading edge, the levels only dropped off only marginally behind, suggesting that PIP_3 levels were now high at all cell junctions and that the front/back gradient of PIP_3 was largely lost (Figure 44 Biii, D). Additionally, we observed the distribution of PIP_3 along the apico-basal axis in embryos lacking maternal and zygotic expression of PTEN. PIP_3 was still absent from the apical and basal surfaces, indicating that either PIP_3 is solely generated at cell junctions or that it is degraded in a PTEN independent manner on the apical and basal surfaces (Figure 44 Biii inset). From these data we can conclude that PTEN plays a major role in polarising PIP_3 levels within DME cells during DC.

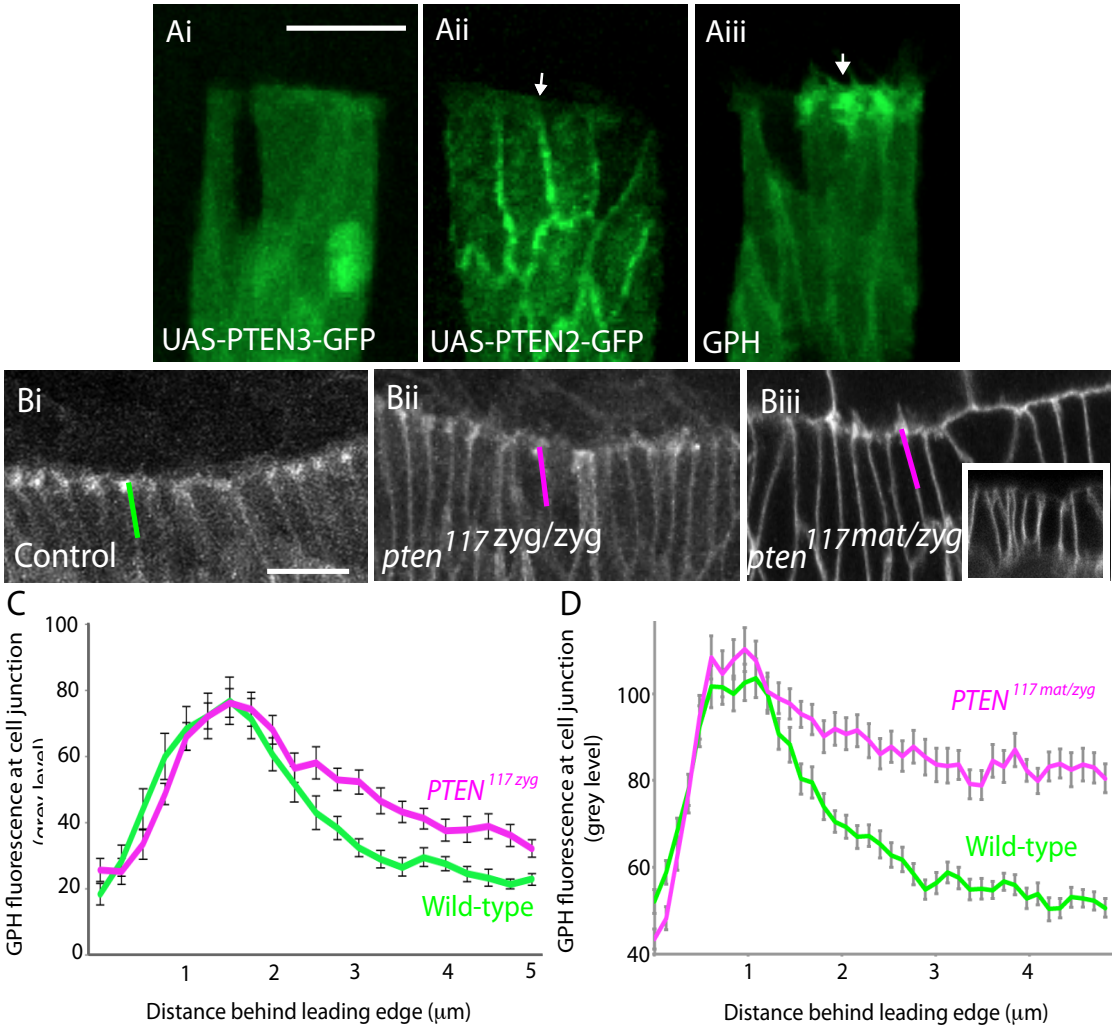

Figure 44. Leading edge gradient of PIP_3 can be affected by reducing the levels of PTEN. Ai) UAS-PTEN3-GFP displays a diffuse localisation in DME cells. Aii) UAS-PTEN2-GFP is localised to cell junctions, the arrow indicates where it is absent from the leading edge. Aiii) GPH specifically localises to cell junctions at the leading edge (arrow), corresponding to the region where UAS-PTEN2-GFP is absent. GPH localisation (indicating PIP_3 levels) in Bi) control embryos, Bii) embryos lacking zygotic expression of PTEN and Biii) embryos lacking zygotic and maternal expression of PTEN. Inset in Biii shows Z-section through the epidermis of *pten*$^{117\ mat/zyg}$ embryo (apical is to the top). Membrane levels of GPH (and therefore PIP_3) were quantified by measuring fluorescence intensity along a 5 μm stretch of each junction beginning immediately in front of the leading edge, as indicated by green and magenta lines in Bi-ii. Distribution of PIP_3 along cell junctions in C) embryos lacking zygotic expression of PTEN and D) embryos lacking zygotic and maternal expression of PTEN. n ≥ 40 junctions from at least 7 embryos. Error bars indicate S.E.M. Scale bar represents 10 μm.

5.2 PTEN distribution is determined by Baz during DC

The PTEN splice variants PTEN2 and PTEN3 exhibit different localisations in DME cells during DC, however they only differ by five amino acids, thus these five amino acids must be responsible for the difference in localisation. PTEN2 contains five additional amino acids at the C-terminus, which form a PDZ-binding domain (Smith *et al* 1999). This PDZ-binding domain has been shown to mediate the binding of PTEN2 to Baz, which is the *Drosophila* homologue of Par3 (von Stein *et al*. 2005).

To determine if Baz is responsible for localising PTEN2 during DC, we first determined the localisation of Baz by co-expressing UAS-m-Cherry-Baz (McGill *et al.* 2009) and UAS-GFP-PTEN2 under the control of *en*-Gal4. This allowed us to observe the localisation of both proteins simultaneously during DC. We found that m-Cherry-Baz and GFP-PTEN2 co-localised, with m-Cherry-Baz also localising to cell junctions except those at the leading edge, as previously observed for GFP-PTEN2 (Figure 45 A). To determine whether Baz is necessary for the localisation of PTEN2 to junctions, we observed the localisation of GFP-PTEN2 in hemizygous baz^{815-8} embryos (Krahn *et al.* 2010). In these embryos, GFP-PTEN2 did not localise to cell junctions; instead it displayed a cytosolic localisation, similar to that observed for PTEN3 (Figure 45 B), demonstrating that Baz is necessary for the localisation of PTEN2 to cell junctions in DME cells. These data suggested that Baz might indirectly regulate PIP_3 distribution during DC by controlling the distribution of PTEN2. To test this idea we first compared the distribution of Baz and PIP_3 by co-expressing UAS-m-Cherry-Baz and UAS-GPH under the control of *en*-Gal4. We found that in DME cells, Baz displays a precise reciprocal distribution to that of PIP_3, with Baz localising at the rear and sides of DME cells, where PIP_3 levels are low, but being absent from the leading edge where PIP_3 levels are high (Figure 45 C). To determine if Baz is regulating PIP_3 distribution in DME cells, we investigated the localisation of PIP_3 in embryos lacking zygotic expression of Baz. Expressing tGPH in hemizygous baz^{815-8} embryos and measuring fluorescence intensity allowed us to objectively analyse the levels of PIP_3 along cell junctions, in a similar manner to measuring PIP_3 levels in $pten^{117}$ embryos. In embryos lacking zygotic expression of Baz, we observed that PIP_3 is no longer strongly polarised in DME cells, with the leading edge PIP_3 peak much reduced (Figure 45 D, E). These data suggest that Baz recruits PTEN to cell junctions away from the DC leading edge, which in turn dephosphorylates PIP_3 specifically at the back at the sides of the cell, resulting in the PIP_3 gradient observed.

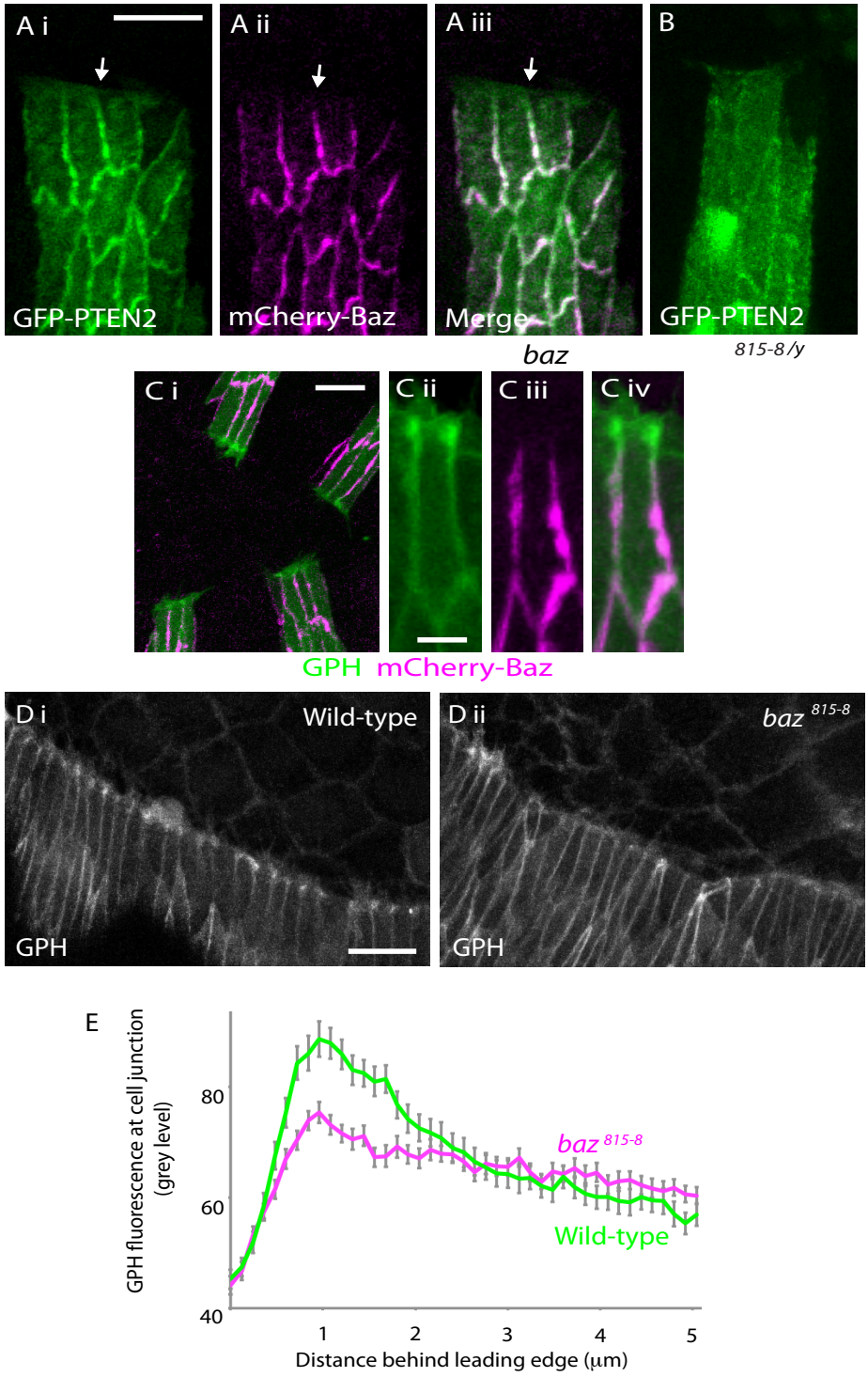

Figure 45. Baz is required for the polarised distribution of PIP_3. A) Co-localisation of GFP-PTEN2 and Baz in DME cells. B) GFP-PTEN2 loses its membrane localisation in *baz*$^{815-8}$ embryos. C) Reciprocal localisation of Cii) PIP_3 and Ciii) Baz. Expression of GPH in Di) wild-type embryos or Dii) *baz*$^{815-8}$ embyros during DC. E) Distribution of PIP_3 along junctions between DME cells in wild-type or *baz*$^{815-8}$ embryos. Quantified measurements of GPH fluorescence intensity along a 5 μm stretch of each junction, commencing immediately in front of the leading edge. n ≥ 68 junctions from at least 11 embryos. Error bars indicate S.E.M. Scale bar represents 10 μm.

If our hypothesis is correct, and Baz is responsible for restricting the localisation of PIP_3 to the leading edge, then we would expect mis-localising Baz to the leading edge of DME cells would prevent PIP_3 from accumulating at the leading edge. To mislocalise Baz, we used a strategy previously described by Laplante and Nilson who demonstrated that expressing the homophillic adhesion protein Echinoid in the amnioserosa during DC resulted in Baz being present at the leading edge, when it would normally be absent (Laplante and Nilson 2011). Consistent with the findings of Laplante and Nilson, we found that Baz is indeed present at the leading edge when Echinoid was expressed in the amnioserosa (Figure 46 B), in contrast to control embryos where it is absent (Figure 46 A). GPH was expressed ubiquitously in these embryos to allow visualisation of the effect of this redistribution of Baz on PIP_3 distribution. This revealed that the leading edge accumulation of PIP_3 observed in control embryos is lost when Baz was present at the leading edge (Figure 46).

5.3 Endogenous Baz displays a reciprocal relationship with actin in DME cells.

Our work indicates that Baz is required for the leading edge accumulation of PIP_3, and we therefore hypothesise that Baz is an upstream regulator of actin structures during DC. However, as we have previously determined Baz localisation by expressing an exogenous GFP-tagged Baz, we sought to determine the localisation of endogenous Baz in relation to actin structures in DME cells. Immunostaining of E-cadherin (green), Baz (red) and F-actin (blue), demonstrated that E-cadherin localises evenly round the periphery of DME cells except at the leading edge cell junctions where it is slightly enriched. Baz co-localises with E-cadherin on most cell junctions of DME cells, except at the leading edge, where Baz, but not E-cadherin, is absent. F-actin is enriched at the leading edge of DME cells (Figure 47 A-C). Merging the images clearly shows the absence of Baz from the leading edge, where F-actin accumulates (Figure 47 D, E). This reciprocal relationship between F-actin and Baz is similar to that observed for Baz and PIP_3 in overexpression experiments (Figure 45 C)

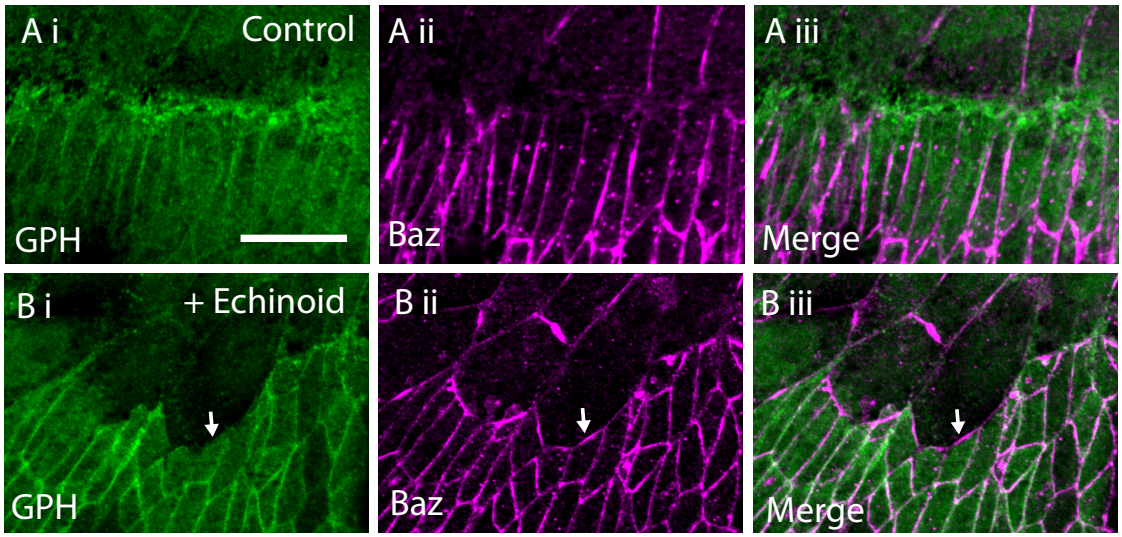

Figure 46. Localising Baz to the leading edge results in loss of PIP_3. Immunofluorescence staining of GPH (green) and Baz (magenta) in Ai-iii) control embryos and Bi-iii) those expressing exogenous Echinoid in the amnioserosa. Arrow indicates a loss of leading edge PIP_3 accumulation corresponding to the re-localisation of Baz. Scale bar represents 10 μm.

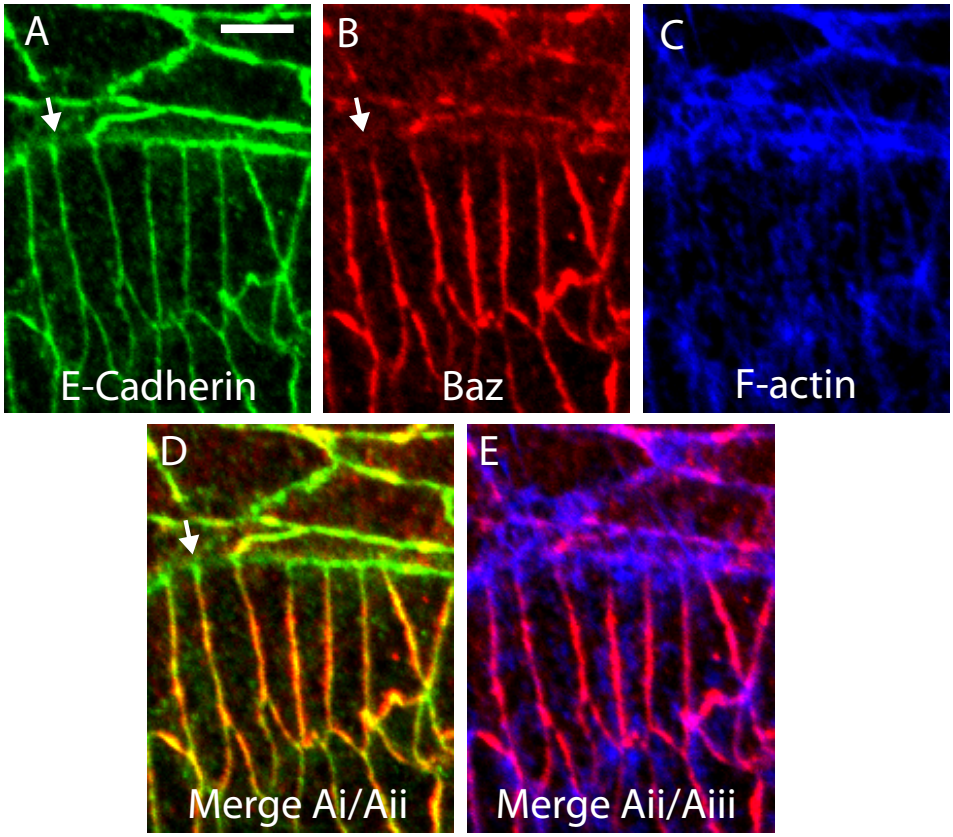

Figure 47. Distribution of E-cadherin, Baz and F-actin during DC. Immunofluorescence of A) E-cadherin, B) Baz and C) F-actin in DME cells. D) Co-localisation of E-Cadherin and Baz demonstrates Baz localising to cell junctions of DME cells, but absent from the leading edge (indicated by the arrow). E) Co-localisation of Baz and F-actin demonstrates a reciprocal localisation with F-actin localising to the front of DME cells, whilst Baz is restricted to the rear and lateral cell junctions. Scale bar represents 5 μm.

5.4 Loss of Baz impairs the formation of filopodia at the DC leading edge.

We have demonstrated that Baz is required to recruit PTEN to cell junctions on the rear and the sides of DME cells and affects the cellular distribution of PIP_3. Given that PIP_3 regulates filopodia formation during DC, we propose that Baz is also a regulator of filopodia in DME cells. To test this hypothesis we expressed UAS-GFP-Moesin under the control of *en*-Gal4 in control or baz^{815-8} mutant embryos and observed filopodial activity at the DC leading edge. We observed a significant decrease in filopodia in baz^{815-8} mutant embryos (3.42 ± 0.49 filopodia per stripe in baz^{815-8} embryos, compared to 5.56 ± 0.57 filopodia per stripe in control embryos, $p<0.0001$) (Figure 48). This result demonstrates that Baz affects the formation of filopodia during DC.

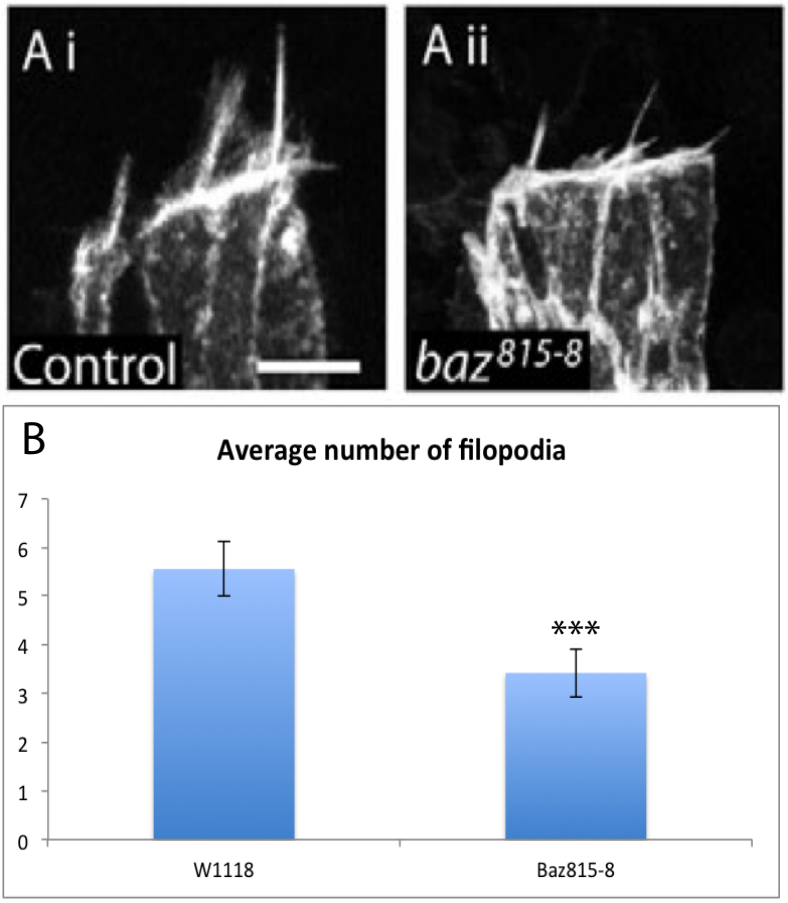

Figure 48. Filopodia number is reduced in embryos lacking zygotic expression of Baz. Filopodia of DME cells imaged in embryos expressing UAS-GFP-Moesin in Ai) control embryos or Aii) embryos lacking zygotic expression of Baz. B) Number of filopodia per *engrailed* stripe in control and mutant embryos. n ≥ 12 embryos. *** indicates a significant difference from controls of $p<0.0001$. Error bars indicate S.E.M. Scale bar represents 5 μm.

Chapter 5 discussion

5.5 PTEN2 regulates the accumulation of PIP_3 during DC

PTEN metabolises PIP_3 and has been shown to be responsible for generating PIP_3 gradients in a variety of contexts including *Dictyostelium* migration and apicobasal polarity in *Drosophila* epithelia (Funamoto *et al.* 2002; von Stein *et al.* 2005). We therefore sought to determine if PTEN could be responsible for the specific leading edge accumulation of PIP_3 observed during DC. Live imaging revealed different localisations for the two PTEN splice variants tested, with PTEN2 displaying a specific localisation to cell junctions. This recruitment of PTEN2 to junctions is consistent with it containing a PDZ-binding domain, allowing it to bind to junction-associated PDZ-containing proteins (Smith *et* al. 1999; Maehama *et al*. 2004). Whilst PTEN3, which lacks this PDZ-binding domain, showed no specific localisation, it did accumulate in the nucleus, where PTEN is known to play a role in a variety of processes including DNA repair, cellular stability and cell cycle arrest (reviewed by Planchon *et al.* 2008). Interestingly, while PTEN2 is localised to cell junctions, it is excluded from leading edge junctions where PIP_3 is present. This reciprocal localisation of PTEN2 and PIP_3 in DME cells is consistent with their localisation in *Dictyostelium* cells, where PTEN localises to the rear of migrating cells, whilst PIP_3 is observed at the front (Funamoto *et al*. 2002). In the case of *Dictyostelium* the restriction of PIP_3 to the leading edge is required for actin cytoskeletal reorganisation.

Analysing the localisation of GPH (and so the distribution of PIP_3) in embryos lacking expression of zygotic and maternal PTEN, showed that PIP_3 now localised homogeneously to all DME cell junctions indicating that in the absence of PTEN, PIP_3 is no longer accumulated solely at the front of DME cells. This is consistent with our hypothesis that PTEN is acting to restrict PIP_3 accumulation to the leading edge of DME cells. However, from our analysis we could still observe a small peak of GPH fluorescence at the front of the cell, indicating that there is still a slight accumulation of PIP_3. This suggests that the PIP_3 gradient could be partially regulated by a second parallel mechanism. It is possible, that in a similar manner to chemotaxing *Dictyostelium* cells, PI3K becomes localised at the leading edge, increasing the amount of PIP_3 formed at leading edge cell junctions (Funamoto *et al.* 2002). In control embryos, with the exception of the leading edge of DME cells, PIP_3 is maintained at low levels by PTEN. This suppression of PIP_3 is likely to be important as it is known to regulate a variety of processes such as cell growth, proliferation and apicobasal polarity (Shewan *et al*. 2010; Vanhaesebroeck *et* al. 2012), and as such needs to be tightly regulated. Our data shows that in DC, PTEN restricts PIP_3 to the front of DME cells by dephosphorylating it at the back and sides of the cells. In this manner, it is ensured that PIP_3 will only accumulate and activate downstream signalling pathways where required.

5.6 Recruitment of PTEN2 by Baz is responsible for PIP_3 localisation and actin polymerisation in DME cells during DC.

Baz is required for the recruitment of PTEN2 to cell junctions, which in turn is responsible for the formation of the PIP_3 gradient observed at the DC leading edge. We observed Baz to be localised to the rear and the sides of the DME cells during DC, as observed for PTEN2. This specific localisation of Baz is consistent with previous work in *Drosophila*, where it was observed that prior to the initiation of DC, Baz is localised on all cell junctions of DME cells, however, once DC commences Baz is gradually lost from the leading edge, but remains localised to lateral and rear DME cell junctions (Laplante and Nilson. 2011). An interaction between Baz and PTEN2 has also been shown in a variety of other contexts including S2 cell culture (*Drosophila* cell line), *Drosophila* embryonic extracts and *Drosophila* photoreceptors (von Stein *et al.* 2005; Pinal *et al*. 2006), consistent with our hypothesis that PTEN2 is recruited to cell junctions by Baz during DC. The work by von-Stein *et al*. demonstrated that PTEN2 bound Baz via its PDZ binding domain, resulting in its localisation to junctions. This recruitment of PTEN2 by Baz has also been demonstrated in the basal domain of developing photoreceptors, where recruitment of PTEN2 by Baz was responsible for the accumulation of PIP_3 at the apical domain (Pinal *et al* 2006). The association between PTEN2 and Baz is well established and shown to be required for apicobasal polarity and we propose that the same relationship occurs in the development of planar polarity during DC.

Given that Baz controls the localisation of PTEN2, it is not surprising that it also controls the gradient of PIP_3 in DME cells during DC. Interestingly, when the fluorescence intensity of GPH was analysed (so revealing PIP_3 distribution), we noticed that there was only a minor peak of GPH at the leading edge of cells in baz^{815-8} embryos (figure 45). It is likely that this is because PTEN2 is no longer sequestered to cell junctions at the back and sides of DME cells in baz^{815-8} embryos and therefore PTEN2 is now cytosolic, allowing it to dephosphorylate PIP_3 throughout the cell, including the leading edge. This work demonstrates that in DME cells, Baz is required to recruit PTEN2 to the back and the sides of the cell, so restricting PIP_3 accumulation to the front of the cell. Relocating Baz to the front of DME cells resulted in a loss of leading edge PIP_3 accumulation, further verifying that Baz is required for the formation of the PIP_3 gradient in DME cells. We also observed a change in the morphology of DME cells where Baz was recruited to the leading edge. It is possible that the loss of PIP_3 from the front of these cells inhibits cytoskeletal rearrangements at the leading edge required for efficient DC, in a similar manner to that observed in neutrophils and *Dictyostelium* (Weiner *et al*. 2002; Devreotes and Janetopoulos 2003; Yoo *et al*. 2010). It has previously been shown that accumulation of Baz at the leading edge results in the loss of the actin cable (Laplante and Nilson 2011), which would account for the disorganised leading edge. Throughout our studies, we have not shown PIP_3 to be required for actin cable formation during DC, however, it is possible that the role it plays in actin polymerisation for protrusion formation could also

have an effect on generating F-actin required for formation of the actin cable. However, a major role for PIP_3 in cable formation is unlikely, given that when PIP_3 is reduced throughout the embryo the leading edge was not disorganised as is observed in embryos expressing Echinoid in the amnioserosa. A more likely explanation for the absence of a cable in these embryos is that loss of polarisation in leading edge cells prevents the recruitment of other actin regulators required for the formation of an actomyosin cable (Laplante and Nilson 2011).

This ability of Baz to regulate the localisation of PIP_3 in DME cells is also important for ensuring actin polymerisation occurs where required. We demonstrated that Baz localises in a reciprocal manner to F-actin, and when Baz is lost, the gradient of PIP_3 is lost and the formation of filopodia at the DC leading edge is impaired. The ability of Baz to regulate the localisation of PIP_3 is consistent with previous work in embryonic epithelia, where von Stein *et al*. demonstrated the ability of Baz and PTEN2 to co-localise at the apical cortex of developing epithelia. Additionally, the authors demonstrated that during the development of the *Drosophila* embryo, PTEN was essential for the reorganisation of the actin cytoskeleton. It is assumed that the effect of loss PTEN on the actin cytoskeleton is as a result of a ubiquitous increase in PIP_3 levels, which is consistent with our observations in DC (von Stein *et al*. 2005).

Baz has also been shown to have antagonistic roles to Cdc42-Par6-aPKC in the formation of basolateral protrusions (Georgiou and Baum 2010). In the developing Drosophila pupal thorax, the authors showed that typically Baz is localised to the apical domain of epithelial cells, and overexpressing Baz resulted in a reduction in the numbers of both intermediate and basal-level protrusions. The authors proposed that this observation is due to Baz acting as a cue to polarise the dynamic actin cytoskeleton, restricting it to the basal compartment, where Par6-aPKC-Cdc42 regulates reorganisation of the actin cytoskeleton into protrusions. Furthermore, Baz can recruit PTEN in the development of *Drosophila* photoreceptors (Pinal *et al*. 2006), where it has been shown to restrict the localisation of F-actin and in this case, the apical formation of microvilli required for correct photoreceptor development. This is consistent with our observation of Baz restricting the formation of actin structures to the front of the cell in a reciprocal localisation to itself. We propose that the restriction of Baz to the rear and the sides of DME cells is responsible for generating the leading edge accumulation of PIP_3, so regulating where MBC is recruited and Rac is activated.

5.7 Summary

We have shown that during DC, Baz is localised to the back and sides of DME cells, where it recruits PTEN2 via its PDZ binding domain. This accumulation of PTEN2 on lateral and rear cell junctions dephosphorylates PIP_3 in these locations, restricting PIP_3 to the leading edge where Baz and PTEN2 are absent. The resulting PIP_3 accumulation at the leading edge is

necessary for the regulation of actin protrusions in DME cells required for efficient DC. It has previously been shown that Baz can recruit PTEN2 (von Stein *et al*. 2005), and that Baz can restrict the formation of filopodia to one cellular location (Georgiou and Baum 2010), however these studies have been carried out in the context of apical-basal polarity. We propose that the same Baz/PTEN/PIP_3 pathway functions in planar polarity in DME cells and is required for the formation of filopodia at the front of DME cells during zippering.

At present, we do not know what determines Baz localisation during DC, however it has been shown that during axis elongation in the *Drosophila* embryo, Rho Kinase phosphorylates Baz, inhibiting its ability to bind to phosphoinositides and hence membranes (Simões *et al*. 2010). We propose that as Rho kinase is required for actin cable contractility (Kimura *et al*. 1996; Mizuno *et al.* 2002), it interacts with and phosphorylates Baz at the front of DME cells (where the actin cable is present), excluding it from the leading edge when the actin cable starts to contract at the onset of DC. It would be interesting to observe the localisation of Baz in embryos lacking expression of Rho kinase. If Rho kinase was responsible for the loss of Baz from the leading edge at the onset of DC, we would expect to observe Baz remaining at the DC leading edge, and no accumulation of PIP_3. In control embryos, the exclusion of Baz from the front of DME cells results in the formation of a PIP_3 gradient, which is required for the formation of actin protrusions required for zippering.

Chapter 6. The role of PIP_3 and downstream effectors in *Drosophila* epidermal wound healing

Filopodia have been shown to be vital for re-epithelialisation, in particular during the final phases of joining together epithelial edges where they make contact with filopodia from the opposing epithelial edge and 'pull' the wound closed (Wood *et al.* 2002). In addition to this role in the final sealing of the wound, they have recently been shown to be required throughout the whole process, contributing to the contraction of the wound by reaching across the wound and making contact with the other side (Abreu-Blanco *et al.* 2012). Cdc42 can regulate the formation of filopodia during wound healing in a variety of systems including *Drosophila* and *Xenopus* embryos and adult mice, with a reduction in levels of Cdc42 resulting in less actin protrusions and slower or failed re-epithelialisation (Wood *et al*. 2002; Davidson *et al*. 2002; Anttonen *et al.* 2012). Additionally, during *Drosophila* larval wound healing, the JNK pathway appears to be required for the formation of actin protrusions (Bosch *et al*. 2005). Other than Cdc42 and JNK our knowledge of protrusion regulation during re-epithelialisation is limited and it is vital that it is improved.

DC has been shown to have many parallels to wound healing (Wood *et al*. 2002), therefore we sought to determine if the PIP_3-MBC-Rac pathway observed in the regulation of filopodia during DC also functions during re-epithelialisation in the *Drosophila* embryo. Rac has previously been shown to be important in the process of re-epithelialisation in both adult mice and *Drosophila* larvae, where loss of Rac was shown to result in a delay in re-epithelialisation, due to a decreased rate of migration, cell polarisation and adhesion (Tscharntkne *et al*. 2007; Baek *et al*. 2010). Contrasting this, Rac has been shown to be dispensable for the process of *Drosophila* embryonic wound healing (Wood *et al*. 2002). The roles of PIP_3 and MBC in re-epithelialisation have not previously been shown, however, given the function of PIP_3 in cell migration and actin cytoskeletal reorganisation, and our previous data in DC, we felt that PIP_3 and its downstream effectors are good candidates as regulators of actin protrusions formation during epithelial wound healing.

6.1 PIP_3 is required for re-epithelialisation

6.1.1 Reducing levels of PIP_3 reduces actin protrusions during re-epithelialisation

To determine if PIP_3 is required for the process of re-epithelialisation, we first investigated its distribution in the epidermis during wound healing. To do this, we laser wounded embryos expressing tGPH (to visualise the localisation of PIP_3), using a micropoint laser attached a Nikon A-1R confocal microscope and live imaged the process of wound closure. Prior to wound healing, GPH (PIP_3) is localised weakly to cell junctions throughout the epidermis

indicating that there is little PIP_3 present. Within 10 minutes of wounding, we observed GPH accumulating strongly to the wound edge, primarily at cell junctions, indicating an accumulation of PIP_3 at these junctions (Figure 49 A). Over time, this localisation became more pronounced, with GPH accumulating at every wound edge cell junction, in a similar manner to the localisation observed during DC. The distribution of PIP_3 is thus polarised in wound edge cells, with the edge of the cell facing the wound having higher levels of PIP_3 than the rest of the cell.

The accumulation of PIP_3 at cell junctions at the wound edge over time suggested that it may be playing a role in wound healing, so we next sought to determine whether healing was affected by depletion of PIP_3. To reduce levels of PIP_3 we expressed UAS-PTEN3 throughout the embryonic epidermis under the control of a double epidermal driver, *e22c*-Gal4, *I67D*-Gal4 (this experiment was carried out by Juliana Alves-Silva, a post doc in the Millard lab). Additionally, UAS-m-Cherry-Moesin was also expressed to visualise F-actin throughout the epidermis. Two drivers were used to maximise PTEN3 expression and therefore maximise PIP_3 degradation and also to provide high levels of m-Cherry-Moesin expression to improve imaging.

Using the micropoint laser, small wounds of 150-250 μm in size were made in the epidermis of the *Drosophila* embryo. These wounds would generally take around 30-60 minutes to close allowing the whole process of wound healing to be observed and multiple wounds to be imaged in reasonable time periods. Use of m-Cherry-Moesin to visualise F-actin allowed the observation of both the actin cable and actin protrusions during wound healing. To analyse the effects of reducing PIP_3 on wound healing, we first analysed the percentage of the wound covered in actin protrusions between 20 and 40 minutes post wounding. As wound edge filopodia tended to be shorter than those observed during DC, it is harder to distinguish between individual filopodia, as such we found analysing area covered by protrusions to be a more accurate representation of total protrusive activity during wound healing than counting individual protrusions. Using percentage coverage rather than absolute area allowed us to more accurately compare wounds of different sizes. Actin protrusion coverage was measured between 20 and 40 minutes, as this was the period when protrusions were consistently present and easy to measure. We found that in embryos in which PIP_3 levels were reduced by expression of PTEN3, the percentage of wound area covered by protrusions was significantly decreased when compared to controls (19.68% ± 5.99 and 28.18 ± 4.32 respectively. $p=0.0031$) (Figure 49 B, C).

Additionally, we sought to determine if this change in protrusions resulted in a delay in re-epithelialisation. We quantified the time taken for wounds to reach 95% closure of the original wound area as opposed to 100% closed, as the amount of protrusions present during the final stages of re-epithelialisation makes it challenging to accurately determine the precise moment

when closure is complete. Wounds made in embryos expressing UAS-PTEN3 throughout the epidermis took slightly longer to close 95% of the original wound size (49.2 ± 4.33 minutes), when compared to wounds in control embryos (42 ± 4.64 minutes). However, this decrease in duration of wound closure was not statistically significant (p=0.2214) (Figure 49 B, C, E).

As the overall time taken to close 95% of the wound was only slightly increased, we analysed the extent of wound closure over time to determine if one phase of closure is particularly affected (Figure 49 F). There was a general trend for embryos expressing UAS-PTEN3 to be larger than controls throughout the process, with wounds being significantly larger at the 14 and 30 minute time points (p= 0.0086 and p=0.0356 respectively)), and the other time points all close to significance (10 minutes p= 0.0501, 18 minutes p=0.1123, 22 minutes p= 0.1114, 26 minutes p=0.0583).

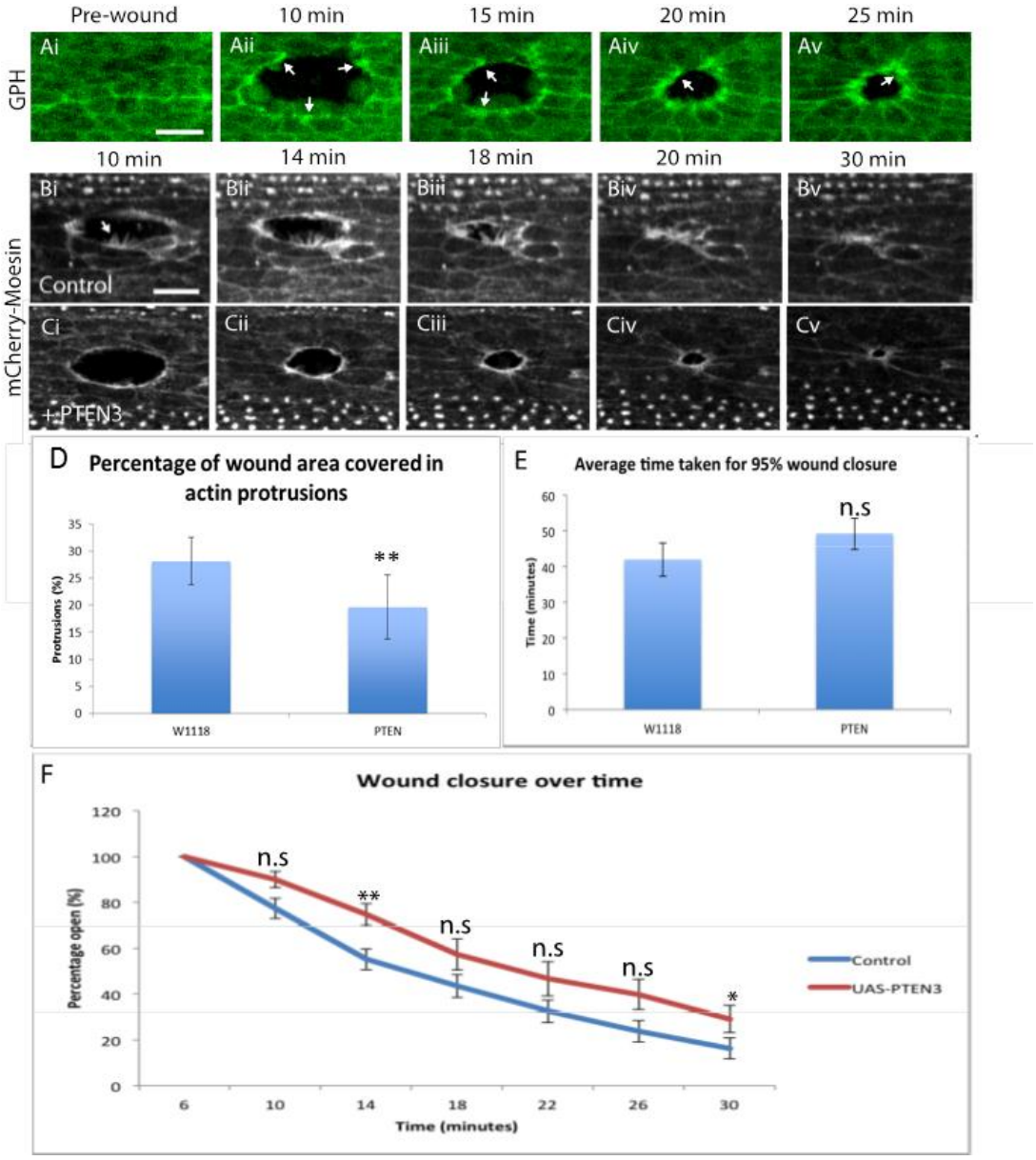

Figure 49. PIP_3 is required for re-epithelialisation. A) GPH localisation during re-epithelialisation. Arrows indicate an accumulation of GPH at wound edge cell junctions. Time-lapse image of wound healing in B) control embryos and C) UAS-PTEN3 expressing embryos. UAS-m-Cherry-Moesin is also expressed under the control of *e22c*-Gal4, *I67D*-Gal4. D) Quantitation of the average number of protrusions present between 20 and 40 minutes post wounding and E) the time taken for the wounds to close 95% of their original area. F) Quantitation of the average size of the wounds over time in embryos with reduced levels of PIP_3 when compared to controls. ** indicates $p< 0.01$, * indicates $p< 0.05$, n.s indicates no significant difference from controls. Error bars indicate S.E.M. Scale bar represents 10 µm. Whole sequence of GPH accumulating at wound edge cell junctions is shown in movie 9 in appendix 2.

6.2 Increasing levels of PIP_3 results in increased protrusions during wound healing

Having shown that reducing the levels of PIP_3 resulted in a modest decrease in the rate of wound healing, probably due to a reduction in the amount of protrusions present, we investigated if wound healing is affected by increasing levels of PIP_3. To increase PIP_3 levels, we used two approaches; expressing UAS-CA-PI3K and generating embryos lacking maternal and zygotic expression of PTEN.

6.2.1 Expression of CA-PI3K increases the amount of actin protrusions present during wound healing.

As expression of UAS-CA-PI3K in DC resulted in an increase in PIP_3 (as determined by observing GPH distribution), we used the same approach to increase PIP_3 during wound healing, expressing UAS-CA-PI3K throughout the embryonic epidermis under the control of *e22c*-Gal4 and *I67D*-Gal4. UAS-m-Cherry-Moesin was expressed alongside UAS-CA-PI3K to allow visualisation of F-actin throughout the epidermis. Analysis of the % protrusion coverage between 20 and 40 minutes post wounding revealed that embryos expressing UAS-CA-PI3K formed significantly more protrusions (50% ± 4.66) than control embryos (35.59% ± 3.73) ($p<0.0001$) (Figure 50 A, B, D).

Laser wounding (as described above) of embryos expressing UAS-CA-PI3K throughout the epidermis resulted in wounds that took 35 ± 4.33 minutes to close, compared to 41.33 ± 3.6 minutes in control embryos ($p=0.2754$). To investigate if the increase in protrusions had an effect on wound healing at any phase of closure, we compared wound size at comparable times between embryos expressing UAS-CA-PI3K and controls. We found that there was a trend for wounds in embryos expressing UAS-CA-PI3K to be smaller than those in controls at all time points, however at no point did the difference reach significance (Figure 50 E).

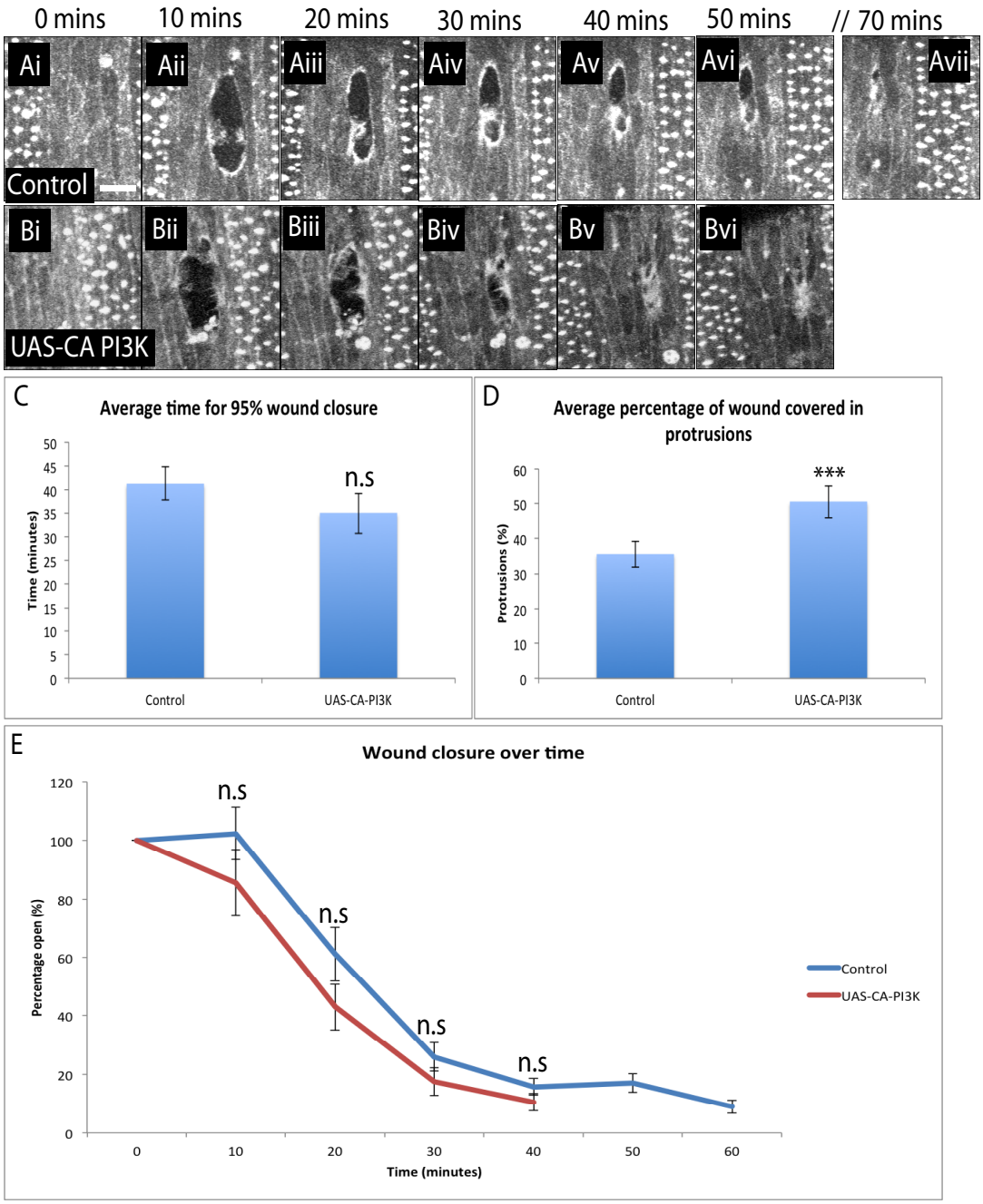

Figure 50. Expression of UAS-CA-PI3K increases the number of protrusions during wound healing. Time lapse images taken from wound healing in A) Control embryos and B) embryos expressing UAS-CA_PI3K throughout the epidermis. C) Quantitation of the time taken for the embryos to close 95% of the original wound area. D) Quantitation of the number of protrusions formed at the wound leading edge. n ≥ 8. *** indicates a significant difference from controls P<0.001. n.s. indicates no significant difference from controls. Error bars indicate S.E.M. Scale bar represents 10 μm. Whole sequence is shown in movie 10 in appendix 2

6.2.2 Embryos lacking expression of PTEN exhibit significantly more protrusions during wound healing

As expressing UAS-CA-PI3K did not result in a significant increase in the rate of wound healing, we adopted an alternative approach to increase the amount of PIP_3 during healing. We made embryos that lacked both maternal and zygotic expression of PTEN. As shown in chapter 3, these embryos exhibit elevated PIP_3 levels.

Expressing GFP-Moesin ubiquitously throughout the embryos allowed visualisation of the F-actin throughout the embryonic epidermis. As previously, control embryos sealed the wounds using both an actin cable and protrusions, with both structures becoming visible within 20 minutes post wounding. Wounds in control embryos took on average 54 ± 5.85 minutes to close 95% of the original wound size. Embryos lacking expression of both maternal and zygotic PTEN showed a significant increase in the amount of protrusions observed at the wound edge (45.35% ± 4.01 and 30.47% ± 4.46 of the total wound area respectively, p=0.0011) (Figure 51 A, B, D) although the rate of re-epithelialisation was not significantly altered, taking on average 44 ± 5.46 minutes to close 95% of the original wound size (p= 0.3512) (figure 51 A-C). When the size of the wounds were analysed, we found that although there was a trend for wounds to be smaller, the difference is only very small and showed no significance at any point in wound healing (Figure 51 E).

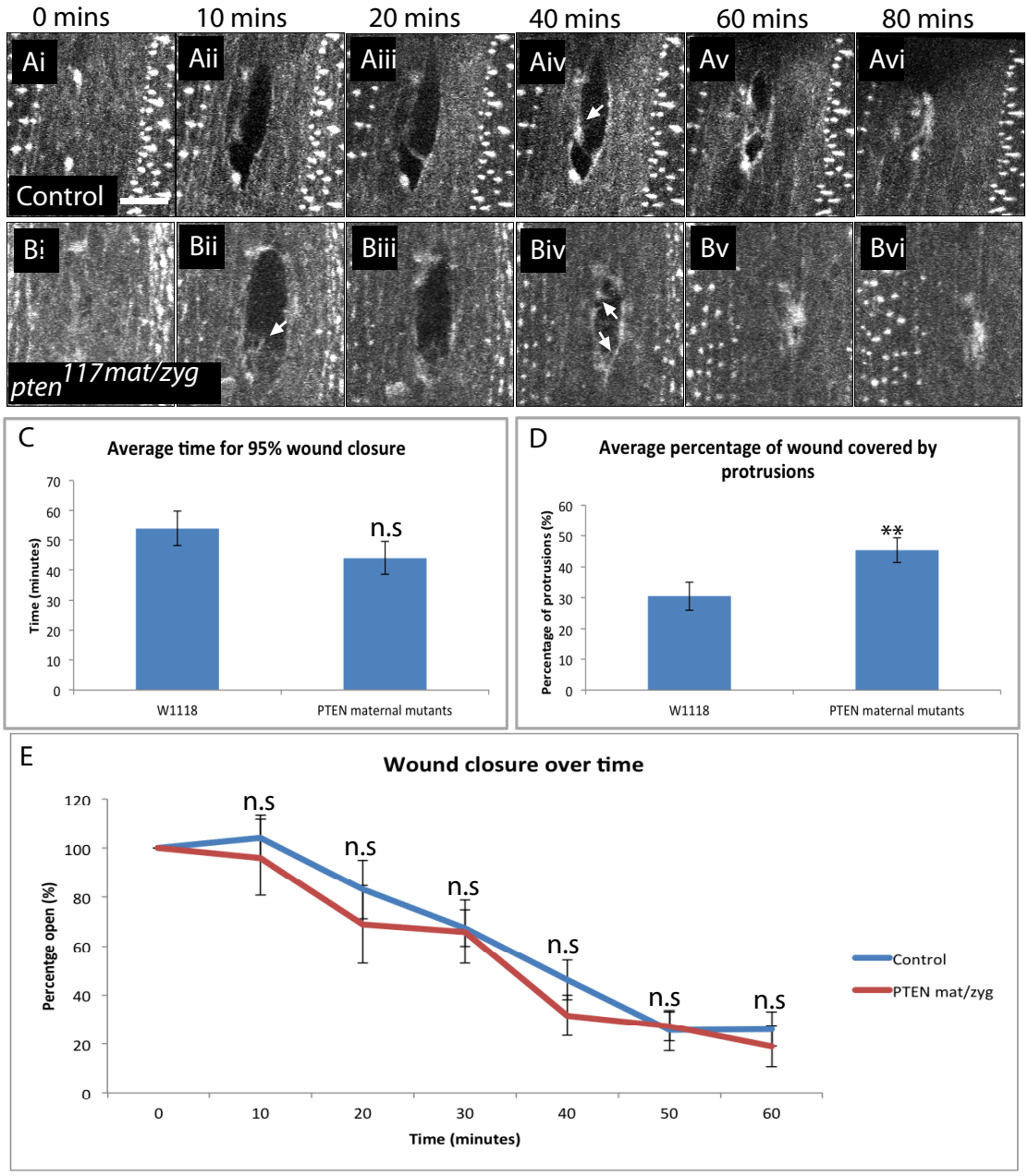

Figure 51. Reduction in PTEN results in slightly quicker wound healing and more protrusions. Time lapse images of A) control embryos and B) embryos lacking expression of maternal and zygotic PTEN. Arrows show the formation and persistence of actin protrusions throughout wound healing. C) Quantitation of the time taken for the wound to heal to 95% of the original size. D) Quantitation of the percentage of the wound covered in protrusions between 20 and 40 minutes of wound healing. n > 7. ** indicates significant difference to the control p<0.005. n.s indicates no significant difference observed from the controls. Error bars indicate S.E.M. Scale bar represents 10 μm. Whole sequence is shown in movie 11 in appendix 2

6.3 MBC is required for efficient wound healing

Having demonstrated that PIP_3 regulates actin protrusions during epithelial wound healing, we next sought to determine whether the downstream signalling pathway components identified during DC also function during re-epithelialisation. We hypothesised that in a similar manner to DC, MBC could be required for re-epithelialisation by regulating the formation of actin protrusions.

To investigate the role of MBC during re-epithelialisation we analysed the effect of loss of MBC on actin protrusions and wound closure speed. Using the mbc^{C1} null allele, we expressed constitutive GFP-Moesin to visualise F-actin in embryos zygotically null for *mbc* to determine if MBC has any role in re-epithelialisation. As previously, wounding control embryos resulted in wounds that formed an actin cable and protrusions by 20 minutes with protrusions on average covering 29.93 % ± 4.18 and 95% closure taking 32 ± 4.68 minutes (Figure 52 A). Embryos lacking zygotic expression of MBC formed some protrusions by 20 minutes, along with an actin cable (Figure 52 B). However, on average the amount of protrusions formed was reduced with 28.29% ± 3.52 ($p < 0.0001$) of the wound covered (Figure 52 D). Additionally, the time taken for the wounds to reach 95% closure was significantly greater than observed in control embryos (52 minutes ± 7.92 $p= 0.0379$) (Figure 52 C). Furthermore, throughout wound healing the wounds appeared to be larger than controls and the final phase of re-epithelialisation appeared more affected than controls (Figure 52 E). However, the biggest difference between the two sets of data occurred within the first 10 minutes after wounding, where controls appeared to close much quicker than those lacking expression of MBC. These data indicate that MBC is important in the regulation of actin protrusions and wound closure during re-epithelialisation in *Drosophila* embryos.

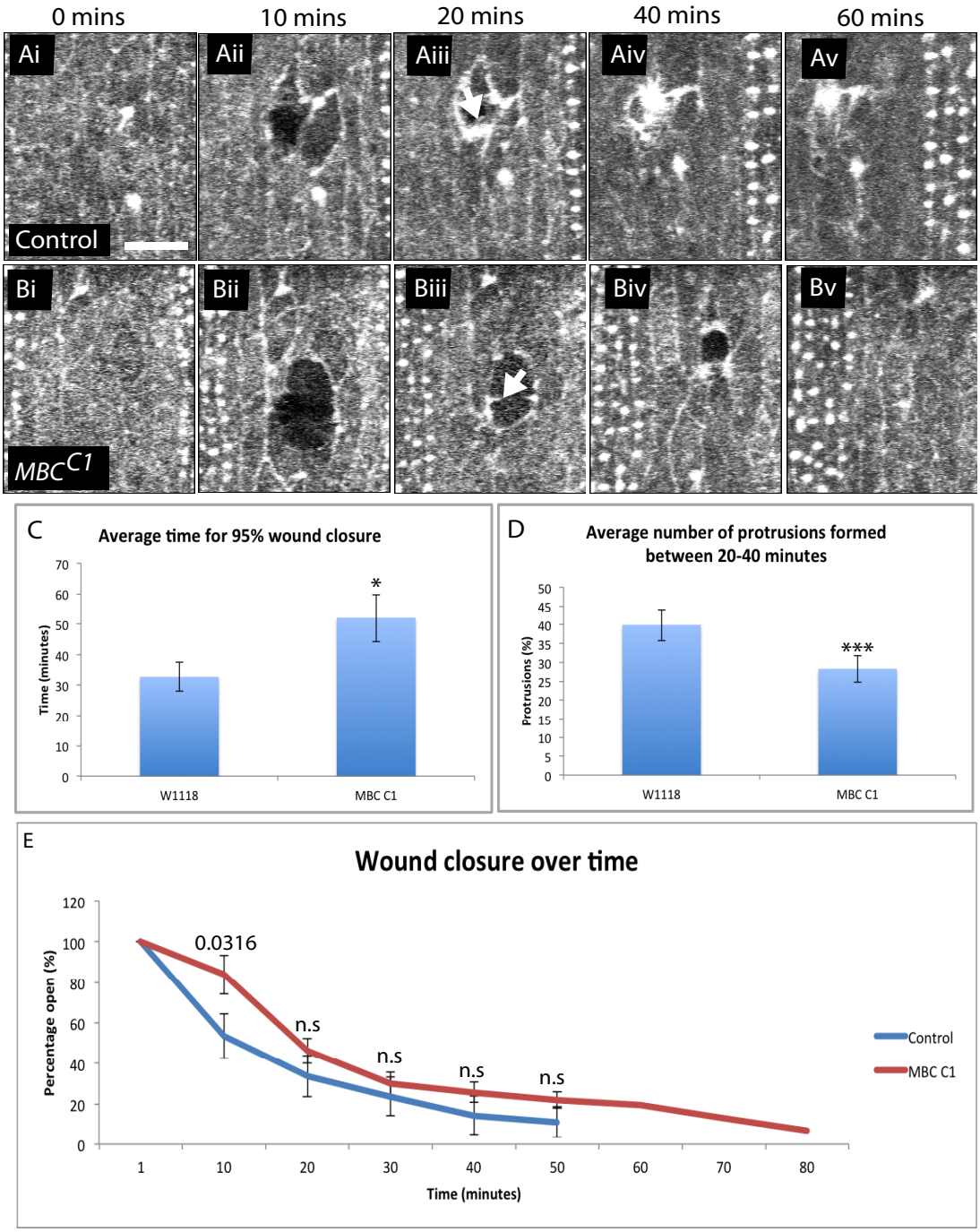

Figure 52. Reduction in levels of MBC results in slower wound healing. Time lapse images of wound healing in A) control and B) *mbc*^{C1} mutant embryos. Arrows indicate the formation of actin protrusions. C) Quantitation of the average time taken for embryos to close 95% of the original wound area. D) Quantitation of the average number of protrusions formed between 20 and 40 minutes of wound healing. n = 11. *** indicates a significant difference from the control P<0.001. * indicates a significant difference from the control P<0.01. Error bars indicate S.E.M. Scale bar represents 10 µm. Whole sequence is shown in movie 12 in appendix 2.

6.4 Rac is required for efficient wound healing

Previous data has shown that Rac is a downstream effector of PIP_3 and MBC during DC, and as these are both are involved in epithelial wound healing, we hypothesised that Rac would also be involved in wound healing.

6.4.1 Loss of Rac results in slower wound healing

To evaluate if Rac has a role in re-epithelialisation in *Drosophila* embryos, we analysed the formation of actin protrusions and the rate of wound healing in embryos zygotically null for all three *Drosophila rac* genes. In chapter 4, two triple *rac* mutant lines, rac^{J10} and rac^{J11}, were analysed, both of which display DC defects. We analysed the actin dynamics during wound healing in both mutant lines by expressing constitutive GFP-Moesin to visualise F-actin. Embryos were wounded as described previously, with an actin cable and protrusions forming within 20 minutes of wounding in control embryos (Figure 53 A).

As previously, actin protrusions between 20 and 40 minutes post wounding were analysed and the time for wounds to reach 95% of their original wound size was calculated. In control embryos, an average of 21.12 % ± 3.81 of the wound area was covered with protrusions and wounds took 41.81 minutes ± 5.51 to reach 95% closure (Figure 53 A, D, E). In comparison, in both *rac* mutant lines, the percentage of wound covered with protrusions was reduced when compared to control embryos (30.85% ± 4.16 wound coverage for rac^{J10} and 22.77% ± 2.48 for rac^{J11} compared to 28.12 ± 3.81 for the controls p=0.023 and <0.0001 respectively) (Figure 53 B, C, E). Additionally, wound healing was delayed in rac^{J11} embryos, but not in rac^{J10} embryos. In rac^{J10} embryos the wounds took on average 59 ± 12.42 minutes to close (p=0.3375 when compared to wounds in control embryos), but the rac^{J11} mutant embryos took significantly longer to heal the wounds than controls (65.5 ± 7.06 minutes, p=0.0103) (Figure B, C, D).

To further determine whether Rac is important for re-epithelialisation, we compared the average size of the wounds over time to those of control embryos (Figure 53 F). Although there was a trend for wounds lacking zygotic expression of Rac to be larger than controls at the equivalent time point after wounding, at no point did this difference reach significance for either Rac mutant line, however this data did indicate that rac^{J11} embryos took longer to complete the final re-sealing phase of re-epithelialisation.

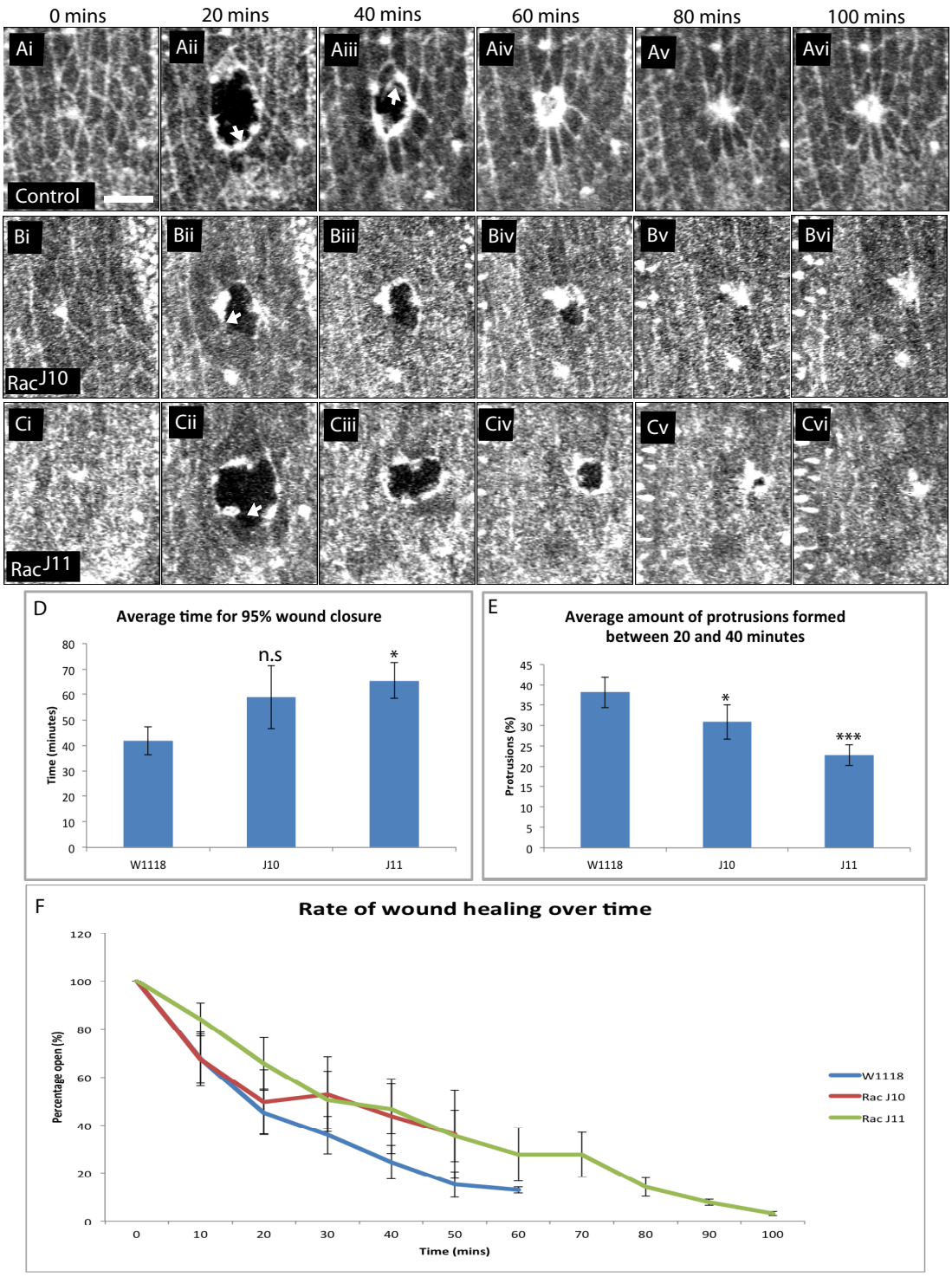

Figure 53. Loss of Rac results in slower wound healing. A-C) Images taken from time-lapse movies of wound healing in Control, *rac*^{J10} and *rac*^{J11} mutant embryos. Arrows indicate the presence of an actin cable and protrusions. D) Quantitation of time taken for embryos to close 95% of the original wound size. E) Quantitation of the average number of protrusions observed between 20 and 40 minutes of wound healing. n ≥ 7 embryos *** indicates a significant difference from controls P<0.001, * indicates a significant difference of P<0.05 and n.s indicates no significant difference from controls. Error bars indicate S.E.M. Scale bar represents 10 µm. Whole sequence is shown in movie 13 in appendix 2

6.4.2 Increasing levels of Rac increases the speed of wound healing

We have previously shown that expressing UAS-Rac1-wt during DC resulted in an increase in the number of filopodia and so we hypothesised that increasing the levels of Rac would result in an increase in the number of protrusions present at the wound edge and thus increase the rate of re-epithelialisation. Using the double epidermal driver used previously (*e22c*-Gal4; *I67D*-Gal4), we expressed UAS-Rac1-wt alongside UAS-m-Cherry-Moesin throughout the embryonic epidermis and wounded embryos as previously described using the Micropoint laser attached to the Nikon confocal. As expected, control embryos formed an actin cable and protrusions by 10 minutes, with the cable thickening over time (Figure 54 A) and on average the wounds in control embryos had closed 95% of their original size by 42 ± 5.65 minutes (Figure 54 C). When UAS-Rac1-wt was expressed throughout the epidermis, the actin cable and protrusions were also formed within 10 minutes (Figure 54 B), however on average a greater proportion of the wound area was covered in protrusions than controls (44.95% ± 4.25 compared to 36.41% ± 4.97 in the control embryos $p<0.0001$), and embryos expressing UAS-Rac1-wt reached 95% closure quicker than controls (30.5 ± 2.24 minutes, $p=0.0257$) (Figure 54 C, D).

To investigate if increasing the amount of Rac present had an effect on any particular phase of re-epithelialisation, we analysed the average size of the wound during healing (Figure 54 E). It can be seen that throughout wound healing, embryos expressing UAS-Rac1-wt had a trend for slightly smaller wounds and interestingly, the shape of the graph differed in the first 10 minutes indicating an initial increase in wound size in control embryos resulting in a significant difference in wound area ($p=0.0412$). These data show that Rac is important in the regulation of actin dynamics during wound closure and that by manipulating the levels of Rac, the rate of re-epithelialisation can be altered.

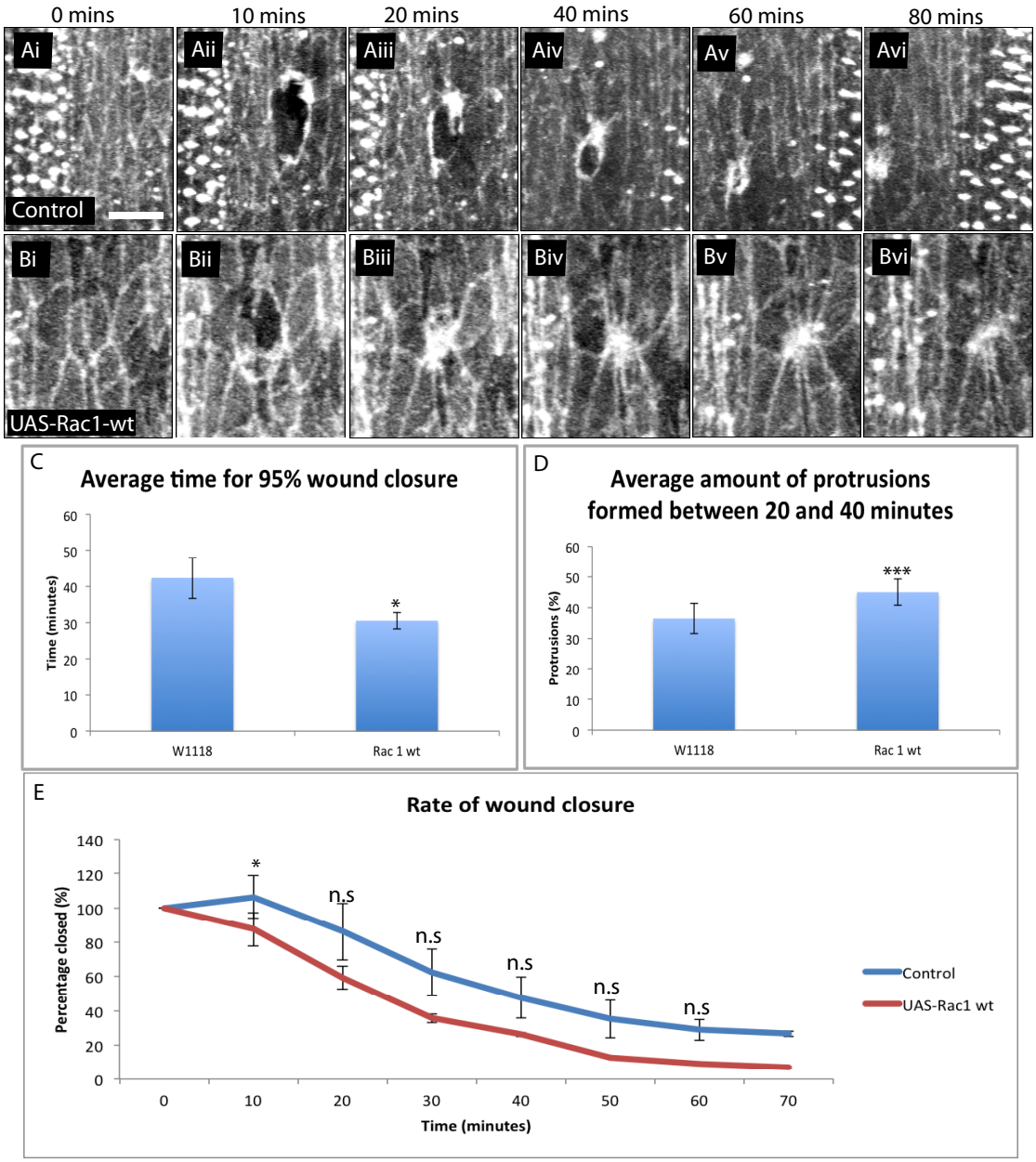

Figure 54. Increasing levels of Rac increases the speed of wound healing. Time lapse images of wound healing in A) control embryos and B) embryos overexpressing UAS-Rac1-wt under the control of *e22c*-Gal4; *I67D*-Gal4. C) Quantitation showing the time taken for the embryos to close 95% of the original wound size. D) Quantitation of the amount of protrusions formed between 20 and 40 minutes of wound healing. n ≥ 14 embryos. *** indicates significant difference from control P<0.001. * indicates significant difference from control P<0.05. Error bars indicate S.E.M. Scale bar represents 10 μm. Whole sequence is shown in movie 14 in appendix 2.

6.5 Baz and actin exhibit a reciprocal relationship during epithelial wound healing

During DC, sequestration of PTEN to cell junctions behind the leading edge by Baz results in PIP_3 accumulation at the leading edge and this drives actin protrusion formation. We sought to determine if a similar mechanism may operate at the wound edge. Embryos expressing UAS-GFP-Baz and UAS-m-Cherry-Moesin under the control of a double epidermal driver (*e22c*-Gal4; *I67D*-Gal4) were laser wounded. Expression of UAS-GFP-Baz and UAS-m-Cherry-Moesin allows visualisation of Baz and F-actin dynamics during wound healing. Prior to wounding Baz localises to cell junctions throughout the epidermis (Figure 55 Ci). Following wounding, Baz begins to be lost from cell junctions at the wound edge and this correlates with the accumulation of actin at the wound edge (within 8 minutes post wounding) (Figure 55 Civ). This result suggests that during epidermal wound healing, in a similar manner to DC, the loss of Baz from the wound edge is required for the formation of actin structures required for wound healing.

In addition to studying the localisation of Baz and F-actin by overexpressing fluorescently tagged proteins, we also analysed the localisation of the endogenous protein by immunofluorescence. Co-staining fixed, wounded embryos with rabbit anti-Baz (red), rat anti-E-cadherin (green) and Alexa647-phalloidin (blue), we were able to compare the localisation of Baz, E-cadherin and F-actin at the wound edge. As observed for GFP-Baz, endogenous Baz is absent from the leading edge and is restricted to cell junctions at the back and sides of wound edge cells. Merging the images of Baz and E-cadherin demonstrates that Baz is present on cell junctions away from the wound edge, whilst merging the images of Baz and F-actin display a reciprocal distribution with F-actin accumulating at the leading edge where endogenous Baz is absent (Figure 56). These results indicate that in both DC and wound healing, Baz exhibits a reciprocal distribution to PIP_3 and F-actin, suggesting the same mechanism may be responsible for promoting leading edge PIP_3 accumulation and hence protrusion formation.

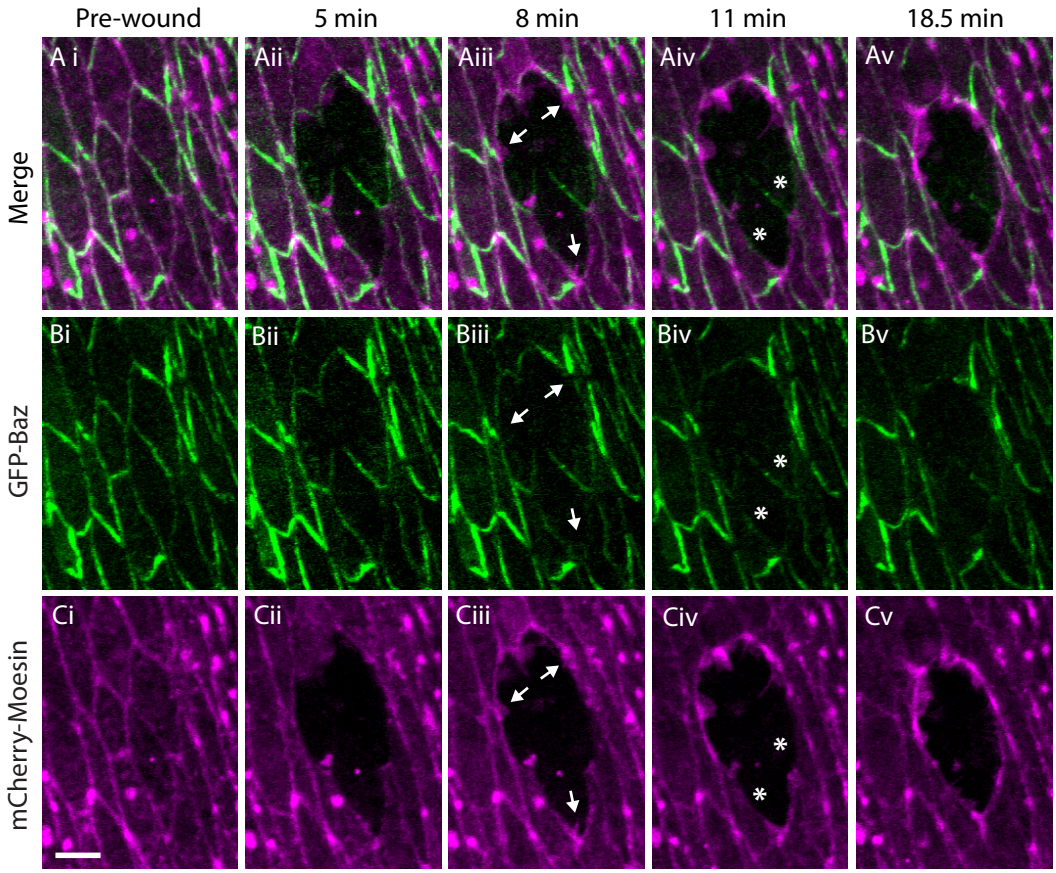

Figure 55. Reciprocal localisation of Baz and actin during epidermal wound healing. Time-lapse images of laser wounded embryos expressing UAS-m-Cherry-moesin and UAS-GFP-Baz demonstrating a loss of Baz corresponding with an accumulation of actin (arrows Ciii). Later in wound healing, asterisks indicate sites where Baz is still present at the wound edge, but actin accumulation is minimal. Scale bars represent 5 μm. Whole sequence is shown in movie 15 in appendix 2

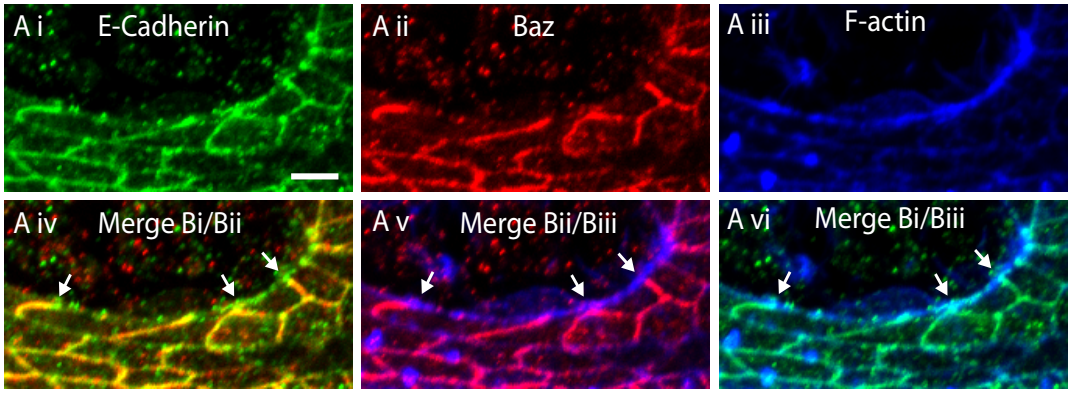

Figure 56. Localisation of endogenous Baz during re-epithelialisation.
Immunofluorescence staining of epithelial wounds with Ai) E-Cadherin (green), Aii) Baz (red) and Aiii) F-actin (blue). A iv- vi) Arrows in merged images indicate where F-actin and E-cadherin are present but Baz is absent. Scale bar represents 5 μm.

Chapter 6 discussion

We have previously shown the requirement of a PIP_3-MBC-Rac pathway in the regulation of actin protrusions during DC. In this chapter we demonstrated that this pathway probably also functions during epithelial wound healing. Additionally, we showed that as in DC, it is likely that redistribution of Baz is responsible for triggering this pathway.

6.6 PIP_3 plays a role in re-epithelialisation

6.6.1 PIP_3 accumulates at epidermal wound edges in a Baz dependent manner

We demonstrated that PIP_3 becomes accumulated at cell junctions at the wound edge in a reciprocal manner to Baz. This observation of PIP_3 accumulating at the front of wound edge cells is consistent with the localisation in DC and cell culture where PIP_3 has been shown to accumulate at the front of DME or migrating cells, where it triggers actin assembly to generate protrusions in the direction of movement (Chapter 3, *et al*. 2001; Funamoto *et al*. 2002; Yoo *et al*. 2010). It is likely that during epithelial wound healing, as with DC, Baz is responsible for generating the specific accumulation of PIP_3 to the front of the wound edge cells where it is required for cell polarisation and the generation of actin protrusions required for efficient wound closure.

Prior to wounding, Baz and actin co-localise on all cell junctions, however once wounded, Baz is lost from the epithelial edge as actin and PIP_3 accumulate. The actin structures formed include an actin cable and actin protrusions, both of which have been shown to be required for efficient wound healing (Martin and Lewis 1992; Wood *et al*. 2002). Although we have not shown it directly, we can assume from the work carried out in DC (Chapter 5), that as Baz is lost from the wound edge, PTEN2 is also lost from the wound edge. This loss of leading edge PTEN2 would then explain the PIP_3 accumulation observed at the wound edge (Figure 44).

Whilst we have demonstrated a role for Baz in epithelial wound healing, it is possible that PI3K is also involved in determining the PIP_3 gradient at epithelial edges. It has previously been shown in MTLn3 rat adenocarcinoma cell culture, that PI3K-mediated lamellipodia are formed in response to EGF signalling, demonstrating that the PI3K signalling pathway can be activated in response to secreted growth factors (Yip *et al.* 2007). Additionally, In *Drosophila* larvae, it has been shown that Pvr (a tyrosine kinase receptor) signalling is required for wound epidermal cells to extend actin protrusions into the gap, and this activation is stimulated by the ligand for Pvr, Pvf1 (which is similar to platelet derived growth factor and vascular endothelial growth factor). It could be that tissue damage, results in exposure of the Pvr receptor to Pvf1, resulting in the activation of downstream signalling pathways, possibly including the PI3K

signalling pathway, required for the regulation of actin dynamics (Wu *et al*. 2009). These data demonstrate that it is possible that growth factors or other secreted molecules are released in response to a wound and could contribute to the production of PIP_3 observed in wound edge cells. From our work, we believe that PTEN polarisation in response to Baz redistribution contributes to wound edge PIP_3 accumulation, but this does not preclude the possibility that activation of PI3K also makes a contribution.

6.6.2 Reduction in PIP_3 levels reduces actin protrusions and delays re-epithelialisation

To determine if PIP_3 plays a role in wound healing, we reduced its levels in the epidermis. Decreasing the levels of PIP_3 throughout the embryonic epidermis by overexpression of PTEN3 resulted in a decrease in protrusions at the wound edge, although this did not result in a significant delay in re-epithelialisation when compared to controls. The loss of protrusions observed in embryos expressing UAS-PTEN3, is consistent with previous work, where we determined that PIP_3 promotes filopodia formation during DC (Chapter 3). That we observe a slight slowing of re-epithelialisation is likely due to the reduction in protrusions at the wound edge. This is consistent with previous work where actin protrusions have been shown to be required for all stages of wound closure (Abreu-Blanco *et al*. 2012). Interestingly, while we observed that embryos with reduced levels of PIP_3 and thus reduced numbers of protrusions were able to undergo re-epithelialisation, previous work has demonstrated that wounds in embryos lacking the ability to form protrusions fail to close their wounds (Wood *et al*. 2002). It is possible that in our experiments, filopodia are mainly involved in the final phase of re-sealing, which is difficult to analyse, and as such we were unable to detect significant changes in re-epithelialisation when PIP_3 levels were reduced. Alternatively, it is possibly that filopodia were not completely eliminated and those remaining are sufficient to accomplish the final re-sealing required to complete re-epithelialisation. This would suggest that either overexpression of PTEN3 does not reduce PIP_3 levels sufficiently, or there is an alternative PIP_3-independent pathway that promotes actin protrusion formation during re-epithelialisation. One possibility for this is Cdc42, which has been shown in both DC and wound healing to be vital for the formation of protrusions required for epithelial fusion (Jacinto *et al*. 2000; Wood *et al*. 2002).

We have shown that reducing the levels of PIP_3 in the embryonic epidermis results in a slight delay in re-epithelialisation, however, given the effect of loss of PIP_3 in DC, we were expecting a more dramatic effect. It could be that protrusions play a larger role in DC than in wound healing and as such their removal has a greater effect on the process of DC. Consistent with this theory, the filopodia observed in DC are longer and greater in number than in wound healing, indicating they may be more important during DC. Additionally, it is possible that during wound healing, the actin cable plays a larger role than it does during DC, and is the main driver of wound closure, with only a small number of protrusions being required for

efficient closure (Martin and Lewis 1992; McCluskey and Martin 1995). An additional explanation for the lack of a significant reduction in speed of wound closure is that there is substantial variation in the closure speed between embryos, making it difficult to reach a statistical significance when observing a relatively modest change.

6.6.3 Increasing PIP_3 levels increases protrusions during wound healing.

Given that reducing PIP_3 levels resulted in a significant decrease in protrusions but not in rate of wound healing, we next sought to determine whether increasing the levels of PIP_3 could enhance epithelial wound healing. Expressing UAS-CA-PI3K throughout the epidermis, or wounding embryos lacking maternal and zygotic expression of PTEN resulted in more wound edge actin protrusions, and slightly faster re-epithelialisation, with wounds appearing smaller throughout wound healing. This trend for smaller wounds that close faster is consistent with the increased number of protrusions observed. Although we did not examine the PIP_3 levels directly in these embryos, we assume that there would be an increase in PIP_3 at the wound edge in both embryos expressing UAS-CA-PI3K and *pten*$^{117\ mat/zyg}$ embryos when compared to wounds in control embryos. In a similar manner to DC, we propose that this elevation of PIP_3 was sufficient to stimulate the formation of additional protrusions aiding the closure of the wound, especially in the final 'knitting-together' stage. The lack of a significant increase in wound healing in these embryos could be due to PIP_3 being elevated on all cell junctions, not just the leading edge, meaning that polarisation is reduced. However, it is also possible that the amount of protrusions present is not the main determinant of closure speed. It is likely that throughout wound healing the actin cable is the main determinant of closure speed, especially as it has shown to be a main driver in re-epithelialisation (Martin and Lewis 1992; Wood *et al*. 2002).

Since filopodia are believed to be most important in the final stages of wound closure, it is possible that this phase of closure is faster on increasing PIP_3 levels, but since it is very difficult to image this phase clearly, we are failing to observe this change. We did not observe any difference in the actin cable on changing the levels of PIP_3, suggesting that it is regulated by a different mechanism to the protrusions.

6.7 MBC and Rac are required for epithelial wound healing

6.7.1 MBC is required for epithelial wound healing

Embryos lacking zygotic expression of MBC produced fewer protrusions at the wound edge than controls and this reduction in protrusions, resulted in slower re-epithelialisation. Wounds appeared to be slightly larger throughout wound healing, but the most noticeable characteristic

of these wounds was a delay in response to injury. Within the first 10 minutes, wounds did not undergo substantial contraction when compared to controls, this could be due to wound egde cells failing to reorganise the actin cytoskeleton sufficiently to contract in size. In addition to the lack of initial response it appears that the wounds take longer in the final re-sealing of the epithelium. We propose that this delay in the final phase of wound healing is a result of a lack of actin protrusions, however, due to imaging constraints we are unable to analyse this clearly. However, this would be consistent with previous work which has shown the importance of actin protrusions in this final re-sealing phase (Wood *et al* 2002).

Although no previous work has looked directly at the role of MBC in wound healing (or its homologue Dock180 in other systems), it has been implicated in a range of cell motility processes including chemotaxis (Erickson *et al.* 1997; Nolan *et al.* 1998). This is consistent with our observation in both DC and wound healing that MBC is a regulator of actin protrusion formation, required for re-epithelialisation.

6.7.2 Rac is important for re-epithelialisation in *Drosophila* embryos

As discussed above, we have identified PIP_3 and MBC to be regulators of actin protrusion formation during re-epithelialisation. As we have shown that PIP_3 regulates the actin cytoskeleton in an MBC-Rac dependent manner during DC, we next investigated the importance of Rac during re-epithelialisation. To investigate the role of Rac in wound healing, we took two approaches; reducing the levels of Rac by using embryos lacking zygotic expression of all three *rac* genes (rac^{J10} and rac^{J11} mutant embryos), and increasing the total level of Rac by expressing UAS-Rac1-wt throughout the epidermis of the embryos. Embryos expressing UAS-Rac1-wt or rac^{J11} embryos displayed significant changes in both the amount of wound covered in protrusions and the speed in re-epithelialisation. Wounding of the rac^{J10} allele, resulted in a slight reduction in the amount of protrusions at the wound edge, however this did not result in a significant change in the time taken for re-epithelialisation to occur. The failure to observe significant changes in the time taken for 95% closure to be reached in rac^{J10} embryos may be due high variability in the data, and that the number of embryos analysed was smaller (n=7) when compared to controls (n=13) or rac^{J11} (n=12). Interestingly, we did observe a significant change in both the amount of protrusions formed at the wound edge and the time taken for wounds to heal in rac^{J11} null embryos.

Increasing the levels of Rac in the epidermis was sufficient to increase the rate of wound closure, likely due to the increase in the amount of protrusions. Embryos expressing UAS-Rac1-wt appear to respond rapidly to the formation of a wound as there is no lag before the wound starts to contract, as can be observed in the control embryos. This could be because Rac stimulates actin polymerisation through activating the WAVE complex (and thus the Arp2/3 complex) (Steffen *et al.* 2004). Therefore, increasing levels of Rac leads to faster

formation of actin filaments at the wound edge, resulting in faster assembly of protrusions and cable. Although the wound size is slightly smaller than controls throughout wound healing in Rac1-wt expressing cells, the major difference occurs in the initial response to the wound, suggesting that once the closure process is established, Rac is not having a major role in determining the closure speed.

Our data showing a role for Rac in regulating protrusions during wound healing is consistent with previous work in DC, where we (and others) have shown the importance of Rac in the regulation of filopodia formation and epithelial closure (chapter 4, Woolner *et al*. 2005). Additionally, these data correspond with work in adult mice and *Drosophila* larvae where it has been shown that Rac is important for regulating the actin cytoskeleton required for re-epithelialisation. However, these results are inconsistent with previous wound healing studies in *Drosophila* embryos. Wood *et al.* (2002) demonstrated that in embryos lacking zygotic expression of Rac, re-epithelialisation was not delayed. This discrepancy between the two studies can be explained in a number of ways; firstly, Wood *et al.* used the rac^{J10} mutant allele, and as we have shown rac^{J10} did not elicit a significant retardation of re-epithelialisation, indicating that the rac^{J10} mutants may be a weaker allele than rac^{J11} for which we did observe a change. Additionally, the embryos used in the Wood *et al.* study were collected at stage 15, whilst ours were late stage 15 to stage 16. As our embryos were slightly older, there was probably less maternally contributed Rac present. Finally, there was no mention about the criteria for the size of wounds used in the study by Wood *et al*. We found that the rate of wound healing varied greatly between smaller and larger sized wounds, which is why we restricted analysis to wounds that were 150-250 μm in size. It is possible that in the previous study, there was a greater variation in the size of wounds resulting in more fluctuation between rates of wound closure and so no significant difference in the rate of wound healing was observed. From this study, we conclude that, as during DC, Rac is a regulator of protrusion formation during wound healing.

One difference that was noticeable throughout the wound healing studies is the initial response to injury in the controls. We found a lot of variation between studies, with some embryos gaping after wounding, whilst some were able to contract and begin wound closure rapidly. This does not appear to be an artefact of wound size as all data was collected from wounds that were between 150-250 μm. It is possible that the observed difference in gaping could be a result of difference in tension within the embryos, affecting the response of individual embryos to respond to the presence of the wound. However, it is also possible that this is natural variation that occurs between embryos, which at present we cannot explain.

6.8 Summary

We have shown during re-epithelialisation that PIP_3, MBC and Rac are all required for efficient wound healing, and loss of any of these signals results in a reduction in actin protrusions and a reduced rate of re-epithelialisation. This observation combined with the genetic interactions identified in DC suggests that the same pathway is operating in both DC and wound healing.

One interesting difference between the DC and wound healing studies is that while in both cases loss of PIP_3, Rac or MBC resulted in significant reductions in protrusions, in wound healing it didn't always result in a significant change in closure speed, whereas it did in DC. One possible explanation for this is that protrusions play a greater role in determining the rate of DC than they do in wound healing, where the actin cable seems to be main driver of closure. Another possible explanation is that there is greater variation in closure rate between samples in wound healing than DC, meaning that it is more difficult to obtain significant differences for comparatively small changes. During the wound closure studies, we measured total protrusion area as opposed to filopodia number, as there is a mixture of both filopodia and lamellipodia formed at the wound edge, making it difficult to discern between the two. As such, it is probable that PIP_3 is capable of affecting the formation of both lamellipodia and filopodia during wound healing, especially given that it is required for the re-organisation of the actin cytoskeleton into pseudopods and lamellipodia during *Dictyostelium* chemotaxis (Funamoto *et al*. 2002). Given that increasing PIP_3 did not result in an increase in the rate of re-epithelialisation, but was sufficient to increase actin protrusions, suggests that the actin cable may be the main driving force that controls the speed of re-epithelialisation, and as altering levels of PIP_3 did not have any discernible effect on the cable, the rate of closure was not greatly altered. We suggest that protrusions are required for closure, but not in great numbers, so that a partial loss of protrusions does not have a major impact on closure. To further investigate the role and regulation of filopodia during re-epithelialisation, it would be interesting to carry out wound healing experiments in embryos lacking an actin cable (*rho* mutant embryos), this would enable us to observe more significant differences associated with changes in actin protrusions.

Also consistent with DC is the role of Baz, which appears to regulate the region of the cell in which F-actin accumulates and as such determines the localisation of actin structures. Given that Baz re-localises to cell junctions at the rear and sides of wound edge cells upon injury, we propose that Baz works in a similar manner to DC; sequestering PTEN2 away from the leading edge, allowing PIP_3 to accumulate at the front of the cell, where it regulates the formation of actin protrusions in an MBC-Rac dependent manner.

Chapter 7. Investigation of PIP_3 function during cell extrusion in the amnioserosa

Multiple mechanical forces contribute to the closure of the dorsal hole during DC, including forces provided by the actin cable, zippering and contraction of the amnioserosa (Jacinto *et al*. 2002; Jacinto *et al*. 2002b; Toyama *et al.* 2008; Solon *et al.* 2009). The amnioserosa is a very dynamic tissue which contributes to dorsal hole closure in three ways; firstly, the cells in the amnioserosa change shape to become tall and thin, thus reducing the size of the dorsal hole, secondly, amnioserosa cells undergo apical contractions pulling the leading edges towards one another, and thirdly, cells are extruded from the amnioserosa, basally into the cavity of the embryo (Toyama *et al.* 2008; Solon *et al*. 2009). Although not fully understood, it has been shown that the actomyosin constrictions of amnioserosal cells are regulated by the Par polarity complex, with Baz promoting the duration of the pulses, whilst Par6/aPKC controls the amount of time between pulses (David *et al*. 2010). The signalling pathways and mechanisms required for amnioserosa cell extrusion (also called delamination) are also not fully understood, however there appears to be multiple forces associated with this process. The delaminating cell itself constricts apically and the surrounding cells elongate in the direction of movement. This elongation of surrounding cells could be in response to the presence of a gap, or they could actively play a role in squeezing the cell from the tissue. As yet, the signals that initiate and drive this delamination are not known.

In addition to contracting actomyosin, which has been shown to be vital in the process of cell constriction and delamination (Rosenblatt *et al*. 2001), there are also many highly dynamic actin protrusions formed on the apical surface of the amnioserosa. Although the role of these protrusions has not been studied, it is possible that they could be important for cell constriction or delamination. Given that we have previously shown Baz to be an upstream regulator of PIP_3 in the regulation of protrusions during both DC and wound healing, and that Baz also regulates the duration of pulses of amnioserosal cells, we next investigated if PIP_3 might play a role in the process of cell delamination from the amnioserosa.

7.1 PIP_3 accumulates in the surrounding cells during amnioserosa cell delamination

As the amnioserosa is a highly dynamic tissue, we expressed UAS-GFP-Moesin throughout the epidermis under the control of *e22c*-Gal4 to observe actin structures that are present in the amnioserosa during DC. One notable feature of amnioserosa cells is the presence of filopodia on the apical surface, particular at the junctions between neighbouring cells (Figure 57 A). Given the number of protrusions present, and that we have previously shown PIP_3 to be a regulator of actin protrusion formation at the DC leading edge, we next investigated the localisation of GPH (and so PIP_3) within the amnioserosa.

We expressed tGPH throughout these embryos to observe the localisation of PIP_3 in the amnioserosa. We found that PIP_3 localised very weakly to cell junctions throughout the amnioserosa, but was strongly accumulated around delaminating cells (Figure 57 Bi-v). This accumulation of PIP_3 appeared to be in the apical domain of cells surrounding the delaminating cell, rather than in the cell itself, and persisted throughout the delamination process (Figure 57 Biii). In particular, PIP_3 accumulated at the edge of the cell facing the delaminating cell, and also at the cell junctions to either side. This accumulation of PIP_3 suggests a polarisation of the surrounding cells.

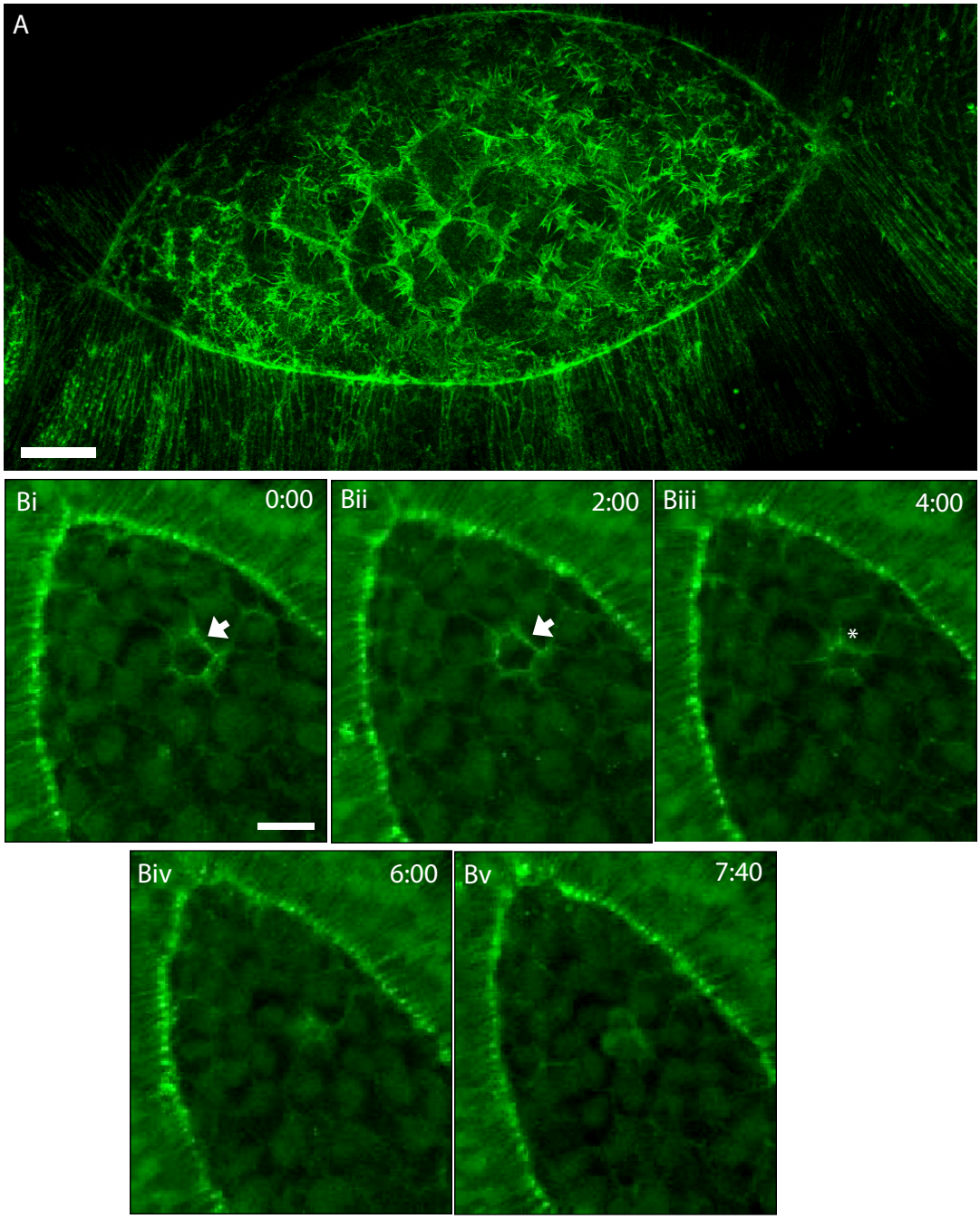

Figure 57. Dynamics of the amnioserosa. A) Embryo expressing UAS-GFP-Moesin under the control of *e22c*-Gal4 shows the numerous actin protrusions on the apical surface of the amnioserosa. B) PIP_3 accumulates around delaminating amnioserosal cells. Time lapse images from embryos expressing tGPH ubiquitously. Arrow indicates the localisation of PIP_3 surrounding a delaminating cell. Asterisk indicates where PIP_3 is localised to the back and sides of the surrounding cells. Scale bar indicates A) 18 µm and B) 40 µm. Whole sequence is shown in movie 16 in appendix 2.

7.2 Reducing PIP_3 levels throughout the whole embryo affects cell delamination and constriction

As PIP_3 accumulates and is polarised in cells surrounding delaminating cells, we next sought to determine if PIP_3 is required for the process of delamination. By expressing UAS-PTEN3 throughout the embryo under the control of *TubP*-Gal4, alongside UAS-GFP-shotgun (E-cadherin) to allow visualisation of cell junctions, we were able to investigate in detail what happens to the delaminating cells and the surrounding cells when PIP_3 levels were reduced. Delamination was observed in early DC to prevent any mechanical input from the advancing leading edges that might contribute to cell delamination. As previously reported (Solon *et al.* 2009; David *et al.* 2010), cells in the amnioserosa oscillate in size throughout DC, so by acquiring time-lapse images, we were able to identify delaminating cells, and measure the apical cell area from early in DC. Measuring apical cell area over time, allowed us to investigate the dynamics of delamination. From analysing the apical area of a delaminating cell, we found that there appears to be a signal which determines when the cells starts delaminating as that cell stops oscillating and starts to constrict or is pushed from the amnioserosa (Figure 58 C).

In control embryos, once cells started to delaminate they took on average 25.9 minutes ± 4.24 to delaminate with the surrounding cells becoming elongated in the direction of extrusion (Figure 58 A, C, D). When levels of PIP_3 were reduced by expression of PTEN3, the time taken for delamination increased to 37.82 minutes ± 6.4 when compared to controls ($p = 0.0035$) and the surrounding cells were less elongated when compared to cells in control embryos (length:width ratio of surrounding cells increased from 1.46 ± 0.17 in control embryos to 1.92 ± 0.23 in embryos expressing UAS-PTEN, $p < 0.0001$) (Figure 58 E).

Additionally we investigated the number of cells in the amnioserosa when the dorsal hole measured 180 μm in width (to ensure embryos were at the same stage), and measured the average size of 10 cells per embryo taken from the middle of the amnioserosa (at least 2 cell widths from the leading edge). Reducing levels of PIP_3 resulted in a slight, but not significant increase in the number of amnioserosal cells (116 ± 4.77 cells compared to 105 ± 4.93 cells in control embryos, $p = 0.0948$) (Figure 58 F). As well as the slight increase in cell number, the average area of cells was significantly reduced in embryos overexpressing UAS-PTEN3 (612.44 ± 75.5 μm compared to 741.45 μm ± 80.04 for control embryos, $p < 0.0001$) (Figure 58 G).

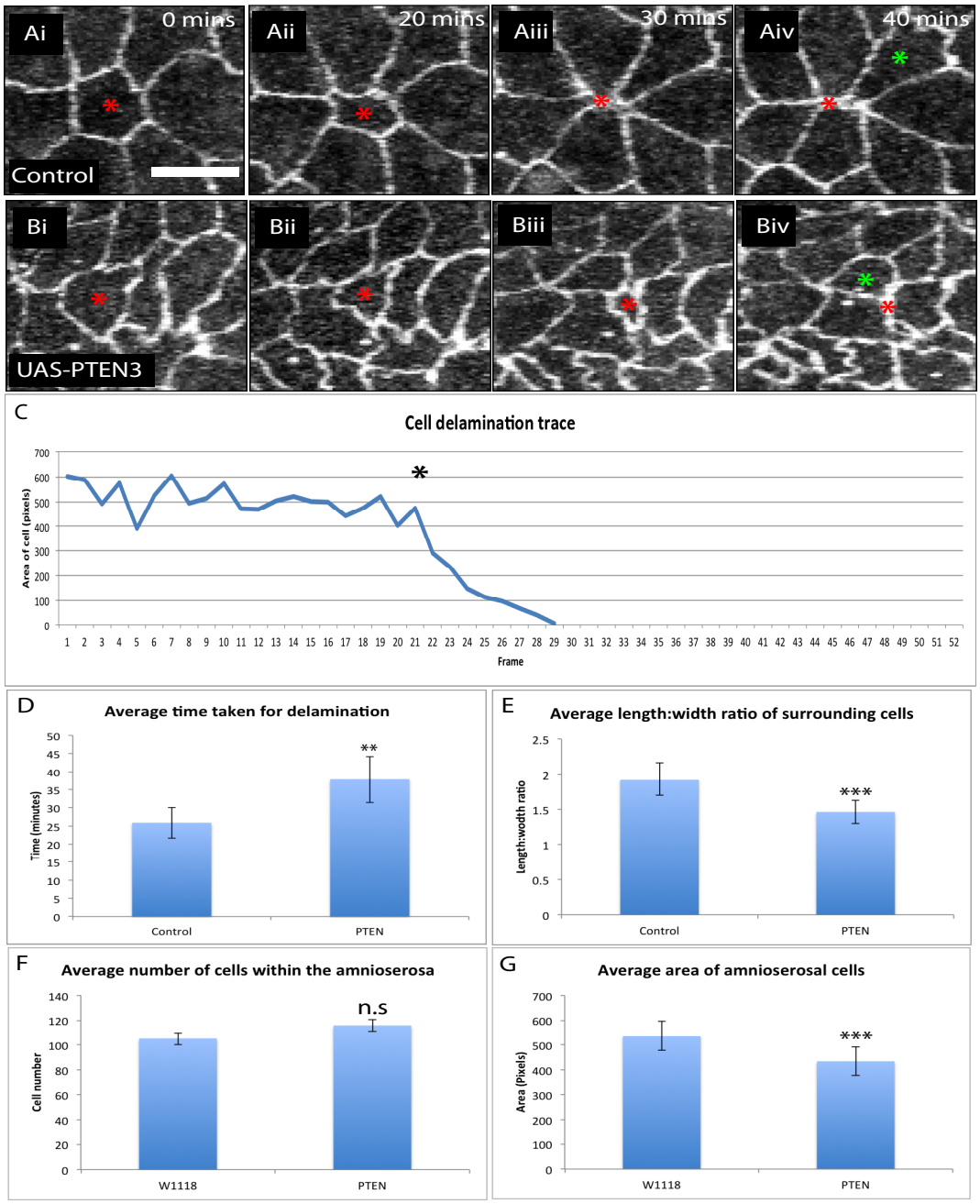

Figure 58. Decreasing PIP_3 throughout the embryo affects delamination. Time lapse images from A) control embryos and B) embryos expressing UAS-PTEN3 under the control of TubP-Gal4, show the delamination of a cell from the amnioserosa. Red asterisk indicates delaminating cell, green asterisk indicates surrounding cells elongated in the direction of delamination. C) Example of a trace measuring a single cell area over time with the asterisk indicating the start of delamination. Quantitation of D) time taken for delamination to occur, E) length:width ratio of surrounding cells F) Average number of cells in the amnioserosa and G) average apical area of amnioserosa cells when the width of the amnioserosa is 180 µm. n ≥ 12. *** indicates a significant difference from the control P< 0.001. ** indicates a significant difference from the control P<0.005. Error bars indicate S.E.M. Scale bar represents 20 µm. Whole sequence is shown movie 17 in appendix 2.

7.3 Altering levels of PIP_3 specifically in the amnioserosa affects cell delamination and constriction

The above experiments demonstrated that reducing the levels of PIP_3 throughout the embryo results in slower delamination and changes in amnioserosa cell morphology. However, given that we know that reducing PIP_3 levels affects zippering, the changes that we observed could be indirect as zippering is known to affect dorsal hole closure, which could have knock-on effects on amnioserosa dynamics. To eliminate this possibility we used an amnioserosa-specific driver (*332.3*-Gal4) to drive expression of either UAS-PTEN3 (to reduce PIP_3 levels) or UAS-CA PI3K (to increase PIP_3 levels) to restrict changes in PIP_3 levels to the amnioserosa. At this point, we switched from UAS-GFP-Shotgun to UAS-GFP-alpha-Catenin to label cell junctions, as expression of UAS-GFP-Shotgun under the control of *332.3*-Gal4 resulted in arrested development at L2 larvae (the reason for this is unknown, however, one possibility is that by L2 there is a lot of GFP present which can be toxic to the individual) and we required adults with expression of both *332.3*-Gal4 and UAS-GFP-Shotgun in order to set up the crosses required to perform the experiments.

We did not observe any significant changes in the amount of time taken for cells to be delaminated from the amnioserosa when either UAS-CA-PI3K or UAS-PTEN3 was expressed in the amnioserosa alone. Expressing UAS-CA-PI3K in the amnioserosa alone did not result in a decrease in the amount of time taken for cells to be delaminated (31.92 minutes ± 4.77 compared to 36.96 minutes ± 3.93 for controls, p=0.38), whereas expressing UAS-PTEN3 throughout the amnioserosa resulted in a slight increase in the amount of time taken for cells to be delaminated from the amnioserosa (45.78 minutes ± 7.18 $p > 0.1236$) although in neither case was the change significant (Figure 59 A). In addition to the rate of delamination, cells surrounding the delaminating cell were also affected, with cells with reduced levels of PIP_3 appearing significantly less elongated than controls (length:width ratio of 1.65 ± 0.21 and 1.89 ± 0.23 respectively, $p = 0.0114$). However, increasing PIP_3 levels did not significantly change elongation of the cells surrounding a delamination event (length:width ratio of 1.97 ± 0.24, p=0.9203) (Figure 59 B).

In addition to changes in rate of delamination, altering the levels of PIP_3 also affected the total cell number and cell area. The cells in the amnioserosa were decreased in number (123.4 ± 2.81 cells in control embryos and 106 ± 3.28 cells in embryos expressing UAS-PTEN3, $p = 0.0028$) and increased in size when levels of PIP_3 were reduced (688.45 μm ± 77.61 for controls and 847.09 μm ± 96.56 when UAS-PTEN3 was expressed, $p = 0.0007$) (Figure 59 C). Consistent with this, when levels of PIP_3 were increased, there were slightly less cells in the amnioserosa (122 ± 3.17 cells for UAS-CA PI3K and 123.42 ± 2.81 cells for controls, $p = 0.0137$), and they were smaller in size than controls (440.04 ± 43.63 pixels for UAS-CA-PI3K and 498 ± 56.24 pixels for control, $p < 0.0001$) (Figure 59 D). This data showed that

increasing the levels of PIP_3 resulted in a similar number of cells in the amnioserosa that were smaller in apical area, whilst decreasing levels of PIP_3 resulted in less amnioserosal cells that were larger in apical area.

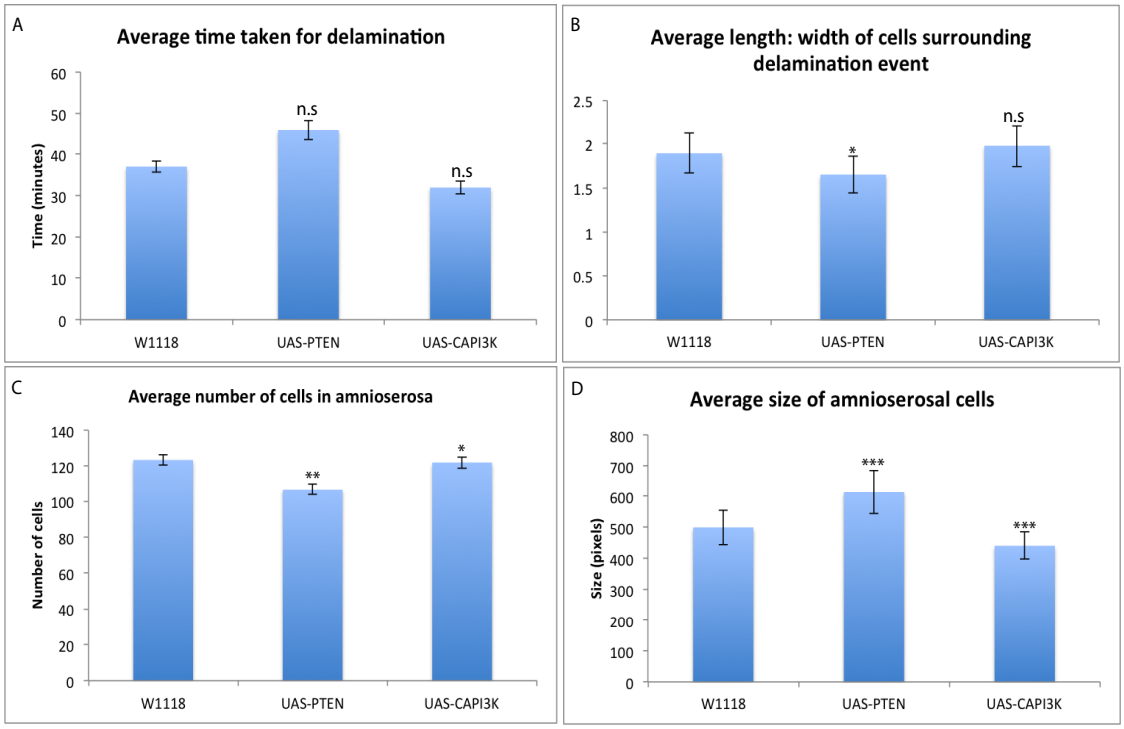

Figure 59. Analysis of cell delamination and morphology in the amnioserosa. Quantification of A) the rate of delamination, B) length:width of cells surrounding a delamination event, C) average number of cells in the amnioserosa and D) the average size of cells in the amnioserosa in embryos expressing UAS-PTEN3 or UAS-CA-PI3K in the amnioserosa under the control of *332.3*-Gal4 when compared to control embryos. n ≥ 7 embryos, ≥ 14 delamination events. *** indicates a significant difference from control of $p < 0.001$, ** indicates $p < 0.01$ and * indicates $p < 0.05$. n.s indicates no significant difference from the controls. Error bars represent S.E.M.

Chapter 7 discussion

7.4 PIP_3 is involved in cell delamination from the amnioserosa

Cell delamination from the amnioserosa closely resembles cell delamination in other tissues, including human colon, *Drosophila* pupal and zebrafish epithelium (Rosenblatt *et* al. 2001; Marinari *et* al. 2012; Eisenhoffer *et al.* 2012). Delamination of a cell from an epithelium has been shown to be a mechanism by which a tissue controls against variations in overgrowth and is observed for both live and apoptotic cells (Eisenhoffer *et* al. 2012; Marinari *et al*. 2012). The extrusion of an apoptotic cell is initiated by the apoptotic cell sending signals to surrounding cells, to form and contract an actomyosin ring which will squeeze out the apoptotic cell (Rosenblatt *et al*, 2001). We observed that PIP_3 accumulates strongly in the cells surrounding delaminated amnioserosa cells, leading us to investigate whether PIP_3 might play a role in regulating this process. We found that PIP_3 does indeed appear to play some role in cell delamination, as altering levels of PIP_3 led to a slight change in the time taken for delamination to occur. Additionally, the length;width ratio of cells surrounding the delaminating cell was also affected. Although the changes observed were slight, it appears that PIP_3 is involved in controlling a mechanism by which the cell is extruded. As we found that PIP_3 localises to the edge of surrounding cells that face the delamination event we believe that PIP_3 may regulate the mechanisms by which surrounding cells contribute to cell delamination, as opposed to playing a role within the delaminating cell itself.

One complication of our findings is that we only observed significant changes in delamination when PIP_3 levels were reduced throughout the embryo, so we cannot rule out that the effect we observed is indirect. One possible explanation for the fact that changes in delamination were modest (and not statistically significant) when PIP_3 was specifically altered in the amnioserosa is that the amnioserosa-specific driver used in these experiments (332.3-Gal4) only yields modest expression of PTEN3 and so PIP_3 levels are not reduced sufficiently. The use of an alternative driver or multiple copies of the PTEN3 transgene might rectify this problem.

Given that we have already determined PIP_3 to be a regulator of actin protrusions during DC and wound healing, and that there are a vast amount of protrusions on the apical surface of amnioserosal cells, it is possible that altering the levels of PIP_3 alters the number of protrusions on the surface of the amnioserosa. It is possible that when a cell is delaminating the surrounding cells respond to it as they would a small wound. The presence of PIP_3 at the front of surrounding cells suggests that they could be polarising in the direction of movement and possibly reorganising the actin cytoskeleton to form protrusions. Given that protrusions are required to close small epithelial wounds, it could be possible that protrusions are also important during cell delamination to maintain tissue integrity, and by reducing PIP_3 in the

amnioserosa; we could be reducing the number of protrusions present, so slowing the process of cell delamination.

Alternatively, PIP_3 could be regulating the formation of the contractile actomyosin ring that appears around delaminating cells. It has been shown that early signals from the apoptotic cell instruct surrounding cells to form an actin cable at the live/dead cell junction. This cable then undergoes contraction in a Rho-mediated manner, squeezing the apoptotic cell out from the epithelium (Rosenblatt *et al*. 2001). Although we have not observed PIP_3 to have an effect on the formation of the actin cable during DC or wound healing, it is possible that in this context, PIP_3 activates downstream actin polymerisation pathways that could be required for the formation of an actin cable. Due to time and imaging constraints, we were unable to directly determine if altering levels of PIP_3 had an effect on either actin protrusions or actomyosin ring formation in cells surrounding a delamination event, however these would certainly be interesting experiments for the future.

More recently, Bardet *et al*. (2013) have shown a role for PTEN in junction dynamics. In particular, they showed that PTEN promotes the elongation of cell junctions by limiting the level of PIP_3. The authors find that during the formation of cell junctions, PIP_3 and Rok (a Rho kinase capable of activating myosin II (Kawano *et al*. 1999)) co-localised and as junctions elongated these levels decreased, presumably due to the increase of PTEN. PTEN was able to regulate epithelial tissue morphogenesis by regulating myosin II distribution. It is possible that during amnioserosa cell delamination, cells surrounding the delaminating cell lose PTEN at the 'front' of the cell, resulting in an accumulation of PIP_3. This accumulation of PIP_3 could then activate Rok, as it has previously been shown to bind to Rho Kinase II, increasing its activity (Yoneda *et al*. 2005), resulting in the contraction of the actomyosin ring, squeezing the cell out of the epithelium. It would be interesting to see using a Rok reporter whether we could observe accumulation of Rok in cells surrounding delamination events. If so, this could indicate a role for PIP_3 in Rok-mediated actin contractility during cell delamination.

As the role of Par polarity proteins in amnioserosal cell oscillations have been investigated, with Baz being shown to be localised to a small patch in the apical surface and required to determine the duration of actomyosin pulses that control oscillations, it would be interesting to observe the localisation of Baz during cell delamination. It could be that in a similar manner to the onset of DC, Baz is lost completely from the delaminating cell and becomes restricted to rear and sides of surrounding cells, promoting the loss of PTEN from the 'front' of the cell, and regulating cell elongation, actin protrusion formation and actin cable formation.

7.5 PIP_3 regulates the number and size of amnioserosa cells

Surprisingly, in addition to observing changes in rate of delamination with changes of PIP_3 levels, we also observed a change in total number and the average size of cells in the amnioserosa. However, the results observed were different depending on the driver used. In embryos where PIP_3 was reduced throughout the embryo (*tubP*-Gal4 driver), there were more amnioserosal cells, which were smaller in apical area than cells in control embryos. By contrast, reducing levels of PIP_3 in the amnioserosa alone (*332.3*-Gal4 driver), resulted in fewer cells, but with a greater apical area, whilst increasing the level of PIP_3 resulted in a similar number of cells that were smaller in apical area, when compared to controls. The effects observed are likely due to early effects on cell proliferation, growth and survival during amnioserosa development, as PIP_3 signalling has been shown to be important in regulating these processes (Leevers *et al* 1996; Benistant *et al.*2000; Gao *et al.* 2000). It is surprising that we observed different effects when using different drivers, but this could be due to differences in the time, duration or level of expression of the transgene induced by the different drivers.

7.6 Summary

We have demonstrated the ability for PIP_3 to regulate the rate at which cells delaminate from the amnioserosa during DC, however we have not investigated the mechanisms through which delamination is achieved. It is likely that in a similar manner to *Dictyostelium* cell migration, PIP_3 is identifying the front of surrounding cells, signalling the direction of elongation and determining where actin re-organisation takes place (Funamoto *et al*. 2002). It would be interesting to investigate how PIP_3 regulates delamination, and if the actin protrusions observed on the apical surface of the embryo are important for the process of cell extrusion. Alternatively, it would also be interesting to determine if PIP_3 can regulate the formation of an actin cable through interactions with Rho kinase II, forming the actin ring required for cell delamination (Rosenblatt *et al.* 2001; Bardet *et al.* 2013).

The ability to use the amnioserosa as a model for cell delamination has many benefits, including working in a genetically tractable model, which is amenable to live imaging. Further work on this process could enhance our understanding on a wide range of events, including tissue homeostasis, which is required to prevent the build-up of excess epithelial cells that could result in the development of cancer.

Chapter 8. Final Discussion

Our analysis of the regulation of actin protrusions during DC and wound healing has identified a PIP_3-MBC-Rac signalling pathway that is required at the front of DME or wound edge cells for the formation of actin protrusions. Additionally we have shown that the Par polarity protein Baz, which is normally associated with apicobasal polarity, is required to restrict the localisation of PIP_3 to the front of the cell in a planar polarised manner. Our key findings and their implications will be summarised below.

8.1 PIP_3 regulates filopodia formation during DC in an MBC and Rac dependent manner

We demonstrate that PIP_3 localises in microdomains at cell junctions at the front of DME cells during DC. These PIP_3 microdomains regulate the formation of filopodia, probably by recruiting and/or activating the Rac specific GEF MBC, which in turn activates Rac. We propose that an increase in Rac activity leads to the activation of downstream pathways that drive actin polymerisation, resulting in filopodia assembly. These filopodia are vital for the process of DC, in particular the process of zippering, which is required to knit together the epithelial edges (Jacinto *et al*. 2000).

It is likely that MBC interacts with PIP_3 via the DHR-1 domain as this interaction has been shown to be responsible for recruiting the MBC homologue Dock180 to PIP_3-rich membranes membrane in CHO cells (Côté *et al*. 2005). We observe some loss of membrane association of GFP-MBC on depletion of PIP_3, so it might be that PIP_3 regulates MBC activity by controlling its cellular localisation. We also demonstrate that MBC is able to act upstream of Rac in the regulation of filopodia during DC. It is probable that this occurs through the interaction of Rac with the DHR-2 domain of MBC which has been shown to result in Rac activation (Wu *et al*. 2011). Expression of forms of MBC with functional domains deleted would enable a more thorough analysis of the mechanism by which MBC links PIP_3 and Rac signalling. We have shown that this PIP_3-MBC-Rac pathway results in the re-organisation of the actin cytoskeleton at the leading edge of DME cells. As Rac has been shown to activate the Scar/WAVE complex, it is possible that this complex is downstream of our proposed pathway, which would in turn activate Arp2/3, resulting in the nucleation of new actin filaments (Steffen *et al.* 2005). Alternatively, Rac1 could promote the association of capping protein with phosphoinositides, resulting in its dissociation from the end of actin filaments (Hartwig *et al.* 1996; Yang *et al*. 1998; Sun *et* al, 2007). This dissociation of capping protein could result in an increased number of free barbed ends for actin polymerisation. It is possible that both of these processes occur simultaneously at the leading edge to increase the formation of filopodia required for DC. Rac is typically associated with the formation of lamellipodia (Nobes and Hall 1999), and as such it was suprising that we observed a change in filopodia when the

levels of Rac were altered, however, this is consistent with other *in vivo* work where Rac has been shown to induce the formation of filopodia (Tahinci *et al*. 2003), indicating that the roles of GTPases *in vivo* is not as defined as *in vitro*. It is possible that the environment has some influence on the type of protrusion formed as during DC we observe an increase in the number of filopodia when levels of Rac were increased, whilst during wound healing, an increase in Rac resulted in an increase in total actin protrusions (including lamellipodia). Alternatively, it is possible that upstream signalling pathways dictate which protrusion type is required, wound signals could signal for lamellipodia, whilst developmental signals could result in the formation of filopodia. It is possible that this type of signalling is through controlling the levels of active Rac present, as high levels of Rac have been shown to induce filopodia, whereas intermediate/low levels of active Rac can induce lamellipodia (Georgiou and Baum 2010).

Perhaps surprisingly, we did not observe a complete loss of leading edge filopodia when we reduced levels of PIP_3. This can be explained one of two ways; either, PIP_3 levels were not reduced sufficiently in our experiments, or there is redundancy with other signalling pathways. This second explanation is probable, as Cdc42 can regulate the formation of filopodia by relieving the autoinhibition of the NPF Wasp, resulting in the activation of the Arp2/3 complex (Miki *et al.* 1998; Rohatgi *et al*. 2000). It is possible that Cdc42 can promote filopodia formation during DC independently of PIP_3. In summary, our analysis has shown PIP_3 to be a regulator of filopodia formation during DC, by activating the downstream MBC-Rac signalling pathway at the leading edge of DME cells.

8.2 Baz is key to generating leading edge accumulation of PIP_3

As mentioned above PIP_3 accumulates at leading edge cell-cell junctions during DC. We propose that this accumulation of PIP_3 is dependent on differences in the cellular distribution of two enzymes; PI3K and PTEN2. We were unable to observe the localisation of PI3K, but based on the distribution of PIP_3 in $pten^{117\ mat/zyg}$ mutant embryos, we believe that it is primarily located at cell-cell junctions but is not planar polarised within DME cells. PTEN2 is also localised to cell-cell junctions, but is absent from junctions along the leading edge, thus resulting in an imbalance between PI3K and PTEN activity at the leading edge, leading to accumulation of PIP_3 specifically in this location. We demonstrate that PTEN2 is localised to cell-cell junctions by the Par polarity protein Baz, which can bind directly to PTEN2 via its PDZ-domain. Baz is present at all cell-cell junctions except those at the leading edge (von Stein *et al*. 2005) and thus PTEN2 is effectively sequestered away from the leading edge by Baz resulting in reduced PIP_3 degradation at the leading edge. We and others (Laplante and Nilson 2011) observe a loss of Baz from the DC leading edge at the onset of DC. It is not known what is responsible for the redistribution of Baz at the beginning of DC, however it is possible that Rho-kinase, which is required for Myosin-II activation (and hence assembly and

contraction of the leading edge actin cable), phosphorylates Baz at the DC leading edge (Simões *et al*. 2010). Rho-kinase phosphorylation of Baz inhibits its ability to interact with phosphoinositides and so could account for its loss from the DC leading edge. In summary, we have shown that at the DC leading edge, Baz is restricted to cell junctions away from the leading edge, sequestering PTEN2 to these cell junctions, allowing the accumulation of PIP_3 at the front of DME cells, where is can promote the formation of filopodia required for efficient DC (Figure 60).

8.3 Actin protrusions are regulated in the same manner during epidermal re-epithelialisation and DC

DC and wound healing have been shown to have many similarities, both in the mechanics and signalling pathways required for the two processes (Wood *et al*. 2002). We propose that the PIP_3-MBC-Rac signalling pathway regulates the formation of actin protrusions during wound healing. We have demonstrated that similar to DC, Baz displays a reciprocal localisation to PIP_3, suggesting that the same mechanism is responsible for the accumulation of PIP_3 at the wound edge. This redistribution of Baz is likely to be required to determine where reorganisation of the actin cytoskeleton occurs. We have not directly demonstrated a genetic interaction between PIP_3, MBC and Rac during wound healing, but given that loss of any of these components resulted in similar reductions in the rate of re-epithelialisation and protrusive activity, and that we had already demonstrated genetic interactions in DC, it is reasonable to suppose that the same pathway operates at the front of wound edge cells. Equally, although we have demonstrated the loss of Baz from wound edge cells, we have not shown that this affects PTEN2 distribution during wound healing. However, given our previous data in DC studies, we propose that Baz controls the localisation of PIP_3 by sequestering PTEN2 away from the wound edge (Figure 60). Notably, where we have performed equivalent experiments to disrupt PIP_3/MBC/Rac signalling in DC and wound healing, we generally observed more significant defects in DC than wound healing. This may suggest that filopodia make a larger contribution to driving epithelial closure during DC than they do during wound healing, where the actin cable appears to be the primary driver of closure. The actin cable seems to be unaffected by disruption of PIP_3 signalling, suggesting that it is regulated by a PIP_3-independent mechanism.

It would be interesting to determine the upstream signalling pathways in both DC and wound healing, as it is likely that different primary signals are responsible for each process, however as yet it is not known what are the initial signals in each migratory event, and it could be possible that this upstream component could account for the difference In protrusions observed in DC and wound healing. This work has furthered our understanding of how a cell

responds to a wound, in particular how a cell reorganises and polarises its actin cytoskeleton in response to tissue damage.

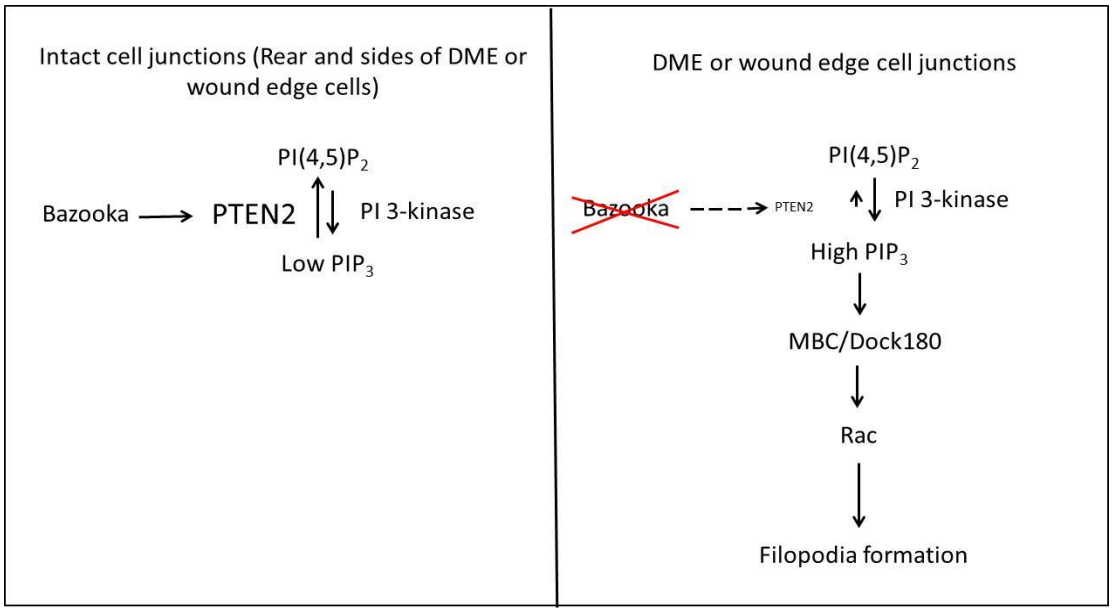

Figure 60. Baz localisation regulates the localisation of downstream actin regulation pathways. A) At the leading edge of DME cells or wound edge cells, Baz is absent, as such PTEN2 is not recruited to these areas and so PIP_3 is not dephosphorylated. This accumulation of PIP_3, recruits/activates MBC, which in turn activates Rac, promoting the polymerisation of new actin filaments required for filopodia formation. B) At the back and sides of DME cells, wound edge cells, or intact cell junctions, Baz is present, it recruits PTEN2, which then dephosphorylates PIP_3, preventing the recruitment/activation of MBC and Rac, and so inhibiting actin polymerisation and filopodia formation.

8.4 PIP_3 regulates amnioserosa cell extrusion during DC

We have also demonstrated a possible role for PIP_3 in the regulation of cell extrusion during DC. PIP_3 appears to regulate the rate at which cells are extruded from the epithelium and the elongation of the cells that surround the extruding cell. Given that PIP_3 accumulates at the front of surrounding amnioserosa cells, it is possible that PIP_3 controls the polarisation of these cells, by identifying a front and reorganising the actin cytoskeleton in the direction of movement. We have not been able to study the role of PIP_3 in these surrounding cells, but we propose that it could contribute to cell extrusion in one of two ways; firstly, as we have already shown a role for PIP_3 in the regulation of filopodia during DC, it is possible that PIP_3 regulates actin protrusion formation that could be required for cell extrusion. Secondly, PIP_3 could regulate the activation of Rho-kinase II, so regulating the contraction of the actomyosin cable surrounding the delaminating cell (Rosenblatt *et al.* 2001; Bardet *et al*. 2013).

Elucidating the mechanisms and signalling pathways by which cells are extruded from an epithelium could further our understanding of the control of tissue growth during development and also how its homogeneity is sustained throughout the life of an organism. This work could also contribute to our knowledge on how tumours are initiated as unregulated tissue growth could result in tumourigenesis.

8.5 Final conclusions

In conclusion, this research has furthered our understanding of the regulation of actin protrusions during epithelial closure events including DC and epithelial wound healing. We have shown that Baz redistribution results in the accumulation of PIP_3 at the leading edge of DME and wound edge cells. This accumulation of PIP_3 recruits and/or activates the Rac GEF MBC, which in turn activates Rac. This activation of Rac leads to activation of downstream actin regulators that promote filopodia formation. These filopodia then drive epithelial closure. Although performed in *Drosophila,* the mechanisms we have identified may well function during epithelial closure processes in other systems such as neural tube closure, palate fusion and vertebrate wound healing.

Appendix 1

Generation of heptane glue coverslips

In order to hold the embryos in place throughout imaging, they were fixed to coverslips using heptane glue. The glue is made by incubating tape (Tesa ♯ D20253), in heptane (Sigma Aldrich ♯ 32287) for 2 days whilst on a rolling platform. Once the glue from the tape has been dissolved, it is pipetted into 2ml microcentrifuge tubes and centrifuged for 60 minutes at 16000 x g. The supernatant is then pipetted into bijou tubes where it is kept until use. When required, the glue is spread onto the coverslip in a homogenous layer and left to dry for at least 20 minutes (Budnik *et al.* 2006).

Apple juice plates

Apple juice plates for overnight egg lays were made by adding 45g agar (Melford M1002) to 1.5L of water, which was then divided between 2 1L bottles, and autoclaved. Whilst autoclaving, 100g sucrose was added to 1L of apple juice in a 2L conical flask, which was then heated, whilst stirring to 80^{O}C on a hot plate, but not allowing it to boil. 3g methyl 4-hydroxybenzoate (Sigma Aldrich Cat ♯5501) was dissolved in 25ml 100% Ethanol (Sigma Aldrich E7023), and added to the apple juice.

Once the agar was autoclaved, it was added to the apple juice/sucrose/methyl 4-hydroxybenzoate and mixed thoroughly by decanting. This was then poured into 35mm dishes (Corning ♯ 430588) so the base of the dish was just covered and left to set for 24 hours before storing at 4^{O}C until use.

Halocarbon oil

A 3:1 mixture of halocarbon oil 700: halocarbon oil 27 (sigma H8898 and H8773 respectively)

PATX

1% Bovine Serum Albumin (Sigma A9647) dissolved in 0.1% triton X-100 (Sigma Aldrich T9284).

Buffer A

100mM Tris HCl (pH 7.6)
100mM EDTA
100mM NaCl
0.5% SDS

10x Phosphate buffered Saline (PBS)

To make 1L
80g NaCl
2g KCl

14.4g Na_2HPO_4

Dissolve in 800ml ddH_20 on a magnetic stirrer, adjust pH to 7.4 with a few drops of 10M NaOH and adjust the final volume to 1L with ddH_20.

Hoyers medium

30g gum Arabic

16ml glycerol

200g chloral hydrate

50ml water

4% paraformaldehyde for embryonic fixation

4ml 10% stock methanol-free formaldehyde (Polysciences ♯ 04018)

6ml ddH_20

Fine pulled needles

Capillary needles were pulled using a Narishige needle puller (PE-22)

Appendix 2

All supplemental movies are provided on a disc at the back of the thesis

Supplementary movie 1: Zippering during DC occurs at a constant rate in control embryos. Live imaging of the final phase of DC in an embryo expressing *en*-Gal4, UAS-m-Cherry-moesin (magenta), constitutive GFP-Moesin (Green), shows that zippering proceeds at a similar rate in *en*-Gal4-expressing stripes and the non-*en*-Gal4 expressing stripes. Images were acquired at 63 x at 120 second intervals. Stills are shown in Figure 24.

Supplementary movie 2: Zippering speed is reduced in cells overexpressing PTEN3. Live imaging of the final phase of DC in an embryo expressing *en*-Gal4, UAS-m-Cherry-Moesin (magenta), constitutive GFP-moesin (green) x UAS-PTEN3 (expressed in magenta stripes), demonstrates that zippering is slower in the *en*-Gal4 stripes expressing UAS-PTEN3, to such an extent that stripes are skipped by the canthus. Images were acquired at 63 x at 120 second intervals. Stills are shown in Figure 24.

Supplementary movie 3: Zippering speed is unaffected in cells expressing UAS-PTEN3-G137E. Live imaging of the final phase of DC in an embryo expressing *en*-Gal4, UAS-m-Cherry-Moesin (magenta), constitutive GFP-moesin (green) x UAS-PTEN3-G137E (expressed in magenta stripes), shows that zippering is unaffected by expression of PTEN3-G137E. Images were acquired at 63 x at 120 second intervals. Stills are shown in Figure 24.

Supplementary movie 4: Zippering speed is increased in cells expressing constitutively active PI3K. Live imaging of the final phase of DC in an embryo expressing *en*-Gal4, UAS-m-Cherry-Moesin (magenta), constitutive GFP-moesin (green) x UAS-CA-PI3K (expressed in magenta stripes), shows that the rate of zippering is increased in stripes expressing UAS-CA-PI3K to the extent that non-*engrailed* stripes are skipped by the canthus. Images were acquired at 63 x at 120 second intervals. Stills are shown in Figure 25.

Supplementary movie 5: Zippering speed is increased in cells expressing constitutively active Ras. Live imaging of the final phase of DC in an embryo expressing *en*-Gal4, UAS-m-Cherry-Moesin (magenta), constitutive GFP-moesin (green) x UAS-CA-Ras (expressed in magenta stripes), shows that the rate of zippering is increased in stripes expressing UAS-CA-Ras, however not to the extent where stripes are skipped by the canthus. Images were acquired at 63 x at 120 second intervals. Stills are shown in Figure 25.

Supplementary movie 6: Zippering speed is increased in cells overexpressing a wild type form of Rac1. Live imaging of the final phase of DC in an embryo expressing *en*-Gal4, UAS-m-Cherry-Moesin (magenta), constitutive GFP-moesin (green) x UAS-Rac1-wt (expressed in magenta stripes), shows that the rate of zippering is increased in stripes

expressing UAS-Rac1-wt. Images were acquired at 63 x at 120 second intervals. Stills are shown in Figure 28.

Supplementary movie 7: Expression of UAS-PTEN3 and UAS-Rac1 wt results in zippering speed similar to that of control embryos. Live imaging of the final phase of DC in an embryo expressing *en*-Gal4, UAS-m-Cherry-Moesin (magenta), constitutive GFP-moesin (green) x UAS-PTEN3, UAS-Rac1-wt (expressed in magenta stripes), shows that the reduced rate of zippering observed in embryos expressing UAS-PTEN3 alone is rescued by the expression of UAS-Rac1-wt. Images were acquired at 63 x at 120 second intervals. Stills are shown in Figure 28.

Supplementary movie 8: Filopodia form from microdomains of PIP_3 at the leading edge. Live imaging of DC in embryos expressing *en*-Gal4, UAS-m-Cherry-Moesin (magenta), UAS-GPH (green), shows the spatial and temporal correlation of PIP_3 accumulation at the leading edge and the initiation of filopodia. Images were acquired at 63 x at 120 second intervals. Stills are shown in Figure 29.

Supplementary movie 9: PIP_3 accumulates at cell-cell junctions at epithelial wound edges. Live imaging of laser wound healing in embryos expressing GPH in the epidermis demonstrates that PIP_3 accumulates at cell junctions at the wound edge. Images were acquired at 63 x at 150 second intervals. Stills are shown in Figure 49.

Supplementary movie 10: Expression of UAS-CA-PI3K increases the amount of wound edge protrusions and rate of re-epithelialisation. Live imaging of laser wound healing in either control embryos (left hand panel), or those also expressing UAS-CA-PI3K (right-hand panel) under the control of *e22c*-Gal4 and *I67D*-Gal4 alongside two copies of UAS-m-Cherry-Moesin, demonstrates an increase in the number of protrusions at the wound edge in embryos expressing UAS-CA-PI3K, and a slightly faster rate of re-epithelialisation. Images were acquired at 63 x at 120 second intervals. Stills are shown in Figure 50.

Supplementary movie 11: *pten*$^{117\ mat/zyg}$ mutant embryos form more actin protrusions at the wound edge than controls. Live imaging of laser wound healing in either control embryos (left-hand panel) or embryos lacking maternal and zygotic expression of PTEN (right hand panel) expressing constitutive GFP-Moesin throughout the embryo, demonstrates an increased number of protrusions and slightly faster re-epithelialisation in embryos lacking expression of PTEN. Images were acquired at 63 x at 120 second intervals. Stills are shown in Figure 51.

Supplementary movie 12: *mbc*^{c1} mutant embryos have less actin protrusions and a slower rate of re-epithelialisation than controls. Live imaging of laser wound healing in

either control embryos (left-hand panel) or embryos lacking zygotic expression of MBC (right-hand panel) expressing constitutive GFP-Moesin throughout the embryo demonstrates a reduced number of protrusions and slower re-epithelialisation in embryos lacking expression of MBC. Images were acquired at 63 x at 120 second intervals. Stills are shown in Figure 52.

Supplementary movie 13: *rac*^{J10} and *rac*^{J11} mutant embryos have less actin protrusions and heal at a slower rate than controls. Live imaging of laser wound healing in either control embryos (left-hand panel), *rac*^{J10} mutant embryos (middle panel) or *rac*^{J11} mutant embryos (right-hand panel) expressing constitutive GFP-Moesin throughout the embryo demonstrate a reduced number of protrusions and slower re-epithelialisation in embryos lacking zygotic expression of Rac. Images were acquired at 63 x at 120 second intervals. Stills are shown in Figure 53.

Supplementary movie 14: Expression of UAS-Rac1-wt increases the amount of wound edge protrusions and rate of re-epithelialisation. Live imaging of laser wound healing in either control embryos (left hand panel) or embryos expressing UAS-Rac1-wt (right-hand panel) under the control of *e22c*-Gal4 and *I67D*-Gal4 alongside two copies of UAS-m-Cherry-Moesin, demonstrates an increase in the number of protrusions at the wound edge in embryos expressing UAS-Rac1-wt and a faster rate of re-epithelialisation. Images were acquired at 63 x at 120 second intervals. Stills are shown in Figure 54.

Supplementary movie 15: Baz is lost from wound edge and displays a reciprocal relationship to F-actin. Live imaging of laser wound healing in embryos expressing UAS-GFP-Baz (green) and UAS-m-Cherry-Moesin (magenta) in the epidermis under the control of *e22c*-Gal4 demonstrates a loss of Baz from the wound edge and an accumulation of F-actin at the front of wound edge cells. Images were acquired at 63 x at 120 second intervals. Stills are shown in Figure 55.

Supplementary movie 16: PIP_3 accumulates around delaminating amnioserosa cells. Live imaging of the amnioserosa during DC in embryos expressing constitutive GPH demonstrates an accumulation of PIP_3 at the front of cells surrounding delaminating cells in the amnioserosa. Images were acquired at 63 x at 150 second intervals. Stills are shown in Figure 57.

Supplementary movie 17: Expression of PTEN3 throughout the embryo slows the rate of amnioserosal cell delamination. Live imaging of the amnioserosa during DC in control embryos (left-hand panel) or those expressing UAS-PTEN3 (right-hand panel) throughout the embryo ender the control of *tubP*-Gal4 alongside UAS-GFP-E-Cadherin, demonstrates a reduction in the rate of cell delamination and a reduction in the elongation of surrounding cells. Images were acquired at 63 x at 150 second intervals. Stills are shown in Figure 58.

PDF 1. A PDF of all of the figures shown in this thesis.

References

Abreu-Blanco MT, Verboon JM, Liu R, Watts JJ, Parkhurst SM. 2012 *Drosophila* embryos close epithelial wounds using a combination of cellular protrusions and an actomyosin purse string. *The Journal of Cell Science* 125 5964-5997

Abmayr SM, Pavlath GK. 2012 Myoblast fusion: lessons from flies and mice. *Development* 139 (4) 641-656

Adams EA, Johnson DI, Longnecker RM, Sloat BF, Pringle JR. 1990 CDC42 and CDC43, two additional genes involved in budding and the establishment of cell polarity in the yeast *Saccharomyces cerevisiae*. *Journal of Cell Biology* 111 (1) 131-142

Aghazadeh B, Zhu K, Kubiseski TJ, Liu GA, Pawson T, Zheng Y, Rosen MK. 1998 Structure and mutagenesis of the Dbl homology domain. *Nature Structural Biology* 5(12) 1098-1107

Amano M, Ito M, Kimura K, Fukaa Y, Chihara K, Nakano T, Matsuura Y, Kaibuchi K. 1996 Phosphorylation and activation of myosin by Rho-associated kinase (Rho-kinase). *The Journal of Biological Chemistry* 271 (34) 20246-20249

Anttonen T, Kiravainen A, Belevich I, Laos M, Richardson WD, Jokitalo E, Brakebusch C, Pirvola U. 2012 Cdc42-dependent structural development of auditory supporting cells is required for wound healing at adulthood. *Scientific Reports* 2 978

Ashburner M, Golic KG, Hawley S. 2005 *Drosophila: A Laboratory Handbook.* Second edition. *Cold Spring Harbor Laboratory Press:* Cold Spring Harbor, New York pp 479-487

Auger KR, Serunian LA, Soltoff S, Libby P, Cantley LC. 1989 PDGF-dependent tyrosine phosphorylation stimulates production of novel phosphoinositides in intact cells. *Cell* 57 (1) 167-175

Bardet PL, Guirao B, Paoletti C, Serman F, Léopold V, Bosveld F, Goya Y, Mirouse V, Graner F, Bellaïche Y. 2013 PTEN controls junction lengthening and stability during cell rearrangement in epithelial tissue. *Developmental Cell* 25 (5) 534-546

Baek SH, Kwon YC, Lee H, Choe KM. 2010 Rho-family small GTPases are required for cell polarisation and directional sensing in *Drosophila* wound healing. *Biochemical and Biophysical Research Communications* 394 (3) 488-492

Bear JE, Svitkina TM, Krause M, Schafer DA, Loureiro JJ, Strasser GA, Maly IV, Chaga OY, Cooper JA, Borisy GG, Gertler FB. 2002 Antagonism between Ena/VASP proteins and actin filament capping regulates fibroblast motility. *Cell* 109 (4) 509-521

Bellacosa A, De Feo D, Godwin AK, Bell DW, Cheng JQ, Altomare DA, Wan M, Dubaeu L, Scambia G, Masciullo V, Ferrandina G, Benedetti Panici P, Mancuso S, Neri G, Testa JR. 1995 Molecular alterations of the Akt2 oncogene in ovarian and breast carcinomas. *International Journal of Cancer* 64 280-285

Bement WM, Forscher P, Mooseker MS. 1993 A novel cytoskeletal structure involved in purse string wound closure and cell polarity maintenance. *The Journal of Cell Biology* 121 (3) 565-578

Bement WM, Mandato CA, Kirsch MN. 1999 Wound-induced assembly and closure of an actomyosin purse string in *Xenopus* oocytes. *Current Biology* 9 (11) 579-587

Bénistant C, Chapuis H, Roche S. 2000 A specific function for phosphatidylinositol 3-kinase alpha (p85alpha-p110alpha) in cell survival and for phosphatidylinositol 3-kinase beta (p85alpha-p110beta) in de novo DNA synthesis of human colon carcinoma cells. *Oncogene* 19 (44) 5083-5090

Bijian K, Takano T, Papillon J, Le Berre L, Michaud JL, Kennedy CRJ, Cybulsky AV. 2005 Actin cytoskeleton regulates extracellular matrix-dependent survival signals in glomerular epithelial cells. *American Journal of Physiology – Renal Physiology* 289 F1313-F1323

Bishop AL, Hall A. 2000 Rho GTPases and their effector proteins. *Biochemical Journal* 348 (pt1) 241-255

Blanchoin L, Pollard TM. 1998 Interaction of actin monomers with *Acanthamoeba* actophorin (ADF/cofilin) and profilin. *The Journal of Biological Chemistry* 273 25106-15111

Blondeau F, Laporte J, Bodin S, Superti-Furga G, Payrastre B, Mandel JL. 2000 Myotubularin, a phosphatase deficient in myotubular myopathy, acts on phosphatidylinositol 3-kinase and phosphatidylinositol 3-phosphate pathway. *Human Molecular Genetics* 9 (15) 2223-2229

Bloor JW, Kiehart DP. 2002 *Drosophila* RhoA regulates the cytoskeleton and cell-cell adhesion in the developing epidermis. *Development* 129 (13) 3173-3183

Boczkowska M, Rebowski G, Petoukhov MV, Hayes DB, Svergun DI, Dominguez R. 2008 X-ray scattering study of activated Arp2/3 complex bound with actin-WCA. *Structure* 16 (5) 695-704

Bosch M, Serras F, Martin-Blance E, Baguñà J. 2005 JNK signalingsignalling pathway required for wound healing in regenerating *Drosophila* wing imagine discs. *Developmental Biology* 280 (1) 73-86

Brand AH, Perrimon N. 1993 Targeted gene expression as a means of altering cell fates and generating dominant phenotypes. *Development* 118 401-415

Bresnick AR. 1999 Molecular mechanisms of nonmuscle myosin-II regulation. *Current Opinion in Cell Biology* 11 (1) 26-33

Britton JS, Lockwood WK, Li L, Cohen SM, Edgar BA. 2002 *Drosophila's* insulin/PI3-kinase pathway coordinates cellular metabolism with nutritional conditions. *Developmental Cell* 2(2) 239-249

Brock AR, Wang Y, Berger S, Renkawitz-Pohl R, Han VC, Wu Y, Galko M. 2012 Transcriptional regulation of Profilin during wound closure in *Drosophila* larvae. *The Journal of Cell Science* 125 5667-5676

Brock C, Scaefer M, Reusch HP, Czupalla C, Michalke M, Spicher K, Schultz G, Nümberg B. 2003 Roles of Gβγ in membrane recruitment and activation of p110γ/p101 phosphoinositide 3-kinase γ. *Journal of Cell Biology* 160 (1) 89-99

Brock J, Midinter K, Lewis J, Martin P. 1996 Healing of incisional wounds in the embryonic chick wing bud: Characterisation of the actin purse-string and demonstration of a requirement for Rho activation. *The Journal of Cell Biology* 135 (4) 1097-1107

Brown RA, Sheperd PR. 2001 Growth factor regulation of the novel class II phosphoinositide 3-kinases. *Biochemical Society transactions* 29 part 4 535-537

Brugnera E, Haney L, Grimsley C, Lu M, Walk SF, Tosello-Trampoint AC, Macara IG, MAdhani H, Fink GR, Ravichandran KS. 2002 Unconventional Rac-GEF activity is mediated through the Dock180-ELMO complex. *Nature Cell Biology* 4 (8) 574-582

Brunet A, Bonni A, Zigmond MJ, Lin MZ, Juo P, Hu LS, Anderson MJ, Arden KC, Blenis J, Greenberg ME. 1999 Akt promotes cell survival by phosphorylating and inhibiting forkhead transcription factor. *Cell* 96 (6) 857-868

Budnik V, Gorczyca M, Prokop A. 2006 Selected methods for the anatomical study of *Drosophila* embryonic and larval neuromuscular junctions. *International Review of Neurobiology* 75 323-365

Burgering BM, Coffer PJ. 1995 Protein kinase B (c-Akt) in phosphatidylinositol-3-OH kinase signal transduction. *Nature* 376 (599-602)

Bustelo XR. 2000 Regulatory and signaling properties of the Vav family. *Molecular Cell Biology* 20 (5) 1461-1477

Cain RJ, Ridley AJ. 2009 Phosphoinositide 3-kinases in cell migration. *Biology of the Cell* 101 (1) 13-29

Caldwell JE, Heiss SG, Mermall V, Cooper JA. 1989 Effects of CapZ, and actin capping protein of muscle, on the polymerisation of actin. *Biochemistry* 28 (21) 8506-8514

Campa F, Yoon HY, Ha VL, Szentoetery Z, Balla T, Randazzo PA. 2009 A PH domain in the Arf GTPase-activating protein (GAP) ARAP1 binds phosphatidylinositol 3,4,5-triphosphate and regulates Arf GAP activity independently of recruitment to the plasma membranes. *Journal of Biological Chemistry* 284 (41) 28069-28083

Campbell IG, Russell SE, Choong DYH, Montgomery KG, Ciavarella ML, Hool CSF, Cristiano BE, Pearson RB, Phillips WA. 2004 Mutation of the PIK3CA gene in ovarian and breast cancer. *Cancer Research* 64 (21) 7678-7681

Campos I, Geiger JA, Santos AC, Carlos V, Jacinto A. 2010 Genetic screen in *Drosophila melanogaster* uncovers a novel set of genes required for embryonic epithelial repair. *Genetics* 184 (1) 129-140

Cao L, Graue-Hernandez EO, Tran V, Reid B, Pu J, Mannis MJ, Zhao M. 2011 Downregulation of PTEN at corneal wound sites accelerates wound healing through increased cell migration. *Investigative Ophthalmology and Visual Science* 52 (5) 2272-2278

Carlier MF, Laurent V, Santolini J, Melki R, Didry D, Xia GX, Hong Y, Chua NH, Pantaloni D. 1997 Actin depolymerizing factor (ADF/cofilin) enhances the rate of filament turnover: implication in actin-based motility. *Journal of Cell Biology* 136 (6) 1307-1322

Carpten JD, Faber AL, Horn C, Donoho GP, Briggs SL, Robbins CM, Hostetter G, Boguslawski S, Moses TY, Savage S, Uhlik M, Lin A, Du J, Qian YW, Zackner DJ,

Tucker-Kellogg G, Touchman J, Patel K, Mousses S, Bittner M, Schevitz R, Lai MH, Blanchard KL, Thomas JE. 2007 A transforming mutation in the pleckstrin homology domain of Akt1 in cancer. *Nature* 448 (7152) 439-444

Chardin P. 1988 The *ras* superfamily proteins. *Biochemie* 70 865-868

Charest PG, Firtel RA. 2006 Feedback signaling controls leading-edge formation during chemotaxis. *Current Opinion in Genetics and Development* 16 339-347

Chatriwala MK, Betts L, Worthylake DK, Sondek J. 2007 The DH and PH domains of Trio coordinately engage Rho GTPases for their efficient activation. *Journal of Molecular Biology* 368 (5) 1307-1320

Chaung TH, Bohi BP, Bokoch GM. 1993 Biologically inactive lipids are regulators of Rac GDI complexation. *Journal of Biological Chemistry* 268 (25) 26206-26211

Chen F, Ma L, Parrini MC, Mao X, Lopez M, Wu C, Marks PW, Davidson L, Kwiatowski DJ, Kirchhausen T, Orkin SH, Rosen FS, Mayer BJ, Kirschner MW, Alt FW. 2000 Cdc42 is required for PIP2-induced actin polymerisation and early development but not for cell viability. *Current Biology* 10 (13) 758-765

Chereau D, Keriff F, Graceffa P, Grabarek Z, Langstemo K, Dominguez R. 2005 Actin-bound structures of Wiskott-Aldrich syndrome protein (WASP)-homology domain 2 and the implications for filament assembly. *Proceedings of the National Academy of Science* 102 (46) 16644-16649

Cherfils J, Chardin P. 1999 GEFs: structural basis for their activation of small GTP-binding proteins. *Trends in Biochemical Science* 24 (8) 306-311

Clark AG, Miller AL, Vaughan E, Yu HYE, Penkert R, Bement WM. 2009 Integration of single and multicellular wound responses. *Current Biology* 19 (16) 1389-1395

Cooper JA, Schafer DA. 2000 Control of actin assembly and disassembly at filament ends. *Current Opinion in Cell Biology* 12 (1) 97-103

Côté JF, Vuori K. 2002 Identification of an evolutionarily conserved superfamily of DOCK180-related proteins with guanine nucleotide exchange activity. *Journal of Cell Science* 115 (24) 4901-4913

Côté JF, Motoyama AB, Bush JA, Vuori K. 2005 A novel binding and evolutionarily conserved PtdIns(3,4,5)P3-binding domain is necessary for DOCK180 signaling. *Nature Cell Biology* 7 (8) 797-807

Côté JF, Vuori K. 2007 GEF what? Dock180 and related proteins help Rac to polarise cells in new ways. *Trends in Cell Biology* 17 (8) 383-393

Cross DA, Alessi DR, Cohen P, Andjelkovich M, Hemmings BA. 1995 Inhibition of glycogen synthase kinase-3 by insulin mediated by protein kinase B. 378 (6559) 785-789

Danjo Y, Gipson IK. 1998 Actin 'purse string' filament are anchored by E-cadherin-mdeiated adherens junctions at the leading edge of the epithelial wound, providing coordinated cell movement. *Journal of Cell Science* 111 (22) 3323-3332

Das B, Shuh X, Day GJ, Han J, Krishna UM, Falck JR, Broek D. 2000 Control of intramolecular interactions between the pleckstrin homology and Dbl homology domains of Vav and Sos1 regulates Rac binding. *The Journal of Biological Chemistry* 275 (20) 15074-15081

David DJV, Tishkina A, Harris TJC. 2010 The PAR complex regulates pulsed actomyosin contractions during amnioserosa apical constriction in *Drosophila*. *Development* 137 (10) 1645-1655

Davidson LA, Ezin AM, Keller R. 2002 Embryonic wound healing by apical contraction and ingression in *Xenopus laevis*. *Cell Motility and the Cytoskeleton* 53 (3) 163-176

Devreotes and Janetopoulos C. 2003 Eukaryotic chemotaxis: Distinctions between directional sensing and polarization. *The Journal of Biological Chemistry* 278 20445-20448

Dhand R, Hara K, Hiles I, Bax B, Gout I, Panayotou G, Fry MJ, Yonezawa K, Kasuga M, Waterfield MD. 1994 PI 3-kinase: structural and functional analysis of intersubunit interactions. *The EMBO Journal* 13 (3) 511-521

DiNubile MJ, Cassimeris L, Joyce M, Zigmond SH. 1995 Actin filmanet barbed-end capping activity in neutrophil lysates: the role of capping protein-beta 2. *Molecular Biology of the Cell* 6 (12) 1659-1671

Di Paolo G, De Camilli P. 2006 Phosphoinositides in cell regulation and membrane dynamics. *Nature* 443 (7112) 651-657

Drubin DG, Nelson WJ. 1996 Origins of cell polarity. *Cell* 84 (3) 335-344

Dutta D, Bloor JW, Rulz-Gomex M, VijayRaghavan K, Kiehart DP. 2002 Real-time imaging of morphogenetic movements in *Drosophila* using Gal4-UAS-driven expression of GFP fused to the actin-binding domain of moesin. *Genesis* 34 (1-2) 146-151

Dvorsky R, Ahmadian MR. 2004 Always look on the bright site of Rho: structural implications for a conserved intermolecular interface. *EMBO Reports* 5(12) 1130-1136

Eisenhoffer GT, Loftus PD, Yoshigi M, Otsuna H, Chien CB, Morcos PA, Rosenblatt J. 2012 Crowding induces live cell extrusion to maintain homeostatic cell numbers in epithelia. *Nature* 484 (7395) 546-549

Erickson MRS, Galletta BJ, Abmayr SM. 1997 *Drosophila myoblast city* encodes a conserved protein that is essential for myoblast fusion, dorsal closure and cytoskeletal organisation. *Journal of Cell Biology 138 (3) 589-603*

Falkenburger BH, Jensen JB, Dickson EJ, Suh BC, Hille B. 2010 Phosphoinositides: lipid regulators of membrane proteins. *Journal of Physiology* 588 (17)3179-3185

Fleming IN, Gray A, Downes CP. 2000 Regulation of the Rac1-specific exchange factor Tiam1 involves both phosphoinositide 3-kinase dependent and –independent components. *Biochemical Journal* 351 (pt1) 173-182

Foster FM, Traer CJ, Abraham SM, Fry MJ. 2003 The phosphoinositide (PI) 3-kinase family. *Journal of Cell Science* 116, 2027-2040

Funamoto S, Milan K, Meili R, Firtel RA. 2001 Role of phosphatidylinositol 3'kinase and a downstream pleckstrin homology domain-containing protein in controlling chemotaxis in *Dictyostelium*. *Journal of Cell Biology* 153 (4) 795-810

Funamoto S, Meili R, Lee S, Parry L, Firtel RA. 2002 Spatial and temporal regulation of 3-phosphoinositides by PI 3-kinase and PTEN mediates chemotaxis. *Cell* 109 (5) 611-623

Galko MJ, Krasnow MA. 2004 Cellular and genetic analysis of wound healing in *Drosophila* larvae. *PLoS Biology* 2 (8) e239

Gao X, Neufeld TP, Pan D. 2000 *Drosophila* PTEN regulates cell growth and proliferation through PI3K-dependent and –independent pathways. *Developmental Biology* 221 (2) 404-418

Garrett MD, Self AJ, Oers CV, Hall A. 1989 Identification of distinct cytoplasmic targets for ras/R-ras and rho regulatory proteins. *Journal of Biological Chemistry*. 264 (1) 10-13

Garvalov BK, Flynn KC, Neukirchen D, Meyn L, Teusch N, Wu X, Brakebusch C, Bamburg JR, Bradke F. 2007 Cdc42 regulates cofilin during the establishment of neuronal polarity. *Journal of Neuroscience* 27 (48) 13117-13129

Gassama-Diagne A, Yu W, ter Beest M, Martin-Belmonte F, Kierbel A, Engel J, Mostov K. 2006 Phosphatidylinositol-3,4,5-triphosphate regulates the formation of the basolateral plasma membrane in epithelial cells. *Nature Cell Biology* 8 (9) 963-970

Gates J, Mahaffey JP, Rogers SL, Emerson M, Rogers EM, Sottile AL, Van Vactor D, Gertler FB, Peifer M. 2007 Enabled plays key roles in embryonic epithelial morphogenesis in *Drosophila*. *Development* 134 2027-2039

Geiger JA, Carvahlo L, Campos I, Santos AC, Jacinto A. 2011 Hole-in-one mutant phenotypes link EGFR/ERK signaling to epithelial tissue repair in *Drosophila*. *PLoS One* 6 (11) e28349

Genova JL, Jong S, Camp JT, Fehon RG. 2000 Functional analysis of *cdc42* in actin filament assembly, epithelial morphogenesis and cell signaling during *Drosophila* development. *Developmental Biology* 221 181-194

Georgiou M, Baum B. 2010 Polarity proteins and Rho GTPases cooperate to spatially organise epithelial actin-based protrusions. *Journal of Cell Science* 123 (7) 1089-1098

Ghosh M, Song X, Mounelmne G, Sigani M, Lawrence DS, Condeelis JS. 2004 Cofilin promotes actin polymerisation and defines the direction of cell motility. *Science* 304 (5671) 743-746

Gibson MC, Perrimon N. 2003 Apicobasal polarisation: epithelial form and function. *Current Opinion in Cell Biology* 15 (6) 747-752

Goberdhan DC, Paricio N, Goodman EC, Mlodzik M, Wilson C. 1999 *Drosophila* tumor suppressor PTEN controls cell size and number by antagonising the ChicoPI3-kinase signaling pathway. *Genes and Development* 13 (24) 3244-3258

Goldschmidt-Clermont PJ, Furman MI, Wachsstock D, Safer D, Nachmias VT, Pollard T. 1992 The control of actin nucleotide exchange by Thymosinβ4 and Profilin. A potential

regulatory mechanism for actin polymerisation in cells. *Molecular Biology of the Cell* 3, 1015-1024

Goley ED, Rodenbusch SE, Martin AC, Welch MD. 2004 Critical conformational changes in the Arp2/3 complex are induced by nucleotide and nucleation promoting factor. *Molecular Cell* 16 (2) 269-279

Goley ED, Welch MD. 2006 The Arp2/3 complex: an actin nucleator comes of age. *Nature Reviews; Molecular Cell Biology* 7, 713-726

Gonçalves-Pimentel C, Gombos R, Mihály J, Sánchez-Soriano N, Prokop A. 2011 Dissecting regulatory networks of filopodia formation in a *Drosophila* growth cone model. *PLoS One* 6 (3) e18340

Govek EE, Newey SE, Aelst LV. 2005 The role of the RHO GTPase in neuronal development. *Genes and Development* 19 (1) 1-49

Graveley BR, Brooks AN, Carlson JW, Duff MO, Landolin JM, Yang L, Artieri CG, van Baren MJ, Boley N, Booth BW, Brown JB, Cherbas L, Davis CCA, Dobin A, Li R, Lin W, Maone JH, Mattiuzzo NR, Miller D, Sturgill D, Tuch BB, Zaleski C, Zhang S, Blanchette M, Dudoit S, Eads B, Green RE, Hammonds A, Jiang L, Kapranov P, Langton L, Perrimon N, Sandler JE, Wan KH, Willingham A, Zhang Y, Zou Y, Andrews J, Bickel PJ, Brenner SE, Brent MR, Cherbas P, Gingeras TR, Hoskins RA, Kauffman TC, Oliver B, Celniker SE. 2011 The developmental transcriptome of *Drosophila melanogaster*. *Nature* 471 (7339) 473-479

Gu Y, Filippi MD, Cancelas JA, Siefring JE, Williams EP, Jasti AC, Harris CE, Lee AW, Prabhakar R, Atkinson SJ, Kwiatkowski DJ, Williams DA. 2003 Hematopoietic cell regulation by Rac1 and Rac2 guanosine triphosphatases. *Science* 302 (5644) 445-449

Gustafson T, Wolpert L. 1961 Studies on the cellular basis of morphogenesis in the sea urchin embryo; directed movements of primary mesenchyme cells in normal and vegetalized larvae. *Experimental Cell Research* 24 64-79

Haataja L, Groffen J, Heisterkamp N. 1997 Characterisation of *RAC3,* a novel member of the Rho family. *The Journal of Biological Chemistry* 272 (33) 20384-20388

Hakeda-Suzuki S, Ng J Tza J, Dietzi G, Sun Y, harms M, Nardine T, Luo L, Dickson BJ. 2002 Rac function and regulation during *Drosophila* development. *Nature* 416 (6879) 438-442

Hakem A, Sanchez-Sweatman O, You-Ten A, Duncan G, Wakeham A, Khokha R, Mak TW. 2005 RhoC is dispensable for embryogenesis and tumor inititation but essential for metastasis. *Genes and Development* 19 (17) 1974-1979

Hall A, Paterson HF, Adamson P, Ridley AJ. 1993 Cellular responses regulated by Rho-related small GTP-binding proteins. *Philosophical Transactions of The Royal Society* 340 (1293) 267-371

Halsell SR, Chu BI, Kiehart DP. 2000 Genetic analysis demonstrates a direct link between rho signaling and non-muscle myosin function during *Drosophila* morphogenesis. *Genetics* 155 (3) 1253-1265

Han J, Luby-Phelps K, Das B, Shu X, Xia Y, Mosteller RD, Krishna UM, Falck JR, White MA, Broek D. 1998 Role of substrates and products of PI 3-kinase in regulating activation of Rac-related Guanosine triphosphatases by Vav. *Science* 279 (5350) 558-560

Harden N, Loh HY, Chia W, Lim L. 1995 A dominant inhibitory version of the small GTP-binding protein Rac disrupts cytoskeletal structures and inhibits developmental cell shape changes in *Drosophila*. *Development* 121 903-914

Harden N, Ricos M, Ong YM, Chia W, Lim L. 1999 Participation of small GTPases in dorsal closure of the *Drosophila* embryo: distinct roles for Rho subfamily proteins in epithelial morphogenesis. *Journal of Cell Science* 112 (3) 273-284

Harden N. 2002 Signaling pathways directing the movement and fusion of epithelial sheets: lessons from dorsal closure in *Drosophila.* Differentuation 70 94-5) 181-203

Harlan JE, Hajduk PJ, Yoon HS, Fesik SW. 1994 Pleckstrin homology domains bind to phosphatidylinositol-4,5-bisphosphate. *Nature* 371 (6493) 168-170

Hartwig JH, Bokoch GM, Carpenter CL, Janmey PA, Taylor LA, Toker A, Stossel TP. 1996 Thrombin receptor ligation and activated Rac uncap actin filament barbed ends through phosphoinositide synthesis in permeabilised human platelets. *Cell* 82 (4) 643-653

Haslam RJ, Kolde HB, Hemmings BA. 1993 Pleckstrin domain homology. *Nature* 363 (642) 309-310

Heasman SJ, Ridley AJ. 2008 Mammalian Rho GTPases: new insights into their functions from *in vivo* studies. *Nature Reviews* 9 690-701

Haviv L, Brill-Kamiely Y, Mahaffy R, Backouche F, Ben-Shaul A, Pollard TD, Bernhelm-Groswasser A. 2006 Reconstitution of the transition from lamellipodium to filopodium in a membrane-free system. *Proceedings of the National Academy of Sciences* 103 (13) 4906-4911

Hirshberg M, Stockley RW, Dodson G, Webb MR. 1997 The crystal structure of human rac1, a member of the rho-family complexed with a GTP-analogue. *Nature Structural Biology* 4 (2) 147-152

Hordijk PL, ten Klooster JP, van der Kammen RA, Michiels F, Oomen LC, Collard JG. 1997 Science Inhibition of invasion of epithelial cells by Tiam1-Rac signaling. *Science* 278 (5342) 1464-1466

Huang H, Potter CJ, Tao W, Li DM, Broglolo W, Hafen E, Sun H, Xu T. 1999 PTEN affects cell size, cell population and apoptosis during *Drosophila* eye development. *Development* 126 (23) 5365-5372

Ihara K, Muraquchi S, Kato M, Shimizu T, Shirakawa M, Kuroda S, Kaibuchi K, Hakoshima T. 1998 Crystal structure of human RhoA in a dominantly active form complexed with a GTP analogue. *The Journal of Biological Chemistry* 273 (16) 9656-9666

Iijima M, Devreotes P. 2002 Tumor suppressor PTEN mediates sensing of chemoattractant gradients. *Cell* 109 (5) 599-610

Innocenti M, Frittoli E, Ponzanelli I, Falck JR, Brachmann SM, Di Fiore PP, Scita G. 2003 Phosphoinositide 3-kinase activates Rac by entering in a complex with Eps8, Abi1, and Sos-1. *Journal of Cell Biology* 160 (1) 17-23

Jacinto A, Wood W, Balayo, Turmaine, Martines-Arias A, Martin P. 2000 Dynamic actin-based epithelial adhesion and cell matching during *Drosophila* dorsal closure. *Current Biology* 10 (22) 1420-1426

Jacinto A, Martinez-Arias A, Martin P. 2001 Mechanisms of epithelial fusion and repair. *Nature Cell Biology* 3 E117-E123

Jacinto A, Woolner S, Martin P. 2002a Dynamic analysis of dorsal closure in *Drosophila*: From genetics to cell biology. *Developmental cell* 3 9-19

Jacinto A, Wood W, Woolner S, Hiley C, Turner L, Wilson C, Martinez-Arias A, Martin P. 2002b Dynamic analysis of actin cable function during Drosophila dorsal closure. *Current Biology* 12 (14) 1245-1250

Jackson B, Peyrollier K, Pedersen E, Basse A, Karlsson R, Wang Z, Lefever T, Ochsenbein AM, Schmidt G, Aktories K, Stanley A, Quondamatteo F, Ladwein, Rottner K, Hengel JF, Brakebusch C. 2011 RhoA is dispensable for skin development, but crucial for contraction and directed migration of keratinocytes. *Molecular Biology of the Cell*. 22 (5) 593-605

Jankovics F, Brunner D. 2006 Transiently reorganised microtubules are essential for zippering during dorsal closure in *Drosophila melanogaster*. *Developmental Cell* 11 (3) 375-385

Jansen S, Collins A, Yang C, Rebowski G, Svitkina T, Dominguez R. 2011 Mechanism of actin filament bundling by Fascin. *The Journal of Billogical Chemistry* 286 30087-30096

Jasper H, Benes V, Schwager C, Sauer S, Clauder-Münster S, Ansorge W, Bohmann D. 2001 The genomic response of the *Drosophila* embryo to JNK signaling. *Developmental Cell* 1 (4) 579-586

Joberty G, Peterson C, Gao L, Macara AG. 2000 The cell-polarity protein Par6 links Par3 and atypical protein kinase C to CDC42. *Nature Cell Biology* 2 (8) 531-539

Kaltschmidt JA, Lawrence N, Morel V, Balayo T, Fernández BG, Pelissier A, Jacinto A, Martinez-Arias A. 2002 Planar polarity and actin dynamics in the epidermis of *Drosophila*. *Nature Cell Biology* 4(12) 937-944

Kamai T, Yamanishi T, Shirataki H, Takagi K, Asami H, Ito Y, Yoshida KI. 2004 Overexpression of RhoA, Rac1 and CDC42 GTPases is associated with progression in testicular cancer. *Clinical Cancer Research* 10 (14) 4799-4805

Kaneko-Kawano T, Takasu F, Naoki H, Sakumura Y, Ishii S, Ueba T, Aiyama A, Okado A, Kawano Y, Suzuki K. 2012 Dynamic regulation of myosin light chain by phosphorylation by rho-kinase. *PLoS One* 7 (6) e39269

Katoh H, Hiramoto K, Negishi M. 2005 Activation of Rac1 by RhoG regulates cell migration. *The Journal of Cell Science* 119 (pt.1) 56-65

Karim FD, Rubin GM. 1998 Ectopic expression of activated Ras1 induces hyperplastic growth and increased cell death in *Drosophila* imaginal tissues. *Development* 125 (1) 1-9

Kawano Y, Fukata Y, Oshiro N, Amano M, Nakamura T, Ito M, Matsumura F, Inagaki M, Kaibuchi K. 1999 Phosphorylation of myosin-binding subunit (Mbs) of myosin phosphatase by Rho-kinase In Vivo. *Journal of Cell Biology* 147 (5) 1023-1038

Keller R, Davidson L, Edlund A, Elul T, Ezin M, Shook D, Skoglund P. 2000 Mechanisms of convergence and extension by cell intercalation. *Philosophical Transactions of the Royal Society B* 355 (1399) 897-922

Ketschek A, Spillane M, Gallo G. 2011 Mechanism of NGF-induced formation of axonal filopodia. *Communicative and Integrative Biology* 4 (1) 55-58

Kimura K, Ito M, Amano M, Chihara K, Fukata Y, Nakafuku M, Yamamori B, Feng J, Nakano T, Okawa K, Iwamatsu A< Kaibuchi K. 1996 Regulation of myosin phosphatase by Rho and Rho-associated kinase (Rho-kinase). *Science* 273 (5272) 245-248

Kiehart DP, Galbraith CG, Edwards KA, Rickoll WL, Montague RA. 2000 Multiple forces contribute to cell sheet morphogenesis for dorsal closure in *Drosophila*. *Journal of Cell Biology* 149 (2) 471

Kim AS, Kakalis LT, Abdul-Manan N, Liu GA, Rosen MK. 2000 Autoinhibition and activation mechanisms of the Wiskott-Aldrich syndrome protein. *Nature* 404 151-158

Kimura K, Ito M, Amano M, Chihara K, Fukata Y, Yamamori B, Feng J, Nakano T, Okawa K, Iwamatsu A, Kaibuchi K. 1996 Regulation of myosin phosphatase by Rho and Rho-associated kinase (Rho-Kinase). *Science* 273 (5272) 245-248

Kiyokawa E, Hasimoto Y, Kobayashi S, Sugimura H, Kuata T, Matsuda M. 1998 Activation of Rac1 by a Crk SH3-binding protein, Dock180. *Genes Development* 12 (21) 3331-3336

Kissil JL, Walmsley MJ, Hanlon L, Haigis KM, Kim CFB, Sweet-Cordero AS, Eckman MS, Tuveson DA, Capobianco AJ, Tybulewicz VLJ, Jacks T. 2007 Requirement for Rac in a K-ras-induced lung cancer in the mouse. *Cancer Research* 67 8089-8094

Kofron M, Heaseman J, Lang SA, Wylie CC. 2002 Plakoglobin is required for maintenance of the cortical actin skeleton in early *Xenopus* embryos and for cdc42-mediated wound healing. *Journal of Cell Biology* 158 (4) 695-708

Kok K, Geering B, Vanhaesebroeck B. 2009 Regulation of phosphoinositide 3-kinase expression in health and disease. *Trends in Biochemical Sciences* 34 (3) 115-127

Kotani K, Yonezawa K, Hara K, Ueda H, Kitamura Y, Sakaue H, Ando A, Chavanleu A, Calas B, Grigorescu F. 1994 Involvement of phosphoinositide 3-kinase in insulin or IFG 1 induced membrane ruffling. *The EMBO Journal* 13 (10) 2313-2321

Kozma R, Ahmed S, Best A, Lim L. 1995 The Ras-related protein CDC42Hs and bradykinin promote formation of peripheral actin microspikes and filopodia in Swiss 3T3 fibroblasts. *Molecular and Cellular Biology* 15 (4) 1942-1952

Krahn MP, Klopfenstein DR, Fischer N, Wodarz A. 2010 Membrane targeting of Bazooka/PAR-3 is mediated by direct binding to phosphoinositide lipids. *Current Biology* 20 (7) 636-642

Lai JP, Dalton JT, Knoell DL. 2007 Phosphatase and tensin homologue deleted on chromosome ten (PTEN) as a molecular target in lung epithelial wound repair. *British Journal of Pharmacology* 152 (8) 1172-1164

Laplante C, Nilson LA. 2011 Asymmetric distribution of Echinoid defines the epidermal leading edge during *Drosophila* dorsal closure. *Journal of Cell Biology* 192 (2) 335-348

Lee T, Luo L. 1999 Mosaic analysis with a repressible cell marker for studies of gene function in neuronal morphogenesis. *Neuron* 22 (3) 451-461

Leevers SJ, Weinkove D, MacDougall LK, Hafen E, Waterfield MD. 1996 The *Drosophila* phosphoinositide 3-kinase Dp110 promotes cell growth

Lesch C, Jo J, Wu Y, Fish GS, Galko MJ. 2010 A targeted UAS-RNAi screen in *Drosophila* larvae identifies wound closure genes regulating distinct cellular processes. *Genetics* 186 (3) 943-057

Li J, Yen C, Liaw D, Podsypanina K, Bose S, Wang SI, Puc J, Miliaresis C, Rodgers L, McCombie R, Bigner SH, Giovanella BC, Ittmann M, Tyko B, Hibshoosh H, Wigler MH, Parsons R. 1997 *PTEN*, a putative protein tyrosine phosphatase gene mutated in human brain, breast and prostate cancer. *Science* 275 (5308) 1943-1947

Li X, Bu X, Avraham H, Flavell RA, Lim B. 2002 The hematopoiesis-specific GTP-binding proteins RhoH is GTPase deficient and modulates activities of other Rho GTPases by an inhibitory function. *Molecular and Cellular Biology* 22 (4) 1158-1171

Liu AX, Rane N, Liu JP, Prendergast GC. 2001 RhoB is dispensable for mouse development, but it modifies susceptibility to tumor formation as well as cell adhesion and growth factor signaling in transformed cells. *Molecular Cell Biology* 21(20) 6906-6912

Liu S, Kapoor M, Leask A. 2009 Rac1 expression by fibroblasts is required for tissue repair *in Vivo*. *The American Journal of Pathology* 2009 1847-1856

Lodish H, Berk A, Zipursky SL, Matsudaira P, Baltimore D, Darnell J. Molecular Cell Biology, 4th edition. New York: W. H. Freeman; 2000. Section 19.1, Microtubule structures. Available from http://www.ncbi.nlm.nih.gov/books/NBK21580

Lomasney JW, Cheng HF, Wang LP, Kuan Y, Liu S, Fesik SW, King K. 1996 Phosphatidylinositol 4,5-bisphosphate binding to the pleckstrin homology domain of phospholipase C-delta 1 enhances enzyme activity. *Journal of Biological Chemistry* 271 (41) 25316-25326

Loovers HM, Postma M, Keizer-Gunnink I, Huang YE, Devreotes PN, van Haastert PJM. 2006 Distinct role of PI(3,4,5)P_3 during chemoattractant signaling in *Dictyostelium*: A quantitative *In vivo* analysis by inhibition of PI3-kinase. *Molecular Biology of the Cell* 17 1503-1513

Lu M, Kinchen JM, Rossman KL, Grimsley C, deBakker C, Brugnera E, Tosello-Trampont AC, Haney LB, Klingele D, Sondek J, Hengartner MO, Ravichandran KS. 2004 PH domain of ELMO functions *in trans* to regulate Rac activation via Dock180. *Nature Structural and Molecular Biology* 11 (8) 756-762

Lu M, Kinchen JM, Rossman KL, Grimsley C, Hall M, Sondek J, Hengartner MO, Yajnik V, Racichandran KS. 2005 A steric-inhibition model for regulation of nucleotide exchange via the Dock180 family of GEFs. *Current Biology* 15 (4) 371-377

Luo L, Liao YJ, Jan LY, Jan YN. 1994 Distinct morphogenetic functions of similar small GTPases: *Drosophila* Drac1 is involved in axonal outgrowth and myoblast fusion. *Genes and Development* 8 (15) 1787-1802

Ma YY, Wei SJ, in YC, Lung JC, Chang TC, Whang-Peng J, Liu JM, Yang DM, Yang WK, Shen CY. 2000 PIK3CA as an oncogene in cervical cancer. *Oncogene* 19 (23) 2739-2744

Ma L, Janetopoulos C, Yang L, Devreotes PN, Iglesias PA. 2004 Two complementary, local excitation, global inhibition mechanisms acting in parallel can explain the chemoattractant-induced regulation of PI(3,4,5)P3 response in *Dictyostelium* cells. *Journal of Biophysics* 87(6) 6764-3774

Maconald KB, Juriloff DM, Harris MJ. 1989 Experimental study of neural tube closure in a mouse stock with high incidence of exencephaly. *Teratology* 39 (2) 195-213

MacDougall L, Domin J, Waterfield MD. 1995 A family of phosphoinoisitide 3-kinases in *Drosophila* identifies a new mediator of signal transduction. *Current Biology* 5 (12) 1404-1415

Machesky LM, Insall RH. 1998 Scar1 and the related Wiskott-Aldrich syndrome protein, WASP, regulate the actin cytoskeleton through the Arp2.3 complex. *Current Biology* 8(25) 1347-1356

Madaule P, Axel R. 1985 A novel Ras-related gene family. *Cell* 41 (1) 31-40

Maehama T, Dixon JE. 1998 The tumor suppressor, PTEN/MMAC1, dephosphorylates the second lipid messenger, phosphatidylinositol, 3,4,5-triphosphate. *Journal of Biological Chemistry* 273 (22) 13375-13378

Maehama T, Kosaka N, Okahara F, Takeuchi KI, Umeda M, Dixon JE, Kanaho Y. 2004 Suppression of a phosphatidylinositol 3-kinase signal by a specific spliced variant of *Drosophila* PTEN. *FEBS Letters* 565 (1-3) 43-47

Malliri A, van der Kammen RA, Clark K, can der Valk M, Michiels F, Collard JG. 2002 Mice deficient in the Rac activator Tiam1 are resistant to Ras-induced skin tumours. *Nature* 417 (6891) 867-871

Marchand JB, Kaiser DA, Pollard TD, Higgs HN. 2001 Interaction of WASP/Scar proteins with actin and vertebrate Arp2/3 complex. *Nature Cell Biology* 3 76-82

Margolis B, Hu P, Katzav S, Li W, Oliver JM, Ullrich A, Weiss A, Schlessinger J. 1992 Tyrosine phosphorylation of Vav proto-oncogene product containing SH2 domain and transcription factor motifs. *Nature* 356 (6364) 71-74

Marinari E, Mehonic A, Curran S, Gale J, Duke T, Baum B. 2012 Live-cell delamination counterbalances epithelial growth to limit tissue overcrowding. *Nature* 484 (7395) 542-545

Martin P. 1997 Wound-healing – aiming for perfect skin regeneration. *Science* 276 75-81

Martin P, Lewis J. 1992 Actin cables and epidermal movement in embryonic wound healing. *Nature* 260 (6400) 179-183

Martin P, Wood W. 2002 Epithelial fusions in the embryo. *Current Opinions in Cell Biology* 14 (5) 569-574

Martin P, D'Souza D, Martin J, Grose R, Cooper L, Maki R, McKercher SR. 2003 Wound healing in the PU.1 null mouse – tissue repair is not dependent on inflammatory cells. *Current Biology* 13 (13) 1122-1128

Martin P, Parkhurst S. 2004 Parallels between tissue repair and embryo morphogenesis. *Development* 131(13) 3021-34

Martin-Belmonte F, Gassama A, Datta A, Yu W, Rescher U, Gerke V, Mostov K. 2007 PTEN-mediated apical segregation of phosphoinositides control epithelial morphogenesis through Cdc42. *Cell* 128 (2) 383-397

Martin-Belmonte F, Mostov K. 2008 Regulation of cell polarity during epithelial morphogenesis. *Current Opinion in Cell Biology* 20 (2) 227-234

Matusek T, Gombos R, Szécsényi A, Sánchez-Soriano N, Czibula A, Pataki C, Gedai A, Prokop A, Raskó I, Mihály J. 2008 Formin proteins of the DAAM subfamily play a role during axon growth. *The Journal of Neuroscience* 28 (39) 13310-13319

Mayer BJ, Ren R, Clark KL, Baltimore D. 1993 A putative modular domain present in diverse signaling proteins. *Cell* 73 629-630

McCluskey J, Martin P. Analysis of the tissue movements of embryonic wound healing – DiI studies in the limb bud stage mouse embryo. *Developmental Biology* 170 102-114

McGill MA, McKinley A, Harris TJC. 2009 Independent cadherin-catenin and Bazooka clusters interact to assemble adherens junctions. *Journal of Cell Biology* 185 (5) 787-796

Mcgough A, Pope B, Chiu W, Weeds A. 1997 Cofilin changes the twist of F-actin: implications for actin filament dynamics and cellular function. *Journal of Cell Biology* 138 (4) 771-781

Mertens AE, Roovers RC, Collard JG. 2003 Regulation of Tiam1-Rac signalling. *Signal Transduction* 1 (3) 11-16

Michiels F, Habets GGM, Stam JC, van der Kammen RA, Collard JG. 1995 A role for Rac in Tiam-1 induced membrane ruffling and invasion. *Nature* 375 (6529) 338-340

Michiels F, Stam JC, Hordijk PL, van der amen RA, Ruuls-Van Stalle L, Feltkamp CA, Collard JG. 1997 Regulated membrane localisation of Tiam1, mediated by the NH2-terminal pleckstrin homology domain, is required for Rac-dependent membrane ruffling and C-Jun NH2-terminal kinase activation. *Journal of Cell Biology* 137 (2) 387-398

Miki H, Sasaki T, Takai Y, Takenawa T. 1998 Induction of filopodium formation by a WASP-related actin-depolymerising protein N-WASP. *Nature* 391 93-96

Millard TH, Martin P. 2008 Dynamic analysis of filopodia interactions during the zippering phase of *Drosophila* dorsal closure. *Development* 135 621-626

Mira JP, Benard V, Groffen J, Sanders LC, Knaus UG. 2000 Endogenous, hyperactive Rac3 controls proliferation of breast cancer cells by a p21-actvated kinase-dependent pathway. *PNAS* 97 (1) 185-189

Misawa H, Ohtsubo M, Copeland NG, Gilbert DJ, Jenkins NA, Yoshimura A. 1998 Cloning and characterisation of a novel class II phosphoinositide 3-kinase containing C2 domain. *Biochemical and biophysical research communications* 244 (2) 531-539

Mizuno T, Tsutsui K, Nishida Y. 2002 *Drosophila* myosin phosphatase and its role in dorsal closure. *Development* 129 (5) 1215-1223

Mockrin SC, Korn ED. 1980 *Acanthamoeba* profilin interacts with G-actin to increase the rate of exchange of actin bound adenosine 5'-triphosphate. *Biochemistry* 19, 5359-5362

Mogilner A, Rubinstein B. 2005 The physics of filopodial protrusion. *Biophysical Journal* 89 782-795

Moissoglu K, Slepchenko BM, Meller N, Horwitz AF, Schwartz MA. 2006 In vivo dynamics of Rac-membrane interactions. *Molecular Biology of the Cell* 17 (6) 2770-2779

Moll J, Sansig G, Fattori E, van der Putten H. 1991 The murine rac1 gene:cDNA cloning, tissue distribution and regulated expression of rac1 mRNA by disassembly of actin microfilaments. *Oncogene* 6 (5) 863-866

Morris JZ, Tissenbaum HA, Ruvkun G. 1996 A phosphatidylinositol-3-OH-kinase family member regulating lobgevity and diapause in *Caenorhabditis elegans*. *Nature* 382(6591) 536-539

Mullins RD, Heuser JA, Pollard TD. 1998 The interaction of Arp2/3 complex with actin: nucleation, high affinity pointed end capping, and formation of branching networks of filaments. *The Proceedings of the National Academy of Science* 95 (11) 6181-6186

Myers MP, Pass I, Batty IH, van der Kaay J, Stolarov JP, Hemmings BA, Wigler MH, Downes CP, Tonks NK. 1998 The lipid phosphatase activity of PTEN is critical for its tumor suppressor function. *Proceedings of the National Academy of Science USA* 95 (23) 13513-13518

Ng J, Nardine T, Harms M, Tzu J, Goldstein A, Sun Y, Dietzl G, Dickson BJ, Luo L. 2002 Rac GTPases control axon growth, guidance and branching. *Nature* 416 (6879) 442-447

Nishimura T, Yamaguchi T, Kato K, Yoshizawa M, Nabeshima Y, Ohno S, Hoshino M, Kaibuchi K. 2005 Par-6-Par-3 mediates CDC42-induced Rac activation through the Rac GEFs STEF/Tiam1. *Nature Cell Biology* 7 (3) 270-277

Nishikimi A, Fukuhara H, Su W, Hongu T, Takasuga S, Mihara H, Cao Q, Sanematsu F, Kanai M, Hasegawa H, Tanaka Y, Shibasaki M, Kanaho Y, Sasaki T, Frohman MA, Fukui Y. 2009 Sequential regulation of Dock2 dynamics by two phospholipids during neutrophil chemotaxis. *Science* 324 (5925) 384-387

Nisho M, Watanabe K, Sasaki J, Taya C, Takasuga S, Iizuka R, Balla T, Yamazaki M, Watanabe H, Itoh R, Kuroda S, Horie Y, Forster I, Mak TW, Yonekawa H, Penninger JM, Kanaho Y, Suzuki A, Sasaki T. 2007 Control of cell polarity and motility by the PtdIns(3,4,5)P_3 phosphatase SHIP1. *Nature Cell Biology* 9 (1) 36-44

Nobes CD, Hall A. 1995 Rho, Rac, and CDC42 GTPases regulate the assembly of multimolecular focal complexed associated with actin stress fibres, lamellipodia and filopodia. *Cell* 31 53-62

Nobes CD, Hall A. 1999 Rho GTPases control polarity, protrusion and adhesion during cell movement. *Journal of Cell Biology* 144 (6) 1235-1244

Nolan KM, Barrett K, Lu Y, Hu KQ, Sylvie V, Settleman J. 1998 Myoblast city, the *Drosophila* homologue of DOCK180/CED-5, is required in a Rac signaling pathway utilized for multiple developmental processes. *Genes and Development* 12 (21) 3337-3342

Oda H, Tsukita S. 1999 Nonchordate classic cadherins have a structurally and functionally unique domain that is absent from chordate classic cadherins. *Developmental Biology* 216 (1) 406-422

Odland G, Ross R. 1968 Human wound repair I. Epidermal regeneration. *Journal of Cell Biology* 39 (1) 135-151

Okada Y, Saika S, Shirai K, Yamanaka O, Kitano A, Wang Z, Yang H, Reinach P. 2009 JNK MAPK signalling contributes in vivo to injury-induced corneal epithelial migration. *Ophthalmic Research* 42 (4) 185-192

Olsen MF, Pasteris NG, Gorski JL, Hall A. 1996 Faciogenital dysplasia protein (FGD1) and Vav, two related proteins required for normal embryonic development, are upstream regulators of Rho GTPases. *Current Biology* 6 (12) 1628-1633

Pai YJ, Abdullah NL, Mohd-Zin SW, Mohammed RS, Rolo A, Greene NDE, Abdul-Aziz NM, Copp AJ. 2012 Epithelial fusion during neural tube morphogenesis. *Birth Defects Research* 94 (10) 817-823

Paterson HF, Self AJ, Garrett MD, Just I, Aktories K, Hall A. 1990 Miroinjection of recombinant p21rho induces rapid changes in cell morphology. *Journal of Cell Biology* 111 (3) 1001-1007

Peng Y, Jiang BH, Yang PH, Cao Z, Shi X, Lin MCM, He ML, Kung HF. 2004 Phosphatidylinositol 3-kinase signaling is involved in neurogenesis during *Xenopus* embryonic development. *The Journal of Biological Chemistry* 279 (27) 28509-28514

Pickering K, Alves-Silva J, Goberdhan D, Millard TH. 2013 Par3/Bazooka and phosphoinositides regulate actin protrusion formation during *Drosophila* dorsal closure and wound healing. *Development* 140 (4) 800-809

Pickett EA, Olsen GS, Tallquist MD. 2008 Disruption of PDGFRalpha-initiated PI3K activation and migration of somite derivatives leads to spina bifida. *Development* 135 (3) 589-598

Pinal N, Goberdhan DC, Collinson L, Fujita Y, Cox IM, Wilson C, Pichaud F. 2006 Regulated and polarized PtdIns(3,4,5)P3 accumulateion is essential for apical membrane morphogenesis in photoreceptor epithelial cells. *Current Biology* 16 (2) 140-149

Planchon SM, Waite KA, Eng C. 2008 The nuclear affairs of PTEN. *Journal of Cell Science* 121 (pt. 3) 249-253

Pollard TD, Cooper JA. 1984 Quantitative analysis of the effect of *Acanthamoeba* profilin on actin filament nucleation and elongation. *Biochemistry* 23 6631-6641

Pollard TD, Borisy GG. 2003 Cellular motility driven by assembly and disassembly of actin filaments. *Cell* 453-465

Pons S, Asano T, Glasheen E, Miralpeix M, Zhang Y, Fisher TL, Myers GM, Sun XJ, White MF. 1995 The structure and function of p55PIK reveal a new regulatory sunbuni gor phosphatidylinositol 3-kinase. *Molecular Cell Biology* 15 (8) 4453-4465

Posakony LG, Raftery LA, Gelbart WM. 1990 Wing formation in *Drosophila melanogaster* requires decapentaplegic gene function along the anterior-posterior compartment boundary. *Mechanical Development* 33 (1) 69-82

Potter CJ, Pedraza LG, Xu T. 2002 Akt regulates growth by directly phosphorylating Tsc2. *Nature Cell Biology* 4 (9) 658-665

Pring M, Weber A, Bubb MR. 1992 Profilin-actin complexes directly elongate actin filaments at the barbed end**.** *Biochemistry* 31 1827-1836

Pyrgaki , Trainor P, Hadjantonaskis AK, Niswander L. 2010 Dynamic imaging of mammalian neural tube closure. *Developmental biology* 344 (2) 941-947

Rämet M, Lanot R, Zachary D, Manfruelli P. 2002 JNK signalling pathway is required for efficient wound healing in *Drosophila*. *Developmental Biology* 241 145-156

Reed BH, Wilk R, Lipshitz HD. 2001 Downregulation of Jun kinase signaling in the amnioserosa is essential for dorsal closure of the *Drosophila* embryo. *Current Biology* 11(14) 1098-1108

Reymond N, Im JH, Garg R, Vega FM, Borda d'Agua B, Riou P , Cox S, Valderrama F, Meschel RJ, Ridley AJ. 2012 CDC42 promotes transendothelial migration of cancer cells through β1 integrin. *The Journal of Cell Biology* 199 (4) 653-668

Ridley AJ, Hall A. 1992 The small GTP-binding protein Rho regulates the assembly of focal adhesions and actin stress fibers in response to growth factors. *Cell* 70 289-299

Ridley AJ, Paterson HF, Johnston, Diekmann D, Hall A. 1992b The small GTP-binding protein rac regulates growth factor-induced membrane ruffling. *Cell* 70 401-410

Ridley AJ. 2001 Rho GTPases and cell migration. *Journal of Cell Science* 114 (pt15) 2713-2722

Rihet S, Vielh P, Camonis J, Goud B, Chevillard S, Gunzburg J. 2001 Mutation status of genes encoding RhoA, Rac1 and Cdc42 GTPases in a pannel of invasive human colorectal and breast tumours. *Journal of Cancer Research an Clinical Oncology* 127 (12) 733-738

Rodriguez-Vicana P, Warne PH, Dhand R, Vanhaesebroeck B, Gout I, Fry MJ, Waterfield MD, Downward J. 1994 Phosphatidylinositol-3-OH kinase as a direct target of Ras. *Nature* 370 527-532

Roggo L, Bernard V, Kovacs AL, Rose AM, Savoy F, Zetka M, Wymann MP, Müller F. 2002 Membrane transport in *Caenorhabditis elegans*: an essential role for VPS34 at the nuclear membrane. *The EMBO Journal* 21 (7) 1673-1683

Rohatgi R, Ho HH, Kirschner MW. 2000 Mechanism of N-Wasp activation by Cdc42 and phosphatidylinositol 4,5-bi-phosphate. *Journal of Cell Biology* 150 (6) 1299-1310

Rosenblatt J, Peluso P, Mitchison TJ. 1995 The bulk of unpolymerised actin in *Xenopus* egg extracts is ATP-bound. *Molecular Biology of the Cell* 6 (2) 227-236

Rosenblatt J, Raff MC, Cramer LP. 2001 An epithelial cell destined for apoptosis signals its neighbours to extrude it by an actin- and myosin-dependent mechanism. *Current Biology* 11 (23) 1847-1857

Rossman KL, Worthylake DK, Snyder JT, Siderovski DP, Campbell SL, Sondek J. 2002 A crystallographic view of interactions between Dbs and Cdc42: PH domain-assisted guanine nucleotide exchange. *The EMBO Journal* 21 (6) 1315-1326

Rossman KL, Der CJ, Sondek J. 2005 GEF means go: turning on Rho GTPases with guanine nucleotide exchange factors. *Nature Reviews Molecular Cell Biology* 6 (2) 167-180

Ruderman NB, Kapeller R, White M, Cantley LC. 1990 Activation of phosphatidylinositol 3-kinase by insulin. *Proceedings of the National Acadamy of Science* 87 1411-1415

Rugendorff A, Younossi-Hartenstein A, Hartenstein V. 1994 Embryonic origin and differentiation of the *Drosophila* heart. *Roux's Archives a century in Developmetal Biology* 203 266-280

Rushton E, Drysdale R, Abmayr SM, Michelson AM, bate M. 1995 Mutations in a novel gene, *myoblast city*, provide evidence in support of the founder cell hypothesis for *Drosophila* muscle development. *Development* 121 (7) 1979-1988

Saltiel AR, Pessin JE. 2002 Insulin signaling pathways in time and space. *Trends in Cell Biology* 12 (2) 65-71

Samuels Y, Wang Z, Bardelli A, Silliman N, Ptak J, Szabo S, Yan H, Gazdar A, Powell SM, Riggins GJ, Willson JKV, Markowitz S, Kinier KW, Vogelstein B, Velculescu VE. 2004 High frequency of mutations of the PIK3CA gene in human cancers. *Science* 304 (5670) 554

Sander EE, van Delft S, Klooster JPT, Reid T, van der Kammen RA, Michiels F, Collard JG. 1998 Matrix-dependent Tiam1/Rac signaling in epithelial cells promotes either cell-cell adhesion or cell migration and it regulated by phosphatidylinositol 3-kinase. *Journal of Cell Biology* 143 (5) 1385-1398

Sarbassov DD, Guertin AD, Ali SM, Sabatini DM. 2005 Phosphorylation and regulation of Akt/PKB by the Rictor-mTOR complex. *Science* 207 (5712) 1098-1101

Sasaki AT, Chun C, Takeda K, Firtel RA. 2004 Localised Ras signalling at the leading edge regulates PI3K, cell polarity and directional cell movement. *Journal of Cell Biology*167 (3) 505-518

Scheffzek K, Ahmadian MR, Kabsch W, Wiesmüller L, Lautwein A, Schmitz F, Wittinghofer A. 1997 The Ras-RasGAP complex: Structural basis for GTPase activation and its loss in oncogenic Ras mutants. *Science* 277 (5324) 333-338

Schirenbeck A, Bretschneider T, Arasada R, Schleicher M, Faix J. 2005 The Diaphanous-related formin dDia2 is required for the formation and maintenance of filopodia. *Nature Cell Biology* 7 619-625

Schmidt A, Hall A. 2002 Guanine nucleotide exchange factors for Rho GTPases: turning on the switch. *Genes and Development* 16 (13) 1587-1609

Schu PV, Takegawa K, Fry MJ, Stack JH, Waterfield MD, Emr SD. 1993 Phosphoinositide 3-kinase encoded by yeast *VSP34* gene essential for protein sorting. *Science* 260 88-91

Shaw L, Rabinovitz I, Wang HHF, Toker A, Mercurio AM. 1997 Activation of phosphoinositide 3-OH kinase by the α6β4 integrin promotes carcinoma invasion. *Cell* 91 (7) 949-960

Shayesteh L, Lu Y, Kuo WL, Baldocchi R, Godfrey T, Collins C, Pinkel D, Powell B, Millis GB, Gray JW. 1999 PIK3CA is implicated as an oncogene in ovarian cancer. *Nature Genetics*

Shirsat NV, Pignolo RJ, Kreider BL, Rovera G. 1990 A member of the ras gene superfamily is expressed specifically in T, B and myeloid hemopoietic cells. *Oncogene* 5 (5) 769-772

Simon CM, Vaughan EM, Bement WM, Edelstein-Keshet L. 2012 Pattern formation of Rho GTPase in single cell wound healing. *Molecular Biology of the Cell* 24 421-432

Simões SdM, Blankenship JT, Weitz O, Farrell DL, Tamada M, Fernandez-Gonzalez R, Zallen JA. 2010 Rho-kinase directs Bazooka/Par2 planar polarity during *Drosophila* axis elongation. *Developmental Cell* 19 (3) 377-388

Sjolander A, Yamamoto K, Huber BE, Lapetina EG. 1994 Association of p21ras with phosphatidylinositol 3-kinase. *Proceedings of the National Academy of Science USA* 88 7908-7912

Skoble J, Auerbuch V, Goley ED, Welch MD, Portnoy DA. 2001 Pivotal role of VASP in Arp2/3 complex-mediated actin nucleation, actin branch-formation, and *Listeria monocytogenes* motility. *Journal of Cell Biology* 155 (1) 89-100

Smith A, Smith A, Airubaie S, Coehlo C, Leevers SJ, Ashworth A. 1999 Alternative splicing of the *Drosophila PTEN* gene. *Biochimica et Biophysica Acta (BBA) – Gene Structure and Expression.* 1447 (2-3) 313-317

Soisson SM, Nimnual AS, Uy M, Bar-Sagi D, Kuriyan J. 1998 Crystal structure of the Dbl and pleckstrin homology domains from the human son of sevenless protein. *Cell* 95 (2) 259-268

Solon J, Kaya-Çopur A, Colombelli J, Brunner D. 2009 Pulsed forces timed by a ratchet-like mechanism drive directed tissue movement during dorsal closure. *Cell* 137(7) 1331-1342

Sone M, Hoshino M, Suzuki E, Kuroda S, Kaibuchi K, Nakagoshi H, Saigo K, Nabeshima YI, Hama C. 1997 Still life, a protein in synaptic terminals of *Drosophila* homologoud to GDP-GTP exhangers. *Science* 275 (5299) 543-547

Sone M, Suzuki E, Hoshino M, Hou D, Kuyomi H, Fukata M, Kuroda S, Kaibuchi K, Nabeshima YI, Hama C. 2000 Synaptic development is controlled in the periactive zones of *Drosophila* synapses. *Development* 127 (19) 4157-4168

Song MS, Salmena L, Pandolfi PP. 2012 The functions and regulation of the PTEN tumour suppressor. *Molecular Cell Biology* 13 283-296

Sossey-Alaoui K, Li X, Ranalli TA, Cowell JK. 2005 Wave3-mediated cell migration and lamellipodia formation are regulated downstream of phosphatidylinositol 3-kinase. *The Journal of Biological Chemistry* 280 (23) 21748-21755

Squarize CH, Castilho RM, Bugge TH, Gutkind JS. 2010 Accelerated wound healing by mTOR activation in genetically defined mouse models. *PLoS One* 5 (5) e10643

Steffen A, Rottner K, Ehinger J, Innocenti M, Scita G, Wehland J, Stradel TEB. 2004 Sra-1 and Nap1 link Rac to actin assembly driving lamellipodia formation. *The EMBO Journal* 23 (4) 749-759

Steffen A, Faix J, Resch GP, Linkner J, Wehland J, Small JV, Rottner K, Stradal TEB. 2006 Filopodia formation in the absence of functional WAVE-and Arp2/3-complexes. *Molecular Biology of the Cell* 17 (6) 2581-2591

Stokoe D, Stephens LR, Copeland T, Gaffney PR, Reese CB, Painter GF, Holmes AB, McCormick F, Hawkins PT. 1997 Dual role of phosphatidylinositol-3,4,5-triphosphate on the activation of protein kinase B. *Science* 227 (5324) 567-570

Stramer B, Wood W, Galko MJ, Redd MJ, Jacinto A< Parkhurts SM, Martin P. 2005 Live imaging of wound inflammation in *Drosophila* embryos reveals key roles for small GTPases during *in vivo* cell migration. *Journal of Cell Biology* 168 (4) 567-573

Stronach B, Perrimon N. 2001 Activation of the JNK pathway during dorsal closure in *Drosophila* requires the mixed lineage kinase, slipper. *Genes Development* 16 (3) 377-387

Sun CX, Downey GP, Zhu F, Koh ALY, Thang H, Glogauer M. 2004 Rac1 is the small GTPase responsible for regulating the neutrophil chemotaxis compass. *Blood* 104 (12) 3758-3765

Sun CX, Magalhães MAO, Glogauer M. 2007 Rac 1 and Rac2 differentially regulate actin free barbed end formation downstream of the fMLP receptor. *The Journal of Cell Biology* 179 (2) 239-245

Suzuki A, de la Ponpa JL, Stambolic V, Elia AJ, Sasaki T, del Barco Barrantes I, Ho A< Wakeham A, Iyie A, Khoo W, Fukumoto M, Mak TW. 1998 High cancer susceptibility and embryonic lethality associated with mutation of the PTEN tumor suppressor gene. *Current Biology* 8 (21) 1169-1178

Svitkina TM, Verkhovsky AB, McQuade KM, Borisy GG. 1997 Analysis of the actin-myosin II system in fisg keratocytes: Mechanism of cell body translocation. *Journal of Cell Biology* 139 (2) 3997-415

Svitkina TM, Borisy GG. 1999 Arp2/3 complex and actin depolymerizing factor/cofilin in dendritic organisation and treadmilling of actin filament array in lamellipodia. *Journal of Cell Biology* 145 (5) 1009-1026

Svitkina TM, Bulanova EA, Chaga OY, Vignjevic DM, Kojima SI, Vasiliev JM, Borisy GG. 2003 Mechanism of filopodia initiation by reorganization of a dendritic network. *Journal of Cell Biology* 160 (3) 409-421

Tahinci A, Symes K. 2003 Distinct functions of Rho and Rac are required for convergent extension during *Xenopus* gastrulation. *Developmental Biology* 259 (2) 318-335

Takahama S, Hirose T, Ohno S. 2008 aPKC restricts the basolateral determinant PtdIns(3,4,5)P3 to the basal region. *Biochemical and Biophysical Research Communications* 368 (2) 249-255

Tolias KF, Cantley LC, Carpenter CL. 1995 Rho family GTPases bind to phosphoinositide kinases. *The Journal of Biological Chemistry* 270 (30) 17656-17659

Toyama Y, Peralta XG, Wells AR, Kiehart DP, Edwards GS. 2008 Apoptotic force and tissue dynamics during *Drosophila* embryogenesis. *Science* 321 (5896) 1683-1686

Tscharntke M, Pofahl R, Kreig T, Haase I. 2005 Ras-induced spreading and wound closure in human epidermal keratinocytes. *The Journal of the Federation of American Societies for Experimental Biology* Published online September 16, 2005

Tscarnkte M, Pofahl R, Chrostek-Grashoff A, Smyth N, Niessen C, Niemann C, Hartwig B, Herzog V, Klein HW, Kreig T, Brakebusch C, Haase I. 2007 Impaired epidermal wound healing *in vivo* upon inhibition or deletion of Rac1. Journal of Cell Science. *120 1480-1490*

Uruno T, Liu J, Zhang P, Fan Y, Egile C, Li R, Mueller SC, Zhan X. 2001 Activation of Arp2/3 complex-mediated actin polymerization by cortactin. *Nature Cell Biology* 3 259-266

Vanhaesebroeck B, Stephens L, Hawkins P. 2012 PI3K signalling: the path to discover and understanding. *Nature Reviews, Molecular Cell Biology* 13 (3) 195-203

Varma S, Lal BK, Zheng R, Breslin JW, Saito S, Pappas PJ, Hobson RW, Durán. 2005 Hyperglycaemia alters PI3K and Akt signaling and leads to endothelial cell proliferative dysfunction. *American Journal of Physiology Heart and circulatory Physiology* 289 (4) H1744-1751

Vega FM, Ridley AJ. 2007 SnapShot: Rho family GTPases. *Cell* 129 (7) 1430e1-1430e2

Vlahos CJ, Matter WF, Hui KY, Brown RF. 1994 A specific inhibitor of phosphatidylinositol 3-kinase, 2-(4-morpholinyl)-8-phenyl-4H-1-benzopyran-4-one (Ly294002). *The Journal of Biological Chemistry* 269 (7) 5241-5248

Vieira OV, Botelho RJ, Rameh L, Brachmann SM, Matsuo T, Davidson HW, Schreiber A, Backer JM, Cantley LC, Grinstein S. 2001 Distinct roles of class I and class III phosphatidylinositol 3-kinases in phagasome formation and maturation. *Journal of Cellular Biology* 155 (1) 19-26

Viglietto G, Motti ML, Bruni P, Melillo RM, D'Alessio A, Califano D, Vinci F, Chiappetta G, Tsichlis P, Bellacosa A, Fusco A, Santoro M. 2002 Cytoplasmic relocalisation and inhibition of the cyclin-dependent kinase inhibitor p27(kip1) by PKB/Akt-mediated phosphorylation in breast cancer. *Nature Medicine* 8 (10) 1136-1144

Vignjevic D, Yarar D, Welch MD, Peloquin J, Svitkina T, Borisy GG. 2003 Formation of filopoida-like bundles in vitro from a dendritic network. *Journal od cell Biology* 160 (6) 951-962

Vincent S, Jeanteur P, Fort P. 1992 Growth-regulated expression of *rhoG*, a new member of the *ras* homolog gene family. *Molecular and Cellular Biology* 12 (7) 3138-3148

Vinson VK, De La Cruz EM, Higgs HN, Pollard TM. 1998 Interactions of *Acanthamoeba* profilin with actin and nucleotides bound to actin. *Biochemistry* 37 (31) 10871 – 10880

Vlahos CJ, Matter WF, Hui KY, Brown RF. 1994 A specific inhibitor of phosphatidylinositol 3-kinase, 2-(4-morpholinyl)-8-phenyl-4H-1-benzopyran-4-one (LY294002). *Journal of Biological Chemistry* 269 (7) 5241-5248

von Stein W, Ramrath A, Grimm A, Müller-Borg M, Wodarz A. 2005 Direct association of Bazooka/Par3 with the lipid phosphatase PTEN reveals a link between the PAR/aPKC complex and phosphoinositide signaling. *Development* 132 1675-1686

Wan H, Liu C, Wert SE, Xu W, Liao Y, Zheng Y, Whitsett JA. 2013 CDC42 is required for structural patterning of the lung during development. *Developmenal Biology* 374 (1) 46-57

Warrington SJ, Strutt H, Strutt D. 2013 The Frizzled-dependent planar polarity pathway locally promotes E-cadherin turnover via recruitment of RhoGEF2. *Development* 140 (5) 1045-1054

Wei SY, Escudero LM, Yu F, Chang LH, Chen LY, Ho YU, Lin CM, Chou CS, Chia W, Modolell J, Hsu JC. 2005 Echinoid is a component of adherens junctions that cooperates with DE-Cadherin to mediate cell adhesion. *Developmental Cell* 8 (4) 493-504

Weiner O, Neilsen PO, Prestwich GD, Kirschner MW, Cantley LC, Bourne HR. 2002 A PtdInsP3- and Rho GTPase-mediated positive feedback loop regulated neutrophil polarity. *Nature Cell Biology* 4 509-512

Weston CR, Davis RJ. 2002 The JNK signal transduction pathway. *Current Opinion in Genetics and Development* 12 (1) 14-21

Weston L, Coutts AS, La Thangue NB. 2012 Actin nucleators in the nucleus: an emerging theme. *Journal of Cell Science* 125 1-9

Wheeler AP, Ridley AJ. 2004 Why three Rho proteins? RhoA, RhoB, RhoC and cell motility. *Experimental Cell Research* 301 (1) 43-49

Whitman M, Downes CP, Keeler M, Keller T, Cantley L. 1988 Type 1 phosphatidylinositol kinase makes a novel inositol phospholipid, phosphatidylinositol-3-phosphate. *Nature* 332 644-646

Witke W, Sharpe AH, Hartwig JH, Azuma T, Stossel TP, Kwiatkowski DJ. 1995 Hemostatic, inflammatory, and fibroblast responses are blunted in mice lacking gelsolin. *Cell* 81 (1) 41-51

Wodarz A, Hinz U, Englebert M, Knust E. 1995 Expression of crumbs confers apical character on plasma membrane domains of ectodermal epithelia of *Drosophila*. *Cell* 82 (1) 67-76

Wood W, Jacinto A, Grose R, Woolner S, Gale J, Wilson C, Martin P. 2002 Wound healing recapitulates morphogenesis in *Drosophila* embryos. *Nature Cell Biology* 4 (11) 907-912

Wood W, Jacinto A. 2005 Imaging cell movement during dorsal closure in *Drosophila* embryos. *Methods of Molecular Biology* 294 203-210

Wood W, Faria C, Jacinto A. 2006 Distinct mechanisms regulate hemocyte chemotaxis during development and wound healing in *Drosophila melanogaster. The Journal of Cell Biology* 173 (3) 405-416

Woolner S, Jacinto A, Martin P. 2005 The small GTPase Rac plays multiple roles in epithelial sheet fusion – Dynamic studies of *Drosophila* dorsal closure. *Developmental Biology* 282 (1) 163-173

Worthylake DK, Rossman KL, Sondek J. 2000 Crystal structure of Rac1 in complex with the guanine nucleotide exchange region of Tiam1. *Nature* 408 (6813) 682-683

Wu Y, Brock AR, Wang Y, Pujitani K, Ueda R, Galko MJ. 2009 A blood-borne PDGF/VEGF-like ligand initiates wound-induced epidermal cell migration in *Drosophila* larvae. *Current Biology* 19 (17) 1473-1477

Wu X, Ramachandran S, Cerione RA, Erickson JW. 2011 A minimal Rac activation domain in the unconventional guanine nucleotide exchange factor Dock180. *Biochemistry* 50 (6) 1070-1080

Wurmser AE, Gary JD, Emr SD. 1999 Phosphoinositide 3-kinases and their FYVE domain-containing effectors as regulators of vascular/lysosome membrane trafficking pathways. *Journal of Biological Chemistry* 274 (14) 9129-9132

Wymann M, Arcaro A. 1994 Platelet-derived growth dactor-induced phosphatidylinositol 3-kinase activation mediates actin rearrangements in fibroblasts. *Biochemical Journal* 298 (pt3) 517-520

Wymann MP, Björklöf K, Calvez R, Finan P, Thomast M, Trifilieff A, Barbier M, Altruda F, Hirsch E, Laffargue M. 2003 Phosphoinositide 3-kinase gamma: a key modulator in inflammation and allergy. *Biochemical Society Transactions* 31 (pt1) 275-280

Yamana N, Arakawa Y, Nishino T, Kurokawa K, Tanji M, Itoh M, Itoh RE, Monypenny J, Ishizaki T, Bito H, Nozaki K, Hashimoto N, Matsuda M, Narummiya S. 2006 The Rho-mDia pathway regulates cell polarity and focal adhesion turnover in migrating cells through mobilizing Apc and c-Src. *Molecular and Cellular Biology* 26 (18) 6844-6858

Yang L, Wang L, Zheng Y. 2006 Gene targeting of Cdc42 and Cdc42GAP affirms the critical involvement of Cdc42 in filopodia, directed migration, and proliferation in primary mouse embryonic fibroblasts. *Molecular Biology of the Cell* 17 (11) 4675-4685

Yang C, Czech L, Gerboth S, Kojima SI, Scita G, Svitkina T. 2007 Novel roles of forming cDia2 in lamellipodia and filopodia formation in motile cells. *PLoS Biology* 5 (11) e317

Yang N, higuchi O, Ohashi K, Nagata K, Wada A, kangawa K, Nishida E, Mizuno K. 1998 Cofilin phosphorylation by LIM_kinase 1 and its role in Rac-mediated actin reorganisation. *Nature* 393 809-

Yang C, Svitkina T. 2011 Filopodia initiation. Focus on the Arp2/3 complex and formins. *Cell Adhesion and Migration* 5 (5) 402-408

Yin J, Lu J, Yu FSX. 2009 Role of small GTPase Rho in regulating corneal epithelial wound signalling. *Investigative Ophthalmology and Visual Science* 49 (3) 1107-1122

Yip SC, El-Sibai M, Coniglio SJ, Mouneimne G, Eddy RJ, Drees BE, Neilsen PO, Goswami S, Symonns M, Condeelis JS, Backer JM. 2007 The distinct roles of Ras and Rac in PI 3-kinase-dependent protrusion during EGF-stimulated cell migration. *Journal of Cell Science* 120 (pt17) 3138-3146

Yoneda A, Malthaupt HAB, Couchman JR. 2005 The Rho kinases I and II regulate different aspects of myosin II activity. *The Journal of Cell Biology* 175 (3) 443-453

Yoo SK, Deng Q, Cavanar PJ, Wu YI, Hahn KM, Huttenlocher A. 2010 Differential regulation of protrusion and polarity by PI3K during neutrophil motility in live zebrafish. *Developmental Cell* 18 (2) 226-36

Yoo SK, Lam PY, Eichelberg MR, Zasadil L, Bement WM, Huttenlocher A. 2012 The role of microtubules in neutrophil polarity and migration in live zebrafish. *Journal of Cell Science* 125 5702-5710

Young PE, Richman AM, Ketchum AS, Kiehart DP. 1993 Morphogenesis in *Drosophila* requires nonmuscle myosin heavy chain function. *Genes Development* 7(1) 29-41

Yuan TL, Cantley LC. 2008 PI3K pathway alterations in cancer: variations on a theme. *Oncogene* 27 (41) 5497-5510

Zanet J, Jayo A, Plaza S, Millard T, Parsons M, Stramer B. 2012 Fascin promotes filopodia formation independent of its role in actin bundling. *Journal of Cell Biology* 197 (4) 477-486

Zeitlinger J, Kockel L, Peverali F, Jackson D, Mlodzik M, Bohmann D. 1997 Defective dorsal closure and loss of epidermal *decapentaplegic* expression in *Drosophila fos* mutants. *The EMBO Journal* 16 7393-7401

Zenz R, Scheuch H, Martin P, Frank C, Eferi R, Kenner L, Sibilia M, Wagner EF. 2003 c-Jun regulates eyelid closure and skin tumor development through EGFR signaling. *Developmental Cell* 4 (6) 879-889

Zheng Y, Bagrodia S, Cerione RA. 1994 Activation of phosphoinositide 3-kinase activity by Cdc42Hs binding to p85. *The Journal of Biological Chemistry* 369 (29) 18727—18730

Zheng Y, Fischer DJ, Santoas MF, Tigyi G, Pasteris NG, Gorski JL, Xu Y. 1996 The faciogenetial dysplasia gene product FGD1 functions as a CDC42HS-specific guanine nucleotide exchange factor. *Journal of Biological Chemistry* 271 (52) 33169-33172

Zhou K, Bokoch G, Traynor-Kaplan AE. 1998 Disruption of Dictyostelium PI3K genes reduces [32P]phosphatidylinositol 3,4 bisphosphate and [32P]phosphatidylinositol triphosphate levels, alters F-actin distribution and impairs pinocytosis. *Journal of Cell Science* 111 (pt2) 283-294

Ziman M, Preuss D, Mulholland J, O'Brien JM, Botstein D, Johnson DI. 1993 Subcellular localisation of Cdc42p, a *Saccharomyces cerevisiae* GTP-binding protein involved in the control of cell polarity. *Molecular Biology of the Cell* 4 (12) 1307-1316

Zuo Y, Wu Y, Chakraborty C. 2012 CDC42 negatively regulated intrinsic migration of highly aggressive breast cancer cells. *Journal of Cellular Physiology* 227 (4) 1399-1407